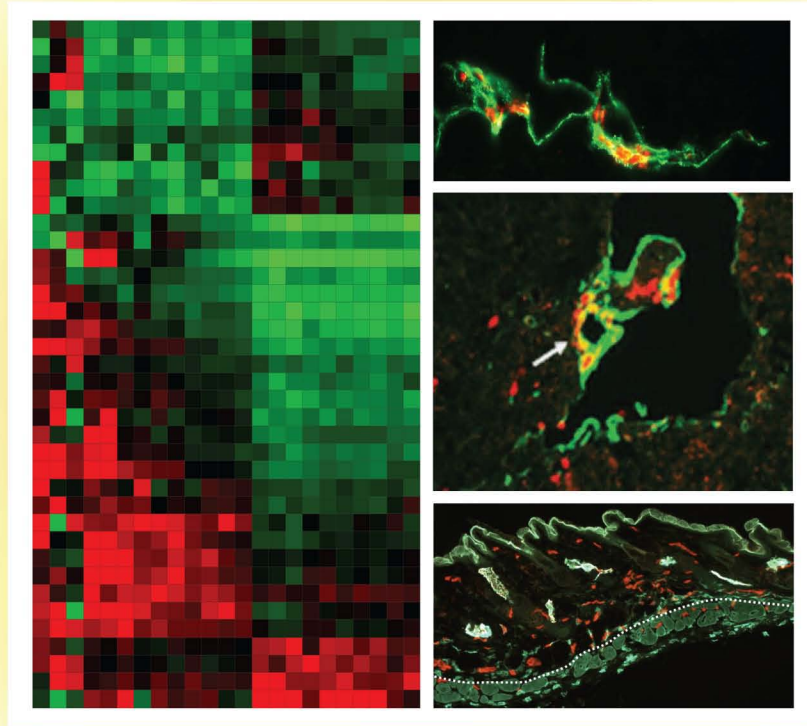DISS. ETH NO. 17752

MOLECULAR MECHANISMS CONTROLLING LYMPHATIC VASCULAR FUNCTION

A dissertation submitted to
ETH Zurich

for the degree of
Doctor of Sciences

presented by

JAE (JAY) WOO SHIN
April 4th, 1981

citizen of
United States of America

accepted on the recommendation of
Prof. Michael Detmar
Prof. Dario Neri

2008

TABLE OF CONTENTS

1 SUMMARY

1.1 <u>Summary</u>

In this thesis, I describe several novel molecular mechanisms controlling lymphatic vascular function during endothelial lineage-specific differentiation and lymphangiogenesis.

The essential functions of the lymphatic vascular system include the maintenance of tissue fluid homeostasis and immune surveillance. Impaired function of the lymphatic system can lead to several diseases such as primary or secondary lymphedema, whereas recent evidence indicates that tumor-induced activation of lymphatic vessels promotes cancer metastasis. In the past, the lack of lymphatic-specific molecular markers has hampered progress in the field of lymphatic vascular biology. However, during the last decade, several key lymphatic-specific markers have been discovered and have been shown to be important molecular regulators during embryonic development, normal fluid balance homeostasis, the afferent immune response, acute and chronic inflammation and cancer spread. In this thesis, I have investigated novel molecular mechanisms regulating lymphatic vascular function, based on the identification of novel lymphatic-specific markers by oligonucleotide microarrays of cultured lymphatic endothelial cells, and on the functional characterization of select lymphatic-specific markers *in vitro* and *in vivo*.

In order to investigate the role of the lymphatic system during embryogenesis, we have recently overexpressed the lymphatic-specific transcription factor Prox1 in cultured blood vascular endothelial cells (BEC), isolated from human foreskin. We found that ectopic overexpression of Prox1 recapitulates, at least in part, the embryonic lymphatic reprogramming of vascular endothelium by downregulating BEC-specific genes and by up-regulating several lymphatic endothelial cell (LEC)-specific genes. In this thesis, I present evidence demonstrating that Prox1 upregulates the expression of Fibroblast Growth Receptor-3 (FGFR-3) during lymphatic reprogramming and that FGF signaling through the upregulated FGFR-3 plays an important role in the early development of the lymphatic vascular system (Chapter 3; Section 1).

Furthermore, using transcriptional profiling by gene microarray technology, I have compared the gene expression profiles of cultured human blood vascular (BEC) and lymphatic (LEC) endothelial cells. These studies have revealed a set of 236 lymphatic signature genes and 342 blood vascular signature genes, many of which have not been previously known to be expressed in a lineage-specific manner. Based on the identification of these signature genes, I have established a Low-Density Microvascular Differentiation Array (LD-MDA), a novel tool to quantify the degree of endothelial lineage-specific differentiation of various endothelial cell types *in vitro* which has also allowed the identification of novel (lymph)angiogenesis factors involved in the chronic inflammatory skin disease psoriasis (Chapter 3; Section 2).

Based on the identification of lymphatic signature genes, I present evidence that an active form of dipeptidyl peptidase IV (DPPIV) is more strongly expressed in lymphatic endothelium as compared to blood vascular endothelium in several different human tissues. To investigate the functional role of DPPIV in LEC biology, I have performed cell proliferation, migration, tube formation and adhesion assays after siRNA-mediated knockdown of DPPIV. These studies have elucidated a dual function of DPPIV in lymphangiogenesis (Chapter 3; Section 3).

Previous studies have revealed that vascular endothelial growth factor-A (VEGF-A) and VEGF-C are upregulated in metastatic cancers, and that they are the major molecular mediators of tumor-induced lymphangiogenesis which promotes lymph node and distant cancer metastasis. Thus, the identification of downstream mediators of the effects of VEGF-A and/or VEGF-C may reveal novel targets for inhibiting lymphangiogenesis and cancer spread. In this thesis, I have performed a comprehensive gene expression profiling screen of LEC stimulated with VEGF-A or VEGF-C for different periods of time. These studies have revealed a number of novel mediators of lymphangiogenesis and, in particular, have identified endocan - also known as ESM1 - as a novel mediator of VEGF-A and of VEGF-C-induced lymphangiogenesis. I demonstrate that endocan significantly promotes LEC proliferation and migration in concert with VEGF-A and VEGF-C, and that silencing of endocan expression significantly attenuates the VEGF-A/VEGF-C induced LEC proliferation and migration *in vitro* and VEGF-A induced lymphatic vessel enlargement *in vivo* (Chapter 3; Section 4).

1.2 <u>Zusammenfassung</u>

In dieser Arbeit beschreibe ich mehrere neue molekulare Mechanismen, welche die Differenzierung lymphatischer Endothelzellen sowie die Lymphangiogenese kontrollieren.

Zu den essentiellen Funktionen des lymphatischen Systems gehören die Regulierung des Flüssigkeitsdrucks im Gewebe sowie die Immunüberwachung des Organismus. Eine Funktionsstörung des lymphatischen Systems kann zu einer Reihe von Krankheiten führen, zum Beispiel dem primären oder sekundären Lymphödem. Jüngste Studien weisen zudem darauf hin, dass die Krebsmetastasierung durch eine Tumor-induzierte Aktivierung lymphatischer Gefässe gefördert wird. Das Fehlen von spezifischen molekularen Markern für lymphatische Gefässe hat die Erforschung der Biologie des lymphatischen Systems lange Zeit behindert. Im vergangenen Jahrzehnt wurden jedoch mehrere entscheidende solcher Marker entdeckt, welche sich auch als wichtige molekulare Regulatoren erwiesen haben für die embryonale Entwicklung des lymphatischen Systems, die Regulierung des Gewebedrucks und die afferente Immunantwort, sowie für pathologische Situationen wie die akute und chronische Entzündung und die Ausbreitung von Krebs.

Basierend auf der Identifizierung neuer spezifischer lympatischer Marker mittels Oligonukleotid-Microarrays kultivierter lymphatischer Endothelzellen, sowie der funktionellen Charakterisierung ausgewählter solcher Marker *in vitro* und *in vivo*, habe ich in dieser Arbeit neue molekulare Mechanismen untersucht, welche lymphvaskuläre Funktionen regulieren.

Um die Rolle des lymphatischen Systems während der Embryogenese zu untersuchen, haben wir kürzlich den Lymphendothel-spezifischen Transkriptionsfaktor Prox1 in aus menschlicher Vorhaut isolierten, kultivierten Blutgefässendothelzellen überexprimiert. Es zeigte sich, dass die Überexpression von Prox1 zumindest teilweise die Umprogrammierung von Blutgefäss- zu Lymphendothelzellen während der embryonalen Entwicklung rekapituliert, indem sie die Expression Blutgefässendothel-spezifischer Gene verringert und die Expression mehrerer Lymphendothel-spezifischer Gene erhöht. Meine Arbeit liefert Hinweise darauf, dass Prox1 während der lymphatischen Umprogrammierung des Blutgefässendothels die

Expression von FGFR-3 verstärkt, und dass FGF-Signale, welche über diesen verstärkt exprimierten Rezeptor vermittelt werden, während der frühen Entwicklung des lymphatischen Systems eine wichtige Rolle spielen (Kapitel 3; Abschnitt 1).

Des weiteren habe ich die Genexpressionsprofile kultivierter humaner Blutgefäss- und Lymphendothelzellen mittels Microarray-Technologie verglichen. Diese Untersuchungen führten zu einem Satz von 236 lymphatischen Signatur-Genen und 342 Blutgefäss-Signatur-Genen, von denen viele noch nicht als spezifisch für den einen oder anderen Endothelzelltyp bekannt waren. Basierend auf der Identifizierung dieser Signatur-Gene habe ich sogenannte „Low Density Microvascular Differentiation Assays" (LD-MDA) entwickelt, mit deren Hilfe sich das Ausmass der lymphatischen oder blutgefässartigen Differenzierung verschiedenster Endothelzell-Typen *in vitro* quantifizieren lässt. Diese Assays haben auch die Identifizierung neuer (lymph)angiogener Faktoren ermöglicht, welche in der chronisch entzündlichen Hautkrankheit Schuppenflechte (Psoriasis) eine Rolle spielen (Kapitel 3; Abschnitt 2).

Ebenfalls basierend auf der Identifizierung lymphatischer Signatur-Gene zeige ich, dass eine aktive Form des Enzyms Dipeptidylpeptidase IV (DPPIV) stärker auf lymphatischem als auf Blutgefässendothel exprimiert wird. Um die funktionelle Bedeutung von DPPIV in lymphatischen Endothelzellen zu untersuchen, habe ich Zellproliferations-, Migrations-, Röhrenbildungs- und Adhäsions-Analysen nach Ausschaltung der DPPIV-Expression mittels siRNA durchgeführt. Diese Versuche haben eine Doppelfunktion von DPPIV in der Lymphangiogenese gezeigt (Kapitel 3; Abschnitt 3).

Aus früheren Studien ist bekannt, dass die Wachstumsfaktoren Vascular Endothelial Growth Factor-A (VEGF-A) und VEGF-C in metastatischen Krebsgeschwüren hochreguliert sind und dass sie die bedeutendsten molekularen Mediatoren der Tumor-induzierten Lymphangiogenese sind, welche ihrerseits Lymphknoten- und entfernte Metastasen begünstigt. Die Identifizierung molekularer Mediatoren der Effekte von VEGF-A und/oder VEGF-C könnte daher zu neuen Zielmolekülen für die Hemmung der Lymphangiogenese und damit der Krebsausbreitung führen. In dieser Arbeit habe ich eine umfassende Untersuchung der Genexpressionsprofile lymphatischer Endothelzellen, welche während unterschiedlicher Zeiträume mit

VEGF-A oder VEGF-C stimuliert wurden, durchgeführt. Diese Studien haben eine Reihe neuer Mediatoren der Lymphangiogenese ergeben, insbesondere habe ich Endocan – auch bekannt als ESM1 – als neuen Mediator der durch VEGF-A und durch VEGF-C induzierten Lymphangiogenese identifiziert. Ich zeige, dass Endocan im Zusammenspiel mit VEGF-A und VEGF-C die Proliferation und Migration lymphatischer Endothelzellen signifikant fördert, und dass Ausschaltung der Expression von Endocan die durch VEGF-A/C induzierte Proliferation und Migration lymphatischer Endothelzellen *in vitro* sowie die durch VEGF-A induzierte Vergrösserung lymphatischer Gefässe *in vivo* signifikant abschwächt (Kapitel 3; Abschnitt 4).

2 INTRODUCTION

2.1 <u>CHARACTERISTICS OF THE LYMPHATIC VASCULATURE</u>

2.1.1 Anatomy and physiology of the lymphatic vasculature

The lymphatic system is composed of a vascular network of thin-walled lymphatic capillaries and thick-walled collecting lymphatic vessels. Unlike blood vessel capillaries, the lymphatic capillaries consist of a single-cell layer of overlapping, flat endothelial cells and are blind-ended structures lacking pericytes, smooth muscle cells and a basement membrane. Endothelial cells in lymphatic capillaries form loose intercellular valve-like junctions and exhibit large interendothelial pores. Anchoring filaments consisting of microfibrils and elastin connect the lymphatic endothelial cells to the extracellular matrix. One of the main functions of the lymphatic vasculature is the maintenance of fluid homeostasis by absorbing interstitial fluid, or lymph. Macromolecules and cells, including extravasated leukocytes, leaked from blood capillaries, as well as activated antigen-presenting cells are taken up by lymphatic capillaries. From here, lymph is transported towards collecting lymphatic vessels (Oliver & Detmar, 2002).

The collecting lymphatic vessels have a smooth muscle cell layer, basement membrane and valves to prevent back flow. The contraction of smooth muscle cells and surrounding skeletal muscles, as well as arterial pulsations, contribute to lymph propulsion (Leu et al, 1999; Petrova et al, 2004). These larger vessels drain into either one of two collecting vessels. The main, longer trunk is the thoracic duct, which runs parallel with the aorta. The thoracic duct empties lymph into the blood stream at the junction of the left subclavian vein with the left internal jugular vein located at the base of the neck. Another, shorter collecting trunk is the right lymphatic duct, which empties its lymph into the right subclavian vein (Ambrose, 2006; Hong et al, 2004c) (**Fig. 2.1.1**).
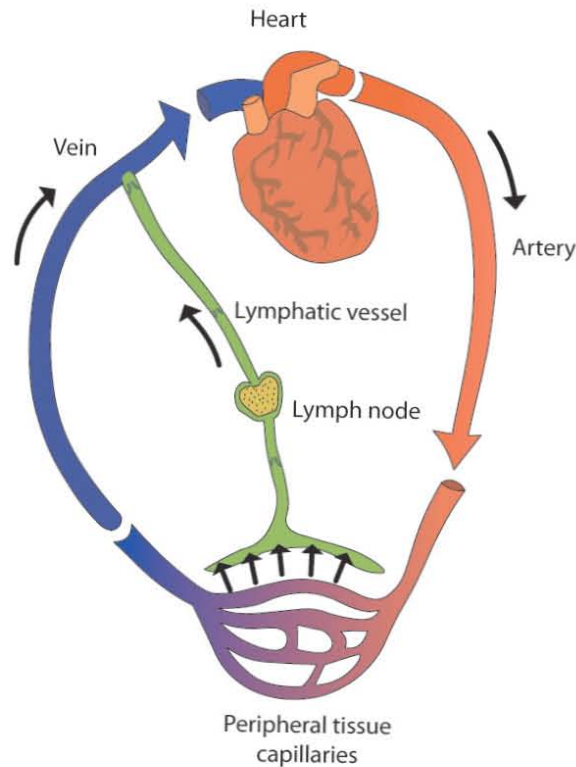
Figure 2.1.1 Schematic illustration of the blood vascular and lymphatic system. *The blood vascular system is a circular and closed system, whereas the lymphatic system is open-ended and linear. Fluids, macromolecules, and cells extravasated from blood capillaries flow into lymphatic capillaries in peripheral tissues and are then transported by means of the larger collecting lymphatic vessels and the thoracic duct back to the blood vascular system for recirculation (Hong et al, 2004c).*

Another important function of the lymphatic system is immune surveillance (Massberg et al, 2007). The lymphatic system includes lymphoid organs such as the lymph nodes, tonsils, Peyer's patches, spleen, and thymus, all of which play an important role in the immune response (Heydtmann et al, 2006; Millington et al, 2007). Lymph, which contains memory T cells, antigens, antigen-bearing dendritic cells and macrophages, is normally filtered through the lymph nodes through collecting-type terminal afferent lymphatics in local peripheral tissues (e.g. skin). It then percolates through the lymphoid tissue and a series of sinuses, and exits the node in the efferent lymphatics (Daynes et al, 1985). The cellular component of the lymph node includes T-cell-dependent paracortical areas, in which naïve T cells from neighboring venules are brought into contact with antigen-presenting dendritic cells (Cavanagh & Von Andrian, 2002). B cells are mainly associated with the germinal follicles in the outer cortex, where naïve B cells acquire the capacity to synthesize epitope-specific antibodies (Randolph et al, 2005). Lymphatic vessels are not

normally present in avascular structures such as the epidermis, hair, nails, cartilage, and cornea, nor are they present in some vascularized organs such as brain and retina (Niederkorn et al, 1989; Oliver & Detmar, 2002).

2.1.2 Genes and mechanisms in lymphatic development

The earliest description of the lymphatic system dates back to the 5th century B.C. Hippocrates' work entitled <u>On Joints</u> stated that "all men have glands, smaller or larger, in the armpit and many other parts of the body" describing the lymph nodes (Withington, 1894). However, the understanding of the lymphatic system only started to augment in the 17th century when Gasparo Aselli (1581 – 1626), a physician in Milan and later Professor of Anatomy in Pavia, observed the lacteals – lymphatic vessels in the intestine - while dissecting a living, well-fed dog, something he had never seen in fasting dogs (Gasparo, 1627). Originally described as "milky veins", the mechanisms controlling the normal development of lymphatic vessels and the molecular regulation of their biological function have remained unclear until the early 20th century. Florence Sabin proposed in 1902 that, in vertebrates, the endothelial cells bud off from the veins during early embryonic development and form primitive lymph sacs. The peripheral lymphatic system then originates from these primary lymph sacs by endothelial sprouting into the surrounding tissues and organs, where local capillaries are formed (Sabin, 1902). A few years after Sabin's "centrifugal" proposal, Hungtington and McClure proposed that the first lymphatics arise independently in the mesenchyme and that they are connected to the venous system only later (Huntington & McClure, 1910). The controversy over the origin of lymphatic vasculature was not resolved until recently. Wigle and Oliver studied mice deficient in the homeodomain protein Prox1 and found that these mice were unable to develop a lymphatic vascular system and that Prox1 was required for a subset of venous endothelial cells in the embryonic cardinal veins to migrate out and to form the initial lymphatic vessels during early embryogenesis (Wigle et al, 2002a). These studies also identified some of the molecular determinants that control the step-wise process of lymphatic competence, commitment, differentiation and maturation (Oliver & Harvey, 2002) as described in the following section:

2.1.2.1 *Endothelial lineage-specific differentiation*

During embryogenesis, an unknown molecular factor(s) regulates the initial stage of lymphatic competence by inducing the lymphatic vessel endothelial hyaluronan receptor 1 (Lyve1) (Banerji et al, 1999) on a few of the endothelial cells that line the anterior cardinal vein of mice at embryonic day (E) 8.5-9.5. This could be considered the first morphologic indication that venous endothelial cells are already competent to respond to a lymphatic-inducing signal (Oliver, 2004). A few hours following the expression of Lyve1 by venous endothelial cells in mice, expression of the transcription factor Prox1 is observed in a subpopulation of venous endothelial cells in a polarized manner. Subsequently, these lymphatic endothelial cell progenitors bud off, proliferate and migrate to form the embryonic lymph sacs and lymphatic vascular network. These cells also express the receptor tyrosine kinase vascular endothelial growth factor receptor-3 (VEGFR-3 or FLT4), the cell surface receptor that binds the lymphangiogenic growth factors, VEGF-C and VEGF-D (Makinen et al, 2005). By E14.5 – 15.5, the primary jugular lymph sacs subsequently sprout to form a primitive lymphatic plexus, which spreads throughout the head and neck, thorax and forelimbs (Oliver & Harvey, 2002). Further maturation and differentiation of the lymphatic vasculature occurs in a progressive manner until the first postnatal days (**Fig. 2.1.2**) (Karpanen et al, 2006; Oliver, 2004; Saharinen et al, 2004).
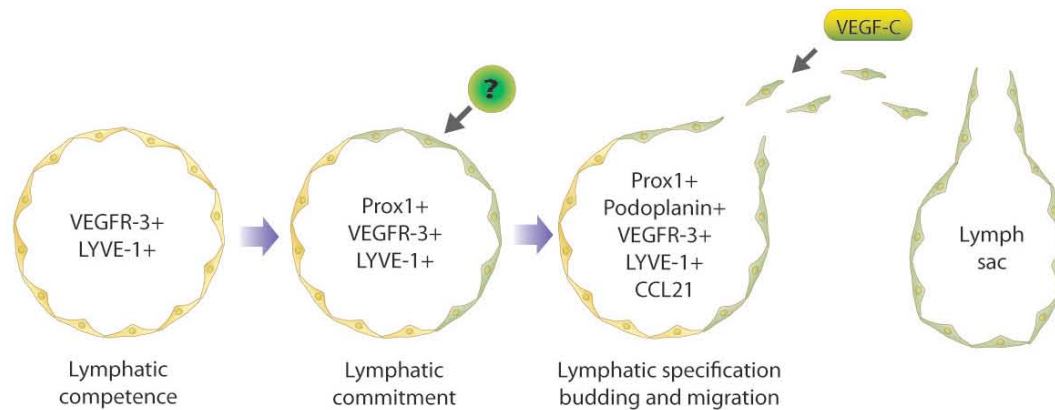
Figure 2.1.2 Current model of the stepwise embryonic development of the mammalian lymphatic system. *At mouse embryonic day (E) 8.5, all endothelial cells of the cardinal vein express the lymphatic markers LYVE-1 and vascular endothelial growth factor recpetor-3 (VEGFR-3) and display lymphatic competency. Upon stimulation by a yet unidentified inductive signal, a subset of venous endothelial cells becomes lymphatically biased and up-regulates Prox1 around E10.5. At E11.5 and thereafter, these Prox1-positive cells bud off and migrate out to form initial lymphatics. They also up-regulate the expression of additional lymphatic-specific molecules such as podoplanin and secondary lymphoid chemokines (SLC). The formation of a mature lymphatic network continues through the first postnatal days.*

In the following section, a detailed description of genes and mechanisms that have been identified as mediators for lymphatic endothelial lineage-specific differentiation is outlines:

2.1.2.1.1 Prox1

Prox1 is a homeodomain protein that was originally isolated due to its high homology to the *Drosophila* protein prospero (Oliver et al, 1993a; Tomarev et al, 1996). Prox1 is an important regulator of cell differentiation and embryogenesis in several tissues such as developing liver, nervous system, pancreas, lens, retina, heart and lymphatic vessels (Oliver et al, 1993a; Sosa-Pineda et al, 2000; Wigle et al, 2002a). Thus far, Prox1 proteins have been identified in human, mouse, chicken, newt, frog, and zebrafish; and their amino acid sequences are highly conserved across these species (Oliver et al, 1993a; Tomarev et al, 1996). In mice, Prox1 expressing endothelial cells are first observed at E10.5 in the jugular vein, from which they migrate to form the first lymphatic sprouts. Endothelial cells of Prox1$^{-/-}$ mice bud from the cardinal vein but fail to express lymphatic endothelial markers and do not migrate further (Wigle et al, 2002a). These findings suggested that Prox1 might specify lymphatic cell fate by

directly reprogramming the transcriptome of embryonic venous endothelial cells. Indeed, Prox1 overexpression in human blood vascular endothelial cells (BEC) suppresses many blood vascular-specific genes and upregulates lymphatic endothelial cell (LEC)-specific transcripts (Hong et al, 2002; Petrova et al, 2002a). Prox1 is also shown to be upregulated in cultured BEC when infected with Kaposi's sarcoma-associated herpes virus (KSHV, also known as HHV-8). This KSHV-mediated upregulation of Prox1 leads to reprogramming of BEC to adopt LEC phenotypes by inducing the expression of more than 70% of major lymphatic-associated genes and by downregulating many BEC-specific genes (Hong et al, 2004a). This Prox1 mediated cell fate reprogramming in KSHV-infected cells provides an additional support to the concept that Prox1 is a master control gene specifying lymphatic endothelial cell fates. Furthermore, Prox1$^{+/-}$ mice develop chylous ascites, and show disorganized and abnormally patterned lymphatic vessels (Harvey et al, 2005). Notably, impaired lymphatic vascular function in Prox1 heterozygotes and in mice with conditional deletion of Prox1 in endothelial cells causes adult onset obesity, indicating an important link between lymphatic function and adipogenesis. So far, treatment of cultured endothelial cells with interleukin-3 and -7 was shown to induce the expression of Prox1; however, the relevance for the *in vivo* regulation of Prox1 expression remains unclear (Al-Rawi et al, 2005; Groger et al, 2004).

2.1.2.1.2 VEGFR-3

VEGFR-3, also known as FLT4, is a member of the fms-like tyrosine kinase family and is structurally related to the two VEGF-A receptors VEGFR-1/FLT1 and VEGFR-2/KDR/FLK1 (Kaipainen et al, 1995; Kaipainen et al, 1993). VEGFR-3 was the first gene to be identified as lymphatic vessel-specific (Kaipainen et al, 1995). VEGFR-3 does not interact with VEGF-A but acts as a signaling receptor for VEGF-C and VEGF-D – the two most potent lymphangiogenic factors known so far. VEGFR-3 deletion in mice leads to defects in blood vessel remodeling and embryonic death at mid-gestation, indicating an early blood vascular function (Dumont et al, 1998). During embryonic development, VEGFR-3 is expressed by venous endothelial cells and also by angioblasts of the head mesenchyme during E8.5 to E12.5 (Kaipainen et al, 1995). Only later in embryogenesis, VEGFR-3 expression becomes

specific for the lymphatic endothelial cells and is gradually down-regulated by venous endothelial cells. VEGFR-3 is known to be specific for lymphatic vessels in adult tissues, however, some tumor-associated and wound-associated blood vessels re-express VEGFR-3 (Hirakawa et al, 2007; Kubo et al, 2000)

2.1.2.1.3 **VEGF-C/D**

VEGF-C and VEGF-D were originally cloned as ligands for VEGFR-3 (Achen et al, 1998; Joukov et al, 1996; Marconcini et al, 1999; Orlandini et al, 1996; Yamada et al, 1997). VEGF-C is expressed by a multitude of cell types, including mesenchymal cells around embryonic veins, activated macrophages, skeletal muscle cells, and smooth muscle cells surrounding large arteries (Eichmann et al, 1998; Joukov et al, 1996; Karkkainen et al, 2004; Kukk et al, 1996). Both VEGF-C and VEGF-D are produced as precursor proteins with N- and C-terminal propeptides flanking the VEGF homology domain (Joukov et al, 1997; Stacker et al, 1999). The secreted factors undergo proteolytic processing that results in increased affinity for both VEGFR-2 and VEGFR-3, and consequently increases their ability to induce angiogenesis (Cao et al, 1998) and lymphangiogenesis *in vivo* (Enholm et al, 2001; Karkkainen et al, 2004; Saaristo et al, 2002). Activation of VEGFR-3 by VEGF-C and/or VEGF-D promotes proliferation, migration, and survival of cultured human LEC (Makinen et al, 2001) and they can also induce lymphangiogenesis in adult tissues (Jeltsch et al, 1997; Veikkola et al, 2001).

The recent inactivation of the Vegf-c gene in mice has provided additional information regarding its role during embryonic lymphangiogenesis (Karkkainen et al, 2004). The mutant embryos showed that Vegf-c activity is essential during the lymphatic development since its functional inactivation results in embryonic lethality. Further analysis demonstrated that Vegf-c activity is essential for promoting the budding and proliferation of Prox1-expressing lymphatic endothelial cells located in the embryonic veins. This suggests that Vegf-c is an essential chemotactic and survival factor during embryonic lymphangiogenesis (Karkkainen et al, 2004). Contrarily, Vegf-d-deficient mice do not exhibit a lymphatic phenotype probably because Vegf-d is not expressed at the critical sites of lymph sac formation in the

embryo (Avantaggiato et al, 1998; Karkkainen et al, 2004). However, exogenous VEGF-D protein rescues the impaired vessel sprouting in Vegfc$^{-/-}$ embryos (Karkkainen et al, 2004).

2.1.2.1.4 LYVE-1

LYVE-1 has been identified as a lymphatic endothelium-specific hyaluronan (HA) receptor. HA is a large mucopolysaccharide polymer (10^{5-7} Daltons) that represents a major component of the extracellular matrix in many tissues (Jackson et al, 2001). LYVE-1 is one of the most widely used markers for lymphatic endothelial cells (Jackson, 2004) and in mice, it is the first marker of lymphatic endothelial commitment (Oliver, 2004). In adults, LYVE-1 expression is downregulated in the collecting lymphatic vessels but remains high in lymphatic capillaries (Makinen et al, 2005). However, Lyve-1-deficient mice appear normal and no obvious lymphatic vascular malfunctions or morphological abnormalities have been detected thus far (Gale et al, 2007).

2.1.2.1.5 Syk and SLP76

The tyrosine kinase Syk and the adaptor protein SLP-76 are involved in controlling the separation of the lymphatic and blood vascular systems during embryogenesis. Recent studies indicate that Syk- and SLP-76-mediated hematopoietic signaling might be required to separate emerging lymphatic vessels from the blood vascular system (Abtahian et al, 2003). Syk is widely expressed in hematopoietic cells and is involved in coupling activated immunoreceptors to downstream signaling events that mediate diverse cellular responses, including proliferation, differentiation, and phagocytosis (Yanagi et al, 2001). The adapter protein SLP-76 (also known as lymphocyte cytosolic protein 2, LCP2) is a substrate of Syk for downstream signaling (Clements, 2003). Syk- or Slp-76-deficient mice that survived to adulthood display arterial-venous-lymphatic shunting and, as a result, exhibit cardiomegaly, elevated cardiac output, and admixture of blood with lymph, suggesting that hematopoietic cells might be involved in the separation of the two vascular systems. Additionally, the lymph-

vascular phenotype of Slp-76-deficient mice was ameliorated when Slp-76 null bone marrow cells were introduced into lethally irradiated wild-type mice (Abtahian et al, 2003). These findings suggest the possibility that hematopoietic precursor cells might influence the development of the lymphatic system. More recent study indicate that deletion of Spred-1 and Spred-2 resulted in embryonic lethality at E12.5 to 15.5 with marked subcutaneous hemorrhage, edema, and dilated lymphatic vessels filled with erythrocytes (Taniguchi et al, 2007), resembling that of Syk^{-/-} and SLP-76^{-/-} mice with defects in the separation of lymphatic vessels from blood vessels.

Table 2.1-1 Genes that mediate lymphatic vasculature formation and patterning

Gene	Model	Phenotype	References
Adhesion molecules			
Integrin α9	KO	Respiratory failure caused by pleural fluid (chylothorax), lymphedema	(Huang *et al.*, 2000)
Growth factors/receptors			
Angiopoietin-1	TG	Hyperplastic lymphatic vessels	(Tammela *et al.*, 2005)
Angiopoietin-2	KO	Hypoplasia, chylous ascites	(Gale *et al.*, 2002)
VEGF-C	KO	No lymphatic vessels (-/-), hypoplasia, chylous ascites, lymphedema (+/-)	(Karkkainen *et al.*, 2004)
VEGF-C	TG	Hyperplastic lymphatic vessels	(Jeltsch *et al.*, 1997)
VEGFR-3	KO	Hyperplastic lymphatic vessels; cardiovascular failure	(Dumont *et al.*, 1998)
VEGFR-3	Chy mice	Lymphedema	(Karkkainen *et al.*, 2001)
Neuropilin-2	KO	Lymphedema, reduction of small lymphatic vessels during development	(Yuan *et al.*, 2002)
HGF	TG	Enhanced formation and enlargment of lymphatic vessels	(Kajiya *et al.*, 2005)
Transcription factors			
Prox1	KO	No lymphatic vasculature developed (-/-), adult-onset obesity, chylous ascites (+/-)	(Wigle and Oliver 1999; Harvey *et al.*, 2005)
FOXC2	KO	Abnormal lymphatic patterning, absent valves, lymphatic dysfunction (-/-), lymphatic vessel and lymph node hyperplasia (+/-)	(Kriederman *et al.*, 2003; Petrova *et al.*, 2004)
Net (Elk3)	KO	Chylothorax, dilated lymphatic vessels	(Ayadi *et al.,* 2001)
SOX18 (ragged)	KO	Generalized edema and chyle in the peritoneum	(Pennisi *et al.*, 2000)
Miscellaneous			
Podoplanin	KO	Lymphedema, dilation of lymphatic vessels and diminished lymphatic transport	(Schacht *et al.*, 2003)
SLP-79 and Syk	KO	Abnormal blood-lymphatic connections	(Abtahian *et al.*, 2003)
Ephrin B2	Mutant	Defective remodeling of lymphatic vascular network, hyperplasia, lack of valves, chylothorax	(Makinen *et al.*, 2005)
Adrenomodullin	KO	Intestitial lymphedema, abnormal lymphatic patterning	(Fritz-Six *et al.*, 2008)
FIAF	KO	Dialated intestinal lymphatic vessels	(Backhed *et al.*, 2007)

FOXC2, forkhead box C2; HGF, hepatocyte growth factor; KO, knock-out; SLP, Src homology 2-domain containing leukocyte protein; SOX18, sex determining region Y-related high mobility group box 18; TG, transgenic; VEGF, vascular endothelial growth factor; VEGFR, vascular endothelial growth factor receptor; FIAF, fasting-induced adipose factor.

2.1.2.2 *Major molecular markers of lymphatic endothelium*

Major advances in lymphatic research have been made possible by the recent establishment of defined cultures of blood vascular endothelial cells (BECs) and lymphatic endothelial cells (LECs) isolated from human skin (Hirakawa et al, 2003; Kriehuber et al, 2001; Makinen et al, 2001; Podgrabinska et al, 2002). Comparative microarray analyses of their specific transcriptomes revealed that approximately 2% of transcribed genes are differentially expressed between BECs and LECs, and this difference may reflect their distinct *in vivo* functions (Hirakawa et al, 2003; Petrova et al, 2002a). However, the arrays used in these analyses included an incomplete set of human genes and a large-scale confirmation of the results by other methods has not been attempted. Very recently, surface-accessible proteins of BECs and LECs were biotinylated, purified by high performance liquid chromatography (HPLC) and analyzed by mass spectrometry (Roesli et al, 2008). This technology has provided the first insight into the surface-accessible, vascular lineage-specific proteome.

The following sections describe well-characterized lymphatic vessel markers and their role in lymphangiogenesis:

2.1.2.2.1 <u>Podoplanin</u>

Podoplanin is a mucin-type transmembrane glycoprotein that is highly expressed by podocytes, keratinocytes, cells of the choroid plexus, alveolar type II lung cells, lymphatic endothelial cells, but not by blood vascular endothelial cells (Hirakawa et al, 2003; Kriehuber et al, 2001; Petrova et al, 2002a; Schacht et al, 2003; Wetterwald et al, 1996). During mouse embryonic development, podoplanin is expressed at around E9 in the central nervous system and the foregut but not yet in the vascular system (Rishi et al, 1995; Schacht et al, 2003). At E11.5-E12.5, podoplanin is expressed by all endothelial cells in the cardinal vein, including the budding Prox1 positive cells, but the expression is progressively down-regulated by venous endothelial cells. At birth, the expression of podoplanin is restricted to LEC (Schacht et al, 2003). Podoplanin deficiency leads to abnormal lung development and perinatal

lethality. Neonatal podoplanin knockout mice displayed abnormal lymphatic function and patterning, mimicking lymphedema, possibly due to impaired migration and adhesion of lymphatic endothelial cells (Schacht et al, 2003).

2.1.2.2.2 <u>FOXC2</u>

The forkhead transcription factor FOXC2 is involved in the specification of the lymphatic capillary versus collecting lymphatic vessel phenotype. FOXC2 is highly expressed in the developing lymphatic vessels as well as in lymphatic valves in adults (Petrova et al, 2004). FOXC2 is essential for the morphogenesis of lymphatic valves and the establishment of a pericyte-free lymphatic capillary network. Mice heterozygous for Foxc2 exhibited a generalized lymphatic vessel and lymph node hyperplasia and rarely exhibited hindlimb swelling, mimicking closely the distinctive lymphatic and ocular phenotype of lymphedema-distichiasis (LD) patients (Kriederman et al, 2003; Yuan et al, 2002).

2.1.2.2.3 <u>Neuropilin2</u>

Neuropilin-1 (Nrp1) and neuropilin-2 (Nrp2) are transmembrane glycoproteins with large extracellular domains that interact with both class 3 semaphorins and VEGFs. While Nrp1 is predominantly expressed in arterial endothelial cells, Nrp2 is mainly expressed in veins and in visceral lymphatic vessels and weakly expressed in the cutaneous lymphatics (Karkkainen et al, 2001). Homozygous Nrp2 mutants show absence or severe reduction of small lymphatic vessels and capillaries during development. Arteries, veins and larger collecting lymphatic vessels developed normally in these mice, suggesting that Nrp2 is selectively required for the formation of small lymphatic vessels and capillaries (Yuan et al, 2002).

2.1.2.2.4 <u>CCL21</u>

CCL21 (CC chemokine ligand 21), also known as secondary lymphoid chemokine (SLC), plays an important role in immunoregulatory and inflammatory processes.

CCL21 is expressed by lymphatic endothelium and is secreted as a 12 KDa protein but it is immobilized by the extracellular matrix (ECM) by binding to sulfated proteoglycans (Patel et al, 2001). It is also expressed in the high endothelial venules and the T cell areas of lymph nodes and Peyer's patches. CCL21 promotes adhesion and stimulates migration of thymocytes, T-lymphocytes, macrophages, and neutrophils through high-affinity binding to chemokine receptor 7 (CCR7) (Gunn et al, 1998; Tangemann et al, 1998). Increased incidence of lymph node metastases has been correlated with the presence of CCR7 on human carcinoma cells (Cabioglu et al, 2005; Gunther et al, 2005; Heresi et al, 2005; Wiley et al, 2001), possibly sensing chemotactic gradients of CCL21 originating from lymphatics (Shields et al, 2007).

2.1.2.2.5 Adrenomedullin

Adrenomedullin (AM) is a multifunctional peptide vasodilator that tranduces its effects through the calcitonin receptor-like receptor (calcrl) when the receptor is associated with a receptor activity-modifying protein (RAMP2) (McLatchie et al, 1998). AM-activated ERK signaling was reported to be greater in human LEC as compared to human BEC and loss of AM signaling resulted in abnormal jugular lymphatic vessels due to reduction in lymphatic endothelial cell proliferation. Additionally, AM-null mice developed intestinal lymphedema and died during mid-gestation (Fritz-Six et al, 2008).

2.1.2.2.6 FIAF/ANGPTL-4

Fasting-induced adipose factor (Fiaf), also known as angiopoietin-like protein 4 (Angptl4), is a glycosylated, secreted, and proteolytically processed protein (Kersten et al, 2000; Kim et al, 2000). Fiaf has been reported to promote endothelial cell survival in the gut after damage from ionizing radiation and reduces VEGF-induced microvascular permeability in the skin (Crawford & Gordon, 2005). Recently, Prox1 has been identified as a downstream target for Fiaf signaling in the intestinal lymphatic endothelium, and Fiaf-deficient mice die during the suckling period with dilated intestinal lymphatic vessels. Fiaf also has been identified as an organ-specific mediator of lymphangiogenesis that is instrumental in sustaining separate blood and

lymphatic circulatory systems in the intestine, and in its supporting mesentery after birth (Backhed et al, 2007).

Table 2.1-2 Specific markers for lymphatic vessels versus blood vessels

Markers	Function	LV	BV	Reference
Prox1	Transcription factor	++	-	(Wigle and Oliver, 1999)
Podoplanin	Transmembrane glycoprotein	++	-	(Wetterwald *et al.*, 1996; Breiteneder-Geleff *et al.*, 1999)
LYVE-1	Hyaluronan receptor	++	-	(Banerji *et al.*, 1999)
VEGFR-3	Growth factor receptor	+	-/(+)[1]	(Kaipainen *et al.*, 1995)
Neuropilin-2	Semaphorin and growth factor receptor	+	-/(+)[2]	(Yuan *et al.*, 2002)
Macrophage mannose receptor 1	L-selectin receptor	+	-	(Irjala *et al.*, 2001)
CCL21	CC-chemokine	+	-	(Gunn *et al.*, 1998)
Desmoplakin	Anchoring protein of adhering junctions	+	-	(Ebata *et al.*, 2001)
Integrin α9	Adhesion molecule, subunit of osteopontin and tenascin receptor, VEGFR-3 coreceptor?	+	-	(Huang *et al.*, 2000; Petrova *et al.*, 2002)
CD44	Hyaluronan receptor	-	+	(Kriehuber *et al.*, 2001)
VEGF-C	Growth factor	-	+	(Kriehuber *et al.*, 2001; Hirakawa *et al.*, 2003)
VEGFR-1	Growth factor receptor	-	+	(Hirakawa *et al.*, 2003)
Neuropilin-1	Semaphorin and growth factor receptor	-	+	(Hong *et al.*, 2002; Petrova *et al.*, 2002)
Endoglin/CD105	Low-affinity receptor for TGF-b	-	++	(Hirakawa *et al.*, 2003)
CD34	L-selectin receptor	-/(+)[3]	++	(Young *et al.*, 1995)
IL-8	CXC-chemokine	-	+	(Petrova *et al.*, 2002)
N-cadherin	Adhesion molecule	-	+	(Petrova *et al.*, 2002; Hirakawa *et al.*, 2003)
ICAM-1/CD54	Adhesion molecule	-	+	(Erhard *et al.*, 1996)
Integrin α5	Adhesion molecule, subunit of fibronectin receptor	-	+	(Petrova *et al.*, 2002; Hirakawa *et al.*, 2003)
Collagen IV	Extracellular matrix protein	-/(+)[4]	++	(Hirakawa *et al.*, 2003)
Versican	Chondroitin sulfate proteoglycan	-	+	(Petrova *et al.*, 2002; Hirakawa *et al.*, 2003)
Laminin	Basement membrane molecule	-/(+)[4]	++	(Barsky *et al.*, 2003; Petrova *et al.*, 2002)
Collagen XVIII	Basement membrane molecule	-/(+)[4]	++	(Petrova *et al.*, 2002; Hirakawa *et al.*, 2003)
PAL-E	Caveolae-associated glycoprotein?	-	++	(Schlingemann *et al.*, 1985; Niemela *et al.*, 2005)

BV, blood vessel; CCL, CC chemokine ligand; LV, lymphatic vessel; LYVE-1, lymphatic vascular endothelial hyaluronan receptor-1;PAL-E, pathologische anatomie leiden-endothelium; VEGF, vascular endothelial growth factor; VEGFR, vascular endothelial growth factor receptor.

[1] VEGFR-3 expression was also found on some blood capillaries during tumor neovascularization and in wound granulation tissue (Valtola et al., 1999; Paavonen et al., 2000).

[2] Neuropilin-2 is also expressed in veins (Yuan et al., 2002).

[3] CD34 expression has also been found on lymphatic endothelial cells (Sauter et al., 1998; Kriehuber et al., 2001).

[4] Peripheral lymphatic vessels sometimes have an incomplete basement membrane, large collecting vessels have a complete one.

2.1.2.3 *Key lymphangiogenic growth factors*

2.1.2.3.1 <u>VEGF-A</u>

Vascular endothelial growth factor A (VEGF-A) is an important signaling protein involved in both **vasculogenesis -** the *de novo* formation of the embryonic circulatory system - and **angiogenesis** - the growth of blood vessels from pre-existing vasculature. VEGF-A activity has been mostly studied in cells of the vascular endothelium, although it also exerts effects on a number of other cell types such as monocytes/macrophages and neurons (Liu et al, 2007). *In vitro*, VEGF-A has been shown to prevent cell apoptosis and to stimulate endothelial cell proliferation, migration, sprouting and tube formation (Ferrara et al, 2003). *In vivo*, the pro-survival effects of VEGF are developmentally regulated. VEGF inhibition results in extensive apoptotic changes in the vasculature of neonatal but not adult mice (Gerber et al, 1999). VEGF-A is also a vasodilator and increases microvascular permeability and, thus, was originally identified as vascular permeability factor (Senger et al, 1983).

VEGF-A binds to VEGFR-1 (FLT1) and VEGFR-2 (FLK1) as well as to the non-kinase receptors neuropilin-1 (NRP1) and NRP2 (Neufeld et al, 1999; Neufeld et al, 1994). Besides its prominent activity on endothelial cells, VEGF-A also induces hematopoietic stem cell mobilization from the bone marrow, monocyte chemoattraction, osteoblast-mediated bone formation and neuronal protection, since these cell types express VEGF receptors (Ferrara et al, 2003; Storkebaum et al, 2004). Moreover, VEGF-A stimulates the recruitment of inflammatory cells such as macrophages and leads to the expression of proteases implicated in pericellular matrix degradation during angiogenesis (Mandriota et al, 1995; Unemori et al, 1992). VEGF-A expression is strongly induced by hypoxia inducible factor (HIF) under hypoxic conditions as well as by many cytokines including platelet-derived growth factor (PDGF), epidermal growth factor (EGF), basic fibroblast growth factors (FGF-2) and transforming growth factors-α (TGFA) (Cao et al, 2002; Detmar et al, 1994; Dvorak et al, 1995; Ferrara, 2004; Pugh & Ratcliffe, 2003; Wu et al, 2000).

The human VEGF-A gene is organized into eight exons (Houck et al, 1991; Tischer et al, 1991). At least nine VEGF-A isoforms of variable amino acid number are produced through alternative splicing: VEGF121, VEGF145, VEGF148, VEGF162, VEGF165, VEGF165b, VEGF183, VEGF189 and VEGF206 (Bates & Harper, 2002; Lange et al, 2003). VEGF121, VEGF165 and VEGF189 are the major forms secreted

by most cell types (Robinson & Stringer, 2001). Among the most commonly observed isoforms, VEGF121 does not bind to heparin and diffuses relatively freely in tissues. In contrast, VEGF189 is sequestered in the extracellular matrix. Enzymatic processing of VEGF189 generates an active form (VEGF110) which lacks the heparin-binding domain (Plouet et al, 1997). This leaves VEGF165 as the most widespread and abundantly expressed splice variant that interacts with heparin sulfate proteoglycans (HSPGs) and neuropilins in a biologically active form. Isoform-specific VEGF-A knockout mice revealed different biological functions of VEGF-A isoforms. Notably, retinal vascular development was normal in mice exclusively expressing the VEGF164 isoform (VEGF$^{164/164}$), indicating that this isoform contains all necessary information for normal outgrowth and remodeling of blood vessels. In contrast, VEGF$^{120/120}$ mice exhibited severe vascular defects, with impaired venous and severely defective arterial vascular development in the retina. VEGF$^{188/188}$ mice had normal venous development, but aborted arterial outgrowth (Carmeliet et al, 1999; Stalmans et al, 2002). Transgenic mice overexpressing VEGF$_{164}$ under the K14 promoter showed a psoriatic phenotype with distinctive vascular changes, epidermal alterations, and inflammatory infiltrates closely resembling human psoriasis (Xia et al, 2003). Mice with a targeted deletion of VEGF in the skin exhibit delayed wound healing and less frequent development of chemically induced papillomas (Rossiter et al, 2004).

2.1.2.3.2 <u>VEGFR-2</u>

VEGFR-2, also known as KDR or FLK1, is a receptor for VEGF-A, VEGF-C and VEGF-D (only in human), and is expressed by both blood vascular and lymphatic endothelium (Hirakawa et al, 2003; Hong et al, 2004b; Kriehuber et al, 2001). The role of VEGFR-2 in angiogenesis has been thoroughly examined, however, the function of VEGF-A signaling through VEGFR-2 in lymphangiogenesis still needs to be further elucidated. Cell proliferation assays demonstrated that VEGF-A potently induced proliferation of lymphatic endothelial cells *in vitro* (Hirakawa et al, 2005b). Additionally, injection of adenoviral murine VEGF-A164 demonstrated pronounced and recurrent *in vivo* lymphangiogenesis in mouse ears (Nagy et al, 2002). Conversely, adenovirus expressing the human VEGF-A165 isoform did not show

distinct lymphangiogenic activity in mouse models (Byzova et al, 2002; Enholm et al, 2001). A likely explanation for this different phenotype may be due to species-specific effects of VEGF-A or due to the tissue-specific lymphangiogenic potency of VEGF-A. Furthermore, Hong *et al.* and Kunstfeld *et al.* have recently revealed that skin-specific overexpression of murine VEGF-A164 resulted in enhanced lymphangiogenesis during tissue repair and in skin inflammation, respectively (Hong et al, 2004b; Kunstfeld et al, 2004). In addition, Hong *et al.* further demonstrated that blocking VEGFR-2 signaling by a VEGFR-2 blocking antibody inhibited both angiogenesis and lymphangiogenesis in healing wounds, indicating the importance of VEGFR-2 for repair-associated lymphangiogenesis (Hong et al, 2004b).

2.1.2.3.3 <u>Angiopoietin-2</u>

Angiopoietin-2 (Ang2) is a ligand for the endothelial cell-specific tyrosine kinase receptor Tie2 and likely acts as an antagonist for angiopoietin-1 (Ang1) (Maisonpierre et al, 1997; Suri et al, 1996). Ang2 destabilizes interactions between blood vascular endothelial cells and surrounding pericytes, resulting in diminished endothelial cell - pericyte contacts. In contrast, Ang1, which interferes with the Ang2 signaling, stabilizes mature blood vessels (Thurston, 2003). Ang2 may induce angiogenic sprouting in the presence of VEGF but may stimulate vessel regression in the absence of VEGF (Holash et al, 1999a; Holash et al, 1999b; Thurston, 2003; Whitehurst et al, 2007). Ang2-deficient mice displayed chylous ascites, lymphedema, and lymphatic dysfunction but replacement of Ang2 with Ang1 was sufficient to rescue the lymphatic vascular phenotype. Although Ang2 is not required during early lymphatic vessel formation, large lymphatic vessels of Ang2 mutant mice were structurally irregular and leaky, and smaller lymphatic vessels displayed abnormal patterning (Gale et al, 2002).

2.1.2.3.4 <u>HGF</u>

Hepatocyte growth factor (HGF, also known as scatter factor) was recently identified as a potent lymphangiogenesis factor (Kajiya et al, 2005). HGF binds directly to its

receptor HGF-R to induce proliferation, migration and tube formation of LEC *in vitro*, exerting its effects independently of the VEGFR-3 pathway. HGF additionally interacts with integrin alpha 9, expressed specifically on LEC, to promote migration. HGF transgenic mice have increased numbers and enlargement of lymphatic vessels and similar results are observed when HGF is delivered subcutaneously, demonstrating that HGF can directly promote lymphangiogenesis *in vivo*.

2.1.2.3.5 **FGF2**

The role of fibroblast growth factor-2 (FGF2) in vascular development and angiogenesis has been well characterized (Auguste et al, 2003a). But recently, studies have shown that FGF2 promotes both lymphatic and blood vessel growth in the mouse cornea assay (Chang et al, 2004; Kubo et al, 2002). FGF2 also promotes proliferation and migration of LEC by directly binding to the receptor FGFR-3, which is upregulated by Prox1 in lymphatic endothelium (Shin et al, 2006). The pro-migratory effect could not be abrogated by neutralization of VEGFR-3, suggesting that FGF2 functions independently of the VEGF-C/VEGFR-3 pathway (Shin et al, 2006).

2.1.2.3.6 **PDGF/IGF**

Recent studies have reported that platelet-derived growth factor-BB (PDGF-BB) and insulin-like growth factor-1 (IGF1) and -2 (IGF2) also induce lymphangiogenesis (Bjorndahl et al, 2005; Cao et al, 2004) in the mouse corneal assay. However, their potential effects on skin lymphangiogenesis still need to be elucidated. Lymphatic vessel formation and growth during physiological and pathological conditions may require interplay of several lymphangiogenic growth factors. Thus, dissecting the molecular mechanisms of these growth factors will provide better insight into understanding lymphangiogenesis in pathologies of the lymphatic vasculature.
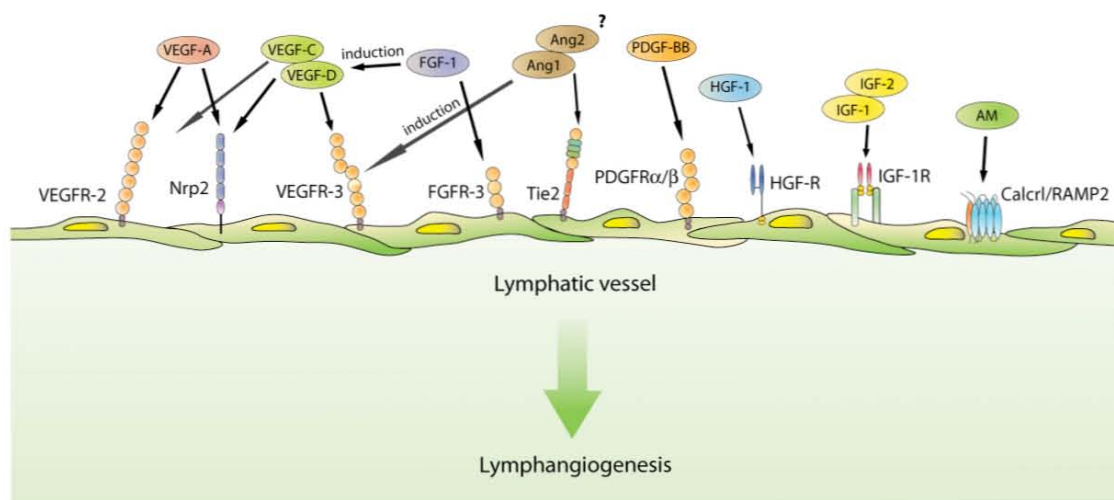
Figure 2.1.3 Schematic representation of lymphangiogenic growth factors and their receptors expressed by lymphatic endothelium. *Several vascular endothelial growth factors (VEGF-A, VEGF-C, VEGF-D) promote lymphangiogenesis by activation of distinct VEGFRs and Nrp2. FGF-2 acts directly through FGFR-3. Angiopoietin-1 (Ang1) activates Tie2 and up-regulates VEGFR-3. HGF, IGF, PDGF-BB, adrenomedullin act directly through their respective receptors HGF-R, IGF-1R, PDGFR and Calcrl/RAMP2.*

2.1.3 Pathologies of the lymphatic vasculature

2.1.3.1 *Lymphatic Dysfunction, Lymphedema*

Abnormal vessel development or damaged lymphatic vessels cause stagnation of proteins and fluid in the interstitium, and lead to lymphedema. This impairment of the lymphatic transport capacity leads to chronic and disabling swelling, tissue fibrosis, adipose degeneration, poor immune function, susceptibility to infections, and impaired wound healing (Rockson, 2001). Primary lymphedemas are rare genetic developmental disorders and are characterized by enlarged lymphatic capillaries and interstitial accumulation of lymph fluid. The symptoms are apparent from birth (Milroy; OMIM:153100) or at puberty (Meige; OMIM:153200) (Witte et al, 1998). Secondary lymphedema is caused by filariasis (elephantiasis) or by trauma due to radiation therapy, surgery or infection. Filariasis is the main cause of lymphedema in tropical countries, with some 100 million people affected worldwide, whereas breast-cancer surgery is a leading cause for secondary lymphedema in industrialized countries (Rockson, 2001). Recent studies have identified mutations in genes that are associated with different human lymphedema syndromes. In Milroy disease, several

heterozygous VEGFR-3 missense mutations result in the expression of an inactive tyrosine kinase (Irrthum et al, 2000; Karkkainen et al, 2000). In lymphedema-distichiasis, an autosomal-dominant disorder with congential lymphedema and double rows of eyelashes (distichiasis), inactivating mutations of the FOXC2 gene were identified in several families (Fang et al, 2000). Additionally, Foxc2-targeted mice have lymphatic abnormalities (Fang et al, 2000; Kriederman et al, 2003; Petrova et al, 2004). Patients with FOXC2 mutations display abnormal mural cell coating of their lymphatic vessels and lack lymphatic valves (Petrova et al, 2004). Moreover, mutations of the SOX18 gene on chromosome 20q13, a SRY-related transcription factor, cause recessive and dominant forms of hypotrichosis-lymphedema-telangiectasia syndrome. Mutations in the DNA-binding domain of SOX18 have been found in the recessive form of the disease whereas the dominant hereditary form is caused by a heterozygous nonsense mutation of the transactivation domain (Irrthum et al, 2003). Recently, a possible lymphedema treatment using viral gene-transfer vectors that encode VEGF-C has been reported. VEGF-C gene therapy was effective in Chy mice that suffer from lymphedema caused by a heterozygous inactivating mutation of VEGFR-3. Moreover, VEGF-C156S, which selectively activates VEGFR-3, successfully induced the formation of a functional cutaneous lymphatic vessel network without blood vessel growth or vascular leakiness - side effects observed with VEGF-C gene therapy due to its activation of VEGFR-2 (Saaristo et al, 2002). More recently, successful regeneration of a lymphatic network was observed after transduction of VEGF-C in lymph node transplantation models (Tammela et al, 2007).

2.1.3.2 *Lymphatic vessels in inflammation and the immune response*

There is increasing evidence that inflammation triggers lymphangiogenesis mediators that may regulate lymphatic vessel function. Lymphatic vessels participate in the regulation of inflammatory responses through their role in the transport of lymphocytes to lymph nodes. Migration of dendritic cells is mediated by the chemokine receptor CCR7 whereas lymphatic vessels express the ligand CCL21 (Ohl et al, 2004). Furthermore, inflammatory infiltrates in human kidney transplants undergoing rejection contain proliferating host lymphatics (Kerjaschki et al, 2004),

and lymphangiogenesis has also been observed in experimental models of chronic airway inflammation (Baluk et al, 2005). Kajiya and Detmar recently found that acute UVB irradiation of the skin results in hyperpermeable, leaky lymphatic vessels that are functionally impaired, and that blockade of VEGFR-3 resulted in prolonged inflammation and edema after UVB irradiation (Kajiya & Detmar, 2006).

Psoriatic skin lesions are characterized by pronounced lymphatic hyperplasia and an increase in the numbers and size of blood vessel (Kunstfeld et al, 2004). The pathogenesis of psoriasis remains unclear, although it is generally accepted that activated T lymphocytes and dendritic cells are important in the maintenance of psoriasis (Gottlieb et al, 2005). Although psoriasis appears to be a human-specific disease, homozygous VEGF transgenic mice spontaneously develop psoriasis-like inflammatory skin lesions at around 6 months of age. Heterozygous VEGF transgenic mice do not develop inflammatory skin lesions, but only upon induction of delayed type hypersensitive reaction (DTH) with oxazolone (Kunstfeld et al, 2004).

2.1.3.3 *Lymphatic involvement in tumor metastasis*

Metastatic tumor spread to regional lymph nodes through lymphatic vessels is the most important prognostic factor for tumors of epithelial origin (Dadras et al, 2005). At present, little is known about the mechanisms how tumor cells gain entry into the lymphatic system and increase their potential for subsequent organ metastasis. The sentinel lymph node is the first regional lymph node to which tumor cells metastasize and it is important in the staging, treatment, and follow up of many solid tumors (Pepper, 2001).

The process of metastasis through the lymphatic vessel system is complex and involves changes in the expression of numerous genes (Ramaswamy et al, 2003). Growth factor-mediated stimulation of lymphatic vessels appears to be required for lymphatic metastasis. Recent studies in animal tumor models have provided evidence that increased levels of VEGF-C and/or VEGF-D promote active tumor lymphangiogenesis and lymphatic tumor spread to regional lymph nodes, and that these effects can be suppressed by blocking VEGFR-3 signaling (Mandriota et al,

2001; Skobe et al, 2001; Stacker et al, 2001). Tumor cells and tumor-associated macrophages secrete VEGF-C and VEGF-D, which induce sprouting of nearby lymphatic vessels, facilitating the egress of tumor cells into the vessel lumen. The lymphatic endothelial cells may also actively attract some tumor cells through the secretion of chemokines, such as CCL21 (Kriehuber et al, 2001). VEGF-A has been shown to induce VEGF-C expression in cultured BEC, and VEGF-A producing transgenic tumors indeed showed higher VEGF-C protein levels than wild-type tumors.

Traditionally, VEGF-A was known as a blood vessel-specific growth factor. However, its major signaling receptor, VEGFR-2, is also expressed on lymphatic endothelial cells *in vitro* and *in situ* (Hirakawa et al, 2003; Hong et al, 2004b; Kriehuber et al, 2001; Saaristo et al, 2002). A high correlation between VEGF-A production and lymph node metastasis in several cancer types, including gastric cancer have been described (Hirakawa et al, 2005b; Kimura et al, 2001). Mice overexpressing VEGF-A in the skin, subjected to a standard chemically-induced skin carcinogenesis regimen, showed active proliferation of VEGFR-2-expressing tumor-associated lymphatic vessels, as well as enhanced tumor metastasis to the sentinel and distant lymph nodes (**Fig. 2.1.4**) (Hirakawa et al, 2005b; Tobler & Detmar, 2006). The pioneering finding of this study was that even before metastasizing, VEGF-A overexpressing primary tumors induced sentinel lymph node lymphangiogenesis, preparing their future metastatic spread (Hirakawa et al, 2005b). The relative contribution of direct (via activation of VEGFR-2 on LECs) versus indirect effects toward the lymphangiogenic activity of VEGF-A remains to be explored.
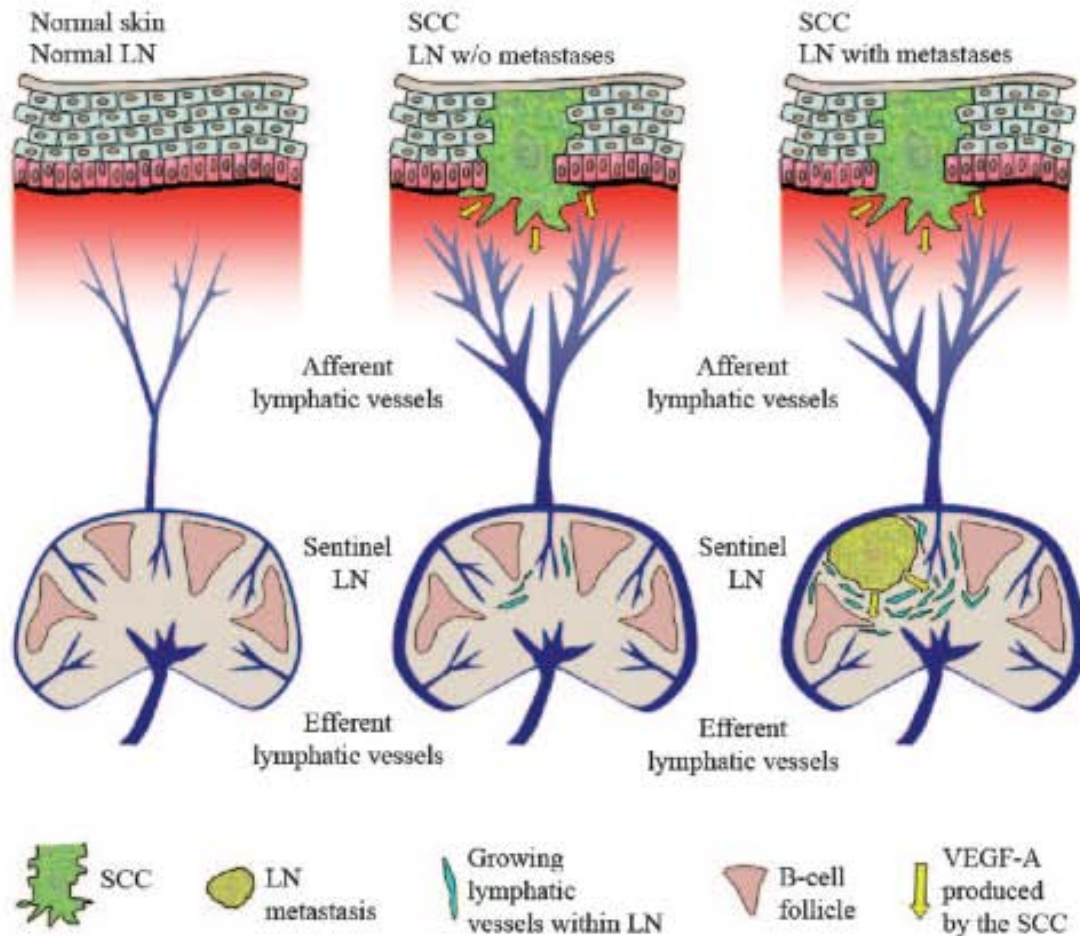
Figure 2.1.4 VEGF-A expressing cancer cells induce tumor and lymph node lymphangiogenesis.
In normal skin, lymphatic vessels are present in the dermis and maintain tissue fluid homeostasis. There is no detectable lymphangiogenesis within draining LN. SCC of K14/VEGF-A transgenic mice induce primary, tumor-associated, lymphatic vessel growth but also lymphangiogenesis within sentinel LN, even before they metastasize, possibly preparing the LN for their later arrival. Metastatic, VEGF-A expressing SCC maintains their lymphangiogenic activity after metastasis to sentinel LN (Tobler & Detmar, 2006).

Recent reports have demonstrated that leukocytes also play an important role in promoting tumor-associated lymphatic vessel growth and activation. Activated macrophages express VEGFR-3, and the lymphangiogenic factor VEGF-C has been shown to enhance macrophage chemotaxis (Schoppmann et al, 2002; Skobe et al, 2001) whereas tumor-associated macrophages secrete VEGF-C to promote lymphangiogenesis (Schoppmann et al, 2002). Recently, VEGF-A secreted by follicular B cells has been implicated in the mediation of lymph node lymphangiogenesis (Angeli et al, 2006), however, the relative contribution of leukocyte-derived lymphangiogenic factors needs to be further elucidated. Bone

marrow-derived progenitor cells and macrophages may physically incorporate into newly formed lymphatic vessels (Kerjaschki, 2005; Maruyama et al, 2005; Schledzewski et al, 2006), but this has not been observed in tumor-associated lymphangiogenesis (He et al, 2004), and it remains unclear whether this mechanism significantly contributes to pathological lymphangiogenesis.

Therapeutically, a soluble VEGFR-3/Fc molecule ("VEGF-C/D trap") inhibited the sprouting and lymphatic vessel enlargement and seemed to restore the integrity of the lymphatic vessel wall (He et al, 2005). Similarly, blocking monoclonal antibodies against VEGF-C/-D or their receptor(s), and small molecules that inhibit the tyrosine kinase catalytic domain of these receptors could be used for the inhibition of lymphangiogenesis and hence tumor metastasis.

2.2   MICROARRAY TECHNOLOGY

The introduction of microarray technology has allowed researchers to examine various biological questions on a genome-wide scale. It has provided a systematic way to study gene expression across the entire transcriptome. The transcriptome is the complete set of transcripts and their relative levels of expression in a particular cell or tissue type under defined conditions (Schena et al, 1995; Shalon et al, 1996).

2.2.1 Oligonucleotide microarray technology

Unlike cDNA microarrays that use expression sequence tags (ESTs) extracted from a sequenced cDNA library, oligonucleotide microarrays contain a series of 25-mer (in case of the Affymetrix platform) or 60-mer (in case of the Applied Biosystems platform) oligonucleotides designed by a computer algorithm to represent known or predicted open reading frames (Kuo et al, 2006). Target labeling is performed using amplified RNA (aRNA) rather than cDNA. The first-strand reverse transcription of poly-A mRNA is performed as for cDNA microarrays, but the poly-dT primer includes a promoter sequence for the enzyme T7 RNA polymerase. After synthesis of the second strand, the T7 enzyme is added and it synthesizes multiple copies of

antisense RNA of the gene, incorporating biotinylated (Affymetrix, http://www.affymetrix.com) or DIG-oxigenin (Applied Biosystems, http://www.appliedbiosystems.com) nucleotides during the reaction (Bammler et al, 2005).

Hybridization to oligonucleotide arrays is a noncompetitive, single-colored per array-approach, and is detected by addition of either a fluorescently labeled streptavidin compound that binds to the biotin group in the aRNA molecule (Affymetrix) or a chemiluminescently labeled anti-digoxigenin-alkaline phosphotase compound that can be detected with digoxigenin in the aRNA molecule (Applied Biosystems).

Some of the advantages of oligonucleotide arrays include the accommodation of higher densities of genes and a lower variability from chip to chip. Researchers can also use this approach without access to microarray construction facilities, and these arrays lend themselves to data comparison across research groups. However, cDNA microarrays are considerably cheaper and offer higher levels of replication that in turn promotes statistical analysis (Wei et al, 2004). They also rely on hybridization over kilobases rather than tens of bases, which may reduce cross-hybridization artifacts, and also minimize effects of intra-specific single nucleotide polymorphisms on the hybridization that could be misinterpreted as strain-specific variation of gene expression (Patterson et al, 2006).

2.2.2 Gene expression data analysis

Microarray technology measures the relative amount of mRNA expressed in two or more experimental conditions (e.g. no-treatment vs. treatment, healthy vs. disease) and generates a differential expression of all known genes (approximately 30,000 genes in humans). Despite the comprehensiveness of microarray technology, one of the main challenges of gene expression profiling is data analysis. The semi-quantitative measurements from microarrays lend themselves to the generation of false positive and false negative results (Breitling, 2006; Couzin, 2006; Magic et al, 2007). In order to circumvent these errors, one can select differentially expressed genes by applying a variety of statistical tests to consider both fold-change and

variability in combination to create a p-value, an estimate of how frequently we would observe these data by chance alone (Chen, 2007; Vardhanabhuti et al, 2006). While the statistical analyses may reliably identify which gene products are differentially expressed under different experimental conditions, making a significant biological extrapolation of differentially expressed genes is key to understand biological effects using microarrays (Breitling, 2006). Having identified some set of differentially expressed genes, the subsequent analysis involves identification of biological patterns within the given set of genes. Gene ontology analysis provides a standard way to define these relationships (Dai et al, 2005; Subramanian et al, 2005). Most genes but not all have several key attributes involved in biological processes, molecular functions and biological pathways. Categorization of regulated genes based on their gene ontology terms generates important relationships between genes and a given condition and thus may generate new hypotheses for further biological investigations (Curtis et al, 2005; Subramanian et al, 2005).

Expression profiling using microarray technology provides exciting new information about what genes do under various conditions. However, the size and complexity of these experiments often results in a wide variety of possible interpretations. Therefore, good experimental design, adequate biological replication and follow-up experiments play key roles in the successful extrapolation of profiling experiments (Couzin, 2006).

3 RESULTS AND DISCUSSION

3.1 Prox1 promotes lineage-specific expression of FGF receptor-3 in lymphatic endothelium

3.1.1 Introduction

Fibroblast growth factor (FGF) signaling plays an important role in a broad range of biological processes of vascular endothelial cells including proliferation, migration, survival, tubulogenesis and differentiation (Javerzat et al, 2002). At least, twenty three different FGFs and four FGF-receptors (FGFR-1 through FGFR-4) have been identified and characterized in vertebrates so far (Javerzat et al, 2002; Ornitz & Itoh, 2001). FGFRs belong to the receptor tyrosine kinase family and commonly consist of three extracellular immunoglobulin-like domains, a single-pass transmembrane domain and a split-tyrosine kinase domain. Alternative splicing generates a wide array of isoforms of FGFRs with distinct physical and biological characteristics (Dell & Williams, 1992; Groth & Lardelli, 2002; Hanneken, 2001; Ornitz, 2000; Terada et al, 2001; Wilkie et al, 2002). The most common variants, the IIIb or IIIc isoform, are formed by alternative splicing of the carboxy-terminal half of the third immunoglobulin domain of FGFR-1, -2 and -3, but not FGFR-4. The alternative splicing is regulated in a tissue-specific manner and also determines their binding specificity for various FGF ligands. In general, the IIIb isoforms of FGFRs are predominantly expressed by epithelial lineage cells, whereas the IIIc variants tend to be expressed in mesenchymal lineages (Alarid et al, 1994; Murgue et al, 1994; Orr-Urtreger et al, 1993; Yan et al, 1993). FGF ligands and their interacting receptor isoforms are often expressed in adjacent tissues.

The roles of FGFs in vascular development have been well characterized in the context of angiogenesis that is associated with tumor development, tissue repair and embryogenesis (Auguste et al, 2003b; Bikfalvi et al, 1998; Javerzat et al, 2002). FGF-2 was one of the first angiogenic factors identified for its potent activity on vascular endothelial cell proliferation (Shing et al, 1984). Recently, FGF-2 was reported to also induce lymphatic vessel growth in mouse cornea assay by promoting the secretion of the potent lymphangiogenic factor, vascular endothelial cell growth factor (VEGF)-C, by blood vascular endothelial cells (Chang et al, 2004; Kubo et al, 2002). Moreover,

systemic treatment with a blocking antibody against VEGFR-3, the major receptor for VEGF-C, reduced the FGF-2-induced corneal lymphangiogenesis (Chang et al, 2004; Kubo et al, 2002). These findings indicate that the effects of FGF-2 on lymphangiogenesis might be largely indirect through activation of the VEGF-C/VEGFR-3 signaling pathway.

The homeodomain transcriptional factor Prox1 was originally isolated due to its homology with the *Drosophila* Prospero protein (Oliver et al, 1993b). Like Prospero, Prox1 plays an important role in cell fate decisions of diverse cell types and serves as a master regulator during embryonic development of the lymphatic vascular system (Hong et al, 2002; Wigle et al, 2002b; Wigle & Oliver, 1999). Upon an inductive signal during early development, Prox1 is upregulated in a subset of venous endothelial cells and reprograms their gene expression profile similar to that of lymphatic endothelial cells. The Prox1-positive venous endothelial cells then further differentiate to adopt lymphatic endothelial cell phenotypes and migrate out to form the primitive lymphatic vessels. Therefore, the Prox1-mediated cell fate reprogramming is the initial and essential step during lymphatic endothelial differentiation (Wigle et al, 2002b; Wigle & Oliver, 1999). In addition, we and others have recently found that ectopic over-expression of Prox1 in cultured blood vascular endothelial cells (BECs) isolated from human foreskin recapitulates the embryonic lymphatic reprogramming by down-regulating the BEC-specific genes and by up-regulating several lymphatic-specific genes (Hirakawa et al, 2003; Hong et al, 2002; Petrova et al, 2002b). However, the molecular mechanisms underlying this lymphatic reprogramming are poorly understood. In this study, we present evidence demonstrating that Prox1 upregulates the expression of FGFR-3 during lymphatic reprogramming and that FGF signaling through the upregulated FGFR-3 plays an important role in the early lymphatic vascular system development.

3.1.2 Results

3.1.2.1 *Ectopic expression of Prox1 in primary BEC upregulates FGFR-3*

We and others have previously reported that ectopic expression of Prox1 in blood vascular endothelial cells (BECs) led to upregulation of several LEC-specific genes (Hong et al, 2002; Petrova et al, 2002b). Detailed microarray analyses further indicate that expression of FGFR-3 is also regulated by the expression of Prox1 in BECs. Real-time RT-PCR analyses confirmed that Prox1 increased FGFR-3 expression by 20-fold (**Fig. 3.1.1A**). The Prox1-mediated upregulation of FGFR-3 was further confirmed by Northern blot analysis by using total RNAs harvested 3, 24 and 48 hours after transduction of BECs with an adenovirus expressing Prox1 (**Fig. 3.1.1B**).

To determine which of the two major FGFR-3 isoforms (IIIb and IIIc) was upregulated by Prox1, RT-PCR was performed by using primers designed to yield a 235-bp product containing an *Apa*I site from the IIIb isoform, or a 229-bp fragment without an *Apa*I site from the IIIc isoform. As controls for the analyses, we also used stably transfected myoblast cells that selectively express either human FGFR-3 IIIb or IIIc isoform (Kanai et al, 1997). As expected, RT-PCR analysis yielded an *Apa*I-sensitive 235-bp product from the IIIb-expressing control cells, and an *Apa*I-insensitive 229-bp fragment from the IIIc-expressing cells (**Fig. 3.1.1C**). The same analysis amplified an *Apa*I-insensitive 229-bp product from BECs infected with the Prox1-adenovirus (**Fig. 3.1.1C**). This indicates that Prox1 predominantly upregulates expression of the FGFR-3 IIIc isoform with a slight activation of the expression of IIIb is also in vascular endothelial cells. Furthermore, RT-PCR of RNA obtained from primary lymphatic endothelial cells generated the *Apa*I-insensitive 229-bp product, whereas unpurified cell mixtures isolated from human foreskins yielded products of both *Apa*I-sensitive and insensitive fragments (**Fig. 3.1.1D**). These data indicate that the FGFR-3 IIIc isoform is the major variant present in LECs and that Prox1 selectively upregulates the IIIc isoform of FGFR-3.
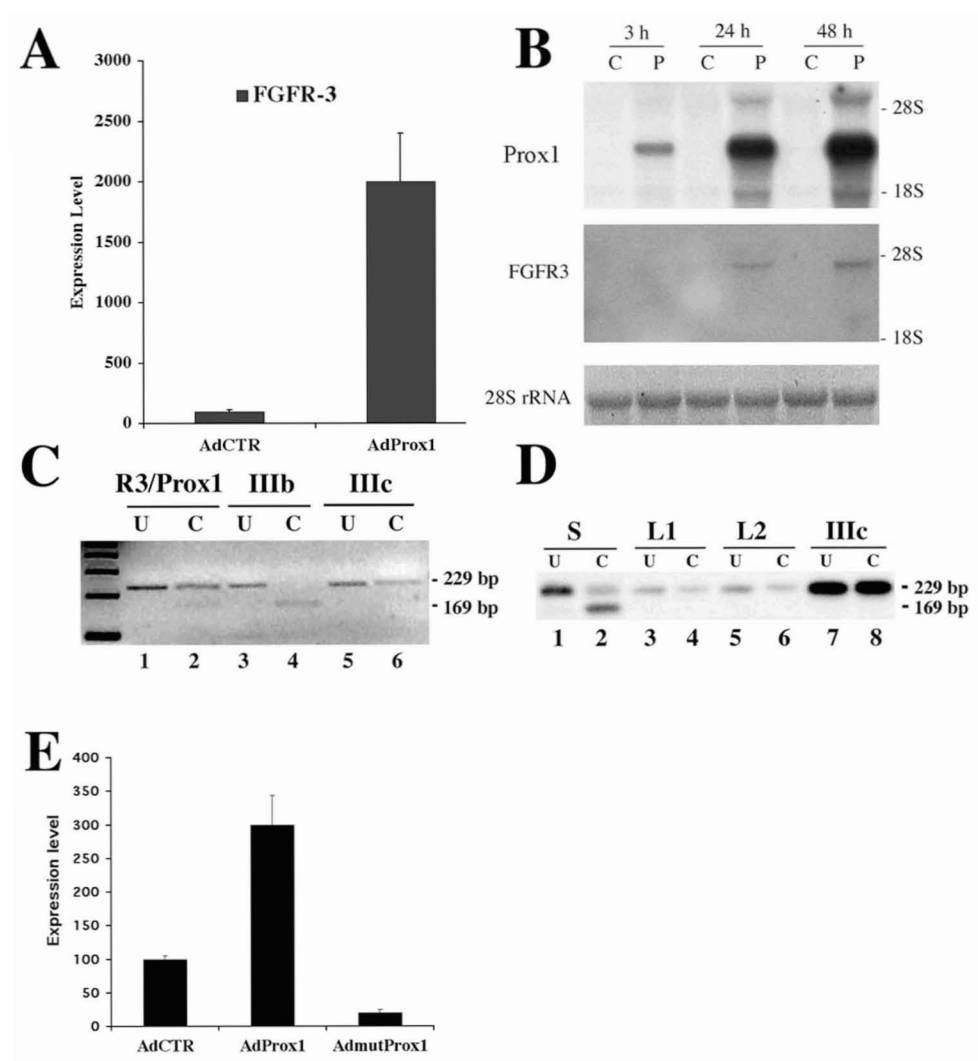
Figure 3.1.1 Prox1 upregulates FGFR-3 expression. *(A) The steady-state level of FGFR-3 mRNA was increased by 20-fold when Prox1 is ectopically overexpressed in BECs. FGFR-3 expression level was measured by real-time RT-PCR in BECs after transduced with control (AdCTR) or Prox1 (AdProx1) adenovirus. Data were normalized by β-actin mRNA levels and expressed as % of the control virus-infected cells (means±SD). (B) Upregulation of FGFR-3 mRNA expression by Prox1 was confirmed by Northern blot analysis of total RNAs obtained from BECs infected with control (C) or Prox1 (P) adenovirus for 3, 24 or 48 hours. (C) Prox1 induces expression of the IIIc isoform of FGFR-3, as determined by a diagnostic ApaI restriction analysis of RT-PCR product (229-bp) amplified from BECs transduced with Prox1-adenovirus for 24 hours (R3/Prox1). As controls, RT-PCR products from FGFR3 IIIb or IIIc-expressing cell lines were digested in parallel. Only the product from the IIIb isoform was digested to yield a 169-bp fragment. (D) Cultured lymphatic endothelial cells (LECs) exclusively express the IIIc isoform of FGFR-3. RT-PCR products of unpurified cell mixture (S) from human neonatal foreskins, two independent batches of LECs (L1, L2) and FGFR-3 IIIc-expressing control cells (IIIc) were subjected to the diagnostic ApaI restriction analysis. While the product from the cell mixture contains both ApaI sensitive and resistant fragments, those of LECs and of FGFR-3 IIIc control cells (IIIc) were resistant to the digestion, indicating that the IIIc is the dominant isoform of FGFR-3 in LECs. U: undigested, C: digested with ApaI. (E) Cultured lymphatic endothelial cells were transduced with adenovirus expressing the wildtype (AdProx1) or mutant (AdmutProx1) Prox1, or with control adenovirus (AdCTR). After 2 days, the expression level of FGFR-3 was determined using real-time RT-PCR.*

To determine if Prox1 is necessary to maintain the expression of FGFR-3 in LECs, we ectopically expressed a mutant Prox1 in cultured lymphatic endothelial cells through the adenovirus gene transfer. The mutant Prox1 protein has two amino-acid substitution mutations in its DNA-binding domain and does not display any transcriptional activity (see below). We found that when expressed in LECs, the mutant Prox1 was able to decrease the expression level of FGFR-3 by 4-fold, while the wildtype Prox1 upregulated FGFR-3 by 3-fold (**Fig. 3.1.1E**). These findings indicate that the mutant Prox1, serving as a dominant negative mutant, may compete with the endogenous Prox1 in LECs and that Prox1 function is necessary to maintain the expression of FGFR-3.

3.1.2.2 *Prox1 binds to the FGFR-3 promoter and activates its transcription*

To study the molecular mechanisms underlying the Prox1-mediated upregulation of FGFR-3, we performed promoter-reporter assays using FGFR-3 promoter-luciferase constructs, which have been previously characterized (McEwen & Ornitz, 1998). A 3-kb promoter fragment was sufficient to mediate transcriptional activation of the firefly luciferase reporter (P1) by Prox1 (**Fig. 3.1.2A**). The Prox1-mediated activation was still maintained even after deleting most of the promoter region to –220 n.t. upstream of the FGFR-3 transcriptional initiation site (P2), but removal of the proximal 220-bp of the promoter sequence abrogated the activation by Prox1 (P3). The Prox1-mediated activation progressively decreased with deletions to –175 and –126 n.t. and then was completely abolished by deletion to -79 n.t. (P4-P6). These data indicate the presence of putative Prox1 response elements (PRE) between -220 to -79 n.t. of the FGFR-3 promoter.
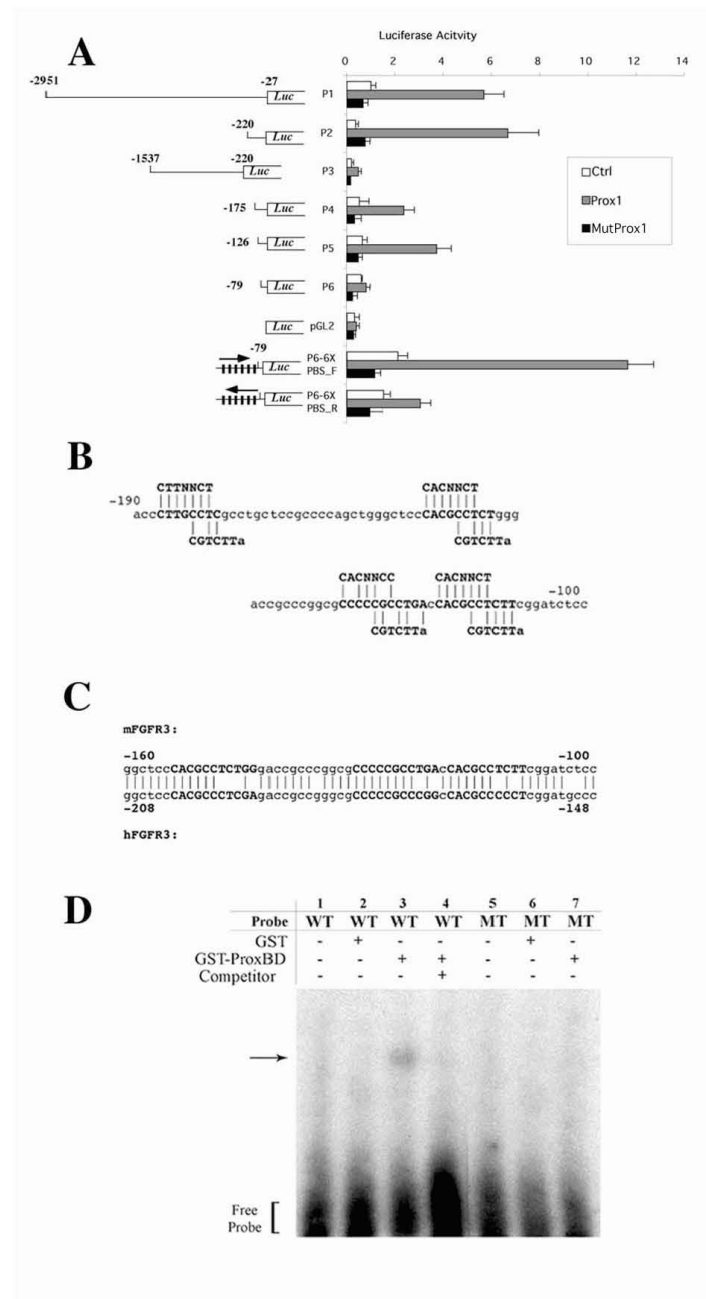
Figure 3.1.2 Prox1 binds to the FGFR-3 promoter to upregulate its transcription. *(A) The FGFR-3 promoter-luciferase (Luc) reporter constructs (P1-P6) and an empty control vector (pGL2) were tested for their luciferase activity in the presence of a vector control (Ctrl), a Prox1-expressing vector (Prox1), or a mutant Prox1-expressing vector (MutProx1). P6-6XPBS contains six-tandem repeats of the Prox1 binding site (PBS, CACGCCTCT) in the P6 construct in the forward- (P6-6XPBS_F) or reverse (P6-6XPBS_R) orientation. Numbers indicate relative locations from the transcriptional initiation site (McEwen & Ornitz, 1998). Data are shown as means±SD. (B) Sequence analysis of the mouse FGFR-3 promoter region revealed four putative Prox1 binding sites. Two previously reported Prospero consensus sequences, C(A/T)(C/T)NNC(T/C) and CGTCTT(A) (Cook et al, 2003; Hassan et al, 1997), are shown above and below the putative Prox1 binding sites (bold), respectively. (C) The proximal three putative Prox1 binding sequences (bold) are conserved between the mouse and human FGFR-3 promoters. (D) Gel electrophoresis mobility shift assays showed that the purified GST-Prox1 fusion protein (GST-ProxBD), but not the GST protein alone, binds to the putative Prox1 binding sequences found in the FGFR-3 promoter. The GST or GST-Prox1 proteins were incubated with ^{32}P-labeled a wild type (WT) or a mutant probe (MT). Arrow indicates a slow migrating complex of GST-Prox1 and the wild-type probe (lane 3). Excessive amount of unlabeled wild type probe (Competitor) competes for the interaction between GST-Prox1 and the labeled wild-type probe (lane 4).*

44

To further determine whether the Prox1-mediated activation of FGFR-3 is dependent on DNA-protein interaction, we introduced two amino acid substitution mutations (N625A and R627A) into the third helix of the homeodomain region that is involved in DNA binding of Prospero, the *Drosophila* homolog of Prox1 (Ryter et al, 2002). Prospero and Prox1 share a high amino acid identity in their DNA-binding domains (Hong & Detmar, 2003b). The Prox1 protein with the two substitution mutations (MutProx1) completely lost its transcriptional activity (**Fig. 3.1.2A**). These findings indicate that a direct DNA-protein interaction is necessary for the Prox1-mediated upregulation of FGFR-3.

3.1.2.3 *Identification of the putative Prox1 binding sites in the FGFR-3 promoter*

Previous reports had identified two seemingly different consensus sequences (C(a/t)(c/t)NNC(t/c) and (T)AAGACG) as putative Prospero binding sites (Cook et al, 2003; Hassan et al, 1997). Interestingly, we found four putative Prox1 binding sites, composed of the two partially overlapping Prospero consensus sites, between -190 and -100 n.t. of the mouse FGFR-3 promoter (**Fig. 3.1.2B**). The proximal three putative Prox1 binding sequences are highly conserved between the mouse and human FGFR-3 promoters (**Fig. 3.1.2C**). To investigate whether these sequence motifs serve as Prox1 binding sites, we performed gel electrophoresis mobility shift assays (EMSA) using a GST-Prox1 fusion protein (Belecky-Adams et al, 1997; Cui et al, 2004). Purified GST-Prox1 fusion protein efficiently bound to a probe containing the putative Prox1 site in the FGFR-3 promoter (**Fig. 3.1.2D**). However, the fusion protein did not bind to a mutant probe whose putative Prox1 site was replaced with random nucleotides. Interaction of the GST-Prox1 protein with the labeled wild-type probe was competed out by addition of excessive unlabeled wild type probe and the GST protein alone did not interact with either probe (**Fig. 3.1.2D**). These data demonstrate that Prox1 bind to the putative Prox1 site present in the FGFR-3 promoter.

We next investigated whether the Prox1 binding site identified in the FGFR-3 promoter is sufficient to mediate transcriptional activation of the reporter gene. We introduced six tandem repeats of the Prox1 binding sequences (PBS, CACGCCTCT)

into the P6 construct in the forward- or the reverse orientation (P6-6XPBS_F and P6-6XPBS_R) (**Fig. 3.1.2A**). The P6 construct was shown to be unable to mediate any transcriptional activation by Prox1. However, introduction of six repeats of the putative Prox1 binding sites in the forward orientation (P6-6XPBS_F) re-instated transcriptional activity to the P6 construct by wild-type, but not by the mutant Prox1 (**Fig. 3.1.2A**). However, when the repeats were introduced in the reverse orientation (P6-6XPBS_R), only marginal activation was observed. These findings indicate that the nine-nucleotide sequence (CACGCCTCT) present in the FGFR-3 promoter is necessary and sufficient to mediate transcriptional activation by Prox1.

3.1.2.4 *Expression of FGFR-3 in developing lymphatic vessels of mouse embryo and of human skin*

We next investigated whether FGFR-3 is expressed in the lymphatically differentiating endothelial cells during mouse embryogenesis. In agreement with our *in vitro* results, many of the Prox1-positive lymphatically differentiating endothelial cells were positively stained for FGFR-3 in E11.5 mouse embryos (**Fig. 3.1.3A-D**). Furthermore, double immunofluorescent stainings for the lymphatic-specific marker LYVE-1 and for FGFR-3 showed that FGFR-3 was strongly and specifically expressed in the newly formed LYVE-1-positive lymphatic vessels (**Fig. 3.1.3E-H**), but not in developing blood vessels (cardinal vein) (**Fig. 3.1.3C and G**). Furthermore, double stainings of human neonatal foreskin for LYVE-1 and FGFR-3 revealed that the lymphatic specific expression of FGFR-3 is also maintained after embryonic development (**Fig. 3.1.3I-L**).
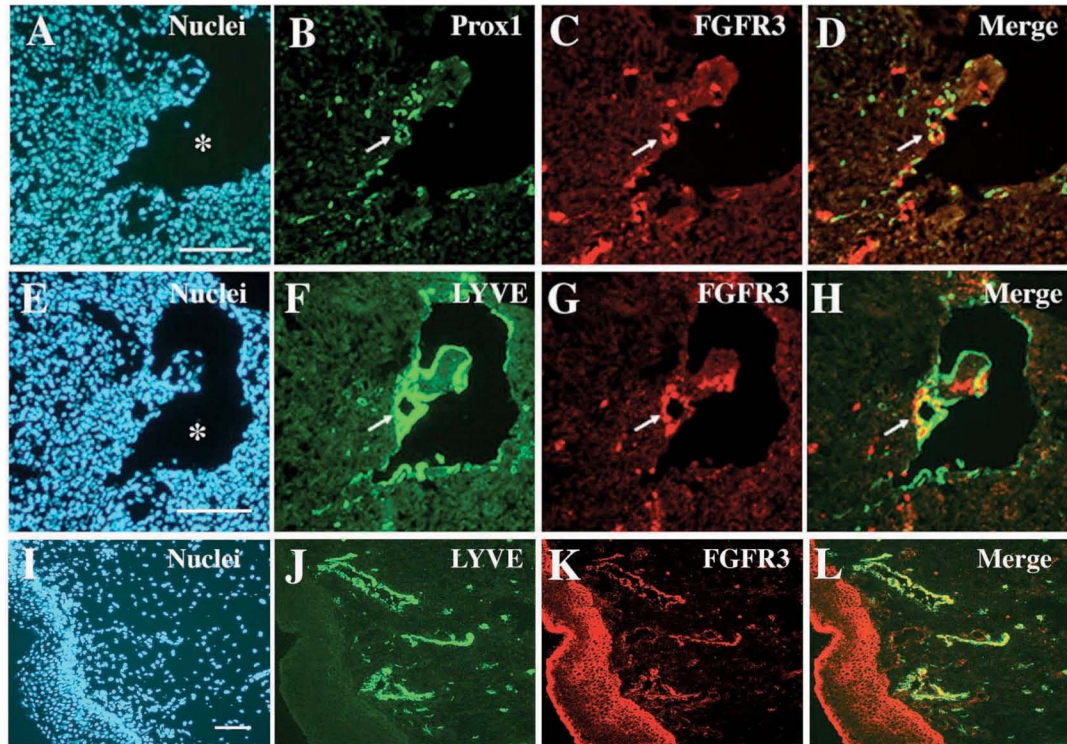
Figure 3.1.3 FGFR-3 expression in lymphatic endothelial cells during and after embryonic development. *Adjacent mouse embryo sections (E11.5) were stained for Prox1 (green) and FGFR-3 (red) (**A-D**), and for LYVE-1 (green) and FGFR-3 (red) (**E-H**). Lymphatically differentiating budding endothelial cells and resident endothelial cells in a newly formed lymphatic vessel are co-stained positively for Prox1 and for FGFR-3 (**D**). Similarly, LYVE-1-positive lymphatic endothelial cells express FGFR-3 (**H**). Arrows indicate a newly formed lymphatic vessel (**B-D and F-H**). A human neonatal foreskin section was co-stained for LYVE-1 and FGFR-3 (**I-L**). Asterisk, cardinal vein; bar, 100 µm.*

3.1.2.5 *Signaling through FGFR-3 promotes LEC proliferation*

To further evaluate the biological role of FGFR-3-mediated signaling, we inhibited expression of FGFR-3 in LECs using small interfering RNAs (siRNAs) and studied the effects on cell proliferation. Real-time RT-PCR analyses revealed that transfection of FGFR-3 siRNAs into LECs decreased the steady state level of FGFR-3 by 50-fold, whereas the expression of FGFR-1 was not altered (**Fig. 3.1.4A**). Notably, knockdown of FGFR-3 resulted in a significant inhibition of proliferation of LECs by 30-40% (**Fig. 3.1.4B**). However, the FGF-2-induced proliferation of LECs was largely unaffected (about two-fold) with or without inhibition of FGFR-3. This may be due to the presence of other functional FGF receptors (FGFR-1, -2 and -4) that

47

may be activated by FGF2. Together, these data demonstrate that the FGFR-3-mediated signaling plays an important role in proliferation of LECs.
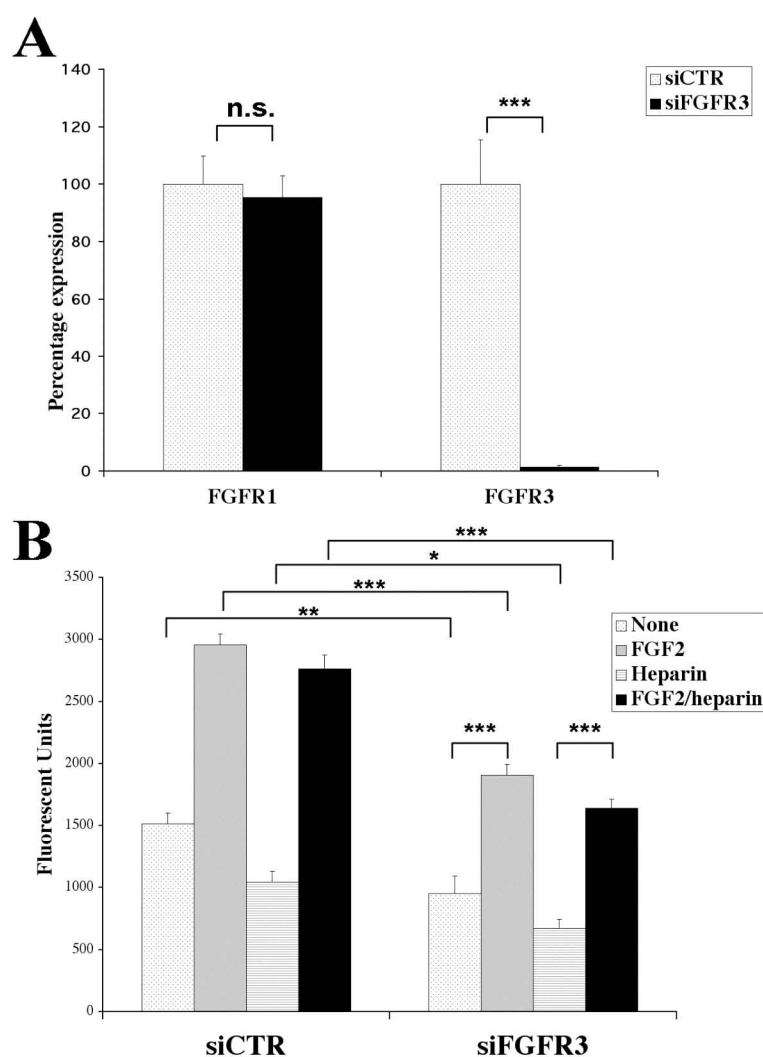
Figure 3.1.4 FGFR-3 mediates proliferation signaling of LECs. *(A) siRNAs against FGFR-3 significantly reduced the steady state levels of FGFR-3, but not of FGFR-1. (B) Knockdown of FGFR-3 inhibits proliferation of LECs in the presence or absence of FGF-2 and its cofactor heparin. Experiments were performed in triplicate twice and LECs with a passage number 2 were used. siCTR, control siRNA for luciferase; siFGFR3, siRNAs for FGFR-3; *, p<0.05; **, p < 0.01; ***, p < 0.001.*

3.1.2.6 *FGF-2 binds directly to low and high affinity receptors in LECs and subsequently internalized for degradation*

We next investigated whether FGF ligands physically interact with FGF receptors present in lymphatic endothelial cells. LECs were incubated with increasing amounts of ^{125}I-FGF-2 and levels of binding to the low and high affinity sites were determined.

^{125}I-FGF-2 was bound in a concentration-dependent manner to LECs but binding was not fully saturable for the low affinity binding sites (**Fig. 3.1.5A**). For low affinity binding (proteoglycans), a Kd of 1 nM and 400,000 binding sites/cell were determined (**Fig. 3.1.5A**). For high affinity binding sites (receptors), maximum binding was detected between 4-6 ng/ml of ^{125}I-FGF-2 (**Fig. 3.1.5B**). Scatchard analysis revealed high affinity binding (Kd of 72 pM) and approximately 5,300 binding sites per cell (**Fig. 3.1.5B**). These values are similar to those found on vascular endothelial cells (Moscatelli, 1987). We then determined internalization of ^{125}I-FGF-2 in LECs. Between 1 to 4 hours, the internalization rate was 0.046 ng/h/10^5 cells (**Fig. 3.1.5C**). This value progressively decreased between 4-8 hours (0.01 ng/h/10^5 cells) and 8-12 hours (0.004 ng/h/10^5 cells), indicating that FGF-2 internalization progressively slows down with time. After 1 hour of internalization, a fragment of 15-kDa (together with the 18-kDa band) was detected (**Fig. 3.1.5D**). At 1.5 and 2 hours, two additional fragments of 10- and 8-kDa appeared and their amounts increased with time. Maximum degradation was observed between 12-24 hours. Interestingly, at 24 hours, 18-kDa FGF-2 was still present in significant amounts in LECs. Taken together, our biochemical study provides a detailed information on binding kinetics of FGF-2 to its receptors and subsequent internalization and degradation patterns of the ligand in lymphatic endothelial cells, which are largely comparable with those of vascular endothelial cells as previously described (Bikfalvi et al, 1989).
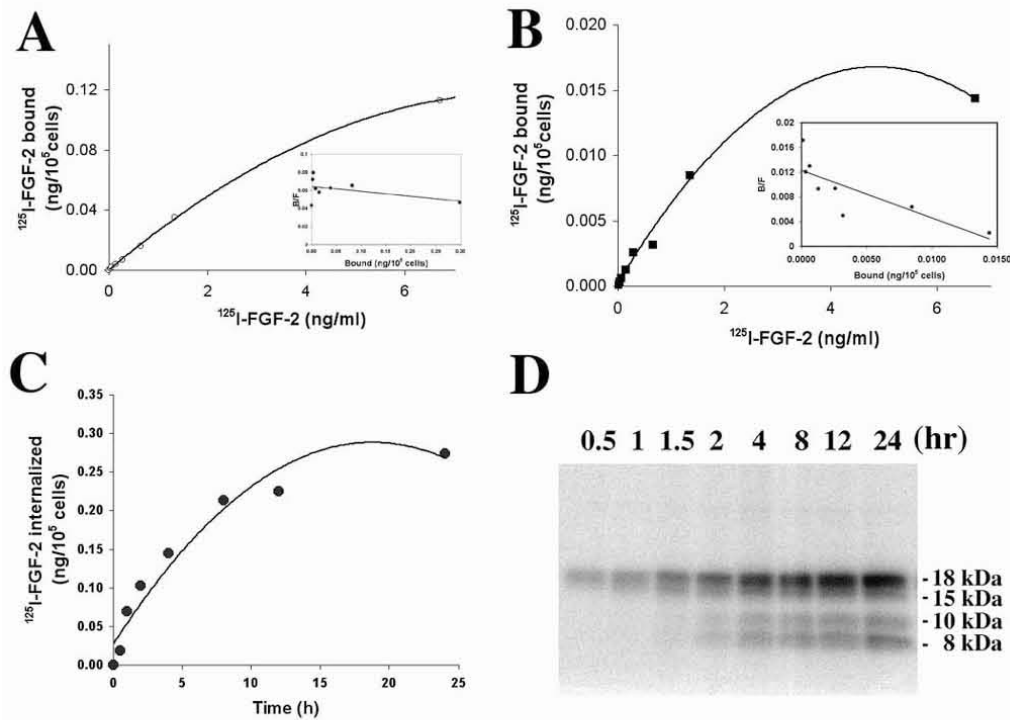
Figure 3.1.5 Binding, internalization and degradation of FGF-2 in LECs. *Concentration dependency of ^{125}I-FGF-2 binding to low affinity sites (**A**) and high affinity receptors (**B**). Cells were incubated with increasing concentrations of ^{125}I-FGF-2 and the specific binding was determined as described in Materials and Methods. Scatchard plots are shown in insets. (**C**) Internalization of ^{125}I-FGF-2 was determined by incubating cells with 10 ng/ml ^{125}I-FGF-2 at 37 °C for specified time intervals. (**D**) After internalization, solubilized cell extracts were run on a 15 % SDS-PAGE gel, dried and processed for autoradiography (PhosphorImager) to visualize the degradation profile. Time (hours) after incubation and molecular mass of the degraded products are shown. The data are representative for two independent experiments performed in duplicates.*

3.1.2.7 *FGF signaling regulates migration, proliferation and apoptosis of cultured primary lymphatic endothelial cells*

We next investigated the effects of two specific FGF ligands on migration, proliferation and apoptosis of primary human LECs. Treatment with recombinant human FGF-1 and FGF-2 significantly enhanced migration and proliferation of LECs (**Fig. 3.1.6A and B**). Furthermore, both FGF ligands protected LECs from apoptosis induced by serum depletion (**Fig. 3.1.6C**). A previous *in vivo* study in mouse corneas indicated that FGF-2 might indirectly promote lymphangiogenesis through activation of the VEGF-C/VEGFR-3 pathway (Kubo et al, 2002). To determine if FGF-2 can stimulate LEC migration *in vitro* directly or indirectly, we studied the effect of FGF-2 in the presence or absence of an anti-VEGFR-3 blocking antibody. Both VEGF-C and

FGF-2 stimulated the migration of LECs at a comparable level (**Fig. 3.1.6D**). However, neutralization of VEGFR-3 abrogated the enhanced migration of LECs by VEGF-C, but not by FGF-2, indicating that FGF-2 can function independently of the VEGF-C/VEGFR-3 pathway *in vitro*.
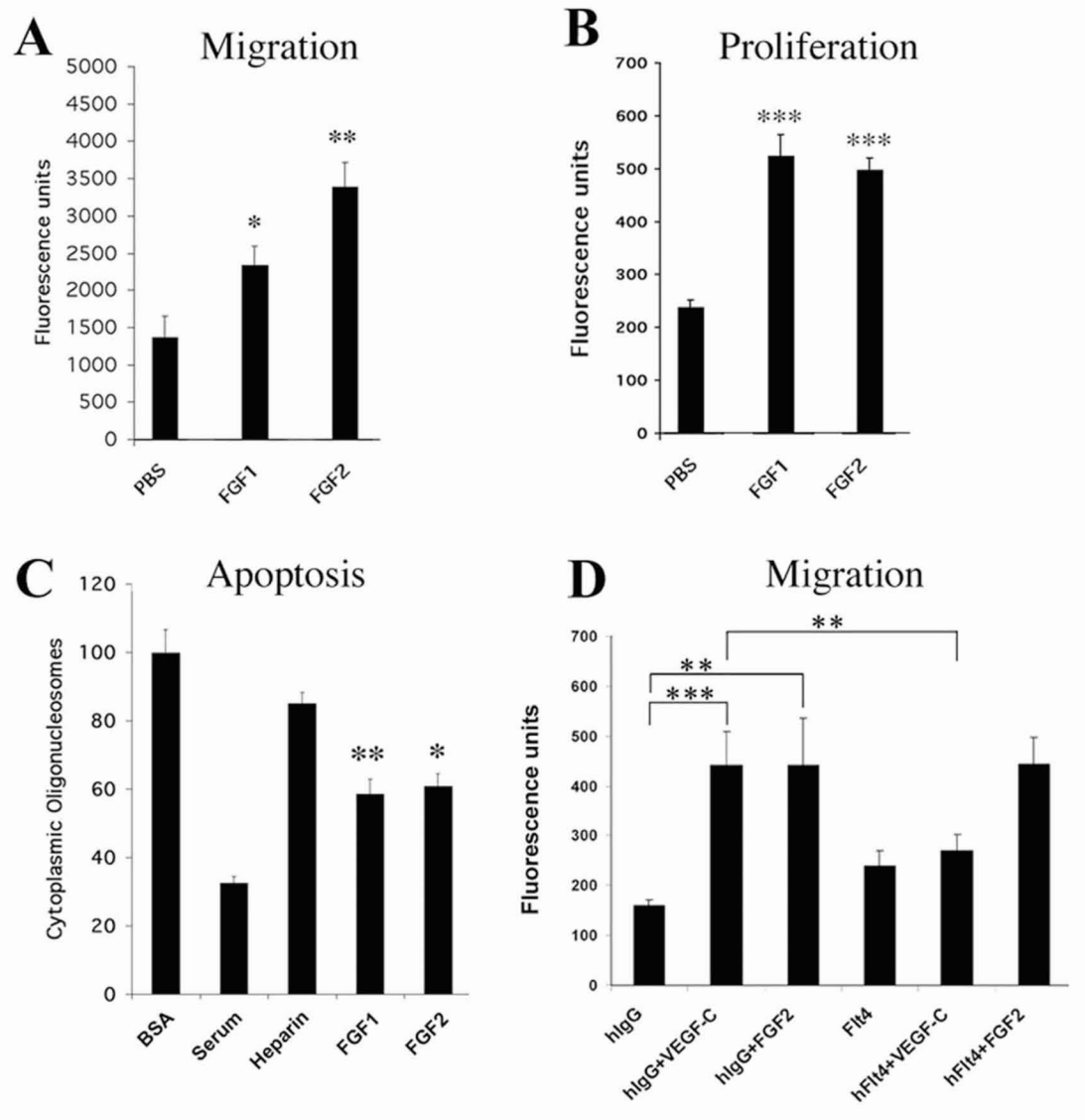
Figure 3.1.6 Stimulatory effects of fibroblast growth factors on proliferation, migration and survival of LECs. *(A) Migration of LECs was promoted by FGF-1 and FGF-2. Cells were allowed to migrate toward fibronectin in serum-free media containing FGF-1 or FGF-2 (10 ng/ml) in the presence of heparin (1 ug/ml). Numbers of migrated cells were quantified by fluorescence assay. (B) FGF-1 and FGF-2 stimulated LEC proliferation. LECs were treated with or without FGFs for 48 hours. Increase in cell numbers was determined using the MUH fluorescence assay. (C) FGF-1 and -2 (10 ng/ml) inhibit LEC apoptosis induced by serum depletion for 24h. Addition of 20% serum, but not of heparin alone, prevented LEC apoptosis. Data are expressed in % of BSA control and are shown as means±SD. (D) FGF-2 directly promoted LEC migration independently from VEGFR-3 activation. LEC migration was stimulated by VEGF-C (100 ng/ml) or FGF-2 (10 ng/ml), but the enhanced migration by VEGF-C was abrogated by addition of an anti-VEGFR-3 blocking antibody. *p<0.05, **p<0.01, ***p<0.001.*

3.1.3 Discussion

The homeodomain protein Prox1 plays an essential role in the lymphatic system development during embryogenesis as a master regulator that induces lymphatic lineage-specific differentiation (Hong & Detmar, 2003b; Hong et al, 2002; Petrova et al, 2002b; Wigle et al, 2002b; Wigle & Oliver, 1999). Furthermore, the LEC lineage-specification occurring during embryogenesis can be post-developmentally recapitulated when Prox1 is ectopically expressed in neonatal BECs (Hong & Detmar, 2003b; Hong et al, 2002; Petrova et al, 2002b). However, the molecular mechanisms underlying the cell fate decision controlled by Prox1 remained to be studied. In this report, we identified FGFR-3 as an initial Prox1 target gene during the early lymphatic system development. This upregulation is mediated at the transcriptional level by a direct binding of Prox1 to the specific sequence elements in the FGFR-3 promoter. Consistently, FGFR-3 is strongly expressed in the vein-derived lymphatically differentiating endothelial cells and in post-developmental lymphatic vessels in neonatal human foreskins. We also found that FGFR-3 plays an important role in mediating proliferating signals of LECs. Furthermore, our biochemical study demonstrated that FGF-2 bind to the low and high affinity receptors in LEC to promote migration, proliferation and cell survival of LECs independently of the VEGF-C/VEGFR-3 signal pathway.

Lymphatic endothelial cells are derived from venous endothelial cells that are of mesodermal origin. Our finding that Prox1 specifically upregulates the IIIc variant of FGFR-3, the major isoform in LEC, is consistent with previous studies that the IIIc forms of FGF receptors (FGFR-1 to -3) are mainly expressed by the mesenchymal lineage cells (Alarid et al, 1994; Orr-Urtreger et al, 1993; Yan et al, 1993). Interestingly, FGF receptors and their splicing variants exhibit strikingly distinct binding affinities to different FGF ligands (Ornitz & Itoh, 2001; Ornitz et al, 1992; Powers et al, 2000). As an example, the FGFR-3 IIIb isoform interacts with FGF-1, but not with FGF-2, FGF-4, or FGF-6, whereas the IIIc isoform is activated by all of these ligands to promote fibroblast proliferation (Kanai et al, 1997; Ornitz et al, 1996). Furthermore, FGFR-3 IIIc also displays a high affinity to FGF-8, FGF-17 and FGF-18 (Liu et al, 2002; Xu et al, 1999; Xu et al, 2000). Given these facts and our

findings presented here, upregulation of FGFR-3 IIIc by Prox1 in the LEC-specific fashion may be essential for mediating proliferation signals for the lymphatic system development, which may be distinct from signals for the blood vascular system development. This notion of differential proliferation signal is highly conceivable because only a subset of endothelial cells in the developing vein needs to be activated to proliferate and migrate out to form initial lymphatic vessels during embryogenesis. Therefore, FGFR-3 may be one of the major players in the molecular mechanism responsible for the LEC differentiation and subsequent lymphatic system development. Furthermore, the expression and maintenance of an additional FGF receptor may be also advantageous for the function of the lymphatic system. Because the lymphatic system plays essential roles in various aspects of the immune system, FGFR-3 may be important for cross talks between LECs and immune cells. It will be interesting to study the role of FGFR-3 during tissue repair, inflammation, and tumor development and metastasis.

We found that interaction of Prox1 with a specific DNA sequence element in the FGFR-3 promoter was necessary for the Prox1-mediated transcriptional activation of FGFR-3. The Prox1-binding sequences found in the FGFR-3 promoter consist of two overlapping consensus binding sequences of Prospero (Cook et al, 2003; Hassan et al, 1997). These sequence motifs, conserved between the mouse and human FGFR-3 genes, form a complex with purified GST-Prox1 protein and were sufficient to re-instate the Prox1-mediated transcriptional activation to a non-activating reporter vector. Previously, functional interactions of Prox1 with other transcriptional regulators were reported in the developing lens. The sequence-specific Six3 repressor antagonizes the Prox1 activation of the γ–crystallin promoter (Lengler et al, 2001). Similarly, Pax-6 occupies a specific sequence motif and prevents Prox1-mediated activation of the βB1-crystallin gene in chicken lens epithelial cells, whereas Prox1 binds to the same site to activate the gene in lens fiber cells (Cui et al, 2004). In contrast, Prox1 was shown to function as a corepressor of Ff1b, the Zebra fish homologue of mammalian steroidogenic factor-1 (SF-1) by a direct protein-protein interaction during embryonic development of the interrenal primordium (Liu et al, 2003b). It remains unknown if these Prox1 interacting partners also play a role in the development of the lymphatic system. Because Prox1 activates some genes but

represses others in lymphatically differentiating endothelial cells, it will be important to characterize transcriptional factors involved in this regulation during lymphatic development.

The VEGF-C/VEGFR-3 signaling was shown to play an essential role in the development of the lymphatic system (Karkkainen et al, 2004). Promotion of lymphangiogenesis by FGF-2 in mouse corneas was suggested to be mediated through upregulation of VEGF-C by stromal cells and FGF-2-induced corneal lymphangiogenesis was abrogated by a neutralizing antibody against VEGFR-3, the major receptor for VEGF-C (Chang et al, 2004; Kubo et al, 2002). In contrast, we found specific expression of FGFR-3 in LECs *in vitro* and *in vivo* and direct binding of FGF-2 to low- and high affinity receptors in LECs. In addition, we found that FGF-1 and FGF-2 can enhance migration, proliferation and survival of LECs and that the FGF-2-mediated activation of LEC migration is not dependent on the function of VEGFR-3. These results clearly indicate that these FGF ligands directly bind to their receptors in LEC and exert a direct role in lymphatic vessel formation. Nonetheless, our data do not rule out an indirect activation of FGF ligands through VEGFR-3 because our experiments involved only purified LECs, but not accompanying other stromal cells, the proposed source of VEGF-C (Chang et al, 2004; Kubo et al, 2002). Therefore, FGF ligands may exert their functions in multiple manners depending on the tissue microenvironment. Our finding that LECs expressed an additional FGF receptor is of particular interest because a recent study showed that lymphangiogenesis occurred at a low dosage of FGF-2 (12.5 ng), a concentration that did not induce accompanying angiogenesis in the mouse cornea assay (Chang et al, 2004). Therefore, it is conceivable that LECs may be more sensitive to FGF-2 stimulation than BECs due to expression of additional FGF receptors.

FGFR-3 has been previously shown to be essential for various developmental processes such as bone morphogenesis, inner ear development and alveogenesis in the lung (Ornitz & Marie, 2002; Weinstein et al, 1998). Because we found that FGFR-3 is a target gene of Prox1 and that Prox1 specifies lymphatic endothelial cell fate, we investigated if FGFR-3 mediates an inductive signal for lymphatic differentiation and found that knockdown of FGFR-3 mRNA significantly inhibited LEC proliferation.

This suggests that the receptor may play an important role in mediating cell proliferation during lymphatic system development. Our preliminary study indicates that the FGFR-3 null mice developed apparently normal lymphatic capillaries in the skin. We believe that this is most likely due to functional complementation by other FGF receptors. This notion of functional cooperation among FGF receptors is further supported by a study of the FGFR-3 and FGFR-4 double knockout mice (Weinstein et al, 1998). Homozygous $fgfr-3^{-/-}fgfr-4^{-/-}$ mutant mice displayed abnormal alveogenesis during lung development, a phenotype that was not present in single knockout mutants, suggesting that the two FGF receptors function together to direct normal lung development. It will be of great interest to evaluate lymphatic vessel development in the $fgfr-3^{-/-}fgfr-4^{-/-}$ mutant mice. Furthermore, mice lacking FGF-18 display a similar mutant phenotype in bone morphogenesis as FGFR-3 null mice, defining FGF-18 as a physiological ligand for FGFR-3 during bone development (Liu et al, 2002). It will be also interesting to see whether FGF-18 single or FGFR-3/FGF-18 double knockout mice develop a normally functioning lymphatic system.

3.2 Quantification of vascular lineage-specific differentiation and molecular characterization of *in vivo* (lymph)angiogenesis by a novel low-density microvascular differentiation array

3.2.1 Introduction

The formation and activation of blood vascular and lymphatic endothelium have an important role in the progression and metastasis of the majority of human cancers (Alitalo et al, 2005; Carmeliet, 2003). Tumors need to induce the growth of new blood vessels (angiogenesis) in order to secure the sufficient supply of oxygen and nutrients, and the growth of new lymphatic vessels (lymphangiogenesis) has been shown to promote cancer metastasis to sentinel lymph nodes and beyond (Hirakawa et al, 2006; Hirakawa et al, 2005b; Mandriota et al, 2001; Skobe et al, 2001; Stacker et al, 2001). Recent studies indicate that both types of endothelium are also involved in chronic inflammatory diseases such as rheumatoid arthritis, inflammatory bowel disease and psoriasis (Alitalo et al, 2005; Carmeliet, 2003; Cueni & Detmar, 2006b). As a result, there has been a surge of interest in identifying novel targets that can be used to specifically image these processes and to target them therapeutically. However, these types of studies have been hampered by the lack of identified lymphatic-specific markers and growth factors.

The lymphatic system is a unidirectional vascular network that drains fluids and cells from peripheral tissues and attracts and transports antigen-presenting cells to mediate the afferent immune response (Oliver & Detmar, 2002). During embryonic development, lymphatic progenitor cells bud off from embryonic veins under the influence of the transcription factor Prox1, migrate, form lymph sacs and eventually form mature lymphatic vessels (Alitalo et al, 2005; Oliver, 2004). Lymphatic endothelial cells (LEC) and blood vascular endothelial cells (BEC) therefore share a large number of common endothelial lineage genes, and there are only a few specific known marker genes, such as the hyaluronan receptor LYVE-1 (Prevo et al, 2001) and the mucin-type glycoprotein podoplanin (Schacht et al, 2003), that distinguish lymphatic vessels from blood vessels (Cueni & Detmar, 2006b).

There have been previous attempts to identify the lineage-specific transcriptomes of LEC and BEC using gene microarrays (Hirakawa et al, 2003; Petrova et al, 2002a; Podgrabinska et al, 2002). However, the arrays used in these analyses included an incomplete set of human genes and a large-scale confirmation of the results by other methods has not been attempted. Gene expression profiling is a time-consuming, relatively expensive process that requires specialized equipment, so it is not practical for use in characterizing the (lymph)angiogenic activity of tissues samples. A simple and rapid assay for the quantitative analysis of *in vitro* vascular differentiation, and of angiogenesis and lymphangiogenesis in tissue samples would provide a major technological advance for research and clinical analysis.

We aimed to comprehensively identify the lineage-specific transcriptomes of primary human LEC and BEC. In this study, we used the Applied Biosystems Human Genome Survey v.2 (AB-HGS), which includes almost all of the known human genes, to identify lymphatic and blood vascular signature genes.

Using the LEC and BEC genes identified, we developed a novel, TaqMan RT-PCR based low-density microvascular differentiation array (LD-MDA) in a microfluidic card format to allow for the simultaneous quantification of 96 genes. Using the LD-MDA we were able to reproducibly identify and quantify the differentiation of LEC and BEC cells *in vitro* based on expression levels of the genes analyzed in the assay. We then designed and developed a computational algorithm to systematically identify genes associated with (lymph)angiogenic activity in tissues samples obtained from patients with the chronic inflammatory skin disease.

3.2.2 Results

3.2.2.1 *Comprehensive identification of vascular lineage-specific gene signatures*

We first analyzed the transcriptional profiles of three matched pairs of LEC and BEC using the AB-HGS microarrays. Genes that were expressed at ≥ 2-fold higher levels in LEC than in BEC (and vice versa) in all three independent pairs of LEC-BEC were

considered to be endothelial lineage-specific signature genes. Based on these criteria we identified a total of 236 LEC signature genes (upregulated ≥2-fold in LEC) and 342 BEC signature genes (upregulated ≥2-fold in BEC) (**Appendix Table 1**). Genes that were highly expressed specifically by LEC included previously identified LEC-associated genes such as Prox1, podoplanin, carcinoembryonic antigen-related cell adhesion molecule-1 (CEACAM1) and soluble guanylate cyclase 1 alpha 3, and genes whose expression was not before associated with LEC, including dipeptidyl peptidase IV (DPPIV) and collectin 12 (COLEC12) (**Table 3.2-1a**). We also identified several BEC signature genes that had not been previously associated with this cell type, including urokinase plasminogen activator (PLAU), membrane metallo-endopeptidase (MME) and endothelial lipase (LIPG) (**Table 3.2-1b**). Together, these results establish a more comprehensive catalogue of endothelial lineage-specific gene signatures.

Table 3.2-1a Top 40 LEC signature genes in all three matched-pair samples by microarray (sorted by median)

LEC gene signature		AB probe ID	Fold change		
Symbol	Gene name		Sample 1	Sample 2	Sample 3
GUCY1A3	guanylate cyclase 1, soluble, alpha 3	170165	497.26	154.95	83.6
GUP1	GRINL1A complex upstream protein	104996	193.23	13.75	9.04
HS3ST1	heparan sulfate (glucosamine) 3-O-sulfotransferase 1	154628	189.98	9.13	2.51
PDK4	pyruvate dehydrogenase kinase, isoenzyme 4	101060	175.09	12.45	14.72
CH25H	cholesterol 25-hydroxylase	117883	130.44	3.56	15.25
MRC1	mannose receptor, C type 1	198568	119.37	6.39	15.29
GIMAP5	GTPase, IMAP family member 5	177981	97.71	6.23	5.6
EDNRB	endothelin receptor type B	150558	83.94	6.56	9.16
HYAL1	hyaluronoglucosaminidase 1	184118	75.23	5.75	7.2
RBP1	retinol binding protein 1, cellular	149921	69.97	13.94	7.51
C6orf123	chromosome 6 open reading frame 123	105756	69.4	10.64	7.36
C2orf23	chromosome 2 open reading frame 23	156624	68.65	13.48	7.75
DKFZP586A0522	DKFZP586A0522 protein	107957	64.69	4.03	12.63
ST6GALNAC3	ST6...N-acetylgalactosaminide alpha-2,6-sialyltransferase 3	189728	55.54	3.78	4.99
CEACAM1	carcinoembryonic antigen-related cell adhesion molecule 1	219223	50.13	11.73	3.9
CD36	CD36 antigen (collagen type I receptor, thrombospondin receptor)	121773	49.85	4.44	10.57
DNASE1L3	deoxyribonuclease I-like 3	167226	49.27	2.55	51.27
SEPP1	selenoprotein P, plasma, 1	169984	48.97	6.42	8.18
IQCA	IQ motif containing with AAA domain	152027	46.85	11.54	4.4
CETP	cholesteryl ester transfer protein, plasma	140569	45.16	3.66	2.84
TFF3	trefoil factor 3 (intestinal)	114445	44.84	8.11	12.68
ADAMTSL3	ADAMTS-like 3	158085	43.95	2.18	25.43
XLKD1	extracellular link domain containing 1	195865	43	0.98	2.01
RBM35B	RNA binding motif protein 35B	167987	41.06	10.21	14.62
TMEM88	transmembrane protein 88	200951	40.58	3.49	5.61
COLEC12	collectin sub-family member 12	114422	39.34	17.2	6.12
CYP1A1	cytochrome P450, family 1, subfamily A, polypeptide 1	135086	39.01	3.21	6.51
PROX1	prospero-related homeobox 1	124383	38.93	6.77	9.56
PPARG	peroxisome proliferative activated receptor, gamma	192239	37.79	60.22	10.05
ZNF467	zinc finger protein 467	184463	36.77	8.26	2.84
GMFG	glia maturation factor, gamma	180184	36.59	2.91	7.12
DPP4	dipeptidylpeptidase 4 (CD26)	209451	35.86	21.59	12.1
ABCA4	ATP-binding cassette, sub-family A (ABC1), member 4	194955	35.51	26.3	7.15
IL7	interleukin 7	127208	34.58	2.55	17.78
PCSK6	proprotein convertase subtilisin/kexin type 6	154864	32.87	3.79	4.71
TRPC6	transient receptor potential cation channel, subfamily C, member 6	101144	32.12	3.07	9.43
PDPN	podoplanin	219722	30.81	2.48	5
C17orf28	chromosome 17 open reading frame 28	115291	29.54	5.41	2.52
MAF	v-maf musculoaponeurotic fibrosarcoma oncogene homolog	186589	28.43	10.69	4.2
C18orf30	chromosome 18 open reading frame 30	171508	28.33	2.77	4.66

Table 3.2-1b Top 40 BEC signature genes in all three matched-pair samples by microarray (sorted by median)

BVEC gene signature			Fold change		
Symbol	Gene name	AB probe ID	Sample 1	Sample 2	Sample 3
COL6A3	collagen, type VI, alpha 3	115643	884.5	44.24	2.82
ADAMTS1	a disintegrin-like and metalloprotease with thrombospondin type 1 motif, 1	216353	477.78	45.43	4.4
COL1A2	collagen, type I, alpha 2	105493	344.17	86.94	3.29
CRISPLD2	cysteine-rich secretory protein LCCL domain containing 2	170538	331.32	29.54	5.35
BEX1	brain expressed, X-linked 1	137034	250.21	88.31	7.02
GPNMB	glycoprotein (transmembrane) nmb	161212	236.81	20.27	4.14
PTGFR	prostaglandin F receptor (FP)	103022	207.64	6.58	5.69
PLAU	plasminogen activator, urokinase	208672	165.63	6.01	126.53
CDH2	cadherin 2, type 1, N-cadherin (neuronal)	187321	163.67	5.19	17.45
NRG1	neuregulin 1	223108	159.16	13.42	8.43
AMIGO2	amphoterin induced gene 2	154434	157	7.48	3.03
GFPT2	glutamine-fructose-6-phosphate transaminase 2	113797	155.06	66.02	3.64
OXTR	oxytocin receptor	200205	155.01	23.39	3.5
FAP	fibroblast activation protein, alpha	164725	131.07	47.35	46.66
GLIPR1	GLI pathogenesis-related 1 (glioma)	117689	118.71	32.66	9.84
MME	membrane metallo-endopeptidase (CALLA, CD10)	197353	117.83	4.74	9.82
CSPG2	chondroitin sulfate proteoglycan 2 (versican)	207524	117.52	21.87	4.79
SYTL2	synaptotagmin-like 2	118410	115.03	22.51	17.59
LOXL1	lysyl oxidase-like 1	156579	102.71	8.15	17.68
PCSK1	proprotein convertase subtilisin/kexin type 1	213177	96.18	8.44	91.13
RGS4	regulator of G-protein signalling 4	165955	93.55	15.49	10.88
FLT1	fms-related tyrosine kinase 1	219494	93.14	21.3	35.73
C7orf10	chromosome 7 open reading frame 10	180432	86.96	15.46	13.27
SHRM	shroom	207317	84.74	10.08	3.83
LOC152573	hypothetical protein BC012029	150646	70.98	8.95	34.85
BASP1	brain abundant, membrane attached signal protein 1	198318	69.8	7.59	25.75
COL5A1	collagen, type V, alpha 1	110570	68.34	5.66	30.97
EMP3	epithelial membrane protein 3	152376	64.94	11.72	14.52
COL6A1	collagen, type VI, alpha 1	215580	63.74	4.99	4
IL1RL1	interleukin 1 receptor-like 1	131513	62.75	36.34	24.5
VEGFC	vascular endothelial growth factor C	170337	59.63	10.14	5.56
LIPG	lipase, endothelial	200619	59.54	112.03	50.64
LCP1	lymphocyte cytosolic protein 1 (L-plastin)	175091	57.18	4.02	12.13
TAGLN	transgelin	172572	56.92	6.98	47.13
NUDT11	nudix (nucleoside diphosphate linked moiety X)-type motif 11	125359	56.13	7.6	9.85
FAM20C	family with sequence similarity 20, member C	199772	54.95	8.38	2.06
FAT	FAT tumor suppressor homolog 1 (Drosophila)	131558	54.78	54.6	8.65
IL7R	interleukin 7 receptor	200834	54.27	7.7	2.93
TCEAL7	transcription elongation factor A (SII)-like 7	130055	53.18	9.41	17.62

3.2.2.2 *Identification of lineage-specific biological functions by in silico analysis*

We next investigated whether the establishment of comprehensive LEC and BEC gene signatures could be used to identify lineage-specific biological functions for each cell type using *in silico* molecular pathway analysis. We found that genes involved in fatty acid, cholesterol and steroid metabolism were significantly over-

represented among LEC signature genes (P < 0.0005), as compared with BEC signature genes (**Table 3.2-2**). In contrast, genes involved in angiogenesis and blood clotting were significantly over-represented among the BEC signature genes (P < 0.005) but not among the LEC signature genes. Genes involved in cell adhesion, immunity and defense, and cell structure and motility were overrepresented in both the LEC and BEC signatures (P < 0.05), indicating common biological functions of both endothelial cell types (**Table 3.2-2**).

Table 3.2-2 Biological process analysis of LEC and BEC signature genes using the Panther Classification System

Biological Process	LEC genes (226)	expected	p-value	BVEC genes (337)	expected	p-value
LEC-specific biological process						
Carbohydrate metabolism	15	4.5	***	7	6.72	ns
Cell cycle control	12	3.06	***	6	4.57	ns
Lipid, fatty acid and steroid metabolism	17	6.04	***	10	9.01	ns
mRNA transcription	27	13.76	***	19	20.51	ns
Nucleoside, nucleotide and nucleic acid metabolism	40	24.68	**	31	36.8	ns
Embryogenesis	5	1.04	**	3	1.56	ns
Neuronal activities	11	4.35	**	10	6.49	ns
BVEC-specific biological process						
Cell adhesion-mediated signaling	6	2.76	ns	22	4.12	***
Skeletal development	1	0.95	ns	12	1.42	***
Proteolysis	11	7.1	ns	25	10.59	***
Extracellular matrix protein-mediated signaling	0	0.51	ns	6	0.76	***
Angiogenesis	2	0.42	ns	5	0.63	***
Blood clotting	1	0.68	ns	5	1.02	**
MAPKKK cascade	4	1.41	ns	7	2.1	**
Endothelial cell-specific biological process						
Signal transduction	63	25.45	***	92	37.95	***
Developmental processes	48	15.99	***	61	23.84	***
Neurogenesis	16	4.35	***	18	6.48	***
Cell proliferation and differentiation	22	8.01	***	26	11.94	***
Cell communication	23	8.9	***	52	13.28	***
Protein modification	20	8.75	***	22	13.04	*
Oncogenesis	11	3.51	***	20	5.23	***
Receptor protein tyrosine kinase signaling pathway	7	1.61	**	6	2.4	*
Cell adhesion	12	4.28	**	31	6.39	***
Protein phosphorylation	13	5.09	**	17	7.59	**
Tumor suppressor	4	0.69	**	8	1.03	***
Cell structure and motility	18	9.32	**	30	13.89	***
Cytokine and chemokine mediated signaling pathway	6	1.93	*	7	2.88	*
Immunity and defense	19	11.34	*	34	16.91	***

*** p-value < 0.0005, ** p-value < 0.005, * p-value < 0.05, ns = not significant

3.2.2.3 *Using the LD-MDA to quantify lineage-specific endothelial cell differentiation*

We next aimed to develop a simple and rapid assay to quantify the degree of lineage-specific differentiation in human endothelial cell samples. We selected 54 genes from the LEC signature and 31 genes from the BEC signature, based upon the degree of specificity determined by array analysis and their potential function (**Appendix Table 1**), and 5 pan-endothelial genes, which are strongly expressed in both cell types (PECAM-1, vWF, KDR, Tie2 and CDH5) as general markers of endothelial lineage differentiation. The expression of these genes and of 6 housekeeping genes were quantified in the TaqMan-based low-density LD-MDA using 384-well microfluidic cards. Using this array, the differential expression levels of all 85 LEC and BEC signature genes were confirmed using mRNA from same three matched pairs of LEC and BEC that were used for the gene array studies (**Appendix Table 1**).

We next investigated whether the LD-MDA might be used to quantify the level of differentiation among different endothelial cell types. The LD-MDA was performed on 10 primary human dermal LEC and 8 human dermal BEC samples previously isolated in our laboratory. Additional samples included human dermal microvascular endothelial cells (HDMEC; n = 2), human umbilical vein endothelial cells (HUVEC; n = 2), the immortalized HDMEC cell line HMEC-1, HaCaT keratinocytes and dermal fibroblasts. We established an 'endothelial lineage score' (ELS) by subtracting the sum of the normalized cycle values (ΔCt) of all 54 LEC-specific genes from the sum of the ΔCt values of all 31 BEC-specific genes. As a measure for the degree of endothelial cell differentiation, the sum of the ΔCt values of the five pan-endothelial marker genes was calculated for each sample and defined as vascular lineage score (VLS). This analysis revealed that all LEC samples clustered together, with ELS scores ranging from 98 to 442, whereas the BEC samples had ELS scores ranging from 825 to 1107 (**Fig. 3.2.1A**). ELS scores for HUVEC fell into the BEC range (1089 and 1081, respectively), in agreement with the blood vascular origin of HUVEC. In contrast, the HMEC-1 cell line had a higher VLS score (96) than the BEC (32-57). This was likely because of the lower levels of expression of the pan-

endothelial markers VE-cadherin, VEGFR-2 and vonWillebrand factor in the HMEC-1 cell line. The two non-endothelial cell types (keratinocytes and dermal fibroblasts) had ELS scores of 987 and 1317 and VLS scores of 179 and 195, respectively, clearly discriminating them from the endothelial cell lines tested in the LD-MDA.
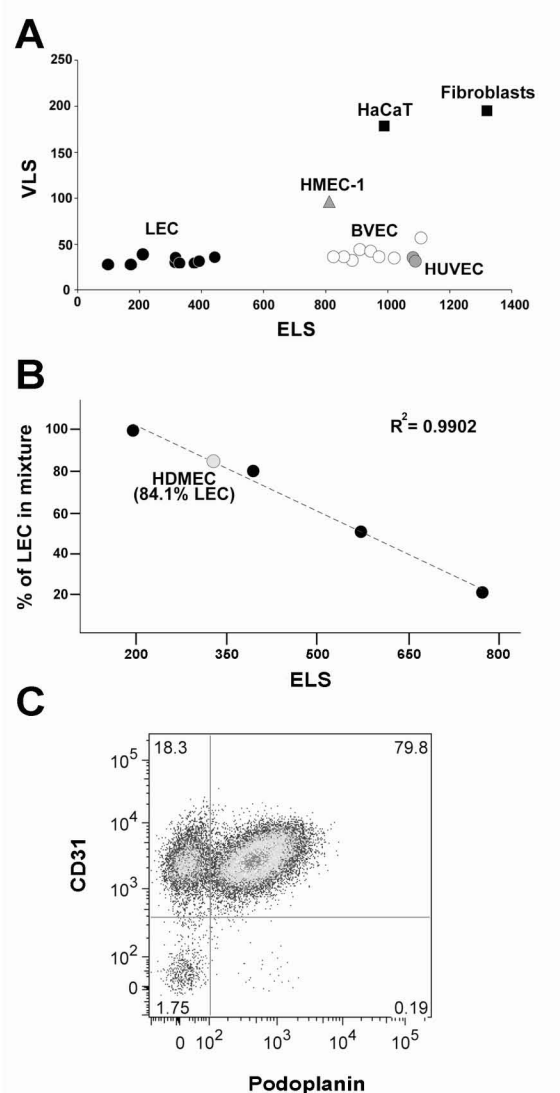
Figure 3.2.1 Quantification of lineage-specific gene expression and differentiation of endothelial and non-endothelial cell types using LD-MDA. *(A) LD-MDAs were performed on total RNA obtained from 10 different primary human LEC (black circles), from 8 BEC (white circles), from 2 HUVEC (grey circles), from HMEC-1 (grey triangle), from HaCaT keratinocytes and from dermal fibroblasts (black squares). Determination of the endothelial lineage score (ELS) and of the vascular lineage score (VLS) revealed that all LEC samples clustered together, whereas the BEC samples were clearly distinguished by their higher ELS scores. ELS scores for HUVEC were indistinguishable from BEC, whereas immortalized HMEC-1 cells did not cluster with BEC, because of their higher VLS score. Keratinocytes and fibroblasts were clearly discriminated from all endothelial cells, based on their VLS scores. (B) Analysis of defined mixtures of LEC and HUVEC by LD-MDA revealed that the distribution of the samples (mixtures) on the ELS-axis showed a linear correlation to the percentage of LEC in each sample ($R^2 = 0.9902$). Using the equation Y (% of LEC) = -1.0865x+3.9474, the percentage of LEC in the examined HDMEC was predicted as 84.1 %. (C) Flow cytometry analysis of the same HDMEC sample stained for the panendothelial marker CD31 and for the LEC-specific marker podoplanin revealed that HDMEC contained approximately 80% LEC.*

To further test this technology, defined mixtures of LEC and HUVEC (percent of LEC: 100, 80, 50, 20, and 0) were analyzed by LD-MDA. The distribution of the samples (mixtures) on the ELS score was indeed proportionally correlated to the percentage of LEC in each sample (**Fig. 3.2.1B**). To investigate whether the LD-MDA could also be used to quantify the percentage of LEC in HDMEC cultures, which represent a mixture of LEC and BEC, we used LD-MDA data from the mixtures of LEC and HUVEC as a standard to derive the linear relationship between ELS and the percentage of LEC in the mixture. A strong linear relationship was identified with R^2 = 0.9902 and the equation of Y (% of LEC) = -1.0865x + 3.9474 (**Fig. 3.2.1B**). Using this equation, we were able to predict the percentage of LEC in a representative HDMEC culture as 84.1 %. Importantly, this prediction - based on the LD-MDA data that were derived from mRNA expression levels - was confirmed at the level of protein expression because FACS analysis revealed that approximately 80% of HDMEC were CD31-positive/podoplanin-positive LEC (**Fig. 3.2.1C**). Together, these findings indicate that the LD-MDA is a new tool for quantifying the degree of endothelial lineage-specific differentiation of cultured cells and for determining the purity of endothelial cell cultures.

3.2.2.4   *Hierarchical clustering according to endothelial lineage-specific gene signatures*

We next asked whether a subset of genes might be identified that shows the most consistent lineage-specific expression. Thirty-nine out of 95 genes selected for the LD-MDA had little variation in expression levels between different samples of the same cell type, but large differences in expression levels between LEC and BEC (**Appendix Table 1**). Based on the expression levels of these core differentiation genes, hierarchical clustering separated the different cell types into four distinct clusters: LEC, BEC, HMEC-1 and non-endothelial cells (**Fig. 3.2.2**). We also identified four groups of genes that were expressed at high levels in one cell type (LEC versus BEC) and at moderate or low levels in another cell type, or that were expressed at moderate levels but were not expressed at all by the other cell type.
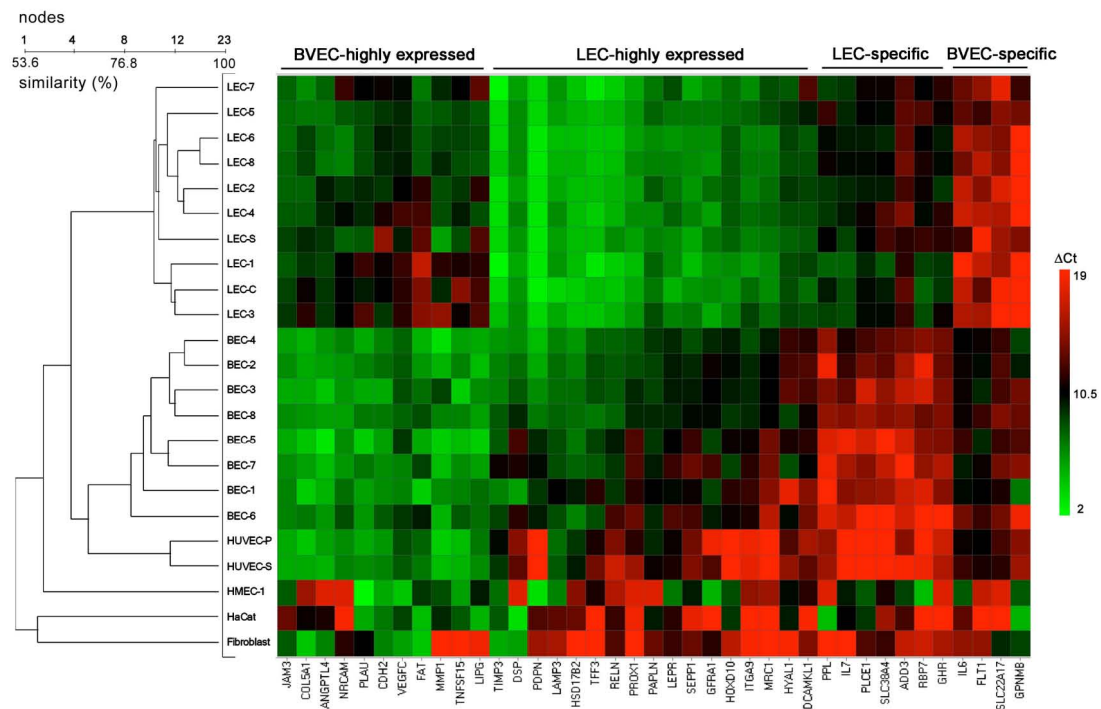
Figure 3.2.2 Hierarchical clustering according to endothelial lineage-specific gene signatures. *Hierarchical clustering, based on the expression levels of 39 core differentiation genes, separated the different cell types into four distinct clusters: LEC, BEC, HMEC-1 and non-endothelial cells. HUVEC cells were separated slightly from the BEC cluster. Two groups of genes were identified for each of the LEC/BEC pairs that were either expressed at high levels in one cell type and at moderate–low levels in the other cell type ("highly expressed genes") or expressed at moderate levels in one cell type and not expressed by the other cell type ("specific genes").*

3.2.2.5 *Identification of (lymph)angiogenic-mediators using a novel Prediction Relevance Ranking analysis*

We next investigated whether the LD-MDA could be used to identify key endothelial signature genes associated with *in vivo* inflammation by quantitatively profiling 43 samples obtained from psoriatic skin lesions. Psoriasis is a chronic inflammatory skin disease with prominent angiogenesis and lymphangiogenesis(Kunstfeld et al, 2004). Half of the skin samples were subjected to differential immunofluorescence analyses by staining for the lymphatic marker LYVE-1 and for the vascular marker CD31 (**Fig. 3.2.3A-D**). The computer-assisted morphologic analysis revealed different degrees of expansion of the dermal lymphatic and blood vascular networks amongst psoriatic lesions, as evaluated by the relative tissue area occupied by lymphatic or blood vessels (**Fig. 3.2.3E**). RNA was isolated from the other half of each sample and was subjected to expression quantification by LD-MDA. We used a Prediction Relevance

Ranking (PRR) analysis to learn all possible models up to degree four:
$$\sum_{k=1}^{4}\binom{90}{k} = 2,676,765$$
. PRR characterized the whole model space and provided a

ranking of the most predictive genes for each of the two targets: lymphatic vessel area (LVA) and blood vessel area (BVA) (**Fig. 3.2.3F**). In addition to PRR analysis, we partitioned the samples into four groups by using the median of LVA and BVA as thresholds. We then applied analysis of variance (ANOVA) to assess the influence of specific genes within these groups. Comparing the group with low LVA and low BVA (**Fig. 3.2.3E;** quadrant IV) against the group with high BVA (**Fig. 3.2.3E;** quadrants II+III) revealed a potential involvement of FLT1, FGF12, ADD3, ALDH1A1, MRC1 and IL7R in inflammatory angiogenesis (**Fig. 3.2.3F).** Furthermore, comparing the group with low LVA and low BVA (**Fig. 3.2.3E;** quadrant IV) against the group with high LVA (**Fig. 3.2.3E;** quadrants I+II) revealed involvement of FLT1, FGF12, IL7R, ADD3, MRC1, INHBA, CDH11, LMO2, RELN and KDR in inflammatory lymphangiogenesis (**Fig. 3.2.3F**). Comparing PRR and ANOVA results revealed FGF12, IL7R and FLT1 as the most significant factors involved. Since FGF12 or IL7 had not been previously implicated in (lymph)angiogenesis, we next treated cultured human LEC and BEC with FGF12 or IL7 and investigated their effects on cellular proliferation. We found that both IL7 and FGF12 significantly induced the proliferation of LEC and of BEC (**Fig. 3.2.3G, H**).
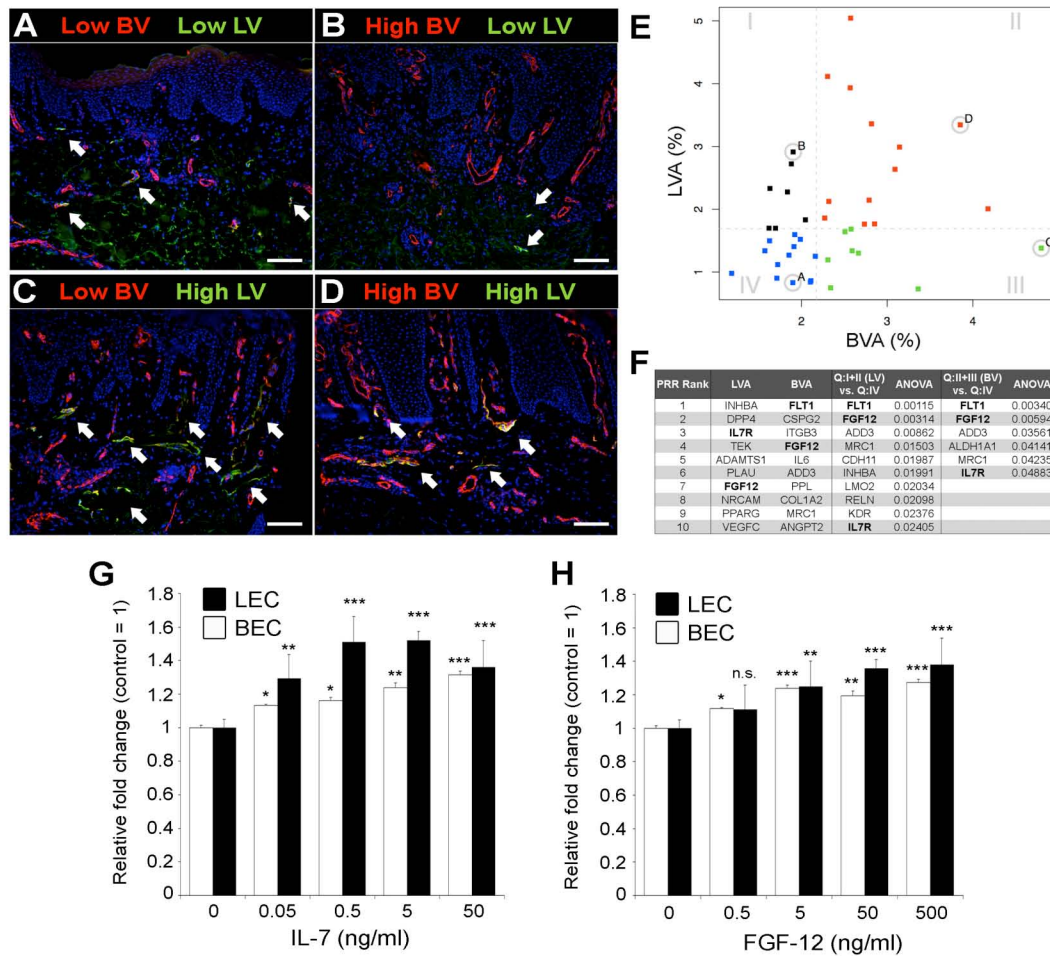
Figure 3.2.3 Identification of (lymph)angiogenic-mediators using Prediction Relevance Ranking test and ANOVA *(A-D) Differential immunofluorescence analysis of psoriatic lesional skin stained for the lymphatic marker LYVE-1 (green; arrows) and for the vascular marker CD31 (red) revealed 4 different patterns: Samples with low blood vessel and lymphatic vessel expansion (**A; quadrant IV in panel E**), strong blood vessel but low lymphatic vessel expansion (**B; quadrant III in panel E**), low blood vessel but strong lymphatic vessel expansion (**C; quadrant I in panel E**) and strong blood vessel and lymphatic vessel expansions (**D; quadrant II in panel E**). Scale bars: 100 µm. BVA = tissue area covered by blood vessels (in %). LVA = tissue area covered by lymphatic vessels (in %). (**F**) Comparative analysis of Prediction Relevance Ranking (PRR) and ANOVA ranking, based on mRNA gene expression profiles of 43 psoriasis skin lesions, revealed FLT1, FGF12, IL7R (bold) to be significantly overrepresented in these analyzes as (lymph)angiogenic-mediators. (**G, H**) Treatment with IL-7 or with FGF-12 for 48 h dose-dependently promoted cellular proliferation of LEC (filled bars) and of BEC (open bars). ***P-value < 0.0005; **P-value < 0.005; *P-value < 0.05.*

3.2.3 Discussion

We have established the first complete lineage-specific transcriptome of cultured human LEC and compared it with that of BEC. Analysis of the molecular pathways associated with the transcriptome of each cell type revealed lineage-specific functions. Furthermore, we developed the LD-MDA to quantify expression of vascular lineage-specific genes in various endothelial cell types and we identified two

novel mediators of (lymph)angiogenesis that are associated with the extent of vascular expansion in the chronic inflammatory skin disease psoriasis.

Using microarray analyses of three matched pairs of human LEC and BEC, we were able to comprehensively characterize the vascular lineage-specific transcriptome of human endothelial cells, and to identify 342 BEC and 236 LEC signature genes. We reliably detected a number of known BEC-specific (Hirakawa et al, 2003; Hong et al, 2004b; Petrova et al, 2002a) and LEC-specific markers (Prevo et al, 2001; Schacht et al, 2003; Wigle et al, 2002a), as well as a number of previously unknown vascular lineage markers (Hirakawa et al, 2003; Petrova et al, 2002a; Podgrabinska et al, 2002). Several of these genes, such as IL7 and glia maturation factor-gamma, might have important roles in endothelial lineage-specific differentiation and development. In fact, mutations in one of the differentially expressed genes in LEC signatures genes, SOX18, cause recessive and dominant forms of hypotrichosis-lymphedema-telangiectasia syndrome(Irrthum et al, 2003). Although a large number of novel lymphatic-specific and blood vascular-specific gene have been identified, more functional characterization of these genes need to be performed.

In silico analysis of the biological pathways associated with LEC and BEC-specific genes revealed that LEC significantly overexpress genes associated with fatty acid and steroid and cholesterol metabolism. These findings are in agreement with the important role of intestinal lymphatic vessels in the uptake of lipids and with recent results observed in mice that are deficient in the lymphatic-specific transcription factor Prox1. Mice with a targeted disruption of Prox1 in the lymphatic endothelium accumulate fat in lymphatic-rich regions (Harvey et al, 2005). Prox1 might therefore directly control the expression of LEC genes involved in lipid metabolism. It has been previously shown that cholesterol 25-hydroxlyase, one of the genes identified in this study as LEC-specific, was strongly up-regulated in cultured endothelial cells transfected with a Prox1-expressing adenoviral vector (Petrova et al, 2002a).

Previously, endothelial cells derived from large vessels such as HUVEC and from microvessels such as HDMEC were believed to have distinct biological functions (Li et al, 2002; Prabhakarpandian et al, 2001; Unger et al, 2002). Our analysis of these

cell types using LD-MDA indicates that differences observed in these cell types might have been caused by varying admixtures of lymphatic and blood vascular endothelial cells in HDMEC preparations, whereas HUVEC are purely of blood vessel origin. So the molecular, transcriptional and functional differences observed between the endothelial cells of small and large vessels should be reevaluated, in light of our findings that LEC represent the majority of cells (at varying percentages, data not shown) in commercially available HDMEC preparations. We advice the routine analysis of the degree of endothelial lineage-specific differentiation that has occurred in each batch of commercial HDMEC, as a quality control step, before these cells are used for research applications. It might also be necessary to evaluate the endothelial cell lines that have been used in previous studies. Using the LD-MDA, we showed that the widely used immortalized HMEC-1 cell line (Ades et al, 1992) has lost several key endothelial-specific characteristics. Results obtained from studies with HMEC-1 should therefore be cautiously interpreted, with regard to their potential relevance to primary endothelial cells. In this regard, the LD-MDA could serve as an easy and reliable tool for quality control analysis of human endothelial cell samples.

Over the recent years, applications of bioinformatics and statistics have generated powerful methods to manage and interpret data, and even to create a statistical model for the prognosis of diseases (Spira et al, 2007; Yu et al, 2008). However, the classical approaches to report only one "best" model failed to characterize the whole model space. High correlations between markers often lead to not only one but also a group of models that perform equally well regarding their predictive power. Hence, the results which report only one of these models are often misleading by ignoring equally good marker combinations. The Prediction Relevance Ranking (PRR) analysis circumvents such problem by counting the number of times each variable shows up in all possible significant models, however, it comes with the drawback of high computation times. Therefore PRR is not suitable for large datasets such as microarrays but it is preferable for biological and clinical datasets which often exhibit a small number of features.

IL7R was identified by PRR and ANOVA as a factor with potential involvement in the mediation of inflammatory angiogenesis and lymphangiogenesis. Previous reports

shown that human microvascular endothelial cells express IL7R, the receptor for IL7(Dus et al, 2003). However, our study demonstrates that human microvascular endothelial cells represent a mixture of both lymphatic and blood vascular endothelium. Based on the LD-MDA analyses of a large number of LEC and BEC, we found that IL7R is indeed more strongly expressed by BEC whereas its ligand IL7 is preferentially expressed by LEC. IL7R is also expressed by myeloid lineage cells and can mediate the production of pro-inflammatory cytokines by monocytes/macrophages (Kilroy et al, 2007; Moller et al, 1996), however, the effect of IL7 on endothelial cells has remained unclear. Our functional *in vitro* studies reveal that IL7 significantly promotes the cellular proliferation of blood vascular and lymphatic endothelium. In this study, we found that FGF12 expression was highly associated with angiogenesis and lymphangiogenesis during chronic inflammation. The specific functions of FGF12 have not yet been determined; however FGF receptors are expressed by vascular endothelium (Suhardja & Hoffman, 2003), and our *in vitro* functional studies show that FGF12 induces LEC and BEC proliferation. These findings indicate that FGF12 and/or IL7 might represent novel therapeutic targets for the treatment of psoriasis and, possibly, other chronic inflammatory diseases that are characterized by extensive angiogenesis and lymphangiogenesis.

3.3   <u>Lymphatic-specific expression of dipeptidyl peptidase IV and its dual role in lymphatic endothelial function</u>

3.3.1 Introduction

The lymphatic vascular system is an open-ended network of endothelial cell-lined vessels that transport extravasated fluid, proteins, metabolites and cells from the interstitial space back to the circulatory system via the thoracic duct (Oliver & Detmar, 2002). Moreover, the lymphatic vascular system also serves as the primary conduit for malignant tumor cell metastasis to regional lymph nodes, and induction of lymphangiogenesis by tumors actively promotes cancer metastasis (Dadras et al, 2005; Hirakawa et al, 2005b; Oliver & Detmar, 2002). There is increasing evidence that lymphatic vessels also actively participate in acute and chronic inflammation. The chronic inflammatory skin disease psoriasis is characterized by pronounced cutaneous lymphatic hyperplasia (Kunstfeld et al, 2004). Kidney transplant rejection is frequently accompanied by lymphangiogenesis (Kerjaschki et al, 2006) and lymphangiogenesis has also been observed in experimental models of chronic airway inflammation (Baluk et al, 2005). However, the molecular mediators of lymphatic vessel activation have remained poorly characterized.

During embryonic development, the transcription factor Prox1 plays a major role in the differentiation and sprouting of lymphatic progenitor cells from the cardinal veins (Hong & Detmar, 2003a). Beginning at embryonic day (E) 9.5 of mouse development, Prox1 is specifically expressed by a subpopulation of endothelial cells that are located on one side of the anterior cardinal vein. These Prox1-positive LECs then bud from the veins to form the primary lymph sacs, which then proliferate and sprout into the periphery to form lymphatic capillaries and vessels (Oliver & Detmar, 2002; Wigle et al, 2002a). Budding and sprouting of LEC from the veins is arrested at ~E11.5-E12.0 in Prox1 null mice (Wigle et al, 2002a). During later stages of development, several genes such as podoplanin (Schacht et al, 2003), neuropilin-2 (Yuan et al, 2002), FOX C2 (Petrova et al, 2004) and angiopoietin-2 (Thurston, 2003) are involved in regulating normal lymphatic vessel patterning and maturation. Although some of these factors are also involved in lymphatic vessel activation under

pathological conditions, the mechanisms controlling lymphatic vessel growth and function have remained poorly understood.

Dipeptidyl peptidase IV (DPPIV) is a membrane glycoprotein that cleaves a conserved proline residue in proteotypically resistant components such as collagens, and that regulates the activities of a number of growth factors and neuropeptides (Bauvois, 2004; Busek et al, 2004; Mentlein, 2004). DPPIV is involved in diverse biological processes, including cell differentiation, adhesion, and apoptosis, functions that are important for controlling neoplastic transformation (Boonacker & Van Noorden, 2003; Houghton et al, 1988; Proost et al, 1999; Wesley et al, 1999). In addition, DPPIV mediates binding to collagen (Bauvois, 1988; Loster et al, 1995) and denatured collagen or gelatin (Ghersi et al, 2002). Despite its role in a number of cellular processes, the potential role of DPPIV for the growth and function of the lymphatic vascular system has remained unknown.

Based on transcriptional profiling studies that revealed an increased expression of DPPIV in cultured lymphatic endothelial cells (LEC) as compared to blood vascular endothelial cells (BEC), we aimed to characterize the vascular expression and function of DPPIV. We found– for the first time – that DPPIV expression is specifically expressed by lymphatic vessels but not by blood vessels in skin, as well as in a number of other organs including the small intestine, esophagus, ovary, breast and prostate glands. Studies in primary human LEC revealed that DPPIV is enzymatically active in these cells, but also promotes adhesion to fibronectin and collagen type I, as well as LEC migration and tube formation. These findings identify DPPIV as a novel lymphatic endothelium-specific marker, and they indicate that DPPIV plays a major role in mediating lymphatic endothelial functions.

3.3.2 Results

3.3.2.1 *Enhanced expression of DPPIV/CD26 by LEC as compared to BEC*

To identify genes that are specifically expressed or up-regulated by LEC, as compared to blood vascular endothelial cells (BEC), we isolated and purified both LEC and BEC from human neonatal foreskins of three independent donors. The three LEC and

BEC cell lines were then subjected to transcriptional profiling by microarray analysis using Applied Biosystems Human Genome Survey 2.0 (Shin et al., manuscript submitted). These studies revealed that DPPIV/CD26 is expressed at higher levels by LEC than by BEC (23.1-fold average increase; n=3). The difference in DPPIV gene expression was confirmed by quantitative TaqMan real-time RT-PCR in three matched pairs of LEC and BEC that were obtained from the same donor each, with an up to 12-fold increase of DPPIV mRNA levels in LEC (**Fig. 3.3.1A**). Western blot analyses of cell lysates confirmed that the enhanced mRNA expression levels correlated with enhanced protein expression of DPPIV in LEC (**Fig. 3.3.1B**).
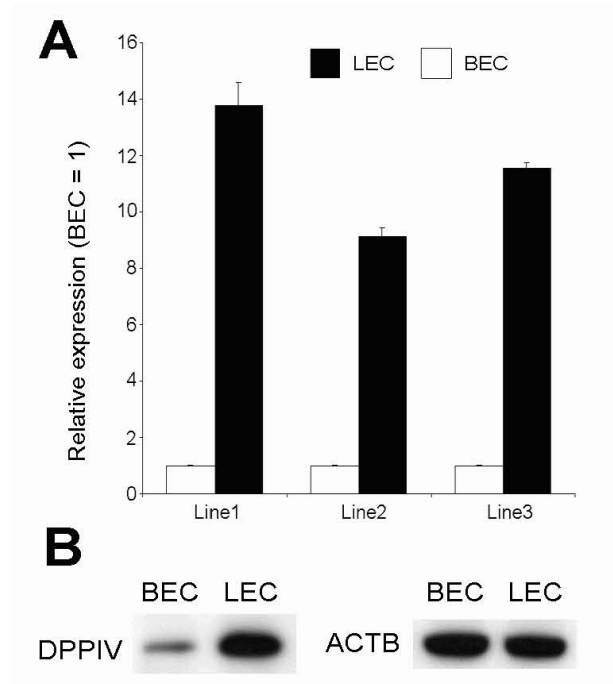
Figure 3.3.1 Enhanced expression of DPPIV/CD26 by LEC as compared to BEC. *(A) Quantitative real-time RT-PCR confirmed that three independently established lines of primary LEC (filled bars) expressed high levels of DPPIV as compared to primary BEC (open bars). (B) Western blot analyses of cell lysates confirmed that LEC expressed much higher levels of DPPIV protein, as compared to BEC (left pane). Western blot analyses for β-Actin were performed for equal loading (right pane).*

3.3.2.2 *Lymphatic vessels in normal skin specifically express DPPIV*

To investigate whether DPPIV is also expressed by lymphatic vessels *in situ*, we next performed double immunofluorescence analyses of normal human skin for DPPIV and for the lymphatic markers LYVE-1, podoplanin and Prox1. LYVE-1-positive (**Fig. 3.3.2B**), podoplanin-positive (**Fig. 3.3.2E**) and Prox1-positive (**Fig. 3.3.2N**) lymphatic vessels also expressed DPPIV ((**Fig. 3.3.2A-F and M-O**). Immunofluorescent staining for the panendothelial marker CD31 revealed a complete

overlap of DPPIV staining with the weakly stained CD31-lymphatic vessels (**Fig. 3.3.2G-I**), whereas strongly stained CD31-positive blood vessels did not express DPPIV. In agreement with these findings, staining for the blood vascular-specific marker CD34 and for DPPIV was mutually exclusive (**Fig. 3.3.2J-L**). Taken together, these findings confirm that DPPIV is specifically expressed by lymphatic vessels and not by blood vessels in human skin.
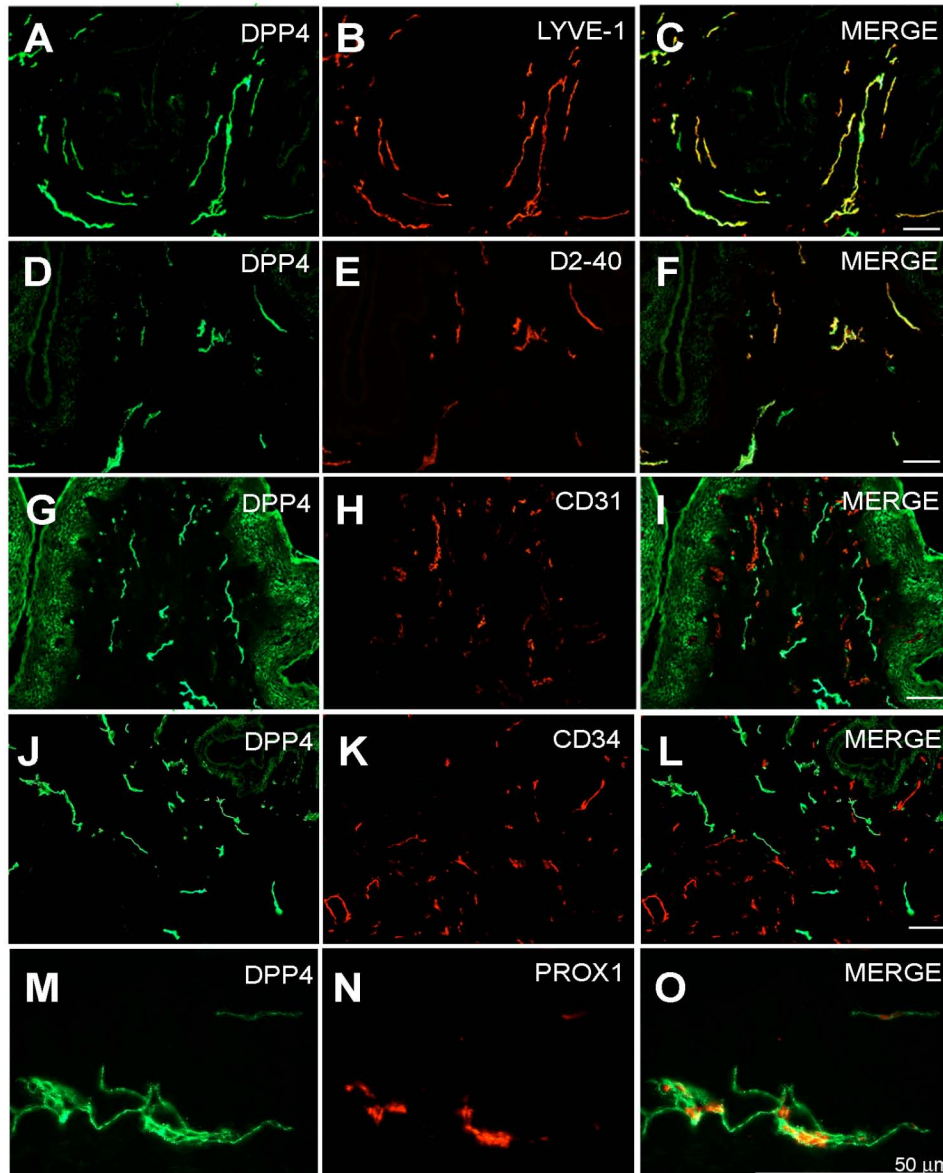
Figure 3.3.2 Specific detection of DPPIV expression by lymphatic endothelium in human skin.
*Double immunofluorescence analyses of normal human skin for DPPIV (green) and for the lymphatic specific markers (**B**) LYVE-1, (**E**) D2-40/podoplanin and (**N**) Prox1 revealed co-localization (**C, F, O**). Immunofluorescent staining for the panendothelial marker CD31 revealed a complete overlap of DPPIV staining with the weakly stained CD31-lymphatic vessels (**G-I**), whereas strongly stained CD31-positive blood vessels did not express DPPIV. Similarly, stainings for DPPIV and for the blood vascular-specific marker CD34 was mutually exclusive (**J-L**). Scale bars: 100 μm.*

3.3.2.3 *DPPIV is expressed by lymphatic vessels in several human organs*

We next investigated whether DPPIV might also serve as a specific marker for lymphatic vessels in other human tissues, in addition to the skin. To this end, we analyzed human tissue microarrays containing a number of sections of normal human organs. We found that lymphatic vessels in the small intestine, esophagus, ovary, breast, peripheral nerve tissue and prostate glands expressed DPPIV (**Fig. 3.3.3A-O**). It is of interest that several glands, including the prostate **(Fig. 3.3.3P, Q, R)**, salivary glands, and adrenal glands (data not shown) showed high expressions of DPPIV by glandular epithelium. Moreover, liver hepatocytes, proximal tubules of the kidney and bile ducts of the liver were also positive for DPPIV (data not shown). In all human tissues examined, DPPIV-positive lymphatic endothelium also expressed the lymphatic-specific marker podoplanin, whereas blood vessels were DPPIV-negative.
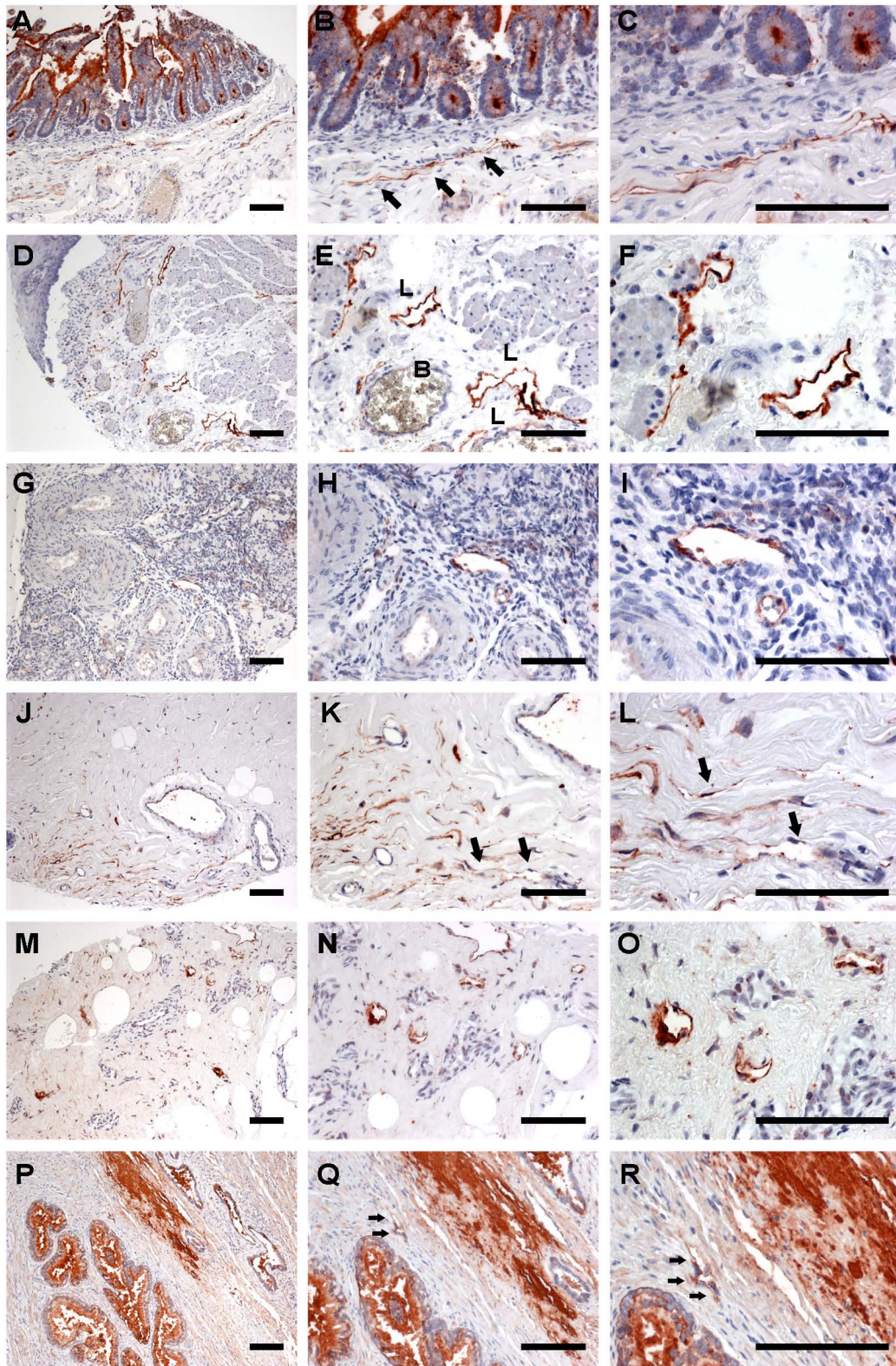
Figure 3.3.3 DPPIV is expressed by lymphatic vessels in several human organs. *We found DPPIV-positive lymphatic vessels in small intestine (A), esophagus (D), cervix (G), breast (J), peripheral nerve (M) and prostate gland (P). Notably, high expressions of DPPIV were found in several glands such as in small intestine (C) and prostate (Q). Scale bars: 100 µm.*

3.3.2.4 *Diprotin A inhibits the enzymatic activity of DPPIV but does not induce LEC proliferation and migration*

To further characterize the potential functional roles of DPPIV in LEC, we next investigated whether DPPIV produced by LEC is enzymatically active. Using a standard DPPIV activity assay for the cleavage of aminoluciferin, we found that the enzymatic activity of DPPIV was significantly higher in LEC than in BEC (p<0.001), and that the activity increased with increasing cell numbers (**Fig. 3.3.4A**). The specificity of the enzymatic activity was confirmed by treatment of LEC with the DPPIV-specific inhibitor diprotin A, which resulted in a significant, dose-dependent repression of DPPIV cleavage activity (**Fig. 3.3.4B**). However, treatment with diprotin A (ranging from 0.01 nM to 10 nM) did not affect LEC proliferation and migration as compared to untreated controls (**Fig. 3.3.4C and D**).
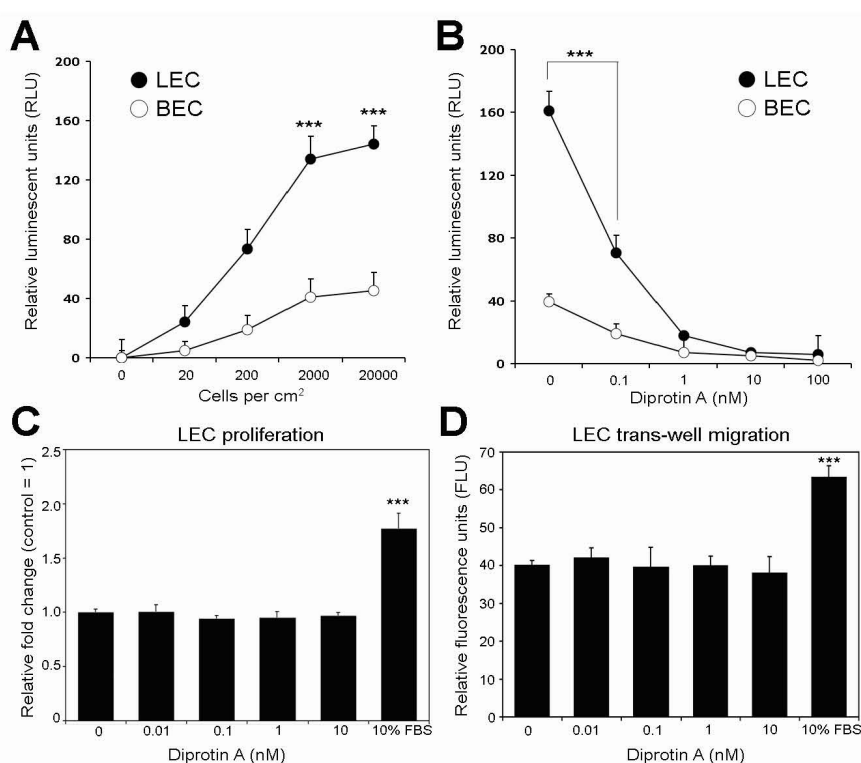
Figure 3.3.4 Diprotin A inhibits the enzymatic activity of DPPIV but does not induce LEC proliferation and migration. *(A) The enzymatic activity was significantly higher in LEC (filled circle) than in BEC (open circle) and that the activity increased with increasing cell numbers. (B) Treatment of LEC with the DPPIV-specific inhibitor diprotin A, significantly and dose dependently repressed DPPIV cleavage activity (from 0.1 nM to 1 nM); treatment of BEC with diprotin A slightly repressed DPPIV cleavage activity (from 0.1 nM to 1 nM). (C, D) Furthermore, treatment with diprotin A (ranging from 0.01 nM to 10 nM) did not affect LEC proliferation and LEC migration, whereas 10% FBS significantly induced both LEC proliferation and migration. ***P-value < 0.0001; **P-value < 0.001; *P-value < 0.01.*

3.3.2.5 *SiRNA-mediated knockdown of DPPIV inhibits LEC adhesion, migration and tube-formation*

In addition - and independently of - its enzymatic activity, DPPIV has also been described to mediate binding to extracellular matrix molecules including fibronectin and collagen (Bauvois, 2004; Loster et al, 1995). We next investigated whether DPPIV inhibition might regulate LEC functions that might play a role in lymphangiogenesis, including cell adhesion, migration and tube formation. Since the inhibition of DPPIV's enzymatic activity by treatment with diprotin A did not affect LEC proliferation and migration, we next aimed to inhibit DPPIV expression by siRNA-mediated knockdown. Using DPPIV-specific siRNA and Amaxa nucleofection, we achieved a > 82% knockdown of DPPIV mRNA expression, as determined by quantitative real-time RT-PCR (**Fig. 3.3.5A**). DPPIV siRNA knockdown inhibited the adhesion of LEC to both fibronectin and to collagen type I, as compared to control LEC ($P<0.005$; **Fig. 3.3.5B**). Trans-well migration assays revealed that LEC transfected with DPPIV siRNA migrated significantly less efficiently towards a FBS gradient when compared to control LEC ($P<0.005$; **Fig. 3.3.5C**). Moreover, DPPIV knockdown also inhibited LEC migration in a monolayer scratch wounding assay ($P < 0.0005$; **Fig. 3.3.5D**). Knockdown of DPPIV in LEC also inhibited the formation of tube-like structures after overlay of confluent cultures with a collagen type I gel (**Fig. 3.3.5G**). In contrast, knockdown of DPPIV did not affect LEC proliferation (data not shown).
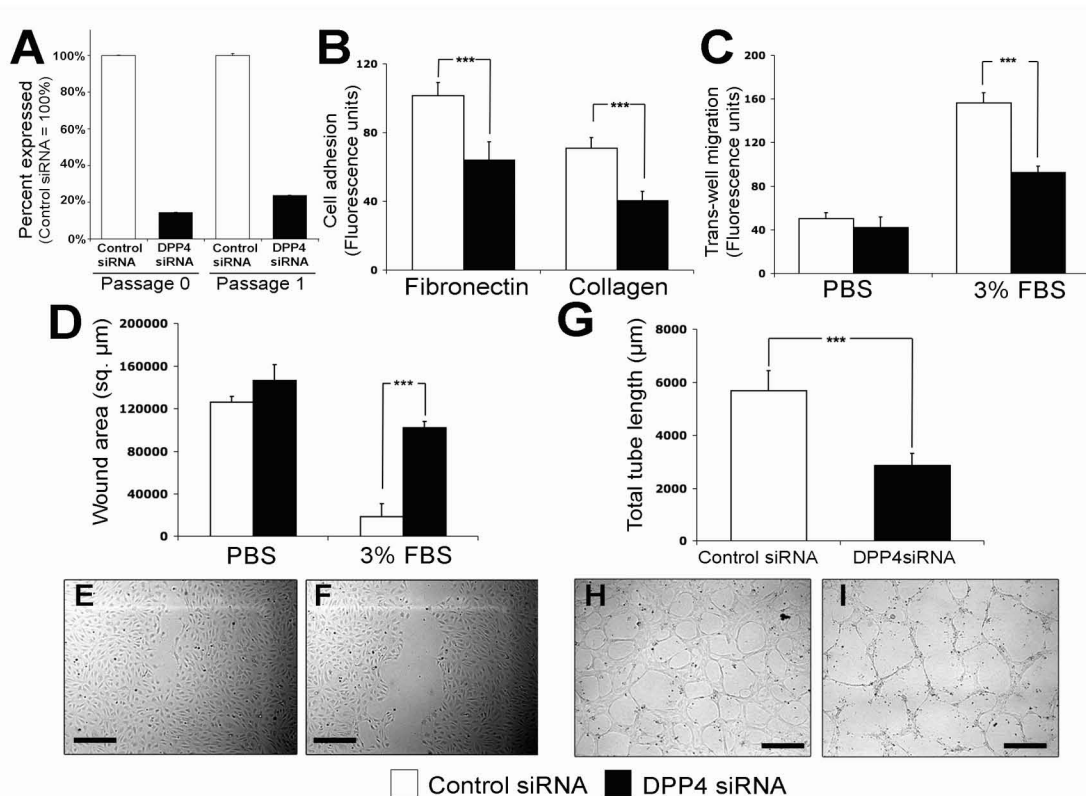
Figure 3.3.5 Knockdown of DPPIV inhibits LEC adhesion, migration and tube formation in vitro. *(A) Greater than 82% knockdown of DPPIV mRNA expression was achieved even after passaging the transfected cells once. (B) DPPIV siRNA knockdown inhibited the adhesion of LEC (filled bars) to both fibronectin and to collagen type I, as compared to control LEC (open bars). (C) Trans-well migration assays revealed that LEC transfected with DPPIV siRNA (filled bars) migrated significantly less efficiently towards a FBS gradient when compared to control LEC (open bars). (D) DPPIV knockdown also inhibited LEC migration in a monolayer scratch wounding assay. Cell culture images reveal repressed wound closure in LEC transfected with DPPIV siRNA (F) when compared to control LEC (E). (G) Knockdown of DPPIV in LEC (I) also inhibited the formation of tube-like structures after overlay of confluent cultures with a collagen type I gel when compared to control LEC (H). Scale bars: 100 μm. ***P-value < 0.0005; **P-value < 0.005; *P-value < 0.05.*

3.3.3 Discussion

In a search for novel pathways involved in lymphatic vessel growth and function, we have used transcriptional profiling of cultured human dermal BEC and LEC to identify enhanced expression of DPPIV in lymphatic endothelium *in vitro*. These results were confirmed by quantitative real-time RT-PCR and by Western blot analyses. We also found that DPPIV promotes LEC adhesion, migration and tube formation.

DPPIV has been implicated in several pathological conditions such as rheumatoid arthritis, Grave's disease and tumor progression (Blazquez et al, 1992; Eguchi et al, 1989; Gerli et al, 1996; Hafler et al, 1985; Wesley et al, 1999). Furthermore, recent

reports indicated that DPPIV might also play a role in endothelial cells (Chen et al, 2003; Zukowska et al, 2003). In this study, we found– for the first time – that DPPIV is specifically expressed by lymphatic vessels but not by blood vessels in the skin and in a number of additional organs, including the small intestine, esophagus, ovary, breast, and prostate glands. However, DPPIV was not detected on lymphatic vessels in the lung, kidney, uterus, liver and stomach (data not shown).

DPPIV has several functions, including serine peptidase activity, binding to the extracellular matrix, and complexing adenosine deaminase (Bauvois, 2004; De Meester et al, 1999). Each of these distinct functions, presumably mediated by distinct domains, might contribute to its role in lymphatic function. Our results indicate that DPPIV, expressed by LEC, efficiently cleaved the DPPIV substrate Gly-Pro-aminoluciferin, demonstrated that DPPIV expressed in LEC is enzymatically active and functional. DPPIV has the ability to cleave other bioactive peptides such as CXCL12, RANTES, MDC and I-TAC (De Meester et al, 1999; Proost et al, 2000; Proost et al, 2001). Therefore, DPPIV expressed by lymphatic vessels may contribute to the activation or deactivation of chemokines which control trafficking of monocytes, lymphocytes and dendritic cells into lymph nodes via lymphatic vessels. Whereas this enzymatic activity of DPPIV was efficiently inhibited by diprotin A, LEC proliferation and migration were not affected. However, we found that siRNA knockdown of DPPIV significantly inhibited LEC adhesion to fibronectin and collagen type I. These results indicate a dual function of DPPIV in lymphatic endothelium: Whereas the peptidase activity modulates the activity of proinflammatory chemokines and other mediators, DPPIV also mediates the interaction of lymphatic vessels with the extracellular matrix, an essential feature for the efficient drainage function of lymphatic vessels and the interstitial transport of macromolecules (Castenholz, 1998; Oliver & Detmar, 2002; Swartz, 2001). Moreover, siRNA-mediated DPPIV knockdown also inhibited LEC migration and tube formation which are essential for developmental and pathological lymphangiogenesis. These results are in agreement with previous studies which indicated that migration of other cell types was mediated by the adhesive properties of DPPIV (Ghersi et al, 2006; Kertesz et al, 2000). Therefore, specifically targeting the adhesive domain of DPPIV might provide a novel strategy for inhibiting pathological lymphangiogenesis. Future studies are needed to investigate whether DPPIV might

also play a role in the mediation of tumor-induced lymphangiogenesis and lymphatic metastasis.

3.4 Transcriptional profiling of VEGF-A and VEGF-C target genes in lymphatic endothelium reveals endocan as a novel mediator of lymphangiogenesis

3.4.1 Introduction

The lymphatic vascular system has an important role in the maintenance of tissue fluid homeostasis, in the afferent phase of the immune response, and in acute and chronic inflammation (Alitalo et al, 2005; Cueni & Detmar, 2006a; Kunstfeld et al, 2004). Recent studies have revealed that lymphatic vessels also play an active role in the metastatic spread of malignant tumor cells to regional lymph nodes (Mandriota et al, 2001; Skobe et al, 2001; Stacker et al, 2001). In particular, tumors can induce lymphangiogenesis via release of the lymphangiogenic growth factors VEGF-C or VEGF-D, leading to enhanced rates of metastasis to the draining sentinel lymph nodes and beyond (Mandriota et al, 2001; Skobe et al, 2001; Stacker et al, 2001). Indeed, studies have revealed that tumor-induced lymphangiogenesis is the most significant prognostic indicator to predict the occurrence of regional lymph node metastasis in malignant melanomas of the skin (Dadras et al, 2005). More recently, it has been found that tumors can also induce lymphangiogenesis within their draining lymph nodes, even before they metastasize (Hirakawa et al, 2007; Hirakawa et al, 2005b) and that induction of lymph node lymphangiogenesis promotes the further metastatic cancer spread to distant lymph nodes and to organs (Hirakawa et al, 2007). Thus, tumor-induced lymphatic growth and activation represents a novel potential target for treating or preventing advanced cancer.

Within the last few years, several mediators of lymphangiogenesis have been identified. Hepatocyte growth factor (HGF, also known as scatter factor) was recently found to induce proliferation, migration and tube formation of lymphatic endothelial cells (LEC) and to promote lymphangiogenesis *in vivo* (Kajiya et al, 2005). Additionally, FGF-2 promotes both lymphatic vessel growth in the mouse cornea (Chang et al, 2004; Kubo et al, 2002), and also promotes proliferation and migration of LEC by binding to its receptor FGFR-3 which is upregulated by the transcription factor Prox1 in lymphatic endothelium (Shin et al, 2006). Other growth factors with

effects on the lymphatic vasculature include platelet-derived growth factor-BB, insulin-like growth factor-1 and -2 (Bjorndahl et al, 2005; Cao et al, 2004), angiopoietin-1 (Gerber et al, 1999) and adrenomedullin (Fritz-Six et al, 2008). Despite the growing number of novel potential lymphangiogenic factors, there is strong evidence that growth factors of the vascular endothelial growth factor (VEGF) family, acting via VEGF receptor-3 (VEGFR-3) and VEGFR-2 on lymphatic endothelium, represent the most important lymphangiogenic stimuli in the majority of human and experimental cancers.

VEGF-C promotes lymphangiogenesis by activating VEGFR-2 and VEGFR-3 on LEC (Makinen et al, 2001). VEGF-C-deficient mice fail to develop a functional lymphatic system (Karkkainen et al, 2004), and transgenic expression of a soluble VEGFR-3 results in pronounced lymphedema (Makinen et al, 2001). Recently, VEGF-A has also been implicated as a strong lymphangiogenic mediator. Indeed, adenoviral delivery of murine VEGF-A164 to the skin of mice strongly promoted lymphatic vessel growth, and transgenic mice overexpressing murine VEGF-A164 specifically in the skin show enhanced lymphangiogenesis during wound healing and inflammation (Hirakawa et al, 2005b; Hong et al, 2004b; Kunstfeld et al, 2004; Nagy et al, 2002). Importantly, when VEGF-A transgenic mice were subjected to a standard chemically-induced multistep skin carcinogenesis regimen, there was enhanced proliferation of VEGFR-2-expressing tumor-associated lymphatic vessels, leading to an increased incidence of lymph node metastasis (Hirakawa et al, 2005b). The relative importance of direct VEGF-A induced signaling via VEGFR-2 versus the potential induction of a paracrine stimulatory loop via upregulation of VEGF-C expression by LEC has remained unclear. Moreover, in contrast to the detailed investigation of the effects of VEGF-A on the blood vasculature (Carmeliet, 2003), the downstream targets of VEGF-A (as well as of VEGF-C) in the lymphatic vasculature have remained unknown.

In this study, we aimed to comprehensively identify downstream molecular targets induced by VEGF-A or VEGF-C in lymphatic endothelium. To this end, we treated human dermal microvascular lymphatic endothelial cells (LEC) with VEGF-A or VEGF-C for up to 24 hours, followed by a time-series transcriptional profiling using gene microarray technology. In these studies we identified a number of genes - many

of them not previously known to be involved in lymphangiogenesis - that clustered either as early response genes, transiently induced genes or progressively induced genes. Endocan, also known as endothelial specific molecule-1 (ESM-1) was one of the genes that were most potently induced by both VEGF-A and VEGF-C. Whereas ESM-1 induction by VEGF-A was mainly dependent on activation of VEGFR-2, VEGF-C-mediated induction depended on the activity of both VEGFR-2 and VEGFR-3. We found that incubation of LEC with ESM-1 enhances the stimulating effects of both VEGF-A and VEGF-C on LEC proliferation and migration, whereas incubation with ESM-1 alone had no effect. Importantly, VEGF-A (or VEGF-C)-induced induction of LEC proliferation and migration was significantly inhibited by siRNA-mediated silencing of ESM-1 *in vitro* and *in vivo*. Together, these studies reveal endocan/ESM-1 as a novel mediator of lymphangiogenesis and as a potential target for the inhibition of VEGF-A- or VEGF-C-induced pathological lymphatic vessel growth and activation.

3.4.2 Results

3.4.2.1 *Microarray analysis reveals novel mediators of VEGF-A and VEGF-C-induced effects on lymphatic endothelial cells*

Both VEGF-A and VEGF-C have been shown to promote lymphangiogenesis *in vivo* and to enhance lymphatic endothelial cell (LEC) proliferation and migration *in vitro* (Hirakawa et al, 2007; Hirakawa et al, 2005b; Hong et al, 2004b; Kunstfeld et al, 2004). To identify genes involved in lymphangiogenesis mediated by these factors, we incubated human dermal microvascular LEC with either VEGF-A or VEGF-C for 0, 1, 4, 8 and 24 hours in triplicates, followed by gene microarray analyses using the chemiluminescence-based Applied Biosystems Human Genome Microarrays platform. We investigated the differentially expressed genes by applying multivariate Empirical Bayes statistics, which ranks genes on the basis of their sequential expression over time and the reproducibility at each time point (Friedman et al, 2000; Liang & Kelemen, 2007; Pan, 2002; Zhang & Zhang, 2007). We next performed Short Time Series Expression Miner (STEM) analysis (Ernst & Bar-Joseph, 2006) to determine which significantly modulated genes cluster together based on their

temporal regulation pattern (**Fig. 3.4.1**). For the VEGF-A treated LEC, we identified 71 genes clustering into the early-response genes group (ER; peak at time point 1h), 49 genes into the transiently induced genes group (TI; peak between 4h and 8h), 79 genes into the progressively induced genes group (PI; progressive increase of expression over time) and 52 into the downregulated genes group (DR; progressive decrease over time). For the VEGF-C treated LEC, 74 genes clustered into ER, 41 into TI, 35 into PI and 38 into DR (**Fig. 3.4.1**). The early response gene cluster revealed the most overlapping genes induced by both VEGF-A and VEGF-C (n=26) as compared to the temporal clusters, and included known early response genes such as EGR-1, EGR-2 and EGR-3 (**Table 3.4-1**). As previously described for blood vascular endothelium (Hesser et al, 2004), DSCR1 was one of the most strongly induced VEGF-A early response genes.
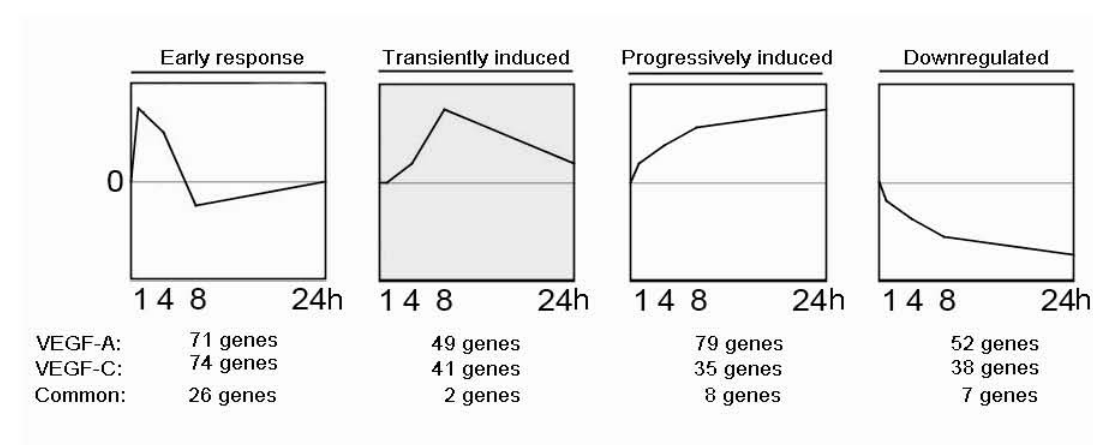
Figure 3.4.1 Microarray time course analysis of LEC treated with VEGF-A or VEGF-C reveals four major temporally regulated gene clusters. *Transcription profiling and Short Time Series Expression Miner (STEM) analysis of LEC stimulated with VEGF-A or VEGF-C for 1h, 4h, 8h or 24h revealed 71/74 genes specifically up-regulated at 1h (early response genes), 49/41 genes upregulated transiently (transiently induced), 79/35 genes upregulated progressively over time (progressively induced) and 52/38 genes down-regulated over time (downregulated).*

Among the progressively induced genes, we identified several genes that have been previously reported to be involved in the mediation of lymphangiogenesis, including VEGF-C and angiopoietin-2 (Thurston, 2003; Veikkola et al, 2001). We additionally found upregulation of asp-like, microcephaly associated (ASPM), TTK protein kinase (TTK) and kinesin family member 14 (KIF14) (**Table 3.4-1**). Fatty acid binding protein 3 (FABP3), SHC SH2-domain binding domain 1 (SHCBP1) and cell division

cycle 2 (CDC2) were highly upregulated by both VEGF-A and VEGF-C in LEC. The list of significantly modulated genes is provided in **Appendix Table 2 and 3**.

Table 3.4-1 **Top 10 genes induced by VEGF-A, VEGF-C or both**

a) Early response genes			b) Transiently induced genes		
VEGF-A	**VEGF-A & VEGF-C**	**VEGF-C**	**VEGF-A**	**VEGF-A & VEGF-C**	**VEGF-C**
NR4A2	EGR3	DUSP5	PLAUR	ANKRD20B	MYO1B
DSCR1	EGR2	LOC387763	LRP8	SLC4A7	LY6H
NR4A3	NR4A1	TncRNA	PLAT		FOXI1
TRIB1	F3	KLF10	GAL		ETV1
AXUD1	FOSB	PFKFB3	ACOT11		CAMTA1
KLF10	FOS	LOC441655	NPAS2		CAMK2B
RRAD	EGR1	TSC22D2	SHC4		KLF5
NUAK2	PTGS2	DKFZP434F0318	UHRF1		IL18R1
TNFAIP3	ATF3	PFKFB3	FLT1		GUCY1A3
MAP3K8	STC1	PELO	SPHK1		CLGN

c) Progressively induced genes			d) Dowregulated genes		
VEGF-A	**VEGF-A & VEGF-C**	**VEGF-C**	**VEGF-A**	**VEGF-A & VEGF-C**	**VEGF-C**
ANGPT2	SHCBP1	LOC338579	CA4	PDK4	FGFR1
ASPM	CDC2	VEGFC	KCTD12	REPS2	CITED1
TOP2A	FABP3	C20orf128	CGNL1	CYP1A1	PGLYRP2
KIF14	ZWINT	ITGB1BP2	GUCY1A3	C2orf23	SCARF2
ARHGAP11A	ESM1	GALNT8	BRUNOL5	LTB	TMC8
NUSAP1	CXCR4	NP	TGFA	TMEM100	UTP14A
KIF2C	ST8SIA4	LDLRAD1	MAN1C1	SPATA12	LAMA2
DGKD	CDC45L	MPHOSPH6	LFNG		WASF2
DAF		CTAGE4	SLC2A12		KCNQ1
TTK		CORO6	IGF1		INE1

We next applied the PANTHER annotation and classification software to identify biological pathways with time-specific regulation by VEGF-A. Among the 14 molecular functions significantly overrepresented after 1h of VEGF-A treatment, were transcription factors and signaling molecules (p<0.0005; **Table 3.4-2a**). Within the transiently and progressively induced gene clusters, genes encoding cytokine receptors and growth factors were significantly overrepresented. The most significantly overrepresented molecular functions after 24 hours included cytoskeletal and microtubule binding proteins (p<0.0005). According to their biological process annotations, genes induced after 1h were significantly involved in mRNA transcription, cell proliferation and cell cycle control (**Table 3.4-2b**). Among the

87

overrepresented pathways after 24h of VEGF-A treatment were protein modification and phosphorylation. The results for VEGF-C treated LEC are provided in **Appendix Table 4**.

Table 3.4-2 **Pathway classification analysis of VEGF-A induced genes in LEC**

Molecular function	1h	4h	8h	24h
Cytokine receptor	++	++	++	++
Phosphorylase	++	++	++	++
Growth factor	+	+++	+	+
Kinase modulator	+	+	+	+
Kinase inhibitor	+	+	++	-
Phosphatase	++	+	+++	-
Basic helix-loop-helix transcription factor	+	+	+	-
Signaling molecule	+++	+++	+	-
Carbohydrate phosphatase	++	+++	+++	-
Kinase	+	+	-	+++
Select regulatory molecule	+	-	+	+
Protein phosphatase	+	-	++	-
Transcription factor	+++	-	-	-
Metalloprotease	+	-	-	-
Defense/immunity protein	-	+	+	-
RNA-binding protein	-	+	+	-
Replication origin binding protein	-	-	+	++
Transaminase	-	-	++	+
Transferase	-	-	+	-
Microtubule binding motor protein	-	-	-	+++
Microtubule family cytoskeletal protein	-	-	-	+++
Cytoskeletal protein	-	-	-	+++
Protein kinase	-	-	-	++
Actin binding motor protein	-	-	-	+
DNA topoisomerase	-	-	-	+
DNA strand-pairing protein	-	-	-	+
DNA helicase	-	-	-	+

Biological process	1h	4h	8h	24h
Cell proliferation and differentiation	+++	+	+	+
Developmental processes	+++	+	+	+
Nucleoside, nucleotide and nucleic acid metabolism	+++	+	+	+
Intracellular signaling cascade	++	++	+	+
MAPKKK cascade	+++	++	+++	-
Immunity and defense	++	++	++	-
Receptor protein tyrosine kinase signaling pathway	+	+	++	-
JNK cascade	+	+	+	-
Signal transduction	+++	+++	+	-
Protein phosphorylation	+++	+	-	+++
Ligand-mediated signaling	+++	+++	-	-
Cell communication	+++	++	-	-
Cell cycle	+	-	+	+++
Cell cycle control	+++	-	+	+++
Protein modification	+	-	-	++
Inhibition of apoptosis	++	-	-	+
Cell surface receptor mediated signal transduction	++	-	-	-
mRNA transcription	+++	-	-	-
Cell adhesion-mediated signaling	+	-	-	-
Neurogenesis	+	-	-	-
Complement-mediated immunity	-	+	+	+
Angiogenesis	-	+	+	+
Amino acid biosynthesis	-	-	+	++
Mitosis	-	-	-	+++
Chromosome segregation	-	-	-	+++
Cytokinesis	-	-	-	+++
DNA replication	-	-	-	++

+++ p-value < 0.0005; ++ p-value < 0.005; + p-value < 0.05; - not significant

3.4.2.2 *ESM-1 expression is potently induced in LEC by VEGF-A and VEGF-C*

Among the progressively increasing gene cluster, endocan (also known as endothelial specific molecule-1; ESM-1), was one of the most potently upregulated genes in LEC after VEGF-A and VEGF-C treatment. Quantitative TaqMan real-time RT-PCR analyses revealed a more than 10-fold induction of ESM-1 mRNA expression at 24h of VEGF-A treatment, and a more than 4-fold induction after treatment with VEGF-C (**Fig. 3.4.2A**), thus confirming the microarray results. Western blot analyses confirmed that ESM1 protein expression was also strongly increased in both LEC lysates and supernatants at 24h and 48h of VEGF-A treatment, compared to control LEC (**Fig. 3.4.2B,C**).

Although VEGF receptor-2 (VEGFR-2) is the only presently known receptor for VEGF-A on LEC, some of the observed VEGF-A effects might have been mediated

by an indirect pathway involving upregulation of VEGF-C which then might have led to VEGFR-3 activation. Moreover, the mature form of human VEGF-C used for the experiments can bind to both VEGFR-2 and VEGFR-3. Thus, we next investigated the relative contribution of VEGFR-2 and VEGFR-3 towards the induction of ESM-1 by VEGF-A and VEGF-C, using blocking antibodies specific for VEGFR-2 or VEGFR-3. Treatment of LEC with VEGF-A strongly induced the expression of ESM-1 in the presence of control IgG, whereas ESM-1 induction was completely inhibited by a VEGFR-2 blocking antibody ($p<0.0001$; **Fig. 3.4.2D**). Incubation with a VEGFR-3 blocking antibody partially reduced the induction of ESM-1 by VEGF-A ($p<0.001$), and a combination of both blocking antibodies inhibited the VEGF-A-mediated ESM-1 induction ($p<0.0001$; **Fig. 3.4.2D**). VEGF-C also induced the expression of ESM1 in the presence of control IgG, though less potently than VEGF-A (**Fig. 3.4.2E**). Incubation with either an anti-VEGFR-2 antibody or an anti-VEGFR-3 antibody only partially blocked the ESM-1 induction by VEGF-C ($p<0.001$ and $p<0.01$, respectively; **Fig. 3.4.2E**). Combined blockade of VEGFR-2 and VEGFR-3 completely prevented VEGF-C-mediated induction of ESM-1 expression ($p<0.0001$).
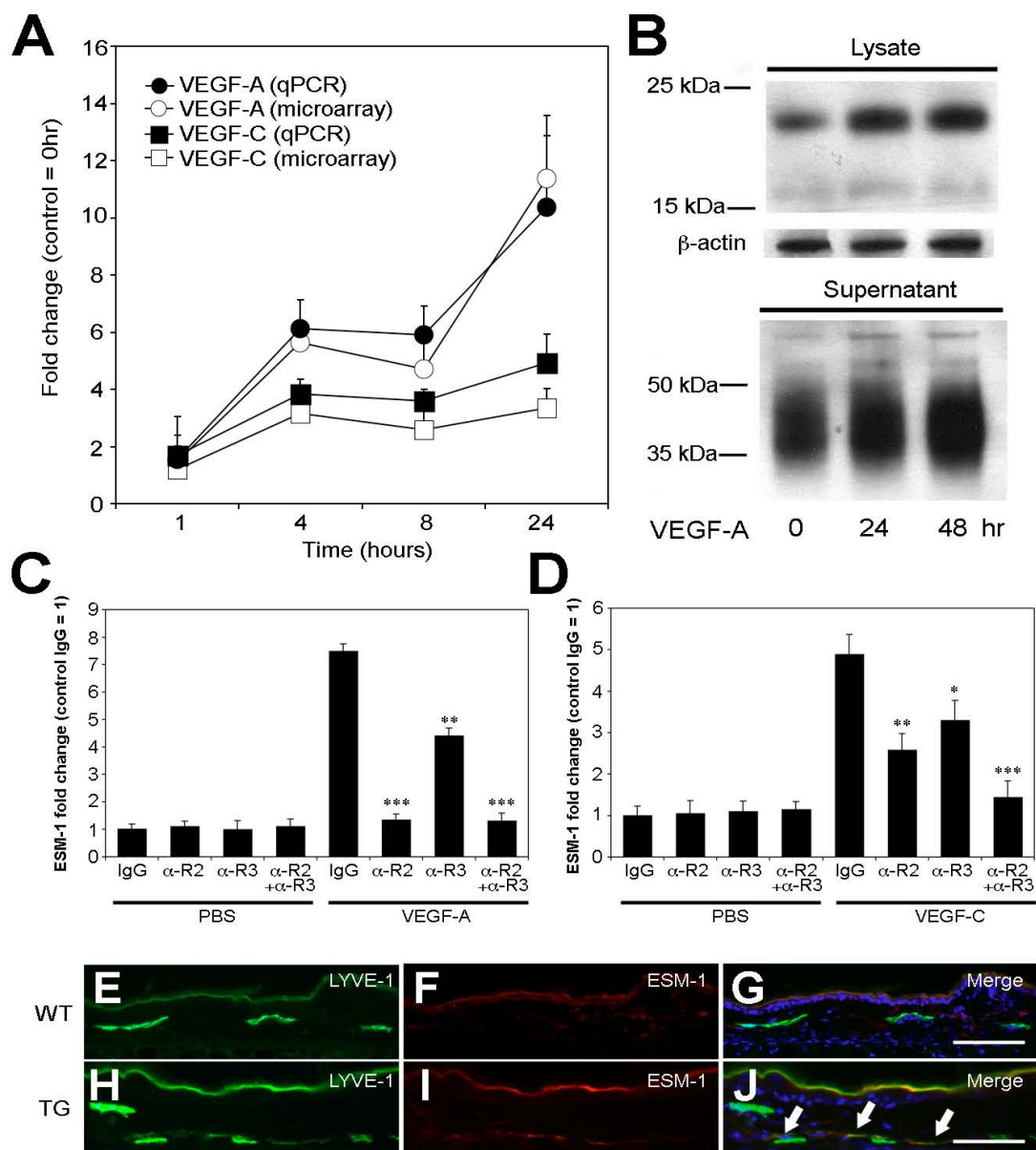
Figure 3.4.2 Expression of ESM1 in LEC is induced by VEGF-A and VEGF-C via VEGFR-2 and VEGFR-3. *(A) When compared to untreated controls, LEC expressed over 10-fold higher levels of ESM1 mRNA after 24h stimulation with VEGF-A (filled circle), and over 4-fold higher levels with VEGF-C (filled square), confirming the microarray expression results (open circles, open squares) by quantitative RT-PCR. (B) Western blot analysis confirmed that LEC stimulated with VEGF-A for 24h or 48h also expressed much higher levels of ESM1 in the cell lysates and in cell supernatants, as compared to untreated controls. (C) Treatment of LEC with VEGF-A strongly induced the expression of ESM-1 in the presence of control IgG, whereas ESM-1 induction was completely inhibited by a VEGFR-2 blocking antibody. Incubation with a VEGFR-3 blocking antibody partially reduced the induction of ESM-1 by VEGF-A, and a combination of both blocking antibodies inhibited the VEGF-A-mediated ESM-1 induction. (D) VEGF-C also induced the expression of ESM1. Incubation with either an anti-VEGFR-2 antibody or an anti-VEGFR-3 antibody only partially blocked the ESM-1 induction by VEGF-C, which was completely prevented by combined blockade of both receptors. ***P-value < 0.0001; **P-value < 0.001; *P-value < 0.01. The LYVE-1 positive lymphatic vessels in the skin of VEGF-A transgenic mice (H-J) expressed ESM-1 (J, arrows), but not the lymphatic vessels in the skin of wildtype mice (E-G). Scale bars: 100 µm.*

To investigate whether ESM-1 expression by lymphatic endothelium might also be upregulated by VEGF-A *in vivo*, we next performed differential immunofluorescence analyses of skin samples obtained from VEGF-A transgenic mice for ESM-1 and the lymphatic-specific hyaluronan receptor LYVE-1. VEGF-A transgenic mice express the murine VEGF-A165 under control of the epidermis-specific keratin 14 promoter, leading to enhanced VEGF-A levels within the skin (Kunstfeld et al, 2004; Xia et al, 2003). The subset of LYVE-1 positive lymphatic vessels in the skin of VEGF-A transgenic mice expressed ESM-1 (**Fig. 3.4.2H-J**), but not the lymphatic vessels in the skin of wildtype mice (**Fig. 3.4.2E-G**).

3.4.2.3 *ESM-1 promotes LEC proliferation and migration induced by VEGF-A and VEGF-C*

Because both VEGF-A and VEGF-C promoted ESM-1 expression by LEC, we investigated whether ESM-1 might modulate the effects of both growth factors on lymphatic endothelial cell functions. Incubation of LEC with ESM-1 alone did not affect LEC proliferation at concentrations ranging from 0.1 ng/ml to 1 µg/ml (**Fig. 3.4.3A** and data not shown). However, addition of ESM1 together with VEGF-A or VEGF-C significantly and dose-dependently increased the stimulatory effects of both growth factors on LEC proliferation (**Fig. 3.4.3A**).

We next investigated whether silencing of ESM-1 expression by small interfering RNAs (siRNAs) might affect the proliferative effects of VEGF-A and -C on LEC. Transfection of LEC with ESM-1 siRNAs efficiently reduced the ESM-1 protein levels, as compared with control siRNA-transfected LEC (**Fig. 3.4.3B**). When ESM-1 siRNA-transfected LEC were treated with VEGF-A or VEGF-C, the proliferation-inducing effects of both growth factors were potently suppressed, as compared with control siRNA-transfected LEC ($p < 0.005$; **Fig. 3.4.3C**). Addition of human recombinant ESM-1 protein to ESM-1 siRNA-transfected LEC partially restored the level of growth stimulation by both VEGF-A and VEGF-C ($p < 0.005$ and $p < 0.05$, respectively; **Fig. 3.4.3C**).

We next investigated whether ESM-1 might also modulate the effects of VEGF-A or -C on LEC migration. Using a standard monolayer wound assay *in vitro*, we found that

addition of ESM-1 at a concentration of 100 ng/ml slightly promoted the migration-enhancing effect of VEGF-A, as compared with VEGF-A treatment only (**Fig. 3.4.3D**). LEC transfected with ESM-1 siRNA showed a significantly reduced migratory response to VEGF-A treatment ($p<0.005$), as compared to control siRNA-transfected LEC. Addition of recombinant ESM-1 protein restored the full stimulatory effect of VEGF-A on LEC migration (**Fig. 3.4.3D**). Comparable results were seen when LEC were treated with VEGF-C (data not shown).
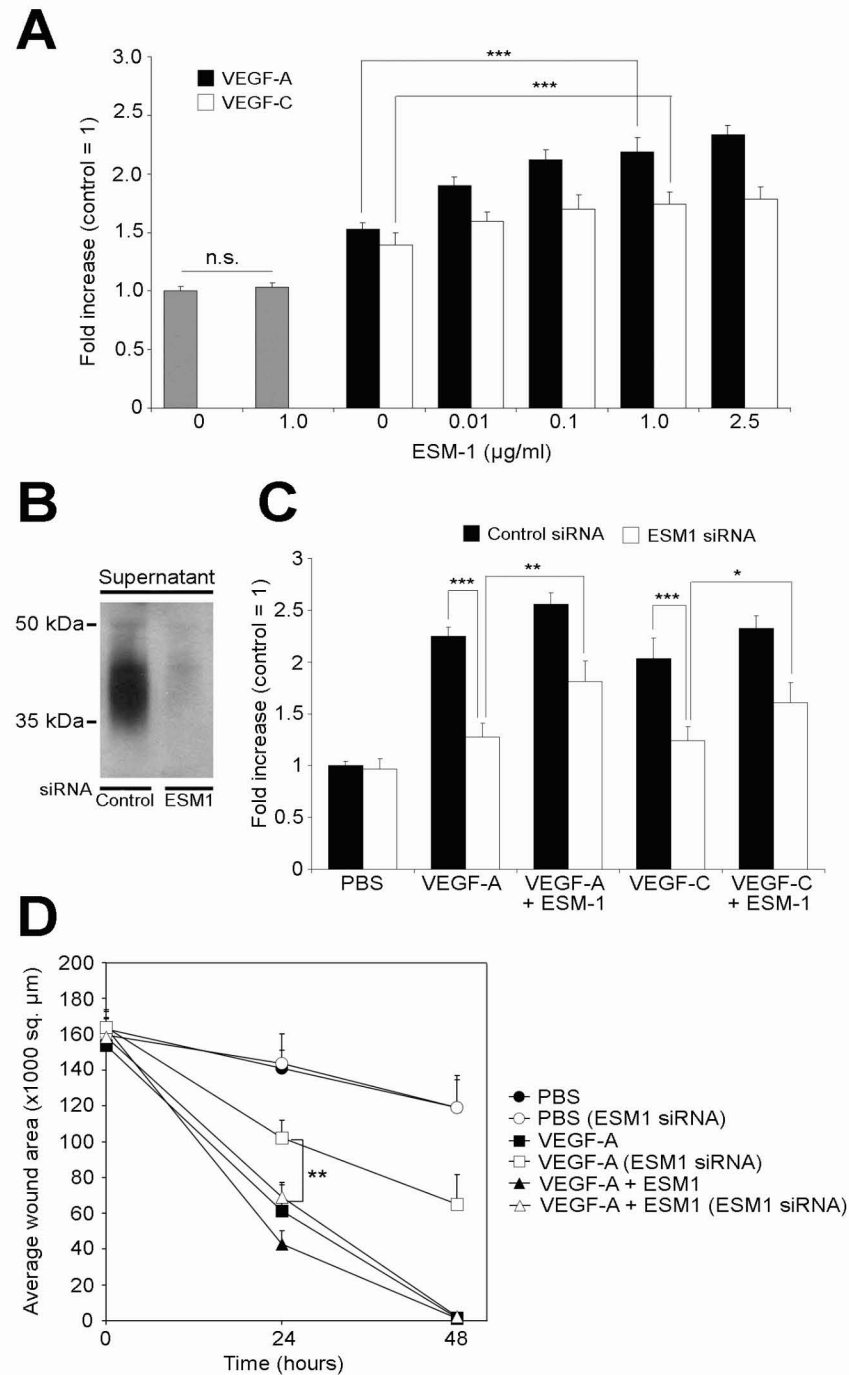
Figure 3.4.3 ESM1 promotes LEC proliferation and migration induced by VEGF-A and VEGF-C. *(A) Addition of ESM1 together with VEGF-A (20 ng/ml) or VEGF-C (100 ng/ml) significantly and dose-dependently increased the stimulatory effects of both growth factors on LEC proliferation, whereas ESM1 alone had no effect.* *(B) Transfection of LEC with ESM-1 siRNAs reduced ESM-1 protein levels compared with control siRNA-transfected LEC.* *(C) The proliferation-inducing effects of VEGF-A and VEGF-C were suppressed in ESM-1 siRNA-transfected LEC but not in control siRNA-transfected LEC. Addition of ESM-1 protein to ESM-1 siRNA-transfected LEC partially restored growth stimulation by VEGF-A and VEGF-C.* *(D) ESM1 (100 ng/ml) slightly promoted the promigratory effect of VEGF-A in a monolayer wound assay, whereas LEC transfected with ESM-1 siRNA showed a significantly reduced migratory response to VEGF-A compared to control siRNA-transfected LEC. Addition of ESM-1 protein restored the effect of VEGF-A on LEC migration. *P-value<0.05; **P-value<0.005; ***P-value<0.0005.*

94

3.4.2.4 *ESM-1 promotes lymphatic vessel activation by VEGF-A in vivo*

Because ESM-1 expression by LEC was strongly upregulated by VEGF-A *in vitro*, and was also upregulated on lymphatic vessels in the skin of VEGF-A transgenic mice, we next investigated whether ESM-1 might also promote the effects of VEGF-A on lymphatic endothelium *in vivo*. To this end, we used an established Matrigel implantation assay in FVB wildtype mice. Matrigels containing PBS or VEGF-A together with either ESM-1 siRNA or with control siRNA were subcutaneously injected into mice. After 7 days, tissue samples were obtained and frozen sections were subjected to differential immunofluorescence analyses for the lymphatic marker LYVE-1 and the panendothelial marker CD31. In the skin surrounding Matrigel implants containing VEGF-A and control siRNA, LYVE-1-positive lymphatic vessels were strongly enlarged (**Fig. 3.4.4B**), as compared to Matrigels containing PBS only (**Fig. 3.4.4A**). In contrast, lymphatic vessels showed a normal morphology and were not enlarged in the skin surrounding Matrigel implants containing VEGF-A and ESM-1 siRNA (**Fig. 3.4.4C**). Computer-assisted morphometric analyses of LYVE-1/CD31 stained sections demonstrated that the density of lymphatic vessels was comparable in all three groups (**Fig. 3.4.4D**). However, the average size of lymphatic vessels was significantly larger in the skin surrounding Matrigel implants containing VEGF-A and control siRNA, as compared to Matrigels containing PBS alone (P<0.005; **Fig. 3.4.4E**). Importantly, lymphatic vessels in the skin surrounding implants containing VEGF-A and ESM-1 siRNA showed a comparable size as found surrounding PBS-containing implants and were significantly smaller than surrounding VEGF-A/control siRNA implants (P<0.005; **Fig. 3.4.4E**). Similarly, the average tissue area covered by lymphatic vessels was significantly increased surrounding VEGF-A/control siRNA implants, as compared to PBS-containing (P<0.0005) or VEGF-A/ESM-1 siRNA containing implants (P<0.05; **Fig. 3.4.4F**).
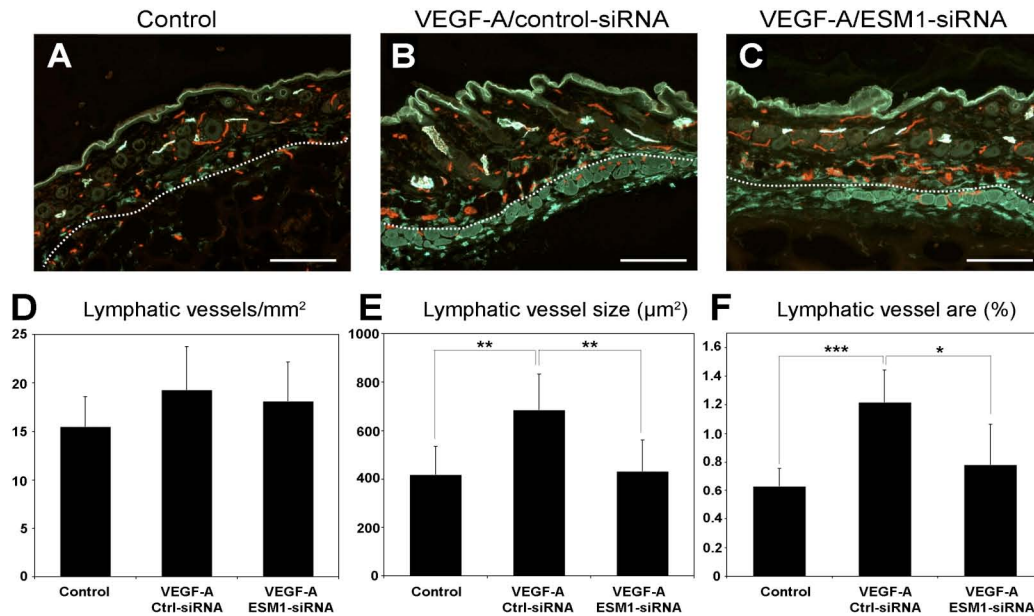
Figure 3.4.4 Targeting ESM1 by siRNA inhibits VEGF-A effects on lymphatic vessels in vivo. *Compared to Matrigels containing PBS (A), LYVE-1-positive lymphatic vessels were enlarged surrounding Matrigels containing VEGF-A and control siRNA (B). Lymphatic vessels were not enlarged surrounding Matrigels containing VEGF-A and ESM-1 siRNA (C). Scale bars: 100 μm. Computer-assisted morphometric analyses of LYVE-1/CD31 stained sections showed comparable density of lymphatic vessels in all groups (D). The average size of lymphatic vessels was significantly larger surrounding Matrigels containing VEGF-A/control siRNA than Matrigels containing PBS (E) or VEGF-A/ESM-1 siRNA. The average tissue area covered by lymphatic vessels was significantly increased surrounding VEGF-A/control siRNA implants, as compared to PBS-containing or VEGF-A/ESM-1 siRNA containing implants (F). *P<0.05; **P<0.005; ***P<0.0005.*

3.4.3 Discussion

In order to comprehensively identify downstream molecular targets induced by VEGF-A or VEGF-C in lymphatic endothelium, we have treated dermal lymphatic endothelial cells with VEGF-A or VEGF-C for up to 24 hours, followed by a time-series transcriptional profiling using gene microarray technology. To our knowledge, this is the first study into the comprehensive downstream mediators of VEGF-A in lymphatic endothelium.

Microarray time course studies provide the ability to monitor the temporal behavior of biological processes of interest through the sequential measurement of the expression of tens of thousands of genes (Martinez et al, 2007; Murphy, 2002; Qian et al, 2003; Storey et al, 2005). However, given the large number of genes evaluated in microarray time course experiments, and the usually rather small number of replicates, the variances are usually poorly estimated. Thus, for the analysis of gene

expression of triplicate samples at 5 different time points, we have applied the multivariate Empirical Bayes (EB) approach to inference (Friedman et al, 2000; Liang & Kelemen, 2007). This is a model-based strategy for introducing moderation into the analysis and has been reported to generate the least number of false positives and false negatives (Huber et al, 2002). Using short time series expression miner (STEM) analysis (Ernst & Bar-Joseph, 2006), we identified distinct temporal clusters of genes modulated by VEGF-A and VEGF-C. Within the early response cluster - with a peak of expression after 1h - we predominantly found transcription factors and signaling molecules. Several of these, such as the early growth response genes EGR1, EGR2 and EGFR3 have been previously described as early VEGF-A target genes in blood vascular endothelium (Liu et al, 2003a; Schoenfeld et al, 2004; Yang et al, 2002). Our finding of Down syndrome critical region protein 1 (DSCR1), an inhibitor of NFAT activity, as one of the most potently induced early response targets in LEC is in agreement with previous results in human umbilical vein endothelial cells (Hesser et al, 2004). It is of interest that the overlap among VEGF-A and VEGF-C targets was highest in the early response cluster, as compared to the transiently induced and the progressively induced gene clusters. Among the cluster of genes with progressively increasing expression after VEGF-A and VEGF-C treatment were - angioipoietin-2 which has been previously shown to be indispensable for the normal development of the lymphatic vasculature in mice (Gale et al, 2002) - as well as VEGF-C, indicating the possible induction of an autocrine growth pathway via VEGFR-3 activation (see below).

Importantly, we found endocan (also known as endothelial specific molecule-1; ESM-1) to be one of the most potently induced genes by both VEGF-A and VEGF-C in cultured LEC - both at the mRNA and the protein level. ESM-1 expression was also detectable on lymphatic vessels in the skin of transgenic mice with chronically elevated levels of VEGF-A but not in the skin of wildtype mice, indicating that ESM-1 is also a target of VEGF-A *in vivo*. ESM-1 is a dermatan sulphate proteoglycan secreted by endothelial cells that has been suggested to play a role in the regulation of cell adhesion in inflammatory disorders and in tumor progression (Bechard et al, 2001b). Whereas the precise function of ESM-1 is still unclear, it has been proposed to inhibit the interaction between intercellular adhesion molecule-1 (ICAM-1) and the integrin LFA-1 on lymphocytes and monocytes (Bechard et al, 2001b). Recently,

increased ESM-1 mRNA expression levels were reported to represent one of the most significant molecular signatures of a poor prognosis in several types of cancer including lung cancer (Grigoriu et al, 2006). Moreover, overexpression of ESM-1 in human embryonic kidney 293 cells, promoted tumor growth in a xenotransplant model in mice (Scherpereel et al, 2003).

Our current study reveals that ESM-1 promoted the mitogenic and promigratory activity of both VEGF-A and VEGF-C on cultured LEC, whereas addition of ESM-1 alone did not affect LEC functions *in vitro*, similar to blood vascular endothelium (Rennel et al, 2007). Moreover, siRNA-mediating ESM-1 silencing inhibited the activation of LEC by VEGF-A and VEGF-C *in vitro* and by VEGF-A *in vivo*. Together, the results indicate that VEGF-A/VEGF-C-mediated induction of ESM-1 represents an autocrine, positive feed-back loop to further promote the stimulatory effects of both growth factors on lymphatic endothelium. ESM-1 has been previously shown to bind to HGF and to increase the HGF mediated proliferation of human embryonic kidney cells in a similar way as heparin, and the single dermatan sulfate chain of the molecule - covalently attached to serine 137 - appears to be required for this effect since the nonglycanated form of ESM-1 did not promote the effects of HGF (Bechard et al, 2001a). Thus, it will be of interest to investigate whether ESM-1 might also bind to VEGF-A and VEGF-C to enhance their interaction with VEGFR-2 and/or VEGFR-3 on LEC.

The relative contribution of direct activation of VEGFR-2 versus possible indirect effects on VEGFR-3 - via induction of its ligand VEGF-C - towards the lymphangiogenic effects of VEGF-A have remained unclear (Hirakawa et al, 2005a). In our study, we found that inhibition of VEGFR-2 with a blocking antibody completely abrogated the VEGF-A-mediated induction of ESM-1 in LEC, clearly indicating that VEGFR-2 is essential for mediating VEGF-A effects. However, specific blockade of VEGFR-3 resulted in a partial inhibition of the ESM-1 induction by VEGF-A. Together with the observed induction of VEGF-C expression after VEGF-A treatment, these findings indicate that VEGF-A might mediate its lymphangiogenic effects indeed in part via activation of an autocrine loop in LEC which leads to VEGFR-3 activation by VEGF-C. It remains at present unclear whether or not VEGF-A might also exert effects on the formation of heterodimers of

VEGFR-2 and VEGFR-3 which might then affect receptor tyrosine phosphorylation (Dixelius et al, 2003). However, one has to keep in mind that the effects of VEGF-A on LEC gene expression were in general stronger than those of VEGF-C, and that the VEGF-A-mediated induction of ESM-1 was only partially blocked by the anti-VEGFR-3 blocking antibody. Our study also demonstrates that both VEGFR-2 and VEGFR-3 are required for the full activity of VEGF-C on LEC gene expression, since inhibition of each receptor alone only partially inhibited the induction of ESM-1 by VEGF-C whereas combined blockade completely abrogated the VEGF-C effect. These findings are in agreement with results demonstrating that the mature form of the VEGF-C protein, which was used for this study, efficiently binds to and activates both receptors (Alitalo et al, 2005). Overall, our studies reveal endocan/ESM-1 as a novel mediator of lymphangiogenesis and as a potential target for the inhibition of VEGF-A- or VEGF-C-induced pathological lymphatic vessel growth and activation.

4 CONCLUSIONS AND OUTLOOK

4.1 Conclusions

In this work, we set out to investigate the molecular mechanisms of lymphatic vascular function during endothelial lineage-specific differentiation and lymphangiogenesis. We demonstrate that the lymphatic-specific transcription factor Prox1 directly binds to putative Prox1 response elements of the FGFR-3 promoter and upregulates the expression of FGFR-3. To validate this finding, we introduced two amino acid substitution mutations into the DNA binding sites of Prospero, the *Drosophila* homolog of Prox1 (Ryter et al, 2002) and revealed that the mutated Prox1 completely lost its transcriptional activity. Additionally, we confirmed the Prox1 binding to the putative Prox1 binding elements by performing gel electrophoresis mobility shift assays (EMSA) and transcriptional activation/luciferase reporter assays. Immunohistochemical analyses further revealed that many of the Prox1-positive differentiating endothelial cells were positively stained for FGFR-3 in E11.5 mouse embryos. In order to show the functional role of FGFR-3 in LEC, we stimulated the cells with FGF1 and FGF2 and revealed significantly enhanced migration and proliferation of LEC – independently of the VEGF-C/VEGFR-3 pathway *in vitro*.

In order to identify other Prox1-modulated genes or LEC-specific genes, we set out to perform a gene expression profiling of human dermal BEC and LEC using oligonucleotide microarrays. This analysis revealed a novel set of 236 lymphatic signature genes and 342 blood vascular signature genes. Based on these endothelial lineage-specific transcripts, we established a novel Low-Density Microvascular Differentiation Array (LD-MDA) that revealed that commercially available HDMEC (human dermal microvascular endothelial cells) are a mixed cell population of LEC and BEC, and contained 84.1% LEC and 15.9% BEC. Using the LD-MDA together with biostatistical analysis, the investigation of the gene expression profiles of 43 psoriatic skin lesions revealed FGF12 and IL7 as novel (lymph)angiogenic-mediators in chronic inflammation. Furthermore, stimulation of LEC and BEC with FGF12 and IL7 significantly enhanced cell proliferation *in vitro*.

In additional experiments - based on the microarray studies where we identified DPPIV as one of the 236 identified lymphatic signature genes - we found that the

active form of dipeptidyl peptidase IV (DPPIV) is more strongly expressed in lymphatic endothelium as compared to blood vascular endothelium in different tissues including skin. Knockdown of DPPIV in LEC significantly repressed cell migration, tube-formation and adhesion to extracellular matrix components. Together, these findings suggest that DPPIV is an essential mediator of lymphangiogenesis.

In addition to DPPIV, several other factors such as VEGF-A and VEGF-C have been reported to regulate lymphangiogenesis. Understanding the molecular mechanisms by which VEGF-A and VEGF-C exert their effects on LEC may reveal novel targets for the prevention of tumor-associated lymphangiogenesis and cancer metastasis. To this end, we stimulated cultured human LEC with VEGF-A or VEGF-C for different time periods and then performed gene microarray analyses. We identified a number of genes that were induced by VEGF-A and/or VEGF-C, either transiently (early response genes) or progressively. In particular, we found that endothelial specific molecule-1 (ESM1), also known as endocan, was significantly upregulated by VEGF-A and VEGF-C. *In vitro* assays revealed that endocan promotes LEC proliferation and migration in concert with VEGF-A and VEGF-C. Furthermore, siRNA-mediated endocan knockdown reduced VEGF-A/-C induced LEC proliferation and migration *in vitro* and also inhibited VEGF-A-induced lymphatic vessel enlargement *in vivo*.

4.2 Outlook

The transcriptional profiling studies have provided exciting new information about novel genes with potential importance for lymphatic vessel growth and/or function. However, only a small fraction of these genes has been characterized thus far. Therefore, further investigations and *in vitro/in vivo* validations will be needed to evaluate the biological role - and possible importance as therapeutic target - of these genes.

In this thesis, we discovered that Prox1 directly binds to the putative Prox1 response elements in the FGFR-3 promoter and upregulates the expression of FGFR-3 during lymphatic reprogramming. However, several other genes have been reported to be involved in the regulation of endothelial lineage-specific differentiation (Hong et al, 2002; Petrova et al, 2002a). Therefore, we plan to systematically locate putative Prox1 response elements in the promoter regions of genes involved in lymphatic reprogramming. A further characterization of these genes will provide more insight into the molecular mechanisms controlling lymphangiogenesis during development.

In this study, the establishment of the LD-MDA allowed a sensitive quantification of endothelial lineage-specific differentiation; however, the genes selected for the LD-MDA and the *in vivo* application of the LD-MDA platform need to be further optimized. We are currently optimizing the platform using 'core' signature genes which show a more comparable expression within a group (e.g. LEC or BEC) but more differential expression between the groups. Furthermore, we try to obtain additional samples of psoriatic skin lesions - in addition to the 43 samples studied in this thesis - to enable an improved statistical analysis and tests for biological significances. The increased sample size could also suggest a possibility to apply the LD-MDA as a prognostic tool to quantify the extent of (lymph)angiogenesis in patients suffering from psoriasis or other angiogenesis-associated diseases.

Additionally, we are currently investigating other possible functions of DPPIV in lymphatic endothelium. The hypothesis that DPPIV cleaves SDF-1α to regulate the chemoattraction of CXCR4-positive cancer cells such as the human breast carcinoma

cell line MDA-MB-231 toward lymphatic endothelial cells, can be tested using transwell migration assays. LEC coated-membranes can be treated or not with diprotin A to regulate the cleavage of SDF-1α, thus creating a gradient of (in)activated SDF-1α to control the motility of CXCR4-positive MDA cancer cells towards LEC. A previous report revealed that *in vivo* neutralization of CXCL12/CXCR4 interactions significantly impaired metastasis of breast cancer cells to regional lymph nodes and lung (Muller et al, 2001). Therefore, injecting MDA cells orthotopically into the mammary fat pad of mice and controlling lymph node metastasis by intravenously delivering diprotin A might shed a new light into the function of DPPIV *in vivo*.

In this thesis, we reported that expression of endocan is induced by VEGF-A and VEGF-C in LEC and we further demonstrated that knockdown of endocan inhibited LEC proliferation and migration *in vitro* and lymphatic vessel enlargement *in vivo*. Recent reports have revealed that increased levels of endocan are observed in the blood of cancer patients (Grigoriu et al, 2006; Scherpereel et al, 2003). Therefore, we are currently planning to investigate the regulation of lymph node metastasis by targeting endocan in experimental tumor models.

Overall, we have identified and characterized several genes that control lymphatic function during differentiation and lymphangiogenesis after performing transcriptional profiling. However, the recent discovery of a multi-layer gene regulation suggests that our biological system of interest is more complex than we have imagined (Chen & Rajewsky, 2006; Kedde et al, 2007). Therefore, systematically identifying microRNAs, single nucleotide polymorphisms (SNPs), epigenetic regulators and RNA-binding proteins controlling the molecular mechanisms of lymphatic vascular function would likely give rise to novel therapeutic targets to prevent lymphatic-associated pathologies.

5 MATERIALS AND METHODS

5.1 *In Vitro*

5.1.1 Cell culture

5.1.1.1 *Isolation of human dermal BEC and LEC*

Neonatal human foreskins were obtained after routine circumcision. After enzymatic digestion, the epidermis was removed and dermal cells were mechanically released (Richard et al, 1998). CD34-positive BEC were isolated by immunomagnetic purification with an anti-human CD34 antibody (BC Pharmigen, San Diego, CA) conjugated to immunomagnetic beads (Dynal, Lake Success, NY). Thereafter, the remaining CD34-negative cells were incubated with an immunomagnetic beads-conjugated anti-human CD31 antibody (Dynal) to isolate LECs. LECs were seeded onto fibronectin-coated (10 µg/ml; BD Biosciences, Bedford, MA) and were propagated in endothelial cell basal medium (Cambrex Corp.; East Rutherford, NJ) containing 20% fetal bovine serum, antibiotics, 2 mmol/L L-glutamine (Invitrogen Corp.; Carlsbad, CA), 10 µg/mL hydrocortisone acetate and 2.5×10^{-2} mg/ml *N*-6,2'-*O*-dibutyryl adenosine-3,5'-cyclic monophosphate (Sigma-Aldrich; St. Louis, MO). Confluent primary BEC cultures were further purified by immunomagnetic E-selectin selection after 6 hours of stimulation with recombinant human tumor necrosis factor-α as described (Richard et al, 1998). The lineage-specific differentiation was confirmed by real-time RT-PCR for the lymphatic vascular markers Prox1, LYVE-1 and podoplanin, and for the blood vascular endothelial markers VEGFR-1 and VEGF-C, as well as by immunostains for CD31, LYVE-1 and Prox1.

5.1.1.2 *Cells*

Human dermal microvascular endothelial cells (HDMEC) and Human umbilical vein endothelial cell (HUVEC) were obtained from Cambrex (Verviers, Belgium) and PromoCell (Heidelberg, Germany). Commercial human LEC were also obtained from Cambrex. Human IMR91 dermal fibroblasts were obtained from the National Institute of Aging, USA. The immortalized human epidermal keratinocyte line HaCaT was a kind gift of Dr. Norbert Fusenig, German Cancer Research Center, Heidelberg,

Germany. The immortalized human microvascular endothelial cell line HMEC-1 (Ades et al, 1992) was obtained from the Center for Disease Control, Atlanta, GA, USA. Stably transfected rat myoblasts expressing human FGFR3 IIIb or FGFR3 IIIc were kind gifts from Dr. Daniel Podolsky, Massachusetts General Hospital (Kanai et al, 1997). HEK293 cells were purchased from American Type Culture Collection (ATCC) (Manassas, VA).

Primary endothelial cells used in all experiments were in their early passages (no greater than passage number 10).

5.2 Target validations

5.2.1 Electrophoretic mobility shift assay

5.2.1.1 *GST-Prox1-DNA complex*

Purification of the GST-Prox1 protein was performed as described (Belecky-Adams et al, 1997; Cui et al, 2004). The GST-Prox1 vector, a kind gift from Dr. M. Duncan (Cui et al, 2004), expresses the C-terminal half of Prox1 (the homeodomain and prospero domains) fused to the GST protein. Rosetta bacterial cells (Novagen, San Diego, CA) were transformed with the GST-Prox1 vector or a control GST vector (pGEX-KG). Bacterial cell extracts were prepared using the BugBuster solution (Novagen). The GST and GST-Prox1 proteins were isolated by Glutathione Sepharose 4B beads (Ahmersham Bioscience, Piscataway, NJ). Five micrograms of purified proteins were incubated in 10 mM Tris (pH 7.5), 10 mM $MgCl_2$, 5 mM EDTA (pH 7.5), 10 mM DTT, 2% NP-40, 10% glycerol, 20% sucrose, 5 μg BSA, and 0.2 μg poly(dI:dC) (poly-deoxy-inosinic-deoxy-cytidylic-acid) for 30 minutes at room temperature, together with 0.05 pmole of ^{32}P-labeled probes (wild-type, ctgggctccCACGCCTCTgggaccgcccg; mutant, ctgggctccACTTAAGCTgggaccgcccg). The protein-DNA complex was separated in a 6% native polyacrylamide gel (30% PA solution, 5X TBE, 10% AP, TEMED) in 0.5X TBE at 200V for 1 hour in an ice-slurry, after a pre-run in 0.5X TBE at 150V at room temperature. For competition

assays, 100-fold molar excess of the unlabeled probe was added to the incubation mixtures.

5.2.2 Quantification of RNA

5.2.2.1 *Detection and quantification of FGF receptor, DPPIV and ESM1 expressions using qRT-PCR*

Dual-labeled TaqMan probe-based real-time RT-PCRs were performed to quantify the expression of FGF receptors (Hong et al, 2002). The sequences of forward and reverse primers and dual-labeled probes are as follows: FGFR-1 (CTCCCGAGGCGGAACC, TGAGCTCGATCCTCCTTTTCA, FAM-CCACGCCGAGCGAGGGTCAG-TAMRA), FGFR-3 (GTCATGGAAAGCGTGGTGC, CCAAACTTGTTCTCCACGACG, FAM-TCGGACCGCGGCAACTACACC-TAMRA), and β-actin (TCACCGAGCGCGGCT, TAATGTCACGCACGATTTCCC, JOE-CAGCTTCACCACCACGGCCGAG-TAMRA).

In addition, conventional RT-PCR was performed for FGFR-3 using forward and reverse primers (GACGGCACACCCTACGTTAC, GGATGCCTGCATACACACTG) that bind to the 7th and 10th exon of human FGFR-3, respectively, along with primers for β-actin (TGGGACGACATGGAGAAAAT, GAGGCGTACAGGGATAGCAC). An FGFR-3 cDNA clone (Clone ID, 180447) from Invitrogen (Carlsbad, CA) was used as a probe for Northern blot analysis. RT-PCR analyses were performed at least three times with comparable results.

The expressions of DPPIV mRNA, ESM1 mRNA were quantified by real-time RT-PCR using the ABI 7900 HT Fast Real-Time PCR System (Applied Biosystems, Foster City, CA). The probes and primers for DPPIV (Hs00175218_m1) and ESM1 (Hs00199831_m1) were pre-designed by Applied Biosystems (Foster City, CA). Each reaction was normalized with the expression of β-actin as an internal control.

5.2.3 Protein

5.2.3.1 *Detection of DPPIV and ESM1 proteins using Western blotting*

For Western blot analysis of DPPIV, LEC were homogenized in lysis buffer. The protein concentrations were determined using NanoOrange® Protein Quantification Kit (Molecular Probes, Eugene, OR). The lysates (100 µg of total protein) were then subjected to SDS-polyacrylamide gel electrophoresis (PAGE), using a NuPAGE™ 10% BT Gel, 1.0 mm, 12 well and NuPAGE™ MES SDS Running Buffer (20x) (both Invitrogen, Carlsbad, CA). The proteins were transferred from SDS gels onto a Trans-Blot® Transfer Medium pure nitrocellulose membrane (BioRad, Hercules, CA) for immunoblot analysis. Blocking was performed with 5% non-fat dry milk in 0.1% Tween®20 (Sigma) in PBS (PBS-T) and then immunoblotted with the anti-DPPIV goat polyclonal antibody (0.2 µg/ml, R&D Systems, Minneapolis, MN). Specific binding was detected by ECL Plus Western Blotting Detection System (GE Healthcare, Buckinghamshire, UK). Equal loading was confirmed with an antibody against β-actin (Sigma, St. Louis, MO).

For Western blot analysis of ESM1, serum-starved (0.1% BSA) LEC were stimulated with 20 µg/ml of VEGF-A for 24h and 48h. The cell lysates were homogenized in lysis buffer and the supernatants were collected at each time point. The protein concentration were determined using NanoOrgane® Protein Quantification Kit (Molecular Probes). The lysates (100 µg total protein) and the supernatants (50 µg) were then subjected to the same method as mentioned above. The membrane was then immunoblotted with the human anti-ESM1 goat polyclonal antibody (0.2 µg/ml, R&D Systems, Minneapolis, MN). Specific binding was detected by ECL Plus Western Blotting Detection System (GE Healthcare, Buckinghamshire, UK). Equal loading was confirmed with an antibody against β-actin (Sigma, St. Louis, MO).

5.2.4 *In situ* expression validations

5.2.4.1 *Tissue samples*

Samples of human skin were from routine circumcision of neonatal foreskin (Massachusetts General Hospital, Boston, MA).

Samples of lesional psoriatic skin were obtained by 8 mm punch biopsy from 43 patients with chronic plaque-type psoriasis (mean age 51.95 years; range from 20 to 76 years) after informed consent was obtained. Approval for this study was obtained from the Human Ethics Committee of the Medical University of Vienna and of the University of Kiel. Samples were cut in half, and one half was stored in RNAlater (Ambion, Austin, Texas) for further RNA isolation. The other half was embedded in optimal cutting temperature (OCT) compound (Sakura Finetek; Torrance, CA, USA) and frozen on dry ice for immunofluorescence analyses.

5.2.4.2 *Immunofluorescence staining of FGFR-3 in human skin and mouse embryo*

Immunofluorescence stainings were performed on frozen sections of 4%-paraformaldehyde-fixed neonatal human foreskin sections or on E11.5 mouse embryo sections as previously described (Hong et al, 2002), using antibodies against human FGFR-3 (MAB 7661, R&D Systems Inc., Minneapolis, MN), mouse FGFR-3 (MAB 710, R&D Systems Inc.), or LYVE-1 (Upstate, Charlottesville, VA). Secondary antibodies labeled with AlexaFluor488 or AlexaFluor594 (Molecular Probes, Eugene, OR) were used to detect respective primary antibodies. Nuclei were counter-stained with 20 μg/ml Hoechst bisbenzimide.

5.2.4.3 *Immunofluorescence of psoriatic skin*

Double immunofluorescence analyses of lymphatic vessels and blood vessels were performed on 8-μm cryostat sections as described (Kunstfeld et al, 2004), using a rabbit polyclonal antibody to the lymphatic-specific hyaluronan receptor LYVE-1 (Upstate/Millipore; Billerica, MA) and a mouse monoclonal antibody to the vascular marker CD31 (Dako Cytomation; Glostrup, Denmark), and corresponding secondary antibodies labeled with AlexaFluor488 or AlexaFluora594 (Invitrogen/Molecular

Probes; Carlsbad, CA). Nuclei were counterstained with 20 μg/ml of Hoechst bisbenzimide. Sections were examined using an Axioscope 2 mot plus (Carl Zeiss AG; Feldbach, Switzerland) and images were captured with a Zeiss AxioCam MRc. Computer-assisted morphometric vessel analyses of representative LYVE-1 and CD31 double-stained sections, including the determination of the relative tissue area covered by lymphatic vessels ("lymphatic vessel area"; LVA) or by blood vessels ("blood vessel area"; BVA) were performed as described (Kunstfeld et al, 2004).

5.2.4.4 *Immunostains of DPPIV*

Differential immunofluorescence stains using an antibody against DPPIV (1:100, R&D systems) together with antibodies against lymphatic-specific or blood vessel-specific markers were performed on 8-μm cryostat sections as described (Kunstfeld et al, 2004). Stainings were performed using antibodies against the lymphatic-specific hyaluronan receptor LYVE-1 (1:1000; Upstate/Millipore, Billerica, MA), the lymphatic-specific glycoprotein podoplanin (D2-40; 1:200; Signet, Dedham, MA), the lymphatic-specific transcription factor Prox-1 (Covance, Princeton, NJ), the panendothelial marker CD31 (1:100, Dako Cytomation, Glostrup, Denmark) or the blood vessel-specific marker CD34 (1:100, BD Pharmingen, San Diego, CA), and corresponding secondary antibodies labeled with AlexaFluor488 or AlexaFluora594 (Invitrogen/Molecular Probes). Nuclei were counterstained with 20 μg/ml of Hoechst bisbenzimide. Immunohistochemical stains were performed on tissue arrays of normal human tissues (MaxArray human normal tissue microarray slides, Zymed, San Francisco, CA) as described previously (Dadras et al, 2003). Briefly, the primary antibody against DPPIV (1:100) was applied, followed by incubation with conjugated anti-goat immunoglobulin using the 3-amino-9-ethylcabazole peroxidase kit (Vector laboratories, Burlingame, CA). Sections were examined using an Axioscope 2 mot plus (Carl Zeiss AG; Feldbach, Switzerland) and images were captured with a Zeiss AxioCam MRc. For staining of lymphatic vessels, the anti-human podoplanin antibody D2-40 (Schacht et al, 2005) (Signet) was used.

5.2.5 Cell culture-based (*in vitro*) assays

5.2.5.1 *Construction of mutant Prox1 and FGFR-3 reporter gene luciferase assays*

To construct a mutant Prox1, two amino acid substitution mutations (N625A and R627A) were introduced into pcDNA/Prox1 (Hong et al, 2002) by using the QuickChange II site-directed Mutagenesis kit (Stratagene, La Jolla, CA). DNA sequences of the primers used for the mutagenesis reaction are CTCATCAAGTGGTTTAGCgcTTTCgccGAGTTTTACTAC and CTGAATGTAGTAAAACTCggcGAAAgcGCTAAACCACTTG. The resulting product (pcDNA/MutProx1) was sequenced to confirm the base-pair changes. The mouse FGFR-3 promoter-luciferase constructs were kindly provided by Dr. David Ornitz (McEwen & Ornitz, 1998). Each luciferase construct was co-transfected into HEK 293 cells in combination with pcDNA (Invitrogen), pcDNA/Prox1 or pcDNA/MutProx1. Forty-eight hours after transfection, 50 μl of the cell lysates were used to measure the activity of firefly luciferase using the Dual-Glo Luciferase Assay System (Promega, Madison, WI). Another 50 μl of the cell lysates was used to measure the protein concentration by using the Bio-Rad Protein Assay (Bio-Rad, Hercules, CA). Luciferase activity was normalized by the total protein amount. The assays were performed in triplicates in three independent experiments.

5.2.5.2 *Binding and internalization of ^{125}I-FGF-2*

FGF-2 was labeled with ^{125}I-Na using iodogen (Pierce, Rockford, IL) as a coupling agent according to the manufacturer's instruction. The specific activity of ^{125}I-FGF-2 was 150,000 cpm/ng. FGF-2 binding to high and low affinity sites was investigated as described (Moscatelli, 1987). Cells were seeded at 2.5 x 10^5/ cm^2 and were cultured in complete medium in 3.5-cm diameter dishes for two days. Cells were washed twice with ice cold PBS and were incubated with the indicated concentrations of ^{125}I-FGF-2 in DMEM containing 20 mM Hepes (pH 7.4) and 0.15 % gelatin for 2 h at 4°C. Cells were then washed three times with cold PBS. ^{125}I-FGF-2 was dissociated from its cellular low affinity binding sites by two 20-second washes with ice cold 20 mM Hepes (pH 7.4), 2 M NaCl, and from its high affinity sites by two 20-second washes

with ice cold 20 mM NaAc (pH 4.0), 2 M NaCl. Bound ^{125}I-FGF-2 was quantified using a Kontron MR 250 gamma-counter (Saint-Quentin-Yvelines, France). Non-specific binding was determined by incubating LECs in separate dishes with ^{125}I-FGF-2 and a 100-fold excess of unlabeled ligand. Specific binding was determined by subtracting non-specific binding from total binding. Experiments were done in duplicates and repeated twice with comparable results. Internalization experiments were performed as described (Perollet et al, 1998). Cells in 3.5-cm diameter dishes were incubated with 10 ng/ml of ^{125}I-FGF-2 and shifted to 37°C. After the specified time points (0-24 h), cells were washed 3 times with PBS and twice for 20 seconds with 20 mM Hepes (pH 7.4) containing 2M NaCl and twice for 20 seconds with ice cold 20 mM NaAc (pH 4.0) containing 2M NaCl, to remove cell surface-associated radioactivity. Cells were then extracted with 5 % Triton X-100, 2 % sodium dodecyl sulfate in PBS pH 7.4 and internalized ^{125}I-FGF-2 was quantified by radioactive counting in a Kontron MR 250 gamma-counter. Experiments were done in duplicates and repeated twice.

5.2.5.3 *Cell proliferation, migration, apoptosis assays and functional inhibition of FGFR-3*

Recombinant human FGF-1 and FGF-2 were purchased from R&D Systems. For proliferation assays, 1,500 LECs were seeded into a fibronectin-coated well of 96 well plates in complete growth medium (Hirakawa et al, 2003). After 24 hours, cells were treated or not with FGFs (10 ng/ml) for 48 hours in low serum medium (2% FBS) containing heparin (1 μg/ml). Cell proliferation was assessed by the MUH fluorescence assay as previously described (Detmar et al, 1990). For migration assays, 24-well FluoroBlok inserts (Falcon, Franklin Lakes, NJ; 8 μm pore size) were coated on the bottom side with 10 μg/ml fibronectin (BD Bioscience) for 1 hour, and then by 100 μg/ml BSA (Sigma) for 1 hour. 750 μl EBM containing 0.2% BSA and heparin (1 μg/ml), supplemented with or without FGFs (10 ng/ml), was added to the bottom chambers. 5×10^4 LECs in serum-free EBM medium (Clonetics, Watersville, MD) containing 0.2% BSA were added into each well. After 3 hours, cells migrated onto the bottom side of the inserts were stained with Calcein-AM (Molecular Probes) and the fluorescence intensity was measured using the Victor2 Fluorometer (PerkinElmer,

Boston, MA). For VEGFR-3 blocking experiments, LECs were pre-incubated with a control IgG or a rat anti-human VEGFR-3 blocking antibody (1 μg/ml) (kindly provided by Dr. Bronek Pytowsky, ImClone Systems Inc., New York, NY) for 10 min. The serum-free EBM media in the bottom chambers contained VEGF-C (100 ng/ml, R&D System) or FGF (10 ng/ml). For apoptosis assays, 4,000 LECs were seeded into a fibronectin-coated well of 96 well plates and cultured for 24 hours. Cells were then incubated for 24 hours in medium containing 0.1% BSA, 20% FBS, 1 μg/ml heparin, with or without FGF-1 or FGF-2 at a concentration of 10 ng/ml. Cytoplasmic histone-associated-DNA-fragments generated by induction of cell death was quantified using the Cell Death Detection ELISA kit (Roche, Indianapolis, IN).

Functional inhibition of FGFR-3 was performed by transfecting cultured LECs (passage 2) with pooled small interfering RNAs (siRNA) for FGFR-3 or siRNA for the luciferase gene as a negative control by using Amaxa HMVEC-L Nucleofector Kit (Amaxa Inc., Cologne, Germany). The siRNA sequences are as follow (FGFR-3: CACGACCUGUACAUGAUCAdTdT, UGCACAACGUCACCUUUGAdTdT and UGCACAACCUCGACUACUAdTdT; Luciferase, CUUACGCUGAGUACUUCGAdTdt). Transfected cells were then plated into two 6-cm dishes. One dish was used to collect total RNAs to quantify the steady-state level of FGFR-3 and the other for cell proliferation assays. Proliferation assays were performed 24 hours after transfection as described above.

5.2.5.4 *LEC and BEC proliferation assays for FGF-12 and IL7*

Recombinant human FGF-12 and IL-7 were purchased from R&D Systems (Minneapolis, MN). BEC and LEC (1.5×10^3) were seeded into fibronectin-coated 96-well plates and were incubated in complete growth medium (Hirakawa et al, 2003). After 24 hours, cells were incubated in medium containing 1% FBS overnight and quintuplicate wells were then treated or not with FGF-12 (0.5 ng/ml – 500 ng/ml) or IL-7 (0.05 ng/ml – 50 ng/ml) in low serum medium (1% FBS). After 48 h, cells were incubated with 4-methylumbelliferyl heptanoate (MUH; Sigma, St. Louis, MO) as described(Detmar et al, 1990). The intensity of fluorescence, proportional to the number of viable cells, was measured using a SpectraMax Gemini EM microplate

reader (Bucher Biotec AG, Basel, Switzerland). Experiments were repeated three times for each treatment. Statistical analyses were performed using the two-tailed unpaired student's *t*-test.

5.2.5.5 *DPPIV enzyme activity assay*

LEC or BEC were seeded into fibronectin-coated wells of 96-well plates in complete growth medium, at a cell density ranging from 20 to 20,000 cells/cm². After 24 hours, cells were washed twice with PBS, incubated with the proluminescent DPPIV substrate Gly-Pro-aminoluciferin (DPPIV-Glo protease assay; Promega, Madison, WI), and gently mixed using a plate shaker at 500 rpm for 30 seconds. Plates were incubated for 2 hours in a buffer system optimized for DPPIV and luciferase activities. Luciferase activity was assessed by a LMAXII 384 luminometer (Bucher Biotec AG, Basel, Switzerland). For enzyme inhibition assays, 2,000 LEC were seeded into fibronectin-coated wells of 96-well plates in complete medium. After 20 hours, cells were washed twice with PBS and were treated with diprotin A (International Peptides, Osaka, Japan) for 4 hours.

5.2.5.6 *LEC transwell migration, scratch-wound, tube formation and adhesion assays and functional inhibition of DPPIV*

siRNA-transfection was performed using Basic Nucleofector Kit for primary mammalian endothelial cells (Amaxa Biosystems, Cologne, Germany) according to the manufacturer's protocol. Predesigned siRNAs against human DPPIV (SI00030212, SI00030219, SI00030226; Qiagen, Hilden, Germany) and control siRNA (Silencer Negative Control #1 siRNA, Ambion, Cambridgeshire, UK) were used for the transfections.

For endothelial cell migration assays, control or DPPIV siRNA-transfected LEC were grown to 100% confluency and serum starved overnight. The following day, a cell-free wound zone was created by scraping the monolayer with a sterile pipette tip. The cells were washed with PBS and then the medium was changed to EBM containing either PBS or 3% FBS. The monolayers were incubated in 5% CO_2 at 37°C for 48 h.

Representative images were taken at 5x magnification directly after wounding and after 48h, using an AxioCam MRm camera attached to an Axiovert 200M microscope (Carl Zeiss AG, Feldbach, Switzerland). Computer-assisted morphometric wound area analyses were performed using the IP-LAB software (Scanalytics, Fairfax, VA).

For trans-well migration assays, 24-well FluoroBlock inserts of 8 μm pore size (BD Bioscience, Bedford, MA) were coated on the bottom side with 10 μg/ml fibronectin (BD Biosciences) or with type I collagen (Vitrogen, Palo Alto, CA) for 1 h, followed by incubation with 100 μg/ml bovine serum albumin (BSA; Sigma) to block the remaining protein-binding sites. Cells ($1x10^6$ cells/ml; 100 μl) were seeded in serum-free EBM medium (Cambrex Bio Science) containing 0.2% delipidized BSA into the upper chambers, and were incubated for 3 h at 37°C in the presence or absence of 3% FBS. Cells on the underside of inserts were stained with Calcein AM (Molecular Probes), and the fluorescence intensity was measured using a Spectra Max Gemini fluorescence reader (Bucher Biotec AG). Cell adhesion assays were performed by coating 96-well plates with fibronectin (10 μg/ml) or type I collagen (50 μg/ml) for 30 min, followed by blocking with 100 μg/ml BSA. Control or DPPIV siRNA-transfected LEC (10^5 cells in 200 μl of serum-free EBM) were seeded into each well and were incubated at 37°C for 45 min. Unattached cells were removed by three gentle washes with serum-free EBM containing 0.5% BSA; attached cells were stained with Calcein AM, fixed with 4% paraformaldehyde, and fluorescence was measured using a Spectra Max Gemini EM. Tube formation assays were performed as described (Schacht et al, 2003). Control or DPPIV siRNA transfected LEC were grown on collagen-coated 24 well plates until confluence. Then, 0.5 ml of neutralized isotonic bovine dermal collagen type I (Vitrogen, Palo Alto, CA) with 3% FBS was added to the cells. After incubation at 37°C for 6 h, cells were fixed with 4% paraformaldehyde for 30 min at 4°C. Representative images were captured and the total length of tube-like structures per area was measured using the IP-LAB software (Scanalytics, Fairfax, VA) as described (Schacht et al, 2003). All studies were repeated three times. Statistical analyses were performed using the unpaired Student's *t*-test.

5.2.5.7 *Functional inhibition of ESM-1, receptor blocking experiment and LEC proliferation and migration assays*

siRNA-transfection was performed using the Basic Nucleofector Kit for primary mammalian endothelial cells (Amaxa Biosystems, Cologne, Germany) according to the manufacturer's protocol. The following siRNAs against ESM1 were used (sense): 5'-GGUUUGUAAAAGAAGAAUCtt-3', 5'-GGUGUCAGCCUUCUAAUGGtt-3' and 5'-GCUGCAUAAGCUGUUAGGUtt-3', as well as control siRNA (silencer negative control #1 siRNA, Ambion, Cambridgeshire, UK).

Antibodies against the extracellular domain of human VEGFR-2 (1121b) (Lu et al, 2000) and of human VEGFR-3 (hF4-3C5) (Persaud et al, 2004), as well as rat negative control IgG were kindly provided by Dr. Bronek Pytowski, Imclone Systems, New York, NY.

LEC ($2x10^3$) were seeded onto fibronectin-coated 96-well plates. Quintuplicate wells were treated with different concentrations of recombinant human ESM1 (0.01 ng/ml to 2500 ng/ml; R&D Systems) and with 20 ng/ml VEGF-A or 100 ng/ml VEGF-C. In some experiments, cells were also incubated with an anti-human ESM1 polyclonal antibody (10 µg/ml) or with control rat-IgG (10 µg/ml). After 72 hours, cells were incubated with 4-methylumbelliferyl heptanoate (MUH; Sigma-Aldrich). The fluorescence intensity, proportional to the number of viable cells, was measured using a Spectra Max GEMINI EM fluorescence reader (Bucher Biotec AG, Basel, Switzerland). For endothelial cell migration assays, control- or ESM-1 siRNA-transfected LEC were grown to 100% confluency and serum starved overnight. The following day, a cell-free wound zone was created by scraping the monolayer with a sterile pipette tip. The cells were washed with PBS and then the medium was changed to EBM/0.1% BSA containing either PBS or VEGF-A (20 ng/ml) or ESM1 (1 µg/ml) or both. The cells were incubated in 5% CO_2 at 37°C for 48h. Representative images were taken at 5x magnification directly after wounding and after 48h, using an AxioCam MRm camera attached to an Axiovert 200M microscope (Carl Zeiss AG). Computer-assisted morphometric wound area analyses were performed using the IP-LAB software (Scanalytics, Fairfax, VA). All experiments were performed three times. Statistical analyses were performed using the unpaired Student's *t*-test.

5.3 *In Vivo*

5.3.1 Mouse experiments

5.3.1.1 *ESM-1 siRNA Matrigel assay, immunofluorescence stainings and morphometric analyses*

Lymphangiogenesis was evaluated *in vivo* by using a matrigel plug assay as described previously (Chae et al, 2004; Kajiya et al, 2005; Zhang et al, 2006). FVB wild-type mice (female, 6-8 weeks old) were anaesthetized and injected subcutaneously into the lower flank skin with 100 µl of Matrigel (BD Biosciences, Bedford, MA) containing either human VEGF-A165 (500 ng/ml) and Silencer Negative control siRNA (10 µg/ml; Ambion, cat. No. 4635) or VEGF-A165 and murine ESM1 siRNA (10 µg/ml; Ambion, cat. no. 16804) (n=5 per group). After 7 days, skin samples were embedded in optimal cutting temperature compound (OCT; Sakura Finetek, Torrance, CA). Immunofluorescence analyses were performed on 8 µm cryostat sections as described (Hong et al, 2004b; Kunstfeld et al, 2004), using a rabbit polyclonal antibody against mouse LYVE-1 (Upstate Biotechnology, Charlottesville, VA) and a monoclonal rat antibody against mouse CD31 (BD Biosciences Pharmingen, San Diego, CA). For the detection of ESM1 in the skin of VEGF-A transgenic mice (female, 8 weeks old) (Kunstfeld et al, 2004; Xia et al, 2003), murine ESM-1 antibody (R&D Systems) was used. Corresponding secondary antibodies were labeled with AlexaFluor488 or AlexaFluor594 (Molecular Probes, Eugene, OR). Nuclei were counterstained with 20 µg/ml Hoechst 33342 (Molecular Probes). Sections were examined by an Axioskop2 microscope (Carl Zeiss AG, Feldbach, Switzerland) and images were captured at 20x magnification with an AxioCam MRm digital camera. Computer-assisted morphometric vessel analyses of representative LYVE-1 and CD31 double-stained sections were performed using the IP-LAB software (Scanalytics, Fairfax, VA) as described (Kunstfeld et al, 2004). Three individual fields per section were examined and the number of vessels per mm^2, the average vessel size and the average tissue area covered by vessels were determined. Statistical analysis was performed using the unpaired Student's *t*-test.

5.4   TRANSCRIPTOMICS

5.4.1   Gene expression profiling using oligonucleotide microarrays

5.4.1.1   *Gene expression profiling of human LEC and BEC*

Total cellular RNA was isolated from confluent BEC and LEC cultures after 2−5 passages using the Trizol reagent (Invitrogen). Digoxigenin-UTP labeled cRNA was generated and linearly amplified from 1 μg of RNA for each sample using the Chemiluminescent RT-IVT Labeling Kit v.2.0 (Applied Biosystems; Foster City, CA) according to the manufacturer's protocol. We obtained the gene expression profiles of three matched pairs (each pair obtained from the same donor) of cultured LEC and BEC by the Applied Biosystems Human Genome Survey Microarray v2.0. Labeling, hybridization, and signal generation and detection were performed according to the manufacturers' protocols.

5.4.1.2   *LEC vs. BEC microarray data analysis*

Quantile normalization, implemented in the statistical language R (http://www.bioconductor.org/), was applied to the datasets to normalize the distribution of probe set intensities for each array. Present calls were set by a signal-to-noise ratio (S/N) ≥3 and quality-flag ≤ 5,000 determined by the AB1700 microarray software tool. The ratio of gene expression was calculated for each matched pair of LEC and BEC, and was expressed as log2 values. For the identification of the LEC-specific transcriptome, probes with present calls in the LEC samples were selected for further analysis. For the identification of the BEC-specific transcriptome, the same filtering was performed on BEC samples. LEC-specific signature genes were identified based on a log2 ratio (LEC/BEC) ≥ 1, whereas BEC-specific signature genes were selected based on a log2 ratio ≤ −1 in each of the three matched pairs of LEC and BEC.

5.4.1.3 *Gene expression profiling for VEGF-A and VEGF-C target genes in LEC*

Primary LEC were serum starved overnight in EBM supplemented with 0.2% bovine serum albumin. Cells were treated or not for 1h, 4h, 8h or 24h with recombinant human VEGF-A$_{165}$ (R&D Systems; 20 ng/ml) or mature human VEGF-C (R&D Systems; 500 ng/ml). Total cellular RNA was isolated using the Trizol reagent (Invitrogen) and was extracted with chloroform, precipitated with isopropanol, washed with 70% ethanol, and dissolved in DNase-free/RNase-free distilled water. The concentration of RNA was measured using a NanoDrop ND-1000 spectrophotometer (Witec AG, Littau, Switzerland), and RNA quality was assessed using a 2100 Bioanalyzer (Agilent Technologies, Palo Alto, CA).

Digoxigenin-UTP labeled cRNA was generated, amplified from 500 ng of total RNA, using the NanoAmp RT-IVT Labeling Kit (Applied Biosystems, Foster City, CA) following the manufacturer's protocol, and was hybridized to Applied Biosystems Human Genome Survey Microarrays V2.0. Chemiluminescence detection, image acquisition and analysis were performed using the Chemiluminescence Detection Kit (Applied Biosystems) and the Applied Biosystems 1700 Chemiluminescent Microarray Analyzer following the manufacturer's protocol. Three biological replicates were generated for each treatment condition (VEGF-A and VEGF-C) and for each time point (0h, 1h, 4h, 8h, 24h).

5.4.1.4 *VEGF-A, VEGF-C stimulated time course data analysis*

Raw data were normalized using Variance Stabilization and Normalization (VSN), a model derived from the variance-versus-mean dependence for microarray intensity data (Huber et al, 2002), available from R/Bioconductor (Gentleman et al, 2004). In a second step, probes which had a signal to noise ratio (S/N ratio) ≥ 3, flag (error) value ≤ 5000 in at least two out of the three replicates for each time point were further subjected to statistical analyses. Differentially expressed genes were identified using the multivariate Empirical Bayes (EB) analysis (R package: time course). The multivariate-EB procedure focuses on moderating the denominator of the multivariate t-statistics, and ranks genes according to the moderated statistic to reduce the number

of false positives and false negatives resulting from very small or very large replicate variances or covariances (www.stat.berkeley.edu/tech-reports/667.pdf). In a next step, Time Series Expression Miner (STEM) (Ernst & Bar-Joseph, 2006) was used to identify early response, transiently upregulated, progressively induced and downregulated clusters. Briefly, STEM implements a clustering method that depends on a set of distinct and representative short temporal expression profiles and each probe in the dataset is assigned to a profile with the closest match. The expected number of probes assigned to each profile is estimated by permutation and the statistically significantly overexpressed (p<0.05) profiles are then identified. The preprocessed datasets of three independent experiments were imported into STEM. Experimental profiles with a minimal correlation of 0.7 with the predetermined model profiles were then clustered together.

5.4.1.5 *Establishment of a Low-Density Microvascular Differentiation Array*

Guided by the gene array results, we selected 54 LEC-specific genes and 31 BEC-specific genes, based upon their consistent and strong specific expression in LEC or BEC, as well as on their assignment to important biological pathways. In addition, the five pan-endothelial cell marker genes PECAM-1, vWF, KDR, TEK, CDH5 and the six endogenous control genes ACTB, GAPDH, PGK1, PPIA, RPLP0 and S18 were included in the design of the LD-MDA (**Appendix Table 1**).

The 384-well micro-fluidic cards were produced with pre-designed primer pairs and FAM-labeled TaqMan probes for each of the 96 selected genes in duplicate, with two sample reservoirs per card. The LD-MDA was then used to evaluate the lineage-specific differentiation of a total of 10 independent lines of primary human dermal LEC, of eight independent lines of primary human dermal BEC, of two independent lines of HUVEC cells, of the immortalized human microvascular endothelial cell line HMEC-1, of the immortalized human epidermal keratinocyte line HaCaT, and of primary human dermal fibroblasts. After extraction of total RNA, the mRNA expression levels of the 96 genes were analyzed by quantitative RT-PCR using the 7900HT Real-Time PCR System (Applied Biosystems). The cDNAs were reverse transcribed from 40 ng of total RNA per sample using random primers provided with

the High Capacity cDNA Archive Kit (Applied Biosystems) at 25°C for 10 minutes, followed by incubation at 37°C for 120 minutes. PCR products were synthesized using the TaqMan Universal PCR Master Mix (Applied Biosystems) at 95°C for 10 minutes, followed by 40 cycles at 95°C for 15 seconds and 60°C for 60 seconds. In additional experiments, total RNA was obtained from frozen samples of 43 psoriatic lesions, using homogenization with a TissueLyser (Qiagen, Hilden, Germany) and RNA extraction with the Trizol reagent.

5.4.1.6 *Endothelial lineage score analysis and identification of core signature genes*

To quantitatively analyze the expression of vascular signature genes, the cycle values (Ct) of PCR amplification were acquired after 40 cycles using the Applied Biosystems SDS 2.2 software. The threshold was set to 0.2 units of fluorescence intensity. Unamplified samples were assigned a Ct value of 41. Normalization of Ct values was performed as follows: $\Delta Ct_{gene} = Ct_{gene} - Ct_{\beta\text{-actin}}$ because out of the six endogenous controls tested, β-actin showed the most consistent expression across different samples. Next, we implemented the 'sum-clustering' method to allocate each sample based on the degree of lymphatic or blood vascular endothelial differentiation. To this end, the sum of the ΔCt values of all 54 LEC-specific genes was subtracted from the sum of the ΔCt values of all 31 BEC-specific genes. This value was defined as the endothelial lineage-specific score (ELS). As a measure for the degree of endothelial cell differentiation, the sum of the ΔCt values of the 5 pan-endothelial marker genes was calculated for each sample and defined as vascular lineage score (VLS).

As a next step, we aimed to identify a subset of the 85 LD-MDA signature genes that had the most consistent lineage-specific 'core genes'. Based on the data obtained from ten LEC and eight BEC cultures, the following standard statistics values were calculated for each gene: delta mean Ct value between the LEC group and the BEC group ($\Delta Ct_{L\text{-}B}$), the mean square (MS) value within the LEC and BEC groups (MS_{within}), and the MS value between the LEC group and the BEC group ($MS_{Between}$). The genes with lower ratios of $MS_{Between}/MS_{within}$ (F-value) and the lower value of

ΔCt_{L-B} were identified as those that were expressed in both LEC and BEC with less specificity. Thus, 19 out of 85 vascular lineage genes that had the lowest F-values and/or ΔCt_{L-B} were removed. The Unweighted Pair Group Method with Arithmetic Mean (UPGMA) (Sokal, 1965) hierarchical clustering was performed using the Spotfire DecisionSite 8.0 software.

5.4.2 Bioinformatics

5.4.2.1 *Microarray data mining tools*

Pathway analyses were performed using the PANTHER (Protein Analysis THrough Evolutionary Relationships) protein classification system (www.pantherdb.org) which classifies proteins into families/sub-families, molecular functions, biological processes and biological pathways. The functional annotation of LEC and BEC signature genes and pathways which were statistically overrepresented in the group of genes upregulated after VEGF-A or VEGF-C treatments were calculated by a random overlapping p-value using binomial tests, with all of the genes represented on the Applied Biosystems Human Genome Survey Microarray serving as the reference list (Cho & Campbell, 2000).

5.4.2.2 *Prediction Relevance Ranking (PRR) analysis*

To investigate the influence of the 90 endothelial-signature genes on lymphatic vessel area and blood vessel area, we used a novel method denoted "Prediction Relevance Ranking" (PRR). It employs multiple linear regression analysis but in contrast to heuristic subset selection methods or regularization techniques like LASSO(Roth, 2004), it enumerates all possible models and investigates the whole model space to produce a ranking of variables based on their predictive power. To prevent overfitting and to estimate the predictive power of each model, 70% of the samples were randomly chosen for training the model and the remaining 30% samples were used for testing; this procedure was repeated 20 times for each model to estimate the distribution of the prediction error. The predictive power was assed by calculating the residual sum of squares (RSS). To characterize the model space for multiple

regression with a continuous target variable (e.g. lymphatic vessel area), PRR uses the linear model which contains the intercept as a reference point. Then, the error distribution of each model, which was lower RSS than average, was compared to the error distribution of the reference model by means of paired Student's *t*-test. The model with the lowest p-value is the single best model. Furthermore, the set of models with a p-value below a predefined threshold (0.05) was further characterized. In order to measure the prediction relevance of a given variable in relation to all other variables, each variable (gene) in a significant set of models was counted and plotted (**Appendix Figure 1**).

6   BIBLIOGRAPHY

Bibliography

Abtahian F, Guerriero A, Sebzda E, Lu MM, Zhou R, Mocsai A, Myers EE, Huang B, Jackson DG, Ferrari VA, Tybulewicz V, Lowell CA, Lepore JJ, Koretzky GA, Kahn ML (2003) Regulation of blood and lymphatic vascular separation by signaling proteins SLP-76 and Syk. *Science* **299**(5604)**:** 247-251

Achen MG, Jeltsch M, Kukk E, Makinen T, Vitali A, Wilks AF, Alitalo K, Stacker SA (1998) Vascular endothelial growth factor D (VEGF-D) is a ligand for the tyrosine kinases VEGF receptor 2 (Flk1) and VEGF receptor 3 (Flt4). *Proc Natl Acad Sci U S A* **95**(2)**:** 548-553

Ades EW, Candal FJ, Swerlick RA, George VG, Summers S, Bosse DC, Lawley TJ (1992) HMEC-1: establishment of an immortalized human microvascular endothelial cell line. *J Invest Dermatol* **99**(6)**:** 683-690

Al-Rawi MA, Watkins G, Mansel RE, Jiang WG (2005) The effects of interleukin-7 on the lymphangiogenic properties of human endothelial cells. *Int J Oncol* **27**(3)**:** 721-730

Alarid ET, Rubin JS, Young P, Chedid M, Ron D, Aaronson SA, Cunha GR (1994) Keratinocyte growth factor functions in epithelial induction during seminal vesicle development. *Proc Natl Acad Sci U S A* **91**(3)**:** 1074-1078.

Alitalo K, Tammela T, Petrova TV (2005) Lymphangiogenesis in development and human disease. *Nature* **438**(7070)**:** 946-953

Ambrose CT (2006) Immunology's first priority dispute--an account of the 17th-century Rudbeck-Bartholin feud. *Cell Immunol* **242**(1)**:** 1-8

Angeli V, Ginhoux F, Llodra J, Quemeneur L, Frenette PS, Skobe M, Jessberger R, Merad M, Randolph GJ (2006) B cell-driven lymphangiogenesis in inflamed lymph nodes enhances dendritic cell mobilization. *Immunity* **24**(2)**:** 203-215

Auguste P, Javerzat S, Bikfalvi A (2003a) Regulation of vascular development by fibroblast growth factors. *Cell Tissue Res* **314**(1)**:** 157-166

Auguste P, Javerzat S, Bikfalvi A (2003b) Regulation of vascular development by fibroblast growth factors. *Cell Tissue Res*

Avantaggiato V, Orlandini M, Acampora D, Oliviero S, Simeone A (1998) Embryonic expression pattern of the murine figf gene, a growth factor belonging to platelet-derived growth factor/vascular endothelial growth factor family. *Mech Dev* **73**(2)**:** 221-224

Backhed F, Crawford PA, O'Donnell D, Gordon JI (2007) Postnatal lymphatic partitioning from the blood vasculature in the small intestine requires fasting-induced adipose factor. *Proc Natl Acad Sci U S A* **104**(2)**:** 606-611

Baluk P, Tammela T, Ator E, Lyubynska N, Achen MG, Hicklin DJ, Jeltsch M, Petrova TV, Pytowski B, Stacker SA, Yla-Herttuala S, Jackson DG, Alitalo K, McDonald DM (2005) Pathogenesis of persistent lymphatic vessel hyperplasia in chronic airway inflammation. *J Clin Invest* **115**(2)**:** 247-257

Bammler T, Beyer RP, Bhattacharya S, Boorman GA, Boyles A, Bradford BU, Bumgarner RE, Bushel PR, Chaturvedi K, Choi D, Cunningham ML, Deng S, Dressman HK, Fannin RD, Farin FM, Freedman JH, Fry RC, Harper A, Humble MC, Hurban P, Kavanagh TJ, Kaufmann WK, Kerr KF, Jing L, Lapidus JA, Lasarev MR, Li J, Li YJ, Lobenhofer EK, Lu X, Malek RL, Milton S, Nagalla SR, O'Malley J P, Palmer VS, Pattee P, Paules RS, Perou CM, Phillips K, Qin LX, Qiu Y, Quigley SD, Rodland M, Rusyn I, Samson LD, Schwartz DA, Shi Y, Shin JL, Sieber SO, Slifer S, Speer MC, Spencer PS, Sproles DI, Swenberg JA, Suk WA, Sullivan RC, Tian R, Tennant RW, Todd SA, Tucker CJ, Van Houten B, Weis BK, Xuan S, Zarbl H (2005) Standardizing global gene expression analysis between laboratories and across platforms. *Nat Methods* **2**(5)**:** 351-356

Banerji S, Ni J, Wang SX, Clasper S, Su J, Tammi R, Jones M, Jackson DG (1999) LYVE-1, a new homologue of the CD44 glycoprotein, is a lymph-specific receptor for hyaluronan. *J Cell Biol* **144**(4)**:** 789-801

Bates DO, Harper SJ (2002) Regulation of vascular permeability by vascular endothelial growth factors. *Vascul Pharmacol* **39**(4-5)**:** 225-237

Bauvois B (1988) A collagen-binding glycoprotein on the surface of mouse fibroblasts is identified as dipeptidyl peptidase IV. *Biochem J* **252**(3)**:** 723-731

Bauvois B (2004) Transmembrane proteases in cell growth and invasion: new contributors to angiogenesis? *Oncogene* **23**(2)**:** 317-329

Bechard D, Gentina T, Delehedde M, Scherpereel A, Lyon M, Aumercier M, Vazeux R, Richet C, Degand P, Jude B, Janin A, Fernig DG, Tonnel AB, Lassalle P (2001a) Endocan is a novel chondroitin sulfate/dermatan sulfate proteoglycan that promotes hepatocyte growth factor/scatter factor mitogenic activity. *J Biol Chem* **276**(51)**:** 48341-48349

Bechard D, Scherpereel A, Hammad H, Gentina T, Tsicopoulos A, Aumercier M, Pestel J, Dessaint JP, Tonnel AB, Lassalle P (2001b) Human endothelial-cell specific molecule-1 binds directly to the integrin CD11a/CD18 (LFA-1) and blocks binding to intercellular adhesion molecule-1. *J Immunol* **167**(6)**:** 3099-3106

Belecky-Adams T, Tomarev S, Li HS, Ploder L, McInnes RR, Sundin O, Adler R (1997) Pax-6, Prox 1, and Chx10 homeobox gene expression correlates with phenotypic fate of retinal precursor cells. *Invest Ophthalmol Vis Sci* **38**(7)**:** 1293-1303

Bikfalvi A, Dupuy E, Inyang AL, Fayein N, Leseche G, Courtois Y, Tobelem G (1989) Binding, internalization, and degradation of basic fibroblast growth factor in human microvascular endothelial cells. *Exp Cell Res* **181**(1)**:** 75-84

Bikfalvi A, Savona C, Perollet C, Javerzat S (1998) New insights in the biology of fibroblast growth factor-2. *Angiogenesis* **1**(2)**:** 155-173

Bjorndahl M, Cao R, Nissen LJ, Clasper S, Johnson LA, Xue Y, Zhou Z, Jackson D, Hansen AJ, Cao Y (2005) Insulin-like growth factors 1 and 2 induce lymphangiogenesis in vivo. *Proc Natl Acad Sci U S A* **102**(43)**:** 15593-15598

Blazquez MV, Madueno JA, Gonzalez R, Jurado R, Bachovchin WW, Pena J, Munoz E (1992) Selective decrease of CD26 expression in T cells from HIV-1-infected individuals. *J Immunol* **149**(9)**:** 3073-3077

Boonacker E, Van Noorden CJ (2003) The multifunctional or moonlighting protein CD26/DPPIV. *Eur J Cell Biol* **82**(2)**:** 53-73

Breitling R (2006) Biological microarray interpretation: the rules of engagement. *Biochim Biophys Acta* **1759**(7)**:** 319-327

Busek P, Malik R, Sedo A (2004) Dipeptidyl peptidase IV activity and/or structure homologues (DASH) and their substrates in cancer. *Int J Biochem Cell Biol* **36**(3)**:** 408-421

Byzova TV, Goldman CK, Jankau J, Chen J, Cabrera G, Achen MG, Stacker SA, Carnevale KA, Siemionow M, Deitcher SR, DiCorleto PE (2002) Adenovirus encoding vascular endothelial growth factor-D induces tissue-specific vascular patterns in vivo. *Blood* **99**(12)**:** 4434-4442

Cabioglu N, Yazici MS, Arun B, Broglio KR, Hortobagyi GN, Price JE, Sahin A (2005) CCR7 and CXCR4 as novel biomarkers predicting axillary lymph node metastasis in T1 breast cancer. *Clin Cancer Res* **11**(16)**:** 5686-5693

Cao R, Bjorndahl MA, Religa P, Clasper S, Garvin S, Galter D, Meister B, Ikomi F, Tritsaris K, Dissing S, Ohhashi T, Jackson DG, Cao Y (2004) PDGF-BB induces intratumoral lymphangiogenesis and promotes lymphatic metastasis. *Cancer Cell* **6**(4)**:** 333-345

Cao R, Brakenhielm E, Li X, Pietras K, Widenfalk J, Ostman A, Eriksson U, Cao Y (2002) Angiogenesis stimulated by PDGF-CC, a novel member in the PDGF family, involves activation of PDGFR-alphaalpha and -alphabeta receptors. *FASEB J* **16**(12)**:** 1575-1583

Cao Y, Linden P, Farnebo J, Cao R, Eriksson A, Kumar V, Qi JH, Claesson-Welsh L, Alitalo K (1998) Vascular endothelial growth factor C induces angiogenesis in vivo. *Proc Natl Acad Sci U S A* **95**(24)**:** 14389-14394

Carmeliet P (2003) Angiogenesis in health and disease. *Nat Med* **9**(6)**:** 653-660

Carmeliet P, Ng YS, Nuyens D, Theilmeier G, Brusselmans K, Cornelissen I, Ehler E, Kakkar VV, Stalmans I, Mattot V, Perriard JC, Dewerchin M, Flameng W, Nagy A, Lupu F, Moons L, Collen D, D'Amore PA, Shima DT (1999) Impaired myocardial

angiogenesis and ischemic cardiomyopathy in mice lacking the vascular endothelial growth factor isoforms VEGF164 and VEGF188. *Nat Med* **5**(5)**:** 495-502

Castenholz A (1998) Functional microanatomy of initial lymphatics with special consideration of the extracellular matrix. *Lymphology* **31**(3)**:** 101-118

Cavanagh LL, Von Andrian UH (2002) Travellers in many guises: the origins and destinations of dendritic cells. *Immunol Cell Biol* **80**(5)**:** 448-462

Chae SS, Paik JH, Furneaux H, Hla T (2004) Requirement for sphingosine 1-phosphate receptor-1 in tumor angiogenesis demonstrated by in vivo RNA interference. *J Clin Invest* **114**(8)**:** 1082-1089

Chang LK, Garcia-Cardena G, Farnebo F, Fannon M, Chen EJ, Butterfield C, Moses MA, Mulligan RC, Folkman J, Kaipainen A (2004) Dose-dependent response of FGF-2 for lymphangiogenesis. *Proc Natl Acad Sci U S A* **101**(32)**:** 11658-11663

Chen JJ (2007) Key aspects of analyzing microarray gene-expression data. *Pharmacogenomics* **8**(5)**:** 473-482

Chen K, Rajewsky N (2006) Natural selection on human microRNA binding sites inferred from SNP data. *Nat Genet* **38**(12)**:** 1452-1456

Chen WT, Kelly T, Ghersi G (2003) DPPIV, seprase, and related serine peptidases in multiple cellular functions. *Curr Top Dev Biol* **54:** 207-232

Cho RJ, Campbell MJ (2000) Transcription, genomes, function. *Trends Genet* **16**(9)**:** 409-415

Cook T, Pichaud F, Sonneville R, Papatsenko D, Desplan C (2003) Distinction between color photoreceptor cell fates is controlled by Prospero in Drosophila. *Dev Cell* **4**(6)**:** 853-864

Couzin J (2006) Genomics. Microarray data reproduced, but some concerns remain. *Science* **313**(5793)**:** 1559

Crawford PA, Gordon JI (2005) Microbial regulation of intestinal radiosensitivity. *Proc Natl Acad Sci U S A* **102**(37)**:** 13254-13259

Cueni LN, Detmar M (2006a) New insights into the molecular control of the lymphatic vascular system and its role in disease. *J Invest Dermatol* **126**(10)**:** 2167-2177

Cueni LN, Detmar M (2006b) New insights into the molecular control of the lymphatic vascular system and its role in disease. *J Invest Dermatol* **126:** 2167-2177

Cui W, Tomarev SI, Piatigorsky J, Chepelinsky AB, Duncan MK (2004) Mafs, Prox1, and Pax6 can regulate chicken betaB1-crystallin gene expression. *J Biol Chem* **279**(12)**:** 11088-11095

Curtis RK, Oresic M, Vidal-Puig A (2005) Pathways to the analysis of microarray data. *Trends Biotechnol* **23**(8)**:** 429-435

Dadras SS, Lange-Asschenfeldt B, Velasco P, Nguyen L, Vora A, Muzikansky A, Jahnke K, Hauschild A, Hirakawa S, Mihm MC, Detmar M (2005) Tumor lymphangiogenesis predicts melanoma metastasis to sentinel lymph nodes. *Mod Pathol* **18**(9)**:** 1232-1242

Dadras SS, Paul T, Bertoncini J, Brown LF, Muzikansky A, Jackson DG, Ellwanger U, Garbe C, Mihm MC, Detmar M (2003) Tumor lymphangiogenesis: a novel prognostic indicator for cutaneous melanoma metastasis and survival. *Am J Pathol* **162**(6)**:** 1951-1960

Dai M, Wang P, Boyd AD, Kostov G, Athey B, Jones EG, Bunney WE, Myers RM, Speed TP, Akil H, Watson SJ, Meng F (2005) Evolving gene/transcript definitions significantly alter the interpretation of GeneChip data. *Nucleic Acids Res* **33**(20)**:** e175

Daynes RA, Spangrude GJ, Roberts LK, Krueger GG (1985) Regulation by the skin of lymphoid cell recirculation and localization properties. *J Invest Dermatol* **85**(1 Suppl)**:** 14s-20s

De Meester I, Korom S, Van Damme J, Scharpe S (1999) CD26, let it cut or cut it down. *Immunol Today* **20**(8)**:** 367-375

Dell KR, Williams LT (1992) A novel form of fibroblast growth factor receptor 2. Alternative splicing of the third immunoglobulin-like domain confers ligand binding specificity. *J Biol Chem* **267**(29)**:** 21225-21229

Detmar M, Brown LF, Claffey KP, Yeo KT, Kocher O, Jackman RW, Berse B, Dvorak HF (1994) Overexpression of vascular permeability factor/vascular endothelial growth factor and its receptors in psoriasis. *J Exp Med* **180**(3)**:** 1141-1146

Detmar M, Imcke E, Ruszczak Z, Orfanos CE (1990) Effects of recombinant tumor necrosis factor-alpha on cultured microvascular endothelial cells derived from human dermis. *J Invest Dermatol* **95**(6 Suppl)**:** 219S-222S.

Dixelius J, Makinen T, Wirzenius M, Karkkainen MJ, Wernstedt C, Alitalo K, Claesson-Welsh L (2003) Ligand-induced vascular endothelial growth factor receptor-3 (VEGFR-3) heterodimerization with VEGFR-2 in primary lymphatic endothelial cells regulates tyrosine phosphorylation sites. *J Biol Chem* **278**(42)**:** 40973-40979

Dumont DJ, Jussila L, Taipale J, Lymboussaki A, Mustonen T, Pajusola K, Breitman M, Alitalo K (1998) Cardiovascular failure in mouse embryos deficient in VEGF receptor-3. *Science* **282**(5390)**:** 946-949

Dus D, Krawczenko A, Zalecki P, Paprocka M, Wiedlocha A, Goupille C, Kieda C (2003) IL-7 receptor is present on human microvascular endothelial cells. *Immunol Lett* **86**(2)**:** 163-168

Dvorak HF, Brown LF, Detmar M, Dvorak AM (1995) Vascular permeability factor/vascular endothelial growth factor, microvascular hyperpermeability, and angiogenesis. *Am J Pathol* **146**(5)**:** 1029-1039

Eguchi K, Ueki Y, Shimomura C, Otsubo T, Nakao H, Migita K, Kawakami A, Matsunaga M, Tezuka H, Ishikawa N, et al. (1989) Increment in the Ta1+ cells in the peripheral blood and thyroid tissue of patients with Graves' disease. *J Immunol* **142**(12)**:** 4233-4240

Eichmann A, Corbel C, Jaffredo T, Breant C, Joukov V, Kumar V, Alitalo K, le Douarin NM (1998) Avian VEGF-C: cloning, embryonic expression pattern and stimulation of the differentiation of VEGFR2-expressing endothelial cell precursors. *Development* **125**(4)**:** 743-752

Enholm B, Karpanen T, Jeltsch M, Kubo H, Stenback F, Prevo R, Jackson DG, Yla-Herttuala S, Alitalo K (2001) Adenoviral expression of vascular endothelial growth factor-C induces lymphangiogenesis in the skin. *Circ Res* **88**(6)**:** 623-629

Ernst J, Bar-Joseph Z (2006) STEM: a tool for the analysis of short time series gene expression data. *BMC Bioinformatics* **7:** 191

Fang J, Dagenais SL, Erickson RP, Arlt MF, Glynn MW, Gorski JL, Seaver LH, Glover TW (2000) Mutations in FOXC2 (MFH-1), a forkhead family transcription factor, are responsible for the hereditary lymphedema-distichiasis syndrome. *Am J Hum Genet* **67**(6)**:** 1382-1388

Ferrara N (2004) Vascular endothelial growth factor: basic science and clinical progress. *Endocr Rev* **25**(4)**:** 581-611

Ferrara N, Gerber HP, LeCouter J (2003) The biology of VEGF and its receptors. *Nat Med* **9**(6)**:** 669-676

Friedman N, Linial M, Nachman I, Pe'er D (2000) Using Bayesian networks to analyze expression data. *J Comput Biol* **7**(3-4)**:** 601-620

Fritz-Six KL, Dunworth WP, Li M, Caron KM (2008) Adrenomedullin signaling is necessary for murine lymphatic vascular development. *J Clin Invest* **118**(1)**:** 40-50

Gale NW, Prevo R, Espinosa J, Ferguson DJ, Dominguez MG, Yancopoulos GD, Thurston G, Jackson DG (2007) Normal lymphatic development and function in mice deficient for the lymphatic hyaluronan receptor LYVE-1. *Mol Cell Biol* **27**(2)**:** 595-604

Gale NW, Thurston G, Hackett SF, Renard R, Wang Q, McClain J, Martin C, Witte C, Witte MH, Jackson D, Suri C, Campochiaro PA, Wiegand SJ, Yancopoulos GD (2002) Angiopoietin-2 is required for postnatal angiogenesis and lymphatic patterning, and only the latter role is rescued by Angiopoietin-1. *Dev Cell* **3**(3)**:** 411-423

Gasparo A (1627) De lactibus sive lacteis venis. *Milan: Mediolani*

Gentleman RC, Carey VJ, Bates DM, Bolstad B, Dettling M, Dudoit S, Ellis B, Gautier L, Ge Y, Gentry J, Hornik K, Hothorn T, Huber W, Iacus S, Irizarry R, Leisch F, Li C, Maechler M, Rossini AJ, Sawitzki G, Smith C, Smyth G, Tierney L, Yang JY, Zhang J (2004) Bioconductor: open software development for computational biology and bioinformatics. *Genome Biol* **5**(10)**:** R80

Gerber HP, Vu TH, Ryan AM, Kowalski J, Werb Z, Ferrara N (1999) VEGF couples hypertrophic cartilage remodeling, ossification and angiogenesis during endochondral bone formation. *Nat Med* **5**(6)**:** 623-628

Gerli R, Muscat C, Bertotto A, Bistoni O, Agea E, Tognellini R, Fiorucci G, Cesarotti M, Bombardieri S (1996) CD26 surface molecule involvement in T cell activation and lymphokine synthesis in rheumatoid and other inflammatory synovitis. *Clin Immunol Immunopathol* **80**(1)**:** 31-37

Ghersi G, Dong H, Goldstein LA, Yeh Y, Hakkinen L, Larjava HS, Chen WT (2002) Regulation of fibroblast migration on collagenous matrix by a cell surface peptidase complex. *J Biol Chem* **277**(32)**:** 29231-29241

Ghersi G, Zhao Q, Salamone M, Yeh Y, Zucker S, Chen WT (2006) The protease complex consisting of dipeptidyl peptidase IV and seprase plays a role in the migration and invasion of human endothelial cells in collagenous matrices. *Cancer Res* **66**(9)**:** 4652-4661

Gottlieb AB, Chamian F, Masud S, Cardinale I, Abello MV, Lowes MA, Chen F, Magliocco M, Krueger JG (2005) TNF inhibition rapidly down-regulates multiple proinflammatory pathways in psoriasis plaques. *J Immunol* **175**(4)**:** 2721-2729

Grigoriu BD, Depontieu F, Scherpereel A, Gourcerol D, Devos P, Ouatas T, Lafitte JJ, Copin MC, Tonnel AB, Lassalle P (2006) Endocan expression and relationship with survival in human non-small cell lung cancer. *Clin Cancer Res* **12**(15)**:** 4575-4582

Groger M, Loewe R, Holnthoner W, Embacher R, Pillinger M, Herron GS, Wolff K, Petzelbauer P (2004) IL-3 induces expression of lymphatic markers Prox-1 and podoplanin in human endothelial cells. *J Immunol* **173**(12)**:** 7161-7169

Groth C, Lardelli M (2002) The structure and function of vertebrate fibroblast growth factor receptor 1. *Int J Dev Biol* **46**(4)**:** 393-400

Gunn MD, Tangemann K, Tam C, Cyster JG, Rosen SD, Williams LT (1998) A chemokine expressed in lymphoid high endothelial venules promotes the adhesion and chemotaxis of naive T lymphocytes. *Proc Natl Acad Sci U S A* **95**(1)**:** 258-263

Gunther K, Leier J, Henning G, Dimmler A, Weissbach R, Hohenberger W, Forster R (2005) Prediction of lymph node metastasis in colorectal carcinoma by expressionof chemokine receptor CCR7. *Int J Cancer* **116**(5)**:** 726-733

Hafler DA, Fox DA, Manning ME, Schlossman SF, Reinherz EL, Weiner HL (1985) In vivo activated T lymphocytes in the peripheral blood and cerebrospinal fluid of patients with multiple sclerosis. *N Engl J Med* **312**(22)**:** 1405-1411

Hanneken A (2001) Structural characterization of the circulating soluble FGF receptors reveals multiple isoforms generated by secretion and ectodomain shedding. *FEBS Lett* **489**(2-3)**:** 176-181

Harvey NL, Srinivasan RS, Dillard ME, Johnson NC, Witte MH, Boyd K, Sleeman MW, Oliver G (2005) Lymphatic vascular defects promoted by Prox1 haploinsufficiency cause adult-onset obesity. *Nat Genet* **37**(10)**:** 1072-1081

Hassan B, Li L, Bremer KA, Chang W, Pinsonneault J, Vaessin H (1997) Prospero is a panneural transcription factor that modulates homeodomain protein activity. *Proc Natl Acad Sci U S A* **94**(20)**:** 10991-10996.

He Y, Rajantie I, Ilmonen M, Makinen T, Karkkainen MJ, Haiko P, Salven P, Alitalo K (2004) Preexisting lymphatic endothelium but not endothelial progenitor cells are essential for tumor lymphangiogenesis and lymphatic metastasis. *Cancer Res* **64**(11)**:** 3737-3740

He Y, Rajantie I, Pajusola K, Jeltsch M, Holopainen T, Yla-Herttuala S, Harding T, Jooss K, Takahashi T, Alitalo K (2005) Vascular endothelial cell growth factor receptor 3-mediated activation of lymphatic endothelium is crucial for tumor cell entry and spread via lymphatic vessels. *Cancer Res* **65**(11)**:** 4739-4746

Heresi GA, Wang J, Taichman R, Chirinos JA, Regalado JJ, Lichtstein DM, Rosenblatt JD (2005) Expression of the chemokine receptor CCR7 in prostate cancer presenting with generalized lymphadenopathy: report of a case, review of the literature, and analysis of chemokine receptor expression. *Urol Oncol* **23**(4)**:** 261-267

Hesser BA, Liang XH, Camenisch G, Yang S, Lewin DA, Scheller R, Ferrara N, Gerber HP (2004) Down syndrome critical region protein 1 (DSCR1), a novel VEGF target gene that regulates expression of inflammatory markers on activated endothelial cells. *Blood* **104**(1)**:** 149-158

Heydtmann M, Hardie D, Shields PL, Faint J, Buckley CD, Campbell JJ, Salmon M, Adams DH (2006) Detailed analysis of intrahepatic CD8 T cells in the normal and hepatitis C-infected liver reveals differences in specific populations of memory cells with distinct homing phenotypes. *J Immunol* **177**(1)**:** 729-738

Hirakawa S, Brown LF, Kodama S, Paavonen K, Alitalo K, Detmar M (2006) VEGF-C-induced lymphangiogenesis in sentinel lymph nodes promotes tumor metastasis to distant sites. *Blood***:** [Epub ahead of print]

Hirakawa S, Brown LF, Kodama S, Paavonen K, Alitalo K, Detmar M (2007) VEGF-C-induced lymphangiogenesis in sentinel lymph nodes promotes tumor metastasis to distant sites. *Blood* **109**(3)**:** 1010-1017

Hirakawa S, Fujii S, Kajiya K, Yano K, Detmar M (2005a) Vascular endothelial growth factor promotes sensitivity to ultraviolet B-induced cutaneous photodamage. *Blood* **105**(6)**:** 2392-2399

Hirakawa S, Hong YK, Harvey N, Schacht V, Matsuda K, Libermann T, Detmar M (2003) Identification of vascular lineage-specific genes by transcriptional profiling of isolated blood vascular and lymphatic endothelial cells. *Am J Pathol* **162**(2)**:** 575-586

Hirakawa S, Kodama S, Kunstfeld R, Kajiya K, Brown LF, Detmar M (2005b) VEGF-A induces tumor and sentinel lymph node lymphangiogenesis and promotes lymphatic metastasis. *J Exp Med* **201**(7)**:** 1089-1099

Holash J, Maisonpierre PC, Compton D, Boland P, Alexander CR, Zagzag D, Yancopoulos GD, Wiegand SJ (1999a) Vessel cooption, regression, and growth in tumors mediated by angiopoietins and VEGF. *Science* **284**(5422)**:** 1994-1998

Holash J, Wiegand SJ, Yancopoulos GD (1999b) New model of tumor angiogenesis: dynamic balance between vessel regression and growth mediated by angiopoietins and VEGF. *Oncogene* **18**(38)**:** 5356-5362

Hong YK, Detmar M (2003a) Prox1, master regulator of the lymphatic vasculature phenotype. *Cell Tissue Res* **314**(1)**:** 85-92

Hong YK, Detmar M (2003b) Prox1, master regulator of the lymphatic vasculature phenotype. *Cell Tissue Res* **314:** 85-92

Hong YK, Foreman K, Shin JW, Hirakawa S, Curry CL, Sage DR, Libermann T, Dezube BJ, Fingeroth JD, Detmar M (2004a) Lymphatic reprogramming of blood vascular endothelium by Kaposi sarcoma-associated herpesvirus. *Nat Genet* **36**(7)**:** 683-685

Hong YK, Harvey N, Noh YH, Schacht V, Hirakawa S, Detmar M, Oliver G (2002) Prox1 is a master control gene in the program specifying lymphatic endothelial cell fate. *Dev Dyn* **225**(3)**:** 351-357

Hong YK, Lange-Asschenfeldt B, Velasco P, Hirakawa S, Kunstfeld R, Brown LF, Bohlen P, Senger DR, Detmar M (2004b) VEGF-A promotes tissue repair-associated lymphatic vessel formation via VEGFR-2 and the alpha1beta1 and alpha2beta1 integrins. *Faseb J* **18**(10)**:** 1111-1113

Hong YK, Shin JW, Detmar M (2004c) Development of the lymphatic vascular system: a mystery unravels. *Dev Dyn* **231**(3)**:** 462-473

Houck KA, Ferrara N, Winer J, Cachianes G, Li B, Leung DW (1991) The vascular endothelial growth factor family: identification of a fourth molecular species and characterization of alternative splicing of RNA. *Mol Endocrinol* **5**(12)**:** 1806-1814

Houghton AN, Albino AP, Cordon-Cardo C, Davis LJ, Eisinger M (1988) Cell surface antigens of human melanocytes and melanoma. Expression of adenosine

deaminase binding protein is extinguished with melanocyte transformation. *J Exp Med* **167**(1): 197-212

Huber W, von Heydebreck A, Sultmann H, Poustka A, Vingron M (2002) Variance stabilization applied to microarray data calibration and to the quantification of differential expression. *Bioinformatics* **18 Suppl 1:** S96-104

Huntington GS, McClure CFW (1910) The anatomy and development of the jugular lymph sac in the domestic cat (Felis domestica). *Am J Anat* **10:** 177-311

Irrthum A, Devriendt K, Chitayat D, Matthijs G, Glade C, Steijlen PM, Fryns JP, Van Steensel MA, Vikkula M (2003) Mutations in the transcription factor gene SOX18 underlie recessive and dominant forms of hypotrichosis-lymphedema-telangiectasia. *Am J Hum Genet* **72**(6): 1470-1478

Irrthum A, Karkkainen MJ, Devriendt K, Alitalo K, Vikkula M (2000) Congenital hereditary lymphedema caused by a mutation that inactivates VEGFR3 tyrosine kinase. *Am J Hum Genet* **67**(2): 295-301

Jackson DG (2004) Biology of the lymphatic marker LYVE-1 and applications in research into lymphatic trafficking and lymphangiogenesis. *Apmis* **112**(7-8): 526-538

Jackson DG, Prevo R, Clasper S, Banerji S (2001) LYVE-1, the lymphatic system and tumor lymphangiogenesis. *Trends Immunol* **22**(6): 317-321

Javerzat S, Auguste P, Bikfalvi A (2002) The role of fibroblast growth factors in vascular development. *Trends Mol Med* **8**(10): 483-489

Jeltsch M, Kaipainen A, Joukov V, Meng X, Lakso M, Rauvala H, Swartz M, Fukumura D, Jain RK, Alitalo K (1997) Hyperplasia of lymphatic vessels in VEGF-C transgenic mice. *Science* **276**(5317): 1423-1425

Joukov V, Pajusola K, Kaipainen A, Chilov D, Lahtinen I, Kukk E, Saksela O, Kalkkinen N, Alitalo K (1996) A novel vascular endothelial growth factor, VEGF-C, is a ligand for the Flt4 (VEGFR-3) and KDR (VEGFR-2) receptor tyrosine kinases. *Embo J* **15**(7): 1751

Joukov V, Sorsa T, Kumar V, Jeltsch M, Claesson-Welsh L, Cao Y, Saksela O, Kalkkinen N, Alitalo K (1997) Proteolytic processing regulates receptor specificity and activity of VEGF-C. *Embo J* **16**(13): 3898-3911

Kaipainen A, Korhonen J, Mustonen T, van Hinsbergh VW, Fang GH, Dumont D, Breitman M, Alitalo K (1995) Expression of the fms-like tyrosine kinase 4 gene becomes restricted to lymphatic endothelium during development. *Proc Natl Acad Sci U S A* **92**(8): 3566-3570

Kaipainen A, Korhonen J, Pajusola K, Aprelikova O, Persico MG, Terman BI, Alitalo K (1993) The related FLT4, FLT1, and KDR receptor tyrosine kinases show distinct expression patterns in human fetal endothelial cells. *J Exp Med* **178**(6): 2077-2088

Kajiya K, Detmar M (2006) An important role of lymphatic vessels in the control of UVB-induced edema formation and inflammation. *J Invest Dermatol* **126**(4)**:** 919-921

Kajiya K, Hirakawa S, Ma B, Drinnenberg I, Detmar M (2005) Hepatocyte growth factor promotes lymphatic vessel formation and function. *Embo J* **24**(16)**:** 2885-2895

Kanai M, Goke M, Tsunekawa S, Podolsky DK (1997) Signal transduction pathway of human fibroblast growth factor receptor 3. Identification of a novel 66-kDa phosphoprotein. *J Biol Chem* **272**(10)**:** 6621-6628

Karkkainen MJ, Ferrell RE, Lawrence EC, Kimak MA, Levinson KL, McTigue MA, Alitalo K, Finegold DN (2000) Missense mutations interfere with VEGFR-3 signalling in primary lymphoedema. *Nat Genet* **25**(2)**:** 153-159

Karkkainen MJ, Haiko P, Sainio K, Partanen J, Taipale J, Petrova TV, Jeltsch M, Jackson DG, Talikka M, Rauvala H, Betsholtz C, Alitalo K (2004) Vascular endothelial growth factor C is required for sprouting of the first lymphatic vessels from embryonic veins. *Nat Immunol* **5**(1)**:** 74-80

Karkkainen MJ, Jussila L, Ferrell RE, Finegold DN, Alitalo K (2001) Molecular regulation of lymphangiogenesis and targets for tissue oedema. *Trends Mol Med* **7**(1)**:** 18-22

Karpanen T, Wirzenius M, Makinen T, Veikkola T, Haisma HJ, Achen MG, Stacker SA, Pytowski B, Yla-Herttuala S, Alitalo K (2006) Lymphangiogenic growth factor responsiveness is modulated by postnatal lymphatic vessel maturation. *Am J Pathol* **169**(2)**:** 708-718

Kedde M, Strasser MJ, Boldajipour B, Vrielink JA, Slanchev K, le Sage C, Nagel R, Voorhoeve PM, van Duijse J, Orom UA, Lund AH, Perrakis A, Raz E, Agami R (2007) RNA-binding protein Dnd1 inhibits microRNA access to target mRNA. *Cell* **131**(7)**:** 1273-1286

Kerjaschki D (2005) The crucial role of macrophages in lymphangiogenesis. *J Clin Invest* **115**(9)**:** 2316-2319

Kerjaschki D, Huttary N, Raab I, Regele H, Bojarski-Nagy K, Bartel G, Krober SM, Greinix H, Rosenmaier A, Karlhofer F, Wick N, Mazal PR (2006) Lymphatic endothelial progenitor cells contribute to de novo lymphangiogenesis in human renal transplants. *Nat Med* **12**(2)**:** 230-234

Kerjaschki D, Regele HM, Moosberger I, Nagy-Bojarski K, Watschinger B, Soleiman A, Birner P, Krieger S, Hovorka A, Silberhumer G, Laakkonen P, Petrova T, Langer B, Raab I (2004) Lymphatic neoangiogenesis in human kidney transplants is associated with immunologically active lymphocytic infiltrates. *J Am Soc Nephrol* **15**(3)**:** 603-612

Kersten S, Mandard S, Tan NS, Escher P, Metzger D, Chambon P, Gonzalez FJ, Desvergne B, Wahli W (2000) Characterization of the fasting-induced adipose factor

FIAF, a novel peroxisome proliferator-activated receptor target gene. *J Biol Chem* **275**(37)**:** 28488-28493

Kertesz Z, Linton EA, Redman CW (2000) Adhesion molecules of syncytiotrophoblast microvillous membranes inhibit proliferation of human umbilical vein endothelial cells. *Placenta* **21**(2-3)**:** 150-159

Kilroy GE, Foster SJ, Wu X, Ruiz J, Sherwood S, Heifetz A, Ludlow JW, Stricker DM, Potiny S, Green P, Halvorsen YD, Cheatham B, Storms RW, Gimble JM (2007) Cytokine profile of human adipose-derived stem cells: expression of angiogenic, hematopoietic, and pro-inflammatory factors. *J Cell Physiol* **212**(3)**:** 702-709

Kim I, Kim HG, Kim H, Kim HH, Park SK, Uhm CS, Lee ZH, Koh GY (2000) Hepatic expression, synthesis and secretion of a novel fibrinogen/angiopoietin-related protein that prevents endothelial-cell apoptosis. *Biochem J* **346 Pt 3:** 603-610

Kimura H, Konishi K, Nukui T, Kaji M, Maeda K, Yabushita K, Tsuji M, Miwa A (2001) Prognostic significance of expression of thymidine phosphorylase and vascular endothelial growth factor in human gastric carcinoma. *J Surg Oncol* **76**(1)**:** 31-36

Kriederman BM, Myloyde TL, Witte MH, Dagenais SL, Witte CL, Rennels M, Bernas MJ, Lynch MT, Erickson RP, Caulder MS, Miura N, Jackson D, Brooks BP, Glover TW (2003) FOXC2 haploinsufficient mice are a model for human autosomal dominant lymphedema-distichiasis syndrome. *Hum Mol Genet* **12**(10)**:** 1179-1185

Kriehuber E, Breiteneder-Geleff S, Groeger M, Soleiman A, Schoppmann SF, Stingl G, Kerjaschki D, Maurer D (2001) Isolation and characterization of dermal lymphatic and blood endothelial cells reveal stable and functionally specialized cell lineages. *J Exp Med* **194**(6)**:** 797-808

Kubo H, Cao R, Brakenhielm E, Makinen T, Cao Y, Alitalo K (2002) Blockade of vascular endothelial growth factor receptor-3 signaling inhibits fibroblast growth factor-2-induced lymphangiogenesis in mouse cornea. *Proc Natl Acad Sci U S A* **99**(13)**:** 8868-8873

Kubo H, Fujiwara T, Jussila L, Hashi H, Ogawa M, Shimizu K, Awane M, Sakai Y, Takabayashi A, Alitalo K, Yamaoka Y, Nishikawa SI (2000) Involvement of vascular endothelial growth factor receptor-3 in maintenance of integrity of endothelial cell lining during tumor angiogenesis. *Blood* **96**(2)**:** 546-553

Kukk E, Lymboussaki A, Taira S, Kaipainen A, Jeltsch M, Joukov V, Alitalo K (1996) VEGF-C receptor binding and pattern of expression with VEGFR-3 suggests a role in lymphatic vascular development. *Development* **122**(12)**:** 3829-3837

Kunstfeld R, Hirakawa S, Hong YK, Schacht V, Lange-Asschenfeldt B, Velasco P, Lin C, Fiebiger E, Wei X, Wu Y, Hicklin D, Bohlen P, Detmar M (2004) Induction of cutaneous delayed-type hypersensitivity reactions in VEGF-A transgenic mice results in chronic skin inflammation associated with persistent lymphatic hyperplasia. *Blood* **104**(4)**:** 1048-1057

Kuo WP, Liu F, Trimarchi J, Punzo C, Lombardi M, Sarang J, Whipple ME, Maysuria M, Serikawa K, Lee SY, McCrann D, Kang J, Shearstone JR, Burke J, Park DJ, Wang X, Rector TL, Ricciardi-Castagnoli P, Perrin S, Choi S, Bumgarner R, Kim JH, Short GF, 3rd, Freeman MW, Seed B, Jensen R, Church GM, Hovig E, Cepko CL, Park P, Ohno-Machado L, Jenssen TK (2006) A sequence-oriented comparison of gene expression measurements across different hybridization-based technologies. *Nat Biotechnol* **24**(7)**:** 832-840

Lange T, Guttmann-Raviv N, Baruch L, Machluf M, Neufeld G (2003) VEGF162, a new heparin-binding vascular endothelial growth factor splice form that is expressed in transformed human cells. *J Biol Chem* **278**(19)**:** 17164-17169

Lengler J, Krausz E, Tomarev S, Prescott A, Quinlan RA, Graw J (2001) Antagonistic action of Six3 and Prox1 at the gamma-crystallin promoter. *Nucleic Acids Res* **29**(2)**:** 515-526

Leu AJ, Gretener SB, Enderlin S, Bruhlmann P, Michel BA, Kowal-Bielecka O, Hoffmann U, Franzeck UK (1999) Lymphatic microangiopathy of the skin in systemic sclerosis. *Rheumatology (Oxford)* **38**(3)**:** 221-227

Li JH, Kluger MS, Madge LA, Zheng L, Bothwell AL, Pober JS (2002) Interferon-gamma augments CD95(APO-1/Fas) and pro-caspase-8 expression and sensitizes human vascular endothelial cells to CD95-mediated apoptosis. *Am J Pathol* **161**(4)**:** 1485-1495

Liang Y, Kelemen A (2007) Bayesian state space models for inferring and predicting temporal gene expression profiles. *Biom J* **49**(6)**:** 801-814

Liu D, Jia H, Holmes DI, Stannard A, Zachary I (2003a) Vascular endothelial growth factor-regulated gene expression in endothelial cells: KDR-mediated induction of Egr3 and the related nuclear receptors Nur77, Nurr1, and Nor1. *Arterioscler Thromb Vasc Biol* **23**(11)**:** 2002-2007

Liu L, Ratner BD, Sage EH, Jiang S (2007) Endothelial cell migration on surface-density gradients of fibronectin, VEGF, or both proteins. *Langmuir* **23**(22)**:** 11168-11173

Liu YW, Gao W, Teh HL, Tan JH, Chan WK (2003b) Prox1 is a novel coregulator of Ff1b and is involved in the embryonic development of the zebra fish interrenal primordium. *Mol Cell Biol* **23**(20)**:** 7243-7255

Liu Z, Xu J, Colvin JS, Ornitz DM (2002) Coordination of chondrogenesis and osteogenesis by fibroblast growth factor 18. *Genes Dev* **16**(7)**:** 859-869

Loster K, Zeilinger K, Schuppan D, Reutter W (1995) The cysteine-rich region of dipeptidyl peptidase IV (CD 26) is the collagen-binding site. *Biochem Biophys Res Commun* **217**(1)**:** 341-348

Lu D, Kussie P, Pytowski B, Persaud K, Bohlen P, Witte L, Zhu Z (2000) Identification of the residues in the extracellular region of KDR important for

interaction with vascular endothelial growth factor and neutralizing anti-KDR antibodies. *J Biol Chem* **275**(19)**:** 14321-14330

Magic Z, Radulovic S, Brankovic-Magic M (2007) cDNA microarrays: identification of gene signatures and their application in clinical practice. *J BUON* **12 Suppl 1:** S39-44

Maisonpierre PC, Suri C, Jones PF, Bartunkova S, Wiegand SJ, Radziejewski C, Compton D, McClain J, Aldrich TH, Papadopoulos N, Daly TJ, Davis S, Sato TN, Yancopoulos GD (1997) Angiopoietin-2, a natural antagonist for Tie2 that disrupts in vivo angiogenesis. *Science* **277**(5322)**:** 55-60

Makinen T, Adams RH, Bailey J, Lu Q, Ziemiecki A, Alitalo K, Klein R, Wilkinson GA (2005) PDZ interaction site in ephrinB2 is required for the remodeling of lymphatic vasculature. *Genes Dev* **19**(3)**:** 397-410

Makinen T, Veikkola T, Mustjoki S, Karpanen T, Catimel B, Nice EC, Wise L, Mercer A, Kowalski H, Kerjaschki D, Stacker SA, Achen MG, Alitalo K (2001) Isolated lymphatic endothelial cells transduce growth, survival and migratory signals via the VEGF-C/D receptor VEGFR-3. *Embo J* **20**(17)**:** 4762-4773

Mandriota SJ, Jussila L, Jeltsch M, Compagni A, Baetens D, Prevo R, Banerji S, Huarte J, Montesano R, Jackson DG, Orci L, Alitalo K, Christofori G, Pepper MS (2001) Vascular endothelial growth factor-C-mediated lymphangiogenesis promotes tumour metastasis. *Embo J* **20**(4)**:** 672-682

Mandriota SJ, Seghezzi G, Vassalli JD, Ferrara N, Wasi S, Mazzieri R, Mignatti P, Pepper MS (1995) Vascular endothelial growth factor increases urokinase receptor expression in vascular endothelial cells. *J Biol Chem* **270**(17)**:** 9709-9716

Marconcini L, Marchio S, Morbidelli L, Cartocci E, Albini A, Ziche M, Bussolino F, Oliviero S (1999) c-fos-induced growth factor/vascular endothelial growth factor D induces angiogenesis in vivo and in vitro. *Proc Natl Acad Sci U S A* **96**(17)**:** 9671-9676

Martinez I, Lombardia L, Garcia-Barreno B, Dominguez O, Melero JA (2007) Distinct gene subsets are induced at different time points after human respiratory syncytial virus infection of A549 cells. *J Gen Virol* **88**(Pt 2)**:** 570-581

Maruyama K, Ii M, Cursiefen C, Jackson DG, Keino H, Tomita M, Van Rooijen N, Takenaka H, D'Amore PA, Stein-Streilein J, Losordo DW, Streilein JW (2005) Inflammation-induced lymphangiogenesis in the cornea arises from CD11b-positive macrophages. *J Clin Invest* **115**(9)**:** 2363-2372

Massberg S, Schaerli P, Knezevic-Maramica I, Kollnberger M, Tubo N, Moseman EA, Huff IV, Junt T, Wagers AJ, Mazo IB, von Andrian UH (2007) Immunosurveillance by hematopoietic progenitor cells trafficking through blood, lymph, and peripheral tissues. *Cell* **131**(5)**:** 994-1008

McEwen DG, Ornitz DM (1998) Regulation of the fibroblast growth factor receptor 3 promoter and intron I enhancer by Sp1 family transcription factors. *J Biol Chem* **273**(9)**:** 5349-5357

McLatchie LM, Fraser NJ, Main MJ, Wise A, Brown J, Thompson N, Solari R, Lee MG, Foord SM (1998) RAMPs regulate the transport and ligand specificity of the calcitonin-receptor-like receptor. *Nature* **393**(6683)**:** 333-339

Mentlein R (2004) Cell-surface peptidases. *Int Rev Cytol* **235:** 165-213

Millington OR, Zinselmeyer BH, Brewer JM, Garside P, Rush CM (2007) Lymphocyte tracking and interactions in secondary lymphoid organs. *Inflamm Res* **56**(10)**:** 391-401

Moller P, Bohm M, Czarnetszki BM, Schadendorf D (1996) Interleukin-7. Biology and implications for dermatology. *Exp Dermatol* **5**(3)**:** 129-137

Moscatelli D (1987) High and low affinity binding sites for basic fibroblast growth factor on cultured cells: absence of a role for low affinity binding in the stimulation of plasminogen activator production by bovine capillary endothelial cells. *J Cell Physiol* **131**(1)**:** 123-130

Muller A, Homey B, Soto H, Ge N, Catron D, Buchanan ME, McClanahan T, Murphy E, Yuan W, Wagner SN, Barrera JL, Mohar A, Verastegui E, Zlotnik A (2001) Involvement of chemokine receptors in breast cancer metastasis. *Nature* **410**(6824)**:** 50-56

Murgue B, Tsunekawa S, Rosenberg I, deBeaumont M, Podolsky DK (1994) Identification of a novel variant form of fibroblast growth factor receptor 3 (FGFR3 IIIb) in human colonic epithelium. *Cancer Res* **54**(19)**:** 5206-5211

Murphy D (2002) Gene expression studies using microarrays: principles, problems, and prospects. *Adv Physiol Educ* **26**(1-4)**:** 256-270

Nagy JA, Vasile E, Feng D, Sundberg C, Brown LF, Manseau EJ, Dvorak AM, Dvorak HF (2002) VEGF-A induces angiogenesis, arteriogenesis, lymphangiogenesis, and vascular malformations. *Cold Spring Harb Symp Quant Biol* **67:** 227-237

Neufeld G, Cohen T, Gengrinovitch S, Poltorak Z (1999) Vascular endothelial growth factor (VEGF) and its receptors. *FASEB J* **13**(1)**:** 9-22

Neufeld G, Tessler S, Gitay-Goren H, Cohen T, Levi BZ (1994) Vascular endothelial growth factor and its receptors. *Prog Growth Factor Res* **5**(1)**:** 89-97

Niederkorn JY, Peeler JS, Ross J, Callanan D (1989) The immunogenic privilege of corneal allografts. *Reg Immunol* **2**(2)**:** 117-124

Ohl L, Mohaupt M, Czeloth N, Hintzen G, Kiafard Z, Zwirner J, Blankenstein T, Henning G, Forster R (2004) CCR7 governs skin dendritic cell migration under inflammatory and steady-state conditions. *Immunity* **21**(2)**:** 279-288

Oliver G (2004) Lymphatic vasculature development. *Nat Rev Immunol* **4**(1)**:** 35-45

Oliver G, Detmar M (2002) The rediscovery of the lymphatic system: old and new insights into the development and biological function of the lymphatic vasculature. *Genes Dev* **16**(7)**:** 773-783

Oliver G, Harvey N (2002) A stepwise model of the development of lymphatic vasculature. *Ann N Y Acad Sci* **979:** 159-165; discussion 188-196

Oliver G, Sosa-Pineda B, Geisendorf S, Spana EP, Doe CQ, Gruss P (1993a) Prox 1, a prospero-related homeobox gene expressed during mouse development. *Mech Dev* **44**(1)**:** 3-16

Oliver G, Sosa-Pineda B, Geisendorf S, Spana EP, Doe CQ, Gruss P (1993b) Prox 1, a prospero-related homeobox gene expressed during mouse development. *Mech Dev* **44**(1)**:** 3-16.

Orlandini M, Marconcini L, Ferruzzi R, Oliviero S (1996) Identification of a c-fos-induced gene that is related to the platelet-derived growth factor/vascular endothelial growth factor family. *Proc Natl Acad Sci U S A* **93**(21)**:** 11675-11680

Ornitz DM (2000) FGFs, heparan sulfate and FGFRs: complex interactions essential for development. *Bioessays* **22**(2)**:** 108-112

Ornitz DM, Itoh N (2001) Fibroblast growth factors. *Genome Biol* **2**(3)**:** REVIEWS3005

Ornitz DM, Marie PJ (2002) FGF signaling pathways in endochondral and intramembranous bone development and human genetic disease. *Genes Dev* **16**(12)**:** 1446-1465

Ornitz DM, Xu J, Colvin JS, McEwen DG, MacArthur CA, Coulier F, Gao G, Goldfarb M (1996) Receptor specificity of the fibroblast growth factor family. *J Biol Chem* **271**(25)**:** 15292-15297

Ornitz DM, Yayon A, Flanagan JG, Svahn CM, Levi E, Leder P (1992) Heparin is required for cell-free binding of basic fibroblast growth factor to a soluble receptor and for mitogenesis in whole cells. *Mol Cell Biol* **12**(1)**:** 240-247

Orr-Urtreger A, Bedford MT, Burakova T, Arman E, Zimmer Y, Yayon A, Givol D, Lonai P (1993) Developmental localization of the splicing alternatives of fibroblast growth factor receptor-2 (FGFR2). *Dev Biol* **158**(2)**:** 475-486.

Pan W (2002) A comparative review of statistical methods for discovering differentially expressed genes in replicated microarray experiments. *Bioinformatics* **18**(4)**:** 546-554

Patel DD, Koopmann W, Imai T, Whichard LP, Yoshie O, Krangel MS (2001) Chemokines have diverse abilities to form solid phase gradients. *Clin Immunol* **99**(1): 43-52

Patterson TA, Lobenhofer EK, Fulmer-Smentek SB, Collins PJ, Chu TM, Bao W, Fang H, Kawasaki ES, Hager J, Tikhonova IR, Walker SJ, Zhang L, Hurban P, de Longueville F, Fuscoe JC, Tong W, Shi L, Wolfinger RD (2006) Performance comparison of one-color and two-color platforms within the MicroArray Quality Control (MAQC) project. *Nat Biotechnol* **24**(9): 1140-1150

Pepper MS (2001) Lymphangiogenesis and tumor metastasis: myth or reality? *Clin Cancer Res* **7**(3): 462-468

Perollet C, Han ZC, Savona C, Caen JP, Bikfalvi A (1998) Platelet factor 4 modulates fibroblast growth factor 2 (FGF-2) activity and inhibits FGF-2 dimerization. *Blood* **91**(9): 3289-3299

Persaud K, Tille JC, Liu M, Zhu Z, Jimenez X, Pereira DS, Miao HQ, Brennan LA, Witte L, Pepper MS, Pytowski B (2004) Involvement of the VEGF receptor 3 in tubular morphogenesis demonstrated with a human anti-human VEGFR-3 monoclonal antibody that antagonizes receptor activation by VEGF-C. *J Cell Sci* **117**(Pt 13): 2745-2756

Petrova TV, Karpanen T, Norrmen C, Mellor R, Tamakoshi T, Finegold D, Ferrell R, Kerjaschki D, Mortimer P, Yla-Herttuala S, Miura N, Alitalo K (2004) Defective valves and abnormal mural cell recruitment underlie lymphatic vascular failure in lymphedema distichiasis. *Nat Med* **10**(9): 974-981

Petrova TV, Makinen T, Makela TP, Saarela J, Virtanen I, Ferrell RE, Finegold DN, Kerjaschki D, Yla-Herttuala S, Alitalo K (2002a) Lymphatic endothelial reprogramming of vascular endothelial cells by the Prox-1 homeobox transcription factor. *Embo J* **21**(17): 4593-4599

Petrova TV, Makinen T, Makela TP, Saarela J, Virtanen I, Ferrell RE, Finegold DN, Kerjaschki D, Yla-Herttuala S, Alitalo K (2002b) Lymphatic endothelial reprogramming of vascular endothelial cells by the Prox-1 homeobox transcription factor. *EMBO J* **21**(17): 4593-4599

Plouet J, Moro F, Bertagnolli S, Coldeboeuf N, Mazarguil H, Clamens S, Bayard F (1997) Extracellular cleavage of the vascular endothelial growth factor 189-amino acid form by urokinase is required for its mitogenic effect. *J Biol Chem* **272**(20): 13390-13396

Podgrabinska S, Braun P, Velasco P, Kloos B, Pepper MS, Skobe M (2002) Molecular characterization of lymphatic endothelial cells. *Proc Natl Acad Sci U S A* **99**(25): 16069-16074

Powers CJ, McLeskey SW, Wellstein A (2000) Fibroblast growth factors, their receptors and signaling. *Endocr Relat Cancer* **7**(3): 165-197

Prabhakarpandian B, Goetz DJ, Swerlick RA, Chen X, Kiani MF (2001) Expression and functional significance of adhesion molecules on cultured endothelial cells in response to ionizing radiation. *Microcirculation* **8**(5)**:** 355-364

Prevo R, Banerji S, Ferguson DJ, Clasper S, Jackson DG (2001) Mouse LYVE-1 is an endocytic receptor for hyaluronan in lymphatic endothelium. *J Biol Chem* **276**(22)**:** 19420-19430

Proost P, Menten P, Struyf S, Schutyser E, De Meester I, Van Damme J (2000) Cleavage by CD26/dipeptidyl peptidase IV converts the chemokine LD78beta into a most efficient monocyte attractant and CCR1 agonist. *Blood* **96**(5)**:** 1674-1680

Proost P, Schutyser E, Menten P, Struyf S, Wuyts A, Opdenakker G, Detheux M, Parmentier M, Durinx C, Lambeir AM, Neyts J, Liekens S, Maudgal PC, Billiau A, Van Damme J (2001) Amino-terminal truncation of CXCR3 agonists impairs receptor signaling and lymphocyte chemotaxis, while preserving antiangiogenic properties. *Blood* **98**(13)**:** 3554-3561

Proost P, Struyf S, Schols D, Opdenakker G, Sozzani S, Allavena P, Mantovani A, Augustyns K, Bal G, Haemers A, Lambeir AM, Scharpe S, Van Damme J, De Meester I (1999) Truncation of macrophage-derived chemokine by CD26/ dipeptidyl-peptidase IV beyond its predicted cleavage site affects chemotactic activity and CC chemokine receptor 4 interaction. *J Biol Chem* **274**(7)**:** 3988-3993

Pugh CW, Ratcliffe PJ (2003) Regulation of angiogenesis by hypoxia: role of the HIF system. *Nat Med* **9**(6)**:** 677-684

Qian J, Lin J, Luscombe NM, Yu H, Gerstein M (2003) Prediction of regulatory networks: genome-wide identification of transcription factor targets from gene expression data. *Bioinformatics* **19**(15)**:** 1917-1926

Ramaswamy S, Ross KN, Lander ES, Golub TR (2003) A molecular signature of metastasis in primary solid tumors. *Nat Genet* **33**(1)**:** 49-54

Randolph GJ, Angeli V, Swartz MA (2005) Dendritic-cell trafficking to lymph nodes through lymphatic vessels. *Nat Rev Immunol* **5**(8)**:** 617-628

Rennel E, Mellberg S, Dimberg A, Petersson L, Botling J, Ameur A, Westholm JO, Komorowski J, Lassalle P, Cross MJ, Gerwins P (2007) Endocan is a VEGF-A and PI3K regulated gene with increased expression in human renal cancer. *Exp Cell Res* **313**(7)**:** 1285-1294

Richard L, Velasco P, Detmar M (1998) A simple immunomagnetic protocol for the selective isolation and long-term culture of human dermal microvascular endothelial cells. *Exp Cell Res* **240**(1)**:** 1-6

Rishi AK, Joyce-Brady M, Fisher J, Dobbs LG, Floros J, VanderSpek J, Brody JS, Williams MC (1995) Cloning, characterization, and development expression of a rat

lung alveolar type I cell gene in embryonic endodermal and neural derivatives. *Dev Biol* **167**(1)**:** 294-306

Robinson CJ, Stringer SE (2001) The splice variants of vascular endothelial growth factor (VEGF) and their receptors. *J Cell Sci* **114**(Pt 5)**:** 853-865

Rockson SG (2001) Lymphedema. *Am J Med* **110**(4)**:** 288-295

Roesli C, Mumprecht V, Neri D, Detmar M (2008) Identification of the surface-accessible, lineage-specific vascular proteome by two-dimensional peptide mapping. *Faseb J*

Rossiter H, Barresi C, Pammer J, Rendl M, Haigh J, Wagner EF, Tschachler E (2004) Loss of vascular endothelial growth factor a activity in murine epidermal keratinocytes delays wound healing and inhibits tumor formation. *Cancer Res* **64**(10)**:** 3508-3516

Roth V (2004) The generalized LASSO. *IEEE Trans Neural Netw* **15**(1)**:** 16-28

Ryter JM, Doe CQ, Matthews BW (2002) Structure of the DNA binding region of prospero reveals a novel homeo-prospero domain. *Structure (Camb)* **10**(11)**:** 1541-1549

Saaristo A, Veikkola T, Enholm B, Hytonen M, Arola J, Pajusola K, Turunen P, Jeltsch M, Karkkainen MJ, Kerjaschki D, Bueler H, Yla-Herttuala S, Alitalo K (2002) Adenoviral VEGF-C overexpression induces blood vessel enlargement, tortuosity, and leakiness but no sprouting angiogenesis in the skin or mucous membranes. *Faseb J* **16**(9)**:** 1041-1049

Sabin FR (1902) On the origin of the lymphatic system from the veins and the development of the lymph hearts and thoracic duct in the pig. *Am J Anat* **1:** 367-391

Saharinen P, Tammela T, Karkkainen MJ, Alitalo K (2004) Lymphatic vasculature: development, molecular regulation and role in tumor metastasis and inflammation. *Trends Immunol* **25**(7)**:** 387-395

Schacht V, Dadras SS, Johnson LA, Jackson DG, Hong YK, Detmar M (2005) Up-regulation of the lymphatic marker podoplanin, a mucin-type transmembrane glycoprotein, in human squamous cell carcinomas and germ cell tumors. *Am J Pathol* **166**(3)**:** 913-921

Schacht V, Ramirez MI, Hong YK, Hirakawa S, Feng D, Harvey N, Williams M, Dvorak AM, Dvorak HF, Oliver G, Detmar M (2003) T1alpha/podoplanin deficiency disrupts normal lymphatic vasculature formation and causes lymphedema. *Embo J* **22**(14)**:** 3546-3556

Schena M, Shalon D, Davis RW, Brown PO (1995) Quantitative monitoring of gene expression patterns with a complementary DNA microarray. *Science* **270**(5235)**:** 467-470

Scherpereel A, Gentina T, Grigoriu B, Senechal S, Janin A, Tsicopoulos A, Plenat F, Bechard D, Tonnel AB, Lassalle P (2003) Overexpression of endocan induces tumor formation. *Cancer Res* **63**(18)**:** 6084-6089

Schledzewski K, Falkowski M, Moldenhauer G, Metharom P, Kzhyshkowska J, Ganss R, Demory A, Falkowska-Hansen B, Kurzen H, Ugurel S, Geginat G, Arnold B, Goerdt S (2006) Lymphatic endothelium-specific hyaluronan receptor LYVE-1 is expressed by stabilin-1+, F4/80+, CD11b+ macrophages in malignant tumours and wound healing tissue in vivo and in bone marrow cultures in vitro: implications for the assessment of lymphangiogenesis. *J Pathol* **209**(1)**:** 67-77

Schoenfeld J, Lessan K, Johnson NA, Charnock-Jones DS, Evans A, Vourvouhaki E, Scott L, Stephens R, Freeman TC, Saidi SA, Tom B, Weston GC, Rogers P, Smith SK, Print CG (2004) Bioinformatic analysis of primary endothelial cell gene array data illustrated by the analysis of transcriptome changes in endothelial cells exposed to VEGF-A and PlGF. *Angiogenesis* **7**(2)**:** 143-156

Schoppmann SF, Birner P, Stockl J, Kalt R, Ullrich R, Caucig C, Kriehuber E, Nagy K, Alitalo K, Kerjaschki D (2002) Tumor-associated macrophages express lymphatic endothelial growth factors and are related to peritumoral lymphangiogenesis. *Am J Pathol* **161**(3)**:** 947-956

Senger DR, Galli SJ, Dvorak AM, Perruzzi CA, Harvey VS, Dvorak HF (1983) Tumor cells secrete a vascular permeability factor that promotes accumulation of ascites fluid. *Science* **219**(4587)**:** 983-985

Shalon D, Smith SJ, Brown PO (1996) A DNA microarray system for analyzing complex DNA samples using two-color fluorescent probe hybridization. *Genome Res* **6**(7)**:** 639-645

Shields JD, Fleury ME, Yong C, Tomei AA, Randolph GJ, Swartz MA (2007) Autologous chemotaxis as a mechanism of tumor cell homing to lymphatics via interstitial flow and autocrine CCR7 signaling. *Cancer Cell* **11**(6)**:** 526-538

Shin JW, Min M, Larrieu-Lahargue F, Canron X, Kunstfeld R, Nguyen L, Henderson JE, Bikfalvi A, Detmar M, Hong YK (2006) Prox1 promotes lineage-specific expression of fibroblast growth factor (FGF) receptor-3 in lymphatic endothelium: a role for FGF signaling in lymphangiogenesis. *Mol Biol Cell* **17**(2)**:** 576-584

Shing Y, Folkman J, Sullivan R, Butterfield C, Murray J, Klagsbrun M (1984) Heparin affinity: purification of a tumor-derived capillary endothelial cell growth factor. *Science* **223**(4642)**:** 1296-1299

Skobe M, Hawighorst T, Jackson DG, Prevo R, Janes L, Velasco P, Riccardi L, Alitalo K, Claffey K, Detmar M (2001) Induction of tumor lymphangiogenesis by VEGF-C promotes breast cancer metastasis. *Nat Med* **7**(2)**:** 192-198

Sokal RR (1965) Statistical Methods in Systematics. *Biol Rev Camb Philos Soc* **40:** 337-391

Sosa-Pineda B, Wigle JT, Oliver G (2000) Hepatocyte migration during liver development requires Prox1. *Nat Genet* **25**(3)**:** 254-255

Spira A, Beane JE, Shah V, Steiling K, Liu G, Schembri F, Gilman S, Dumas YM, Calner P, Sebastiani P, Sridhar S, Beamis J, Lamb C, Anderson T, Gerry N, Keane J, Lenburg ME, Brody JS (2007) Airway epithelial gene expression in the diagnostic evaluation of smokers with suspect lung cancer. *Nat Med* **13**(3)**:** 361-366

Stacker SA, Caesar C, Baldwin ME, Thornton GE, Williams RA, Prevo R, Jackson DG, Nishikawa S, Kubo H, Achen MG (2001) VEGF-D promotes the metastatic spread of tumor cells via the lymphatics. *Nat Med* **7**(2)**:** 186-191

Stacker SA, Stenvers K, Caesar C, Vitali A, Domagala T, Nice E, Roufail S, Simpson RJ, Moritz R, Karpanen T, Alitalo K, Achen MG (1999) Biosynthesis of vascular endothelial growth factor-D involves proteolytic processing which generates non-covalent homodimers. *J Biol Chem* **274**(45)**:** 32127-32136

Stalmans I, Ng YS, Rohan R, Fruttiger M, Bouche A, Yuce A, Fujisawa H, Hermans B, Shani M, Jansen S, Hicklin D, Anderson DJ, Gardiner T, Hammes HP, Moons L, Dewerchin M, Collen D, Carmeliet P, D'Amore PA (2002) Arteriolar and venular patterning in retinas of mice selectively expressing VEGF isoforms. *J Clin Invest* **109**(3)**:** 327-336

Storey JD, Xiao W, Leek JT, Tompkins RG, Davis RW (2005) Significance analysis of time course microarray experiments. *Proc Natl Acad Sci U S A* **102**(36)**:** 12837-12842

Storkebaum E, Lambrechts D, Carmeliet P (2004) VEGF: once regarded as a specific angiogenic factor, now implicated in neuroprotection. *Bioessays* **26**(9)**:** 943-954

Subramanian A, Tamayo P, Mootha VK, Mukherjee S, Ebert BL, Gillette MA, Paulovich A, Pomeroy SL, Golub TR, Lander ES, Mesirov JP (2005) Gene set enrichment analysis: a knowledge-based approach for interpreting genome-wide expression profiles. *Proc Natl Acad Sci U S A* **102**(43)**:** 15545-15550

Suhardja A, Hoffman H (2003) Role of growth factors and their receptors in proliferation of microvascular endothelial cells. *Microsc Res Tech* **60**(1)**:** 70-75

Suri C, Jones PF, Patan S, Bartunkova S, Maisonpierre PC, Davis S, Sato TN, Yancopoulos GD (1996) Requisite role of angiopoietin-1, a ligand for the TIE2 receptor, during embryonic angiogenesis. *Cell* **87**(7)**:** 1171-1180

Swartz MA (2001) The physiology of the lymphatic system. *Adv Drug Deliv Rev* **50**(1-2)**:** 3-20

Tammela T, Saaristo A, Holopainen T, Lyytikka J, Kotronen A, Pitkonen M, Abo-Ramadan U, Yla-Herttuala S, Petrova TV, Alitalo K (2007) Therapeutic differentiation and maturation of lymphatic vessels after lymph node dissection and transplantation. *Nat Med* **13**(12)**:** 1458-1466

Tangemann K, Gunn MD, Giblin P, Rosen SD (1998) A high endothelial cell-derived chemokine induces rapid, efficient, and subset-selective arrest of rolling T lymphocytes on a reconstituted endothelial substrate. *J Immunol* **161**(11)**:** 6330-6337

Taniguchi K, Kohno R, Ayada T, Kato R, Ichiyama K, Morisada T, Oike Y, Yonemitsu Y, Maehara Y, Yoshimura A (2007) Spreds are essential for embryonic lymphangiogenesis by regulating vascular endothelial growth factor receptor 3 signaling. *Mol Cell Biol* **27**(12)**:** 4541-4550

Terada M, Shimizu A, Sato N, Miyakaze SI, Katayama H, Kurokawa-Seo M (2001) Fibroblast growth factor receptor 3 lacking the Ig IIIb and transmembrane domains secreted from human squamous cell carcinoma DJM-1 binds to FGFs. *Mol Cell Biol Res Commun* **4**(6)**:** 365-373

Thurston G (2003) Role of Angiopoietins and Tie receptor tyrosine kinases in angiogenesis and lymphangiogenesis. *Cell Tissue Res* **314**(1)**:** 61-68

Tischer E, Mitchell R, Hartman T, Silva M, Gospodarowicz D, Fiddes JC, Abraham JA (1991) The human gene for vascular endothelial growth factor. Multiple protein forms are encoded through alternative exon splicing. *J Biol Chem* **266**(18)**:** 11947-11954

Tobler NE, Detmar M (2006) Tumor and lymph node lymphangiogenesis--impact on cancer metastasis. *J Leukoc Biol* **80**(4)**:** 691-696

Tomarev SI, Sundin O, Banerjee-Basu S, Duncan MK, Yang JM, Piatigorsky J (1996) Chicken homeobox gene Prox 1 related to Drosophila prospero is expressed in the developing lens and retina. *Dev Dyn* **206**(4)**:** 354-367

Unemori EN, Ferrara N, Bauer EA, Amento EP (1992) Vascular endothelial growth factor induces interstitial collagenase expression in human endothelial cells. *J Cell Physiol* **153**(3)**:** 557-562

Unger RE, Krump-Konvalinkova V, Peters K, Kirkpatrick CJ (2002) In vitro expression of the endothelial phenotype: comparative study of primary isolated cells and cell lines, including the novel cell line HPMEC-ST1.6R. *Microvasc Res* **64**(3)**:** 384-397

Vardhanabhuti S, Blakemore SJ, Clark SM, Ghosh S, Stephens RJ, Rajagopalan D (2006) A comparison of statistical tests for detecting differential expression using Affymetrix oligonucleotide microarrays. *OMICS* **10**(4)**:** 555-566

Veikkola T, Jussila L, Makinen T, Karpanen T, Jeltsch M, Petrova TV, Kubo H, Thurston G, McDonald DM, Achen MG, Stacker SA, Alitalo K (2001) Signalling via vascular endothelial growth factor receptor-3 is sufficient for lymphangiogenesis in transgenic mice. *EMBO J* **20**(6)**:** 1223-1231

Wei C, Li J, Bumgarner RE (2004) Sample size for detecting differentially expressed genes in microarray experiments. *BMC Genomics* **5**(1)**:** 87

Weinstein M, Xu X, Ohyama K, Deng CX (1998) FGFR-3 and FGFR-4 function cooperatively to direct alveogenesis in the murine lung. *Development* **125**(18)**:** 3615-3623

Wesley UV, Albino AP, Tiwari S, Houghton AN (1999) A role for dipeptidyl peptidase IV in suppressing the malignant phenotype of melanocytic cells. *J Exp Med* **190**(3)**:** 311-322

Wetterwald A, Hoffstetter W, Cecchini MG, Lanske B, Wagner C, Fleisch H, Atkinson M (1996) Characterization and cloning of the E11 antigen, a marker expressed by rat osteoblasts and osteocytes. *Bone* **18**(2)**:** 125-132

Whitehurst B, Flister MJ, Bagaitkar J, Volk L, Bivens CM, Pickett B, Castro-Rivera E, Brekken RA, Gerard RD, Ran S (2007) Anti-VEGF-A therapy reduces lymphatic vessel density and expression of VEGFR-3 in an orthotopic breast tumor model. *Int J Cancer* **121**(10)**:** 2181-2191

Wigle JT, Harvey N, Detmar M, Lagutina I, Grosveld G, Gunn MD, Jackson DG, Oliver G (2002a) An essential role for Prox1 in the induction of the lymphatic endothelial cell phenotype. *Embo J* **21**(7)**:** 1505-1513

Wigle JT, Harvey N, Detmar M, Lagutina I, Grosveld G, Gunn MD, Jackson DG, Oliver G (2002b) An essential role for Prox1 in the induction of the lymphatic endothelial cell phenotype. *Embo J* **21**(7)**:** 1505-1513.

Wigle JT, Oliver G (1999) Prox1 function is required for the development of the murine lymphatic system. *Cell* **98**(6)**:** 769-778.

Wiley HE, Gonzalez EB, Maki W, Wu MT, Hwang ST (2001) Expression of CC chemokine receptor-7 and regional lymph node metastasis of B16 murine melanoma. *J Natl Cancer Inst* **93**(21)**:** 1638-1643

Wilkie AO, Patey SJ, Kan SH, van den Ouweland AM, Hamel BC (2002) FGFs, their receptors, and human limb malformations: clinical and molecular correlations. *Am J Med Genet* **112**(3)**:** 266-278

Withington ET (1894) *Medical history from the earliest times*, London: The Scientific Press.

Witte MH, Erickson R, Bernas M, Andrade M, Reiser F, Conlon W, Hoyme HE, Witte CL (1998) Phenotypic and genotypic heterogeneity in familial Milroy lymphedema. *Lymphology* **31**(4)**:** 145-155

Wu LW, Mayo LD, Dunbar JD, Kessler KM, Baerwald MR, Jaffe EA, Wang D, Warren RS, Donner DB (2000) Utilization of distinct signaling pathways by receptors for vascular endothelial cell growth factor and other mitogens in the induction of endothelial cell proliferation. *J Biol Chem* **275**(7)**:** 5096-5103

Xia YP, Li B, Hylton D, Detmar M, Yancopoulos GD, Rudge JS (2003) Transgenic delivery of VEGF to mouse skin leads to an inflammatory condition resembling human psoriasis. *Blood* **102**(1)**:** 161-168

Xu J, Lawshe A, MacArthur CA, Ornitz DM (1999) Genomic structure, mapping, activity and expression of fibroblast growth factor 17. *Mech Dev* **83**(1-2)**:** 165-178

Xu J, Liu Z, Ornitz DM (2000) Temporal and spatial gradients of Fgf8 and Fgf17 regulate proliferation and differentiation of midline cerebellar structures. *Development* **127**(9)**:** 1833-1843

Yamada Y, Nezu J, Shimane M, Hirata Y (1997) Molecular cloning of a novel vascular endothelial growth factor, VEGF-D. *Genomics* **42**(3)**:** 483-488

Yan G, Fukabori Y, McBride G, Nikolaropolous S, McKeehan WL (1993) Exon switching and activation of stromal and embryonic fibroblast growth factor (FGF)-FGF receptor genes in prostate epithelial cells accompany stromal independence and malignancy. *Mol Cell Biol* **13**(8)**:** 4513-4522.

Yanagi S, Inatome R, Takano T, Yamamura H (2001) Syk expression and novel function in a wide variety of tissues. *Biochem Biophys Res Commun* **288**(3)**:** 495-498

Yang S, Toy K, Ingle G, Zlot C, Williams PM, Fuh G, Li B, de Vos A, Gerritsen ME (2002) Vascular endothelial growth factor-induced genes in human umbilical vein endothelial cells: relative roles of KDR and Flt-1 receptors. *Arterioscler Thromb Vasc Biol* **22**(11)**:** 1797-1803

Yu SL, Chen HY, Chang GC, Chen CY, Chen HW, Singh S, Cheng CL, Yu CJ, Lee YC, Chen HS, Su TJ, Chiang CC, Li HN, Hong QS, Su HY, Chen CC, Chen WJ, Liu CC, Chan WK, Li KC, Chen JJ, Yang PC (2008) MicroRNA signature predicts survival and relapse in lung cancer. *Cancer Cell* **13**(1)**:** 48-57

Yuan L, Moyon D, Pardanaud L, Breant C, Karkkainen MJ, Alitalo K, Eichmann A (2002) Abnormal lymphatic vessel development in neuropilin 2 mutant mice. *Development* **129**(20)**:** 4797-4806

Zhang D, Zhang M (2007) Bayesian profiling of molecular signatures to predict event times. *Theor Biol Med Model* **4:** 3

Zhang G, Fahmy RG, diGirolamo N, Khachigian LM (2006) JUN siRNA regulates matrix metalloproteinase-2 expression, microvascular endothelial growth and retinal neovascularisation. *J Cell Sci* **119**(Pt 15)**:** 3219-3226

Zukowska Z, Grant DS, Lee EW (2003) Neuropeptide Y: a novel mechanism for ischemic angiogenesis. *Trends Cardiovasc Med* **13**(2)**:** 86-92

7 APPENDIX

Appendix Table 1

LEC signature genes (sorted by median of AB1700 fold change) confirmed by LD-MDA

LEC gene signature (236)		Fold change by AB1700			Fold change by qPCR				
Gene name	AB probe ID	Sample 1	Sample 2	Sample 3	Sample 1	Sample 2	Sample 3	LD-MDA	Core
guanylate cyclase 1, soluble, alpha 3	170165	497.3	155.0	83.6	1152.2	139.2	60.6	Yes	
deoxyribonuclease I-like 3	167226	49.3	2.6	51.3					
peroxisome proliferative activated receptor, gamma	192239	37.8	60.2	10.1	49.8	58.6	8.6	Yes	
ATP-binding cassette, sub-family A (ABC1), member 4	194955	35.5	26.3	7.2					
ADAMTS-like 3	158085	44.0	2.2	25.4					
dipeptidylpeptidase 4 (CD26)	209451	35.9	21.6	12.1	70.7	13.8	9.1	Yes	
coxsackie virus and adenovirus receptor	108284	23.6	20.9	2.8	47.0	28.4	2.4	Yes	
doublecortin and CaM kinase-like 1	202776	20.0	10.4	28.6	41.5	13.6	15.8	Yes	Yes
interleukin 7	127208	34.6	2.6	17.8	93.9	5.5	24.1	Yes	Yes
collectin sub-family member 12	114422	39.3	17.2	6.1	114.1	21.9	7.1	Yes	
retinol binding protein 7, cellular	129740	16.8	1.4	29.6	426.9	161.5	512.2	Yes	Yes
phosphodiesterase 9A	105408	15.8	16.2	9.4					
follistatin	117261	3.7	15.5	43.6	10.5	17.9	49.9	Yes	
runt-related transcription factor 1; translocated to, 1	122830	24.7	4.9	15.3					
mannose receptor, C type 1	198568	119.4	6.4	15.3	250.3	7.6	9.0	Yes	Yes
cholesterol 25-hydroxylase	117883	130.4	3.6	15.3					
pyruvate dehydrogenase kinase, isoenzyme 4	101060	175.1	12.5	14.7					
RNA binding motif protein 35B	167987	41.1	10.2	14.6					
ras homolog gene family, member U	130933	26.2	4.4	14.1					
retinol binding protein 1, cellular	149921	70.0	13.9	7.5	209.6	30.5	12.7	Yes	
integrin, beta 4	184548	14.9	3.0	13.8	5222.0	375.0	530.4	Yes	
GRINL1A complex upstream protein	104996	193.2	13.8	9.0					
chromosome 2 open reading frame 23	156624	68.7	13.5	7.8					
periplakin	138890	16.8	12.5	12.8	12812.4	591.8	35.2	Yes	Yes
trefoil factor 3 (intestinal)	114445	44.8	8.1	12.7	460.9	14.8	19.5	Yes	Yes
DKFZP586A0522 protein	107957	64.7	4.0	12.6					
solute carrier family 38, member 4	217080	12.5	5.3	17.0	141.5	10.1	21.2	Yes	Yes
carcinoembryonic antigen-related cell adhesion molecule 1	219223	50.1	11.7	3.9	35.4	7.0	3.6	Yes	
growth hormone receptor	190306	13.1	9.0	11.7	33.9	18.2	9.5	Yes	Yes
IQ motif containing with AAA domain	152027	46.9	11.5	4.4					
homeo box D10	166056	17.7	3.3	11.4	39.9	5.2	8.3	Yes	Yes
PDZ domain protein GIPC2	180419	20.8	5.5	11.1	64.1	8.1	20.1	Yes	
v-maf musculoaponeurotic fibrosarcoma oncogene homolog	186589	28.4	10.7	4.2	61.9	12.7	3.7	Yes	
chromosome 6 open reading frame 123	105756	69.4	10.6	7.4					
relaxin 1	122881	11.8	10.6	2.2					
CD36 antigen	121773	49.9	4.4	10.6					
storkhead box 2	199062	9.9	3.2	16.7					
aldehyde dehydrogenase 1 family, member A1	162248	10.1	1.8	9.6	34.2	2.4	13.8	Yes	
reelin	207609	20.1	8.2	9.6	40.4	9.5	7.8	Yes	Yes
prospero-related homeobox 1	124383	38.9	6.8	9.6	134.0	7.9	10.3	Yes	Yes
transient receptor potential cation channel C 6	101144	32.1	3.1	9.4					

LEC gene signature (236) Gene name	AB probe ID	Fold change by AB1700			Fold change by qPCR			LD-MDA	Core
		Sample 1	Sample 2	Sample 3	Sample 1	Sample 2	Sample 3		
pleckstrin homology domain containing, family A member 2	116372	8.5	13.7	9.3					
phospholipase C, epsilon 1	132759	9.3	21.7	9.2	40.3	18.1	119.1	Yes	Yes
endothelin receptor type B	150558	83.9	6.6	9.2	150.8	7.9	15.7	Yes	
heparan sulfate (glucosamine) 3-O-sulfotransferase 1	154628	190.0	9.1	2.5					
cadherin, EGF LAG seven-pass G-type receptor 1	202051	8.8	10.8	3.4	21.1	8.4	2.5	Yes	
hairy/enhancer-of-split related with YRPW motif 1	121998	8.5	2.5	8.6	20.3	5.7	9.8	Yes	
tissue inhibitor of metalloproteinase 3	179538	10.8	8.4	4.3	31.3	11.1	4.5	Yes	Yes
solute carrier family 26, member 4	194103	8.5	4.8	8.3	4.8	7.1	11.1	Yes	
zinc finger protein 467	184463	36.8	8.3	2.8					
selenoprotein P, plasma, 1	169984	49.0	6.4	8.2	86.0	10.3	7.8	Yes	Yes
START domain containing 8	145078	8.1	2.1	11.1					
GDNF family receptor alpha 1	202672	7.9	8.0	106.1	7.6	13.7	42.3	Yes	Yes
ring finger protein 152	217858	7.9	2.4	10.7					
chemokine (C-C motif) ligand 21	138321	7.8	1.0	7.7	5259.7	86.8	42.7	Yes	
leucine rich repeat containing 1	115313	14.0	4.0	7.5					
chromosome 8 open reading frame 55	143619	7.7	7.5	4.6					
calmegin	100646	7.3	30.7	2.4					
tumor necrosis factor receptor superfamily, member 11a	105151	11.8	7.3	5.9					
LIM domain binding 2	127667	24.3	2.6	7.2					
hyaluronoglucosaminidase 1	184118	75.2	5.8	7.2	682.7	9.0	20.2	Yes	Yes
SRY (sex determining region Y)-box 18	126548	26.9	7.2	4.3	98.9	7.4	9.0	Yes	
glia maturation factor, gamma	180184	36.6	2.9	7.1					
ovostatin-2	138125	27.0	5.3	7.1					
tumor necrosis factor (ligand) superfamily, member 10	153282	25.9	6.9	2.6					
homeo box D4	219817	27.9	6.8	4.9					
centrosomal protein 1	203266	6.7	2.8	7.1					
cytochrome P450, family 1, subfamily A, polypeptide 1	135086	39.0	3.2	6.5					
galanin	167511	10.9	2.3	6.5					
klotho beta	120728	6.4	4.6	10.5					
chromosome 10 open reading frame 116	121402	22.9	4.5	6.4					
GTPase, IMAP family member 5	177981	97.7	6.2	5.6					
chromosome 1 open reading frame 34	132797	19.6	2.1	6.0					
coagulation factor C homolog, cochlin (Limulus polyphemus)	189694	7.7	4.7	5.9					
lamin B receptor	159112	8.7	4.3	5.9					
chromatin modifying protein 4C	177868	7.6	5.8	5.3					
NDRG family member 2	153476	21.4	5.8	3.5					
transmembrane protein 88	200951	40.6	3.5	5.6					
sulfotransferase family, cytosolic, 1C, member 2	130755	21.5	5.5	5.0					
leptin receptor	222462	5.5	3.0	6.6	13.6	8.5	9.1	Yes	Yes
serine protease inhibitor, Kunitz type, 2	212742	7.8	3.7	5.4					
chromosome 17 open reading frame 28	115291	29.5	5.4	2.5					
hydroxysteroid (17-beta) dehydrogenase 2	195707	21.5	2.7	5.4	39.9	4.0	9.1	Yes	Yes
phosphatidic acid phosphatase type 2B	133742	5.4	5.8	5.4	10.4	6.0	4.3	Yes	
DEAD (Asp-Glu-Ala-Asp) box polypeptide 10	166102	6.8	3.4	5.4					
kinesin family member 14	121673	2.2	5.4	6.1					
v-rel reticuloendotheliosis viral oncogene homolog (avian)	109539	6.1	5.3	2.4					
integrin, alpha 9	157432	16.7	2.9	5.3	78.6	6.8	2.0	Yes	Yes

LEC gene signature (236)		Fold change by AB1700			Fold change by qPCR				
Gene name	AB probe ID	Sample 1	Sample 2	Sample 3	Sample 1	Sample 2	Sample 3	LD-MDA	Core
fms-related tyrosine kinase 4	204569	19.9	3.0	5.1	83.6	6.6	5.9	Yes	
SH2 domain containing 3A	130169	10.7	3.0	5.1					
YTH domain containing 2	181510	6.0	5.1	2.4					
myosin VIIA and Rab interacting protein	155197	5.7	5.1	2.5					
solute carrier family 24, member 1	216954	5.1	6.0	4.5					
chondroitin beta1,4 N-acetylgalactosaminyltransferase	101140	10.0	5.0	3.3	23.1	6.6	4.1	Yes	
ring finger protein 144	101012	5.0	7.4	2.3					
podoplanin	219722	30.8	2.5	5.0	80.5	3.6	7.2	Yes	Yes
ST6...N-acetylgalactosaminide alpha-2,6-sialyltransferase 3	189728	55.5	3.8	5.0					
chromosome 11 open reading frame 8	108279	5.0	3.0	31.9					
dedicator of cytokinesis 8	106981	8.1	4.9	2.1					
forkhead box C1	195499	4.0	4.9	4.8	8.7	5.5	3.5	Yes	
kelch repeat and BTB (POZ) domain containing 11	208898	9.4	4.1	4.8					
fibroblast growth factor 12	138024	8.7	4.8	2.8	12.7	10.7	2.4	Yes	
proprotein convertase subtilisin/kexin type 6	154864	32.9	3.8	4.7					
chromosome 18 open reading frame 30	171508	28.3	2.8	4.7					
MADS box transcription enhancer factor 2, polypeptide C	179021	12.3	4.7	1.8	30.1	5.6	5.9	Yes	
protein phosphatase 1, regulatory (inhibitor) subunit 9A	198246	11.2	4.6	2.0					
SH3 domain and tetratricopeptide repeats 2	133008	10.5	2.8	4.5					
chromosome 7 open reading frame 29	138101	5.7	3.9	4.5					
multimerin 1	128509	27.1	4.5	3.2					
CTD (carboxy-terminal domain) small phosphatase-like	130122	4.5	4.6	3.6					
zinc finger protein 650	211325	4.4	4.9	2.6					
dehydrogenase/reductase (SDR family) member 3	125937	9.6	4.4	2.8					
phosphodiesterase 6B, cGMP-specific, rod, beta	120762	5.9	4.3	2.2					
toll-like receptor 4	216730	6.2	4.3	2.5					
guanylate cyclase 1, soluble, beta 3	131372	4.3	7.8	3.9					
secreted frizzled-related protein 1	143998	2.6	6.2	4.3					
midline 1 (Opitz/BBB syndrome)	214412	5.2	2.7	4.2					
SMAD, mothers against DPP homolog 9 (Drosophila)	106362	6.4	2.7	4.2					
ADP-ribosylation factor-like 4B	146573	14.1	4.2	3.1					
chromosome 2 open reading frame 31	204611	4.2	4.0	4.2					
chromosome 20 open reading frame 129	199617	4.1	3.2	13.6					
adrenergic, beta-2-, receptor, surface	127856	5.9	3.2	4.1					
phosphoglucomutase 5	186266	6.8	4.1	3.3					
v-yes-1 Yamaguchi sarcoma viral related oncogene homolog	194134	6.6	4.1	3.9	12.9	4.2	3.5	Yes	
B cell RAG associated protein	110602	5.5	4.0	2.0					
neuritin 1	182524	8.7	4.0	3.2					
SET and MYND domain containing 2	141023	4.0	4.0	5.4					
ephrin-A5	158422	23.5	4.0	2.8					
epithelial membrane protein 2	173909	4.0	3.5	7.4					
adducin 3 (gamma)	132668	11.9	3.9	1.7	38.6	10.6	23.6	Yes	Yes
cell division cycle 25B	208879	4.0	2.8	3.9					
serologically defined colon cancer antigen 33	186894	3.9	2.9	4.4					
similar to tumor-associated membrane protein XMP	230120	3.5	3.9	4.7					
transforming growth factor, alpha	180395	18.8	3.3	3.9					
huntingtin-associated protein interacting protein	125617	9.3	3.7	3.9					

153

LEC gene signature (236) Gene name	AB probe ID	Fold change by AB1700			Fold change by qPCR			LD-MDA	Core
		Sample 1	Sample 2	Sample 3	Sample 1	Sample 2	Sample 3		
piccolo (presynaptic cytomatrix protein)	176448	3.8	4.6	2.6					
aquaporin 7 pseudogene 1	108084	19.3	3.8	3.2					
galactosamine... N-acetylgalactosaminyltransferase-like 4	176965	7.5	3.8	2.7					
suppressor of fused homolog (Drosophila)	176456	3.8	2.5	3.8					
kelch-like 3 (Drosophila)	184006	3.1	3.8	4.7					
cholesteryl ester transfer protein, plasma	140569	45.2	3.7	2.8					
tetraspanin 12	215171	10.2	2.4	3.6					
hydroxysteroid (17-beta) dehydrogenase 8	213046	3.3	3.6	3.8					
homeo box D8	217040	7.6	3.6	3.6					
sex comb on midleg-like 2 (Drosophila)	115809	5.5	3.3	3.6					
tribbles homolog 2 (Drosophila)	188922	2.4	3.6	4.1					
protein kinase C, zeta	184015	8.1	3.1	3.5					
LIM domain only 2 (rhombotin-like 1)	207685	20.9	3.5	3.3	48.3	4.5	3.5	Yes	
nitric oxide synthase 3 (endothelial cell)	197614	14.6	3.3	3.5					
chaperone, ABC1 activity of bc1 complex like (S. pombe)	144833	3.6	3.3	3.5					
Rap guanine nucleotide exchange factor (GEF) 5	129115	6.9	3.4	2.8					
glucose-fructose oxidoreductase domain containing 1	137251	2.8	3.4	3.7					
ribosomal protein S6 kinase, 90kDa, polypeptide 5	152363	3.4	2.3	3.7					
transmembrane 4 L six family member 18	125309	19.0	2.3	3.4					
RALBP1 associated Eps domain containing 2	125119	15.9	3.4	2.2					
arrestin, beta 1	111374	9.2	2.8	3.3					
tissue factor pathway inhibitor	126759	5.2	2.2	3.3					
aldehyde dehydrogenase 6 family, member A1	184174	3.3	4.2	2.7					
lysosomal-associated membrane protein 3	194477	9.4	3.3	3.0	29.5	4.7	5.1	Yes	Yes
kinesin family member 20A	118830	3.3	2.5	8.6					
serum deprivation response	156433	20.7	3.2	2.1					
propionyl Coenzyme A carboxylase, alpha polypeptide	126484	3.6	3.2	2.1					
acyl-CoA synthetase long-chain family member 5	180740	8.4	3.2	2.6					
formin binding protein 1	127600	3.2	2.5	59.6					
cyclin-dependent kinase inhibitor 1B (p27, Kip1)	121695	6.0	2.9	3.1					
nudix (nucleoside diphosphate linked moiety X)-type 6	179802	2.1	3.4	3.1					
DNA-damage-inducible transcript 4-like	199024	11.0	2.2	3.1					
suppressor of cytokine signaling 2	108934	3.1	3.1	9.2					
chromosome 20 open reading frame 35	220840	2.3	4.8	3.1					
BTB (POZ) domain containing 3	119684	2.2	3.4	3.1					
HRAS-like suppressor 3	144399	7.7	3.0	2.2					
serine/threonine kinase 32B	178424	3.4	3.0	2.1					
chromosome 6 open reading frame 85	182938	8.8	3.0	2.6					
fibroblast growth factor 13	156333	11.6	3.0	2.2					
protein tyrosine phosphatase, receptor N polypeptide 2	187260	4.1	3.0	2.7					
zinc finger protein 435	101333	8.3	2.9	2.2					
erythrocyte membrane protein band 4.1-like 2	124368	3.8	2.8	2.9					
pellino homolog 1 (Drosophila)	113197	4.1	2.9	2.3					
cAMP responsive element binding protein 3-like 4	203282	2.9	3.0	2.6					
nuclear factor I/B	141557	10.8	2.9	2.6					
F-box and leucine-rich repeat protein 7	178637	2.9	3.0	2.1					
recombination activating gene 1 activating protein 1	210819	2.8	2.2	2.9					

154

LEC gene signature (236)		Fold change by AB1700			Fold change by qPCR				
Gene name	AB probe ID	Sample 1	Sample 2	Sample 3	Sample 1	Sample 2	Sample 3	LD-MDA	Core
protein kinase C binding protein 1	180118	3.2	2.4	2.8					
calsyntenin 3	198222	2.8	2.0	2.9					
homeo box D1	149127	11.8	2.8	2.5					
progestin and adipoQ receptor family member VIII	166596	13.1	2.8	2.1					
t-complex 11 (mouse) like 2	193950	3.1	2.5	2.8					
high-mobility group box 2	177404	2.0	2.8	8.2					
glycine receptor, beta	112304	2.8	3.5	2.1	4.8	4.0	2.1	Yes	
contactin associated protein-like 3	153182	9.7	2.8	2.5					
CNKSR family member 3	173337	5.8	2.3	2.8					
F-box protein 46	162992	2.2	2.8	9.0					
sprouty homolog 3 (Drosophila)	134280	2.8	2.6	3.0					
3-hydroxybutyrate dehydrogenase (heart, mitochondrial)	122515	2.7	2.7	7.0					
nudix (nucleoside diphosphate linked moiety X)-type 4	172746	4.7	2.7	2.4					
Friend leukemia virus integration 1	128011	7.9	2.7	2.3					
BMP2 inducible kinase	162982	4.3	2.3	2.7					
phosphatidic acid phosphatase type 2A	207194	4.5	2.2	2.7					
GTP cyclohydrolase I feedback regulator	215327	2.6	4.0	2.2					
mutS homolog 5 (E. coli)	114236	2.6	2.5	3.0					
Ras protein-specific guanine nucleotide-releasing factor 2	181938	2.6	2.6	2.2					
transcription elongation factor B polypeptide 3B (A2)	212385	2.6	2.1	11.2					
gamma-aminobutyric acid (GABA) A receptor, epsilon	130287	2.5	2.6	2.6					
ankylosis, progressive homolog (mouse)	172690	2.5	2.8	2.6					
protein tyrosine phosphatase, non-receptor type 14	186519	2.8	2.5	2.5					
cyclin B2	169571	2.5	2.1	8.3					
semaphorin 3A	154374	2.5	2.5	5.8					
cyclin-dependent kinase inhibitor 2C (p18, inhibits CDK4)	112997	2.2	2.5	8.0					
MyoD family inhibitor domain containing	191935	2.5	2.5	3.1					
Werner syndrome	188301	2.5	3.0	2.3					
midline 2	206942	4.9	2.5	2.5					
nuclear factor of activated T-cells, calcineurin-dependent 3	198298	3.2	2.5	2.0					
protein phosphatase 3 (calcineurin A alpha)	215875	4.3	2.4	2.2					
adaptor-related protein complex 1, sigma 2 subunit	183970	2.4	2.4	2.4					
SEC15-like 1 (S. cerevisiae)	147612	7.5	2.3	2.4					
nucleoredoxin	160193	2.6	2.4	2.1					
MAP kinase interacting serine/threonine kinase 2	147930	2.8	2.4	2.2					
protein tyrosine phosphatase type IVA, member 3	221359	2.4	2.6	2.1					
hydroxysteroid (17-beta) dehydrogenase 7	149125	2.2	3.1	2.3					
TBC1 domain family, member 8 (with GRAM domain)	214636	8.1	2.3	2.2					
citrate lyase beta like	124662	2.3	2.2	4.1					
Rho GTPase activating protein 25	198348	14.4	2.3	2.3					
forkhead box P1	203381	2.4	2.1	2.3					
chromosome 14 open reading frame 94	187081	2.3	2.0	2.9					
fat-like cadherin FATJ	131034	2.7	2.3	2.2					
Fanconi anemia, complementation group C	205301	2.5	2.3	2.2					
phosphorylase, glycogen; liver	150387	2.5	2.2	2.2					
protocadherin gamma subfamily C, 5	227600	4.4	2.0	2.2					
phosphatidylinositol transfer protein, cytoplasmic 1	117142	2.8	2.2	2.2					

155

LEC gene signature (236)		Fold change by AB1700			Fold change by qPCR			LD-MDA	Core
Gene name	AB probe ID	Sample 1	Sample 2	Sample 3	Sample 1	Sample 2	Sample 3		
papilin, proteoglycan-like sulfated glycoprotein	138764	4.3	1.4	2.2	8.3	2.0	2.1	Yes	Yes
inhibitor of growth family, member 3	168063	2.0	2.1	2.1					
2-hydroxyphytanoyl-CoA lyase	138137	2.1	2.1	2.3					
extracellular link domain containing 1	195865	43.0	1.0	2.0	312.0	3.5	15.2	Yes	
EPH receptor B2	190778	2.2	1.4	1.4	4.8	1.6	0.7	Yes	
angiopoietin 2	193875	3.8	0.5	1.0	10.1	0.9	1.3	Yes	
desmoplakin	170090	1.5	0.4	0.5	2.5	3.5	3.3	Yes	Yes

BEC signature genes (sorted by median of AB1700 fold change) confirmed by LD-MDA

BEC gene signature (342)		Fold change by AB1700			Fold change by qPCR			LD-MDA	Core
Gene name	AB probe ID	Sample 1	Sample 2	Sample 3	Sample 1	Sample 2	Sample 3		
plasminogen activator, urokinase	208672	165.6	6.0	126.5	91.6	6.7	164.8	Yes	Yes
proprotein convertase subtilisin/kexin type 1	213177	96.2	8.4	91.1					
brain expressed, X-linked 1	137034	250.2	88.3	7.0					
collagen, type I, alpha 2	105493	344.2	86.9	3.3	685.5	71.9	5.3	Yes	
glutamine-fructose-6-phosphate transaminase 2	113797	155.1	66.0	3.6					
lipase, endothelial	200619	59.5	112.0	50.6	16.4	117.4	95.8	Yes	Yes
FAT tumor suppressor homolog 1 (Drosophila)	131558	54.8	54.6	8.7	6993.8	55.3	151.9	Yes	Yes
fibroblast activation protein, alpha	164725	131.1	47.4	46.7	16098.5	18.7	9098.3	Yes	
transgelin	172572	56.9	7.0	47.1					
matrix metalloproteinase 1 (interstitial collagenase)	215808	45.6	9.5	85.9	36.3	11.7	73.3	Yes	Yes
ADAM with thrombospondin type 1 motif, 1	216353	477.8	45.4	4.4	140.1	64.1	3.7	Yes	
collagen, type VI, alpha 3	115643	884.5	44.2	2.8					
interleukin 6 (interferon, beta 2)	163241	28.4	40.4	45.8	521.0	52.9	32.1	Yes	Yes
interleukin 1 receptor-like 1	131513	62.8	36.3	24.5					
fms-related tyrosine kinase 1	219494	93.1	21.3	35.7	75.6	19.8	65.3	Yes	Yes
hypothetical protein BC012029	150646	71.0	9.0	34.9					
interleukin 8	176899	34.1	9.0	33.2	26.8	7.6	68.7	Yes	
tumor necrosis factor (ligand) superfamily, member 15	192558	39.1	8.4	32.7	27.3	5.1	139.5	Yes	Yes
GLI pathogenesis-related 1 (glioma)	117689	118.7	32.7	9.8					
collagen, type V, alpha 1	110570	68.3	5.7	31.0	36.5	5.3	83.6	Yes	Yes
cysteine-rich secretory protein LCCL domain containing 2	170538	331.3	29.5	5.4					
angiopoietin-like 4	181959	34.5	25.4	27.6	16.7	15.9	31.6	Yes	Yes
receptor tyrosine kinase-like orphan receptor 1	194924	51.8	8.2	27.0					
brain abundant, membrane attached signal protein 1	198318	69.8	7.6	25.8					
GLI-Kruppel family member GLI3	100093	24.0	2.7	31.3					
latent transforming growth factor beta binding protein 2	116441	23.5	5.5	80.2					
oxytocin receptor	200205	155.0	23.4	3.5					
solute carrier family 22, member 17	140114	23.0	7.4	34.7	15.8	35.2	166.8	Yes	Yes
synaptotagmin-like 2	118410	115.0	22.5	17.6					
chondroitin sulfate proteoglycan 2 (versican)	207524	117.5	21.9	4.8	4986.4	20.7	347.8	Yes	
glutaminyl-peptide cyclotransferase (glutaminyl cyclase)	152127	25.4	4.0	20.6					

BEC gene signature (342)		Fold change by AB1700			Fold change by qPCR			LD-MDA	Core
Gene name	AB probe ID	Sample 1	Sample 2	Sample 3	Sample 1	Sample 2	Sample 3		
glycoprotein (transmembrane) nmb	161212	236.8	20.3	4.1	11700.5	2503.8	42.8	Yes	Yes
high mobility group AT-hook 2	105728	20.3	20.2	3.0					
brain-derived neurotrophic factor	215284	36.8	18.9	8.3					
interferon, alpha-inducible protein 27	152567	18.9	7.3	170.0					
lysyl oxidase-like 1	156579	102.7	8.2	17.7					
transcription elongation factor A (SII)-like 7	130055	53.2	9.4	17.6					
cadherin 2, type 1, N-cadherin (neuronal)	187321	163.7	5.2	17.5	24.5	3.4	14.7	Yes	Yes
dihydropyrimidinase-like 4	161807	17.2	4.7	22.2					
phosphatidic acid phosphatase type 2 domain containing 1	190799	26.1	15.7	3.8					
stanniocalcin 2	184148	39.4	15.7	4.5					
regulator of G-protein signalling 4	165955	93.6	15.5	10.9					
squamous cell carcinoma antigen recognized by T cells 2	187160	15.7	4.6	15.5					
chromosome 7 open reading frame 10	180432	87.0	15.5	13.3					
GULP, engulfment adaptor PTB domain containing 1	137136	18.1	4.6	15.4					
chromosome 6 open reading frame 105	163966	15.2	10.6	24.4					
thrombospondin, type I, domain containing 2	155355	21.9	14.8	11.6					
transient receptor potential cation channel, subfamily C1	158239	14.6	5.5	16.7					
epithelial membrane protein 3	152376	64.9	11.7	14.5					
neuronal cell adhesion molecule	106462	14.4	7.8	29.6	11.5	7.9	26.7	Yes	Yes
leucine rich repeat containing 17	133553	14.1	4.0	48.6					
nuclear receptor interacting protein 3	102896	19.2	9.0	13.8					
ring finger protein 182	106266	31.3	5.6	13.7					
neuregulin 1	223108	159.2	13.4	8.4					
LY6/PLAUR domain containing 1	197493	7.2	12.3	14.1					
lymphocyte cytosolic protein 1 (L-plastin)	175091	57.2	4.0	12.1					
endothelial cell-specific molecule 1	174810	16.1	12.1	6.1					
epithelial V-like antigen 1	129035	12.1	5.2	14.2					
serine (or cysteine) proteinase inhibitor, clade E, member 2	210342	15.7	3.5	12.0					
phosphoglycerate dehydrogenase	210225	33.3	11.9	6.9					
Fc receptor-like and mucin-like 2	173350	30.7	11.8	2.6					
anthrax toxin receptor 1	112158	20.3	11.7	9.0					
v-erb-b2 erythroblastic leukemia viral oncogene homolog 2	105627	11.6	2.8	21.4					
keratin 7	207298	11.5	9.3	21.3					
IGF-II mRNA-binding protein 3	210073	12.5	6.8	11.4					
inhibin, beta A (activin A, activin AB alpha polypeptide)	193064	50.6	5.8	11.2	44.0	4.6	9.4	Yes	
neurexin 3	139725	14.4	11.1	5.5					
transcription factor EC	114012	11.1	6.2	45.3					
transmembrane, prostate androgen induced RNA	158378	11.3	6.5	11.1					
delta-notch-like EGF repeat-containing transmembrane	103310	35.7	10.1	10.9	1977.3	13.3	8699.8	Yes	
myozenin 2	188996	14.6	10.8	5.4					
F-box protein 32	218680	10.7	4.0	16.2					
CD44 antigen	133604	12.8	10.6	3.7	16.8	12.8	7.4	Yes	
sulfatase 1	169414	23.2	3.7	10.6					
matrix metalloproteinase 10 (stromelysin 2)	170985	6.0	10.5	41.2	3.0	7.3	19.6	Yes	
heat shock 22kDa protein 8	165817	10.2	6.8	13.2					
vascular endothelial growth factor C	170337	59.6	10.1	5.6	41.0	6.0	8.9	Yes	Yes

157

BEC gene signature (342)		Fold change by AB1700			Fold change by qPCR				
Gene name	AB probe ID	Sample 1	Sample 2	Sample 3	Sample 1	Sample 2	Sample 3	LD-MDA	Core
shroom	207317	84.7	10.1	3.8					
major facilitator superfamily domain containing 2	170831	25.2	10.1	2.5					
Mst3 and SOK1-related kinase	112198	27.8	3.1	10.0					
RAB23, member RAS oncogene family	122394	15.9	10.0	3.9					
myosin, light polypeptide 9, regulatory	181719	12.4	4.0	9.9					
intercellular adhesion molecule 1 (CD54)	109070	9.9	2.3	20.9	7.3	1.6	40.2	Yes	
nudix (nucleoside diphosphate linked moiety X)-type 11	125359	56.1	7.6	9.9					
membrane metallo-endopeptidase (CALLA, CD10)	197353	117.8	4.7	9.8	7097.8	5.3	40.7	Yes	
solute carrier family 1, member 1	169469	10.6	9.7	2.5					
cyclin-dependent kinase inhibitor 2B (p15, inhibits CDK4)	204006	41.8	6.2	9.6					
spastic paraplegia 3A (autosomal dominant)	190761	10.4	2.1	9.3					
multiple C2 domains, transmembrane 1	136033	4.4	22.8	9.3					
lysyl oxidase-like 2	136648	34.1	3.6	9.2					
synaptotagmin-like 3	171063	9.2	5.4	34.1					
ecotropic viral integration site 1	201951	9.2	3.4	27.3					
transforming growth factor, beta-induced, 68kDa	133906	52.8	9.1	8.0					
spectrin domain with coiled-coils 1	103537	46.5	8.7	9.1					
a disintegrin and metalloproteinase domain 23	177272	9.0	3.7	16.8					
collagen, type VIII, alpha 1	219384	9.2	8.8	2.5					
runt-related transcription factor 3	194489	15.5	8.7	2.2					
fibulin 5	212132	8.5	4.4	19.1					
family with sequence similarity 20, member C	199772	55.0	8.4	2.1					
calmodulin binding transcription activator 1	103913	8.4	2.9	11.7					
tropomyosin 2 (beta)	163441	28.4	8.4	5.1					
leucine-rich repeat-containing G protein-coupled receptor 4	155675	19.7	2.9	8.3					
promethin	123271	8.3	4.2	22.5					
sparc/osteonectin, cwcv and kazal-like domains proteoglycan	125730	8.8	4.3	8.2					
nexilin (F actin binding protein)	139130	8.1	13.3	2.1					
phospholipase A2, group IVA (cytosolic, calcium-dependent)	185568	4.1	18.6	7.9					
prostaglandin-endoperoxide synthase 2	208388	3.3	7.9	8.9					
interleukin 7 receptor	200834	54.3	7.7	2.9	37.0	10.7	9.1	Yes	
cadherin 11, type 2, OB-cadherin (osteoblast)	107867	21.2	7.7	2.1	17.4	12.1	3.6	Yes	
kelch-like 13 (Drosophila)	119847	4.7	8.4	7.7					
zinc finger homeobox 1b	159875	46.6	7.6	5.2					
guanylate binding protein 1, interferon-inducible, 67kDa	145041	7.6	2.6	8.3					
BCL2-associated athanogene 2	113353	17.6	7.5	2.6					
amphoterin induced gene 2	154434	157.0	7.5	3.0					
chromosome 14 open reading frame 37	211103	12.4	5.6	7.4					
ring finger protein 150	213739	47.5	3.2	7.4					
metallothionein 1F (functional)	144569	3.5	7.3	7.6					
transforming growth factor, beta 3	158090	11.0	7.3	6.6					
plasminogen activator, urokinase receptor	208060	14.2	7.2	6.1					
serine (or cysteine) proteinase inhibitor, clade B, member 2	183353	7.5	7.1	3.9					
F-box and leucine-rich repeat protein 16	143089	7.1	2.0	11.6					
UDP-N-acteylglucosamine pyrophosphorylase 1	120981	10.6	7.1	3.1					
chromosome 9 open reading frame 150	194026	7.0	7.0	14.8					

| BEC gene signature (342) | | Fold change by AB1700 | | | Fold change by qPCR | | | | |
Gene name	AB probe ID	Sample 1	Sample 2	Sample 3	Sample 1	Sample 2	Sample 3	LD-MDA	Core
tumor necrosis factor receptor superfamily, member 6b	176555	7.5	3.0	7.0					
asparagine synthetase	219578	13.3	4.0	7.0					
piggyBac transposable element derived 3	218140	4.3	6.9	22.0					
parathyroid hormone-like hormone	143454	8.8	6.8	2.4					
insulin receptor substrate 1	183403	38.2	6.7	3.1					
chromosome 6 open reading frame 115	116829	3.3	6.6	8.1					
prostaglandin F receptor (FP)	103022	207.6	6.6	5.7					
cysteine-rich secretory protein LCCL domain containing 1	113861	15.7	5.1	6.6					
programmed cell death 1 ligand 2	213263	6.4	15.1	3.9					
dual specificity phosphatase 23	140616	12.4	6.4	5.1					
ubiquitin carboxyl-terminal esterase L1	192628	6.4	2.5	13.2					
tumor necrosis factor (ligand) superfamily, member 9	190964	7.0	6.2	2.7					
chromosome 6 open reading frame 188	223249	6.7	6.2	5.4					
ATPase, Na+/K+ transporting, beta 1 polypeptide	199586	6.2	7.6	3.9					
myosin IE	142916	6.2	2.7	10.2					
B-cell CLL/lymphoma 6 (zinc finger protein 51)	151724	7.9	4.9	6.0					
follistatin-like 1	140364	9.4	2.4	6.0					
vitamin D (1,25- dihydroxyvitamin D3) receptor	135316	44.7	5.9	2.5					
sushi-repeat-containing protein, X-linked 2	140054	5.9	3.2	41.8					
chondroitin sulfate synthase 3	223255	7.7	3.2	5.9					
SH3 domain containing ring finger 2	131603	6.6	5.9	2.8					
junctional adhesion molecule 3	100510	5.9	3.6	14.7	2.7	2.8	15.6	Yes	Yes
RGM domain family, member B	223528	12.8	2.7	5.9					
discoidin, CUB and LCCL domain containing 2	114133	6.8	4.5	5.9					
metallothionein 1B (functional)	174119	4.0	8.3	5.8					
proteoglycan 1, secretory granule	133333	5.8	5.4	8.9					
GATA binding protein 6	186512	11.2	5.8	4.9					
synaptogyrin 1	223759	10.2	2.8	5.7					
elongation of very long chain fatty acids-like 4	199358	10.8	5.5	5.6					
interleukin 32	143239	5.0	5.6	35.0					
N-acetyltransferase 2 (arylamine N-acetyltransferase)	105812	5.6	4.6	5.8					
procollagen-proline, 2-oxoglutarate 4-dioxygenase	182482	6.6	2.7	5.5					
metallothionein 1X	226343	4.1	8.2	5.5					
nuclear transport factor 2	212373	4.4	7.7	5.5					
palladin, cytoskeletal associated protein	130541	11.6	2.2	5.4					
chemokine (C-X-C motif) ligand 1	149192	5.4	4.9	5.9					
metallothionein 2A (functional)	204773	4.0	8.5	5.4					
angiotensin II receptor, type 1	105197	39.6	5.3	3.2					
regulator of G-protein signalling 5	192935	4.3	9.0	5.3					
regulator of G-protein signalling 10	128800	10.5	5.2	4.9					
ankyrin repeat domain 42	161072	9.8	2.6	5.2					
Rho GDP dissociation inhibitor (GDI) beta	143589	2.3	5.2	5.5					
regulator of G-protein signalling 20	138203	5.2	5.5	3.0					
myeloid/lymphoid or mixed-lineage leukemia	151049	5.2	2.2	6.3					
dihydropyrimidine dehydrogenase	112355	3.7	5.4	5.1					
bone morphogenetic protein 8b (osteogenic protein 2)	112045	5.3	3.1	5.1					
collagen, type VI, alpha 1	215580	63.7	5.0	4.0	39.4	7.5	14.3	Yes	

159

BEC gene signature (342)		Fold change by AB1700			Fold change by qPCR				
Gene name	AB probe ID	Sample 1	Sample 2	Sample 3	Sample 1	Sample 2	Sample 3	LD-MDA	Core
pleckstrin homology-like domain, family A, member 2	185855	11.7	5.0	4.1					
potassium large conductance calcium-activated channel (Mb1)	213246	5.0	5.2	3.4					
pregnancy specific beta-1-glycoprotein 7	139074	2.8	5.1	4.8					
lymphocyte antigen 6 complex, locus K	100594	17.2	3.6	4.8					
DAZ interacting protein 1	115295	8.8	4.8	2.6					
metallothionein IV	223241	2.6	4.8	5.1					
basic helix-loop-helix domain containing, class B, 2	197538	8.9	3.2	4.8					
matrix metalloproteinase 2 (gelatinase A)	146058	4.7	2.1	17.4					
collagen, type XXVII, alpha 1	224496	6.8	3.1	4.7					
solute carrier family 7, member 14	186645	4.6	6.7	3.9					
SMAD specific E3 ubiquitin protein ligase 2	126729	5.0	4.6	2.8					
metallothionein 1E (functional)	223856	3.1	6.6	4.6					
ADP-ribosylation factor 7	210546	5.4	4.5	3.2					
ATPase, Class I, type 8B, member 1	106683	4.5	2.3	6.7					
interferon induced transmembrane protein 5	163015	2.9	4.7	4.5					
chromosome X open reading frame 53	150469	9.7	2.2	4.5					
pregnancy specific beta-1-glycoprotein 5	101520	4.4	9.2	2.7					
solute carrier family 19 (thiamine transporter), member 2	119822	13.3	3.0	4.4					
ATP-binding cassette, sub-family B (MDR/TAP), member 1	182279	4.4	2.4	13.7					
tumor necrosis factor receptor superfamily, member 12A	137897	13.1	4.3	3.4					
Notch homolog 2 (Drosophila) N-terminal like	128130	4.3	2.1	6.6					
low density lipoprotein-related protein 12	114806	10.0	2.6	4.3					
retinoic acid receptor, beta	109692	19.8	4.3	3.3					
leucine rich repeat containing 16	141737	7.8	4.3	3.7					
ankyrin repeat and SOCS box-containing 9	109802	2.8	4.3	14.8					
integrin, beta 3 (platelet glycoprotein IIIa, antigen CD61)	192782	5.1	4.0	4.2	3.1	2.8	6.1	Yes	
serine (or cysteine) proteinase inhibitor, clade B member 8	226878	11.7	4.2	2.5					
cytoskeleton-associated protein 4	134467	4.2	2.6	4.5					
natriuretic peptide precursor C	146370	21.3	4.2	4.1					
tripartite motif-containing 61	229268	5.6	4.2	2.8					
quinolinate phosphoribosyltransferase	161752	46.4	4.2	2.4					
G protein-coupled receptor 8	169779	2.2	4.2	6.7					
immunoglobulin superfamily, member 4B	149440	13.6	2.7	4.1					
caldesmon 1	185731	4.7	3.3	4.1					
activated leukocyte cell adhesion molecule	115975	6.5	4.1	2.4					
PFTAIRE protein kinase 1	129209	3.3	4.1	4.4					
TBC1 domain family, member 2	205982	6.9	4.1	2.6					
selectin P	114371	4.0	3.7	14.3					
guanylate binding protein 3	221503	5.0	2.5	4.0					
secreted protein, acidic, cysteine-rich (osteonectin)	123437	4.0	2.4	9.2					
cysteine and glycine-rich protein 1	203065	5.4	2.4	4.0					
leukotriene B4 12-hydroxydehydrogenase	210882	4.0	2.7	5.1					
microtubule-associated protein 1A	130759	32.7	3.9	2.9					
carboxypeptidase A3 (mast cell)	100989	3.9	4.3	2.3					
autism susceptibility candidate 2	156350	3.9	2.6	4.3					
laminin, gamma 2	201627	3.9	5.8	3.4					

BEC gene signature (342)		Fold change by AB1700			Fold change by qPCR				
Gene name	AB probe ID	Sample 1	Sample 2	Sample 3	Sample 1	Sample 2	Sample 3	LD-MDA	Core
family with sequence similarity 91, member A1	103214	2.6	4.9	3.9					
BIA2	216429	3.8	8.8	3.2					
zinc finger protein 568	190182	4.1	3.2	3.8					
dual-specificity tyrosine-(Y)-phosphorylation kinase 2	130435	7.1	2.3	3.8					
pleckstrin homology-like domain, family B, member 1	120125	3.8	2.4	3.9					
metallothionein 1J	227956	3.6	11.6	3.7					
2,3-bisphosphoglycerate mutase	178503	5.8	3.6	3.7					
regulator of G-protein signalling 3	221266	3.7	2.0	25.5					
armadillo repeat containing 9	141649	3.7	2.6	4.6					
echinoderm microtubule associated protein like 1	119690	2.6	3.7	5.2					
chromosome 6 open reading frame 168	177450	3.7	3.0	7.8					
S100 calcium binding protein A3	199821	2.7	4.8	3.7					
adenylate cyclase 7	184103	7.4	2.0	3.7					
PDZ and LIM domain 7 (enigma)	121548	5.4	2.5	3.6					
tropomyosin 1 (alpha)	225735	7.0	3.6	2.8					
interleukin 4 receptor	214374	3.6	2.4	17.8					
leukocyte receptor cluster (LRC) member 4	212382	3.6	2.0	6.4					
plasminogen activator, tissue	152725	22.2	3.6	3.6					
piggyBac transposable element derived 5	133539	5.0	2.4	3.6					
exostoses (multiple) 1	190050	5.4	3.6	2.2					
ankyrin repeat domain 1 (cardiac muscle)	209661	3.6	6.1	2.7					
pregnancy specific beta-1-glycoprotein 9	130276	15.0	2.4	3.6					
UL16 binding protein 2	221382	5.9	3.5	3.0					
S100 calcium binding protein A11 (calgizzarin)	145550	3.5	2.7	3.7					
glypican 2 (cerebroglycan)	184349	3.5	3.1	14.9					
protein kinase, cAMP-dependent, catalytic, beta	198878	2.2	3.5	4.9					
Rho GTPase activating protein 24	111787	3.5	2.6	6.1					
testis expressed gene 9	102862	11.4	3.1	3.5					
proline-serine-threonine phosphatase interacting protein 2	141843	3.5	3.5	3.6					
integrin, alpha V	117958	3.5	2.6	6.1	2.0	2.6	5.0	Yes	
fibronectin 1	136386	21.2	3.5	2.5					
SPOC domain containing 1	162279	4.9	3.5	3.5					
protein tyrosine phosphatase, receptor type, G	171586	3.5	2.6	3.6					
fibronectin type III and ankyrin repeat domains 1	173923	3.5	2.5	5.6					
regulating synaptic membrane exocytosis 2	216707	5.2	3.4	2.8					
C2 and WW domain containing E3 ubiquitin protein ligase 2	103552	3.2	3.4	3.7					
La ribonucleoprotein domain family, member 6	150810	8.2	2.4	3.4					
ribonuclease, RNase A family, 1 (pancreatic)	139103	3.4	3.3	197.0					
opioid growth factor receptor-like 1	117428	3.4	2.8	3.6					
adrenergic, beta, receptor kinase 2	213717	4.0	2.2	3.4					
histone 1, H2bk	190073	3.3	2.5	3.7					
meningioma (disrupted in balanced translocation) 1	203105	2.9	3.4	3.3					
poliovirus receptor	149750	6.4	3.3	2.2					
sine oculis homeobox homolog 1 (Drosophila)	113710	5.1	3.3	2.6					
chemokine (C-X-C motif) ligand 6	192528	22.7	3.3	2.1					
cyclin-dependent kinase inhibitor 2A	127523	8.6	3.3	2.5					
homeodomain interacting protein kinase 2	233986	3.7	2.1	3.3					

161

BEC gene signature (342)		Fold change by AB1700			Fold change by qPCR				
Gene name	AB probe ID	Sample 1	Sample 2	Sample 3	Sample 1	Sample 2	Sample 3	LD-MDA	Core
collagen, type V, alpha 3	181976	3.3	2.1	7.8					
Notch homolog 2 (Drosophila)	142906	10.7	2.8	3.3					
ectodermal-neural cortex (with BTB-like domain)	172733	7.5	3.3	3.0					
cyclin-dependent kinase 6	235779	5.6	2.5	3.3					
enabled homolog (Drosophila)	219949	3.1	3.3	5.6					
retinoic acid early transcript 1G	177046	5.3	3.2	3.2					
tubulin, beta 2	194068	3.9	3.2	2.4					
spastic ataxia of Charlevoix-Saguenay (sacsin)	211211	4.8	3.2	2.9					
colony stimulating factor 2 (granulocyte-macrophage)	155234	3.2	2.4	8.1					
phosphatidylinositol transfer protein, membrane-associated 1	128232	3.5	2.3	3.2					
solute carrier family 7, member 11	209308	3.2	4.0	2.9					
ventricular zone expressed PH domain homolog 1	178585	3.1	2.9	6.2					
S100 calcium binding protein A11 pseudogene	187317	3.1	2.7	6.2					
homeo box B2	167151	4.8	3.1	3.1					
glucan (1,4-alpha-), branching enzyme 1	234875	2.3	3.6	3.1					
discoidin, CUB and LCCL domain containing 1	211479	5.5	3.0	2.5					
ras homolog gene family, member Q	142100	3.6	2.9	3.0					
activating transcription factor 3	185687	3.3	2.4	3.0					
zinc finger protein 528	121921	2.2	3.0	3.6					
G protein-coupled receptor 126	134617	3.0	3.1	2.3					
AIF-like mitochondrion-associated inducer of death	129590	3.0	2.0	3.9					
collagen triple helix repeat containing 1	191084	3.0	2.2	11.0					
protein tyrosine phosphatase-like A domain containing 2	205747	2.1	3.0	5.4					
Rho-related BTB domain containing 3	103105	2.9	2.8	5.1					
IBR domain containing 2	234266	4.3	2.9	2.9					
ATPase family homolog up-regulated in senescence cells	222770	2.9	3.1	2.1					
protocadherin 10	116092	12.1	2.8	2.7					
protein kinase, AMP-activated, beta 2 non-catalytic subunit	180648	2.4	2.8	7.5					
apolipoprotein B mRNA editing enzyme	132926	2.1	2.8	3.1					
ecotropic viral integration site 5	124405	2.8	2.8	3.3					
glycosyltransferase-like domain containing 1	215619	2.8	2.0	4.3					
pregnancy specific beta-1-glycoprotein 1	211648	2.6	5.5	2.8					
diacylglycerol kinase, gamma 90kDa	211883	2.0	2.8	6.0					
protocadherin beta 17 pseudogene	218372	3.4	2.3	2.7					
paired-like homeodomain transcription factor 2	167147	16.0	2.7	2.7					
chromosome 6 open reading frame 128	223051	2.3	2.7	11.4					
phosphatidylserine receptor	109646	2.5	2.7	4.6					
pre-B-cell leukemia transcription factor 3	168129	3.2	2.7	2.6					
protocadherin beta 5	169402	2.4	2.7	12.5					
mitogen-activated protein kinase kinase kinase 13	143560	2.6	2.6	6.2					
a disintegrin and metalloproteinase domain 9	183965	3.1	2.3	2.6					
IKK interacting protein	223807	2.9	2.6	2.3					
cathepsin C	190056	2.6	2.6	3.8					
protein kinase C, epsilon	214787	2.6	2.6	7.2					
chemokine (C-C motif) receptor-like 2	112106	2.5	2.6	11.6					
membrane protein, palmitoylated 2 (MAGUK p55 subfamily member 2)	152735	10.5	2.6	2.5					

| BEC gene signature (342) | | Fold change by AB1700 | | | Fold change by qPCR | | | | |
Gene name	AB probe ID	Sample 1	Sample 2	Sample 3	Sample 1	Sample 2	Sample 3	LD-MDA	Core
phosphoprotein enriched in astrocytes 15	220353	3.6	2.1	2.6					
transcription elongation factor A (SII)-like 5	157065	2.5	2.6	6.5					
transient receptor potential cation channel, subfamily V 2	207656	2.5	2.1	7.4					
phosphoglucomutase 3	205937	2.7	2.5	2.1					
chaperonin containing TCP1, subunit 6B (zeta 2)	130061	2.5	2.1	7.6					
trophoblast-derived noncoding RNA	232041	2.5	2.4	3.3					
signal-induced proliferation-associated 1 like 2	169848	2.3	2.5	4.6					
muscle RAS oncogene homolog	101584	3.1	2.4	2.5					
ecotropic viral integration site 2B	139158	8.8	2.3	2.4					
insulin-like growth factor binding protein 6	150353	9.5	2.4	2.0					
serine-arginine repressor protein (35 kDa)	106827	2.4	2.0	2.5					
coagulation factor II (thrombin) receptor	158262	2.4	2.2	6.4					
fibrillin 1 (Marfan syndrome)	147111	10.0	2.4	2.1					
CD109 antigen (Gov platelet alloantigens)	157795	2.4	2.4	3.9					
four and a half LIM domains 2	202137	4.1	2.4	2.4					
TRAF family member-associated NFKB activator	109879	2.3	2.0	4.9					
anthrax toxin receptor 2	191543	2.3	2.7	2.1					
membrane protein, palmitoylated 4	150693	2.3	2.2	3.8					
PDZ and LIM domain 5	103100	2.3	3.0	2.3					
fem-1 homolog c (C.elegans)	127238	4.9	2.3	2.3					
nicotinamide N-methyltransferase	125400	2.6	2.3	2.1					
protein tyrosine phosphatase domain containing 1	128960	2.3	2.1	8.2					
golgi membrane protein SB140	151061	2.3	2.2	2.5					
congenital dyserythropoietic anemia, type I	114892	2.2	2.3	2.3					
DnaJ (Hsp40) homolog, subfamily B, member 5	152148	2.1	2.3	3.8					
solute carrier family 38, member 6	142416	2.3	2.3	2.3					
C1q domain containing 1	106320	2.2	2.3	2.4					
palmdelphin	114289	2.1	2.3	2.8					
related RAS viral (r-ras) oncogene homolog	180365	2.1	2.3	6.4					
SNF1-like kinase	171526	19.1	2.2	2.2					
solute carrier family 35, member D1	135060	2.1	2.6	2.1					
solute carrier family 16, member 3	129361	6.6	2.1	2.1					
retinoic acid early transcript 1K pseudogene	190201	2.2	2.0	2.1					

Appendix Figure 1 Prediction Relevance Ranking analysis. A novel method denoted "Prediction Relevance Ranking" analysis employs multiple linear regression analysis and it enumerates all possible models and investigates the whole model space to produce a ranking of variables (genes) based on their predictive power. The prediction relevance for lymphatic vessel area (LVA; blue bars) revealed INHBA, DPP4, IL7R, TEK and ADAMTS1 as top 5 most frequent variables in a set of all possible regression models. The prediction relevance for blood vessel area (BVA; red bars) revealed FLT1, CSPG2, ITGB3, FGF12 and IL8 as top 5 most frequent variables in a set of all possible significant regression models.
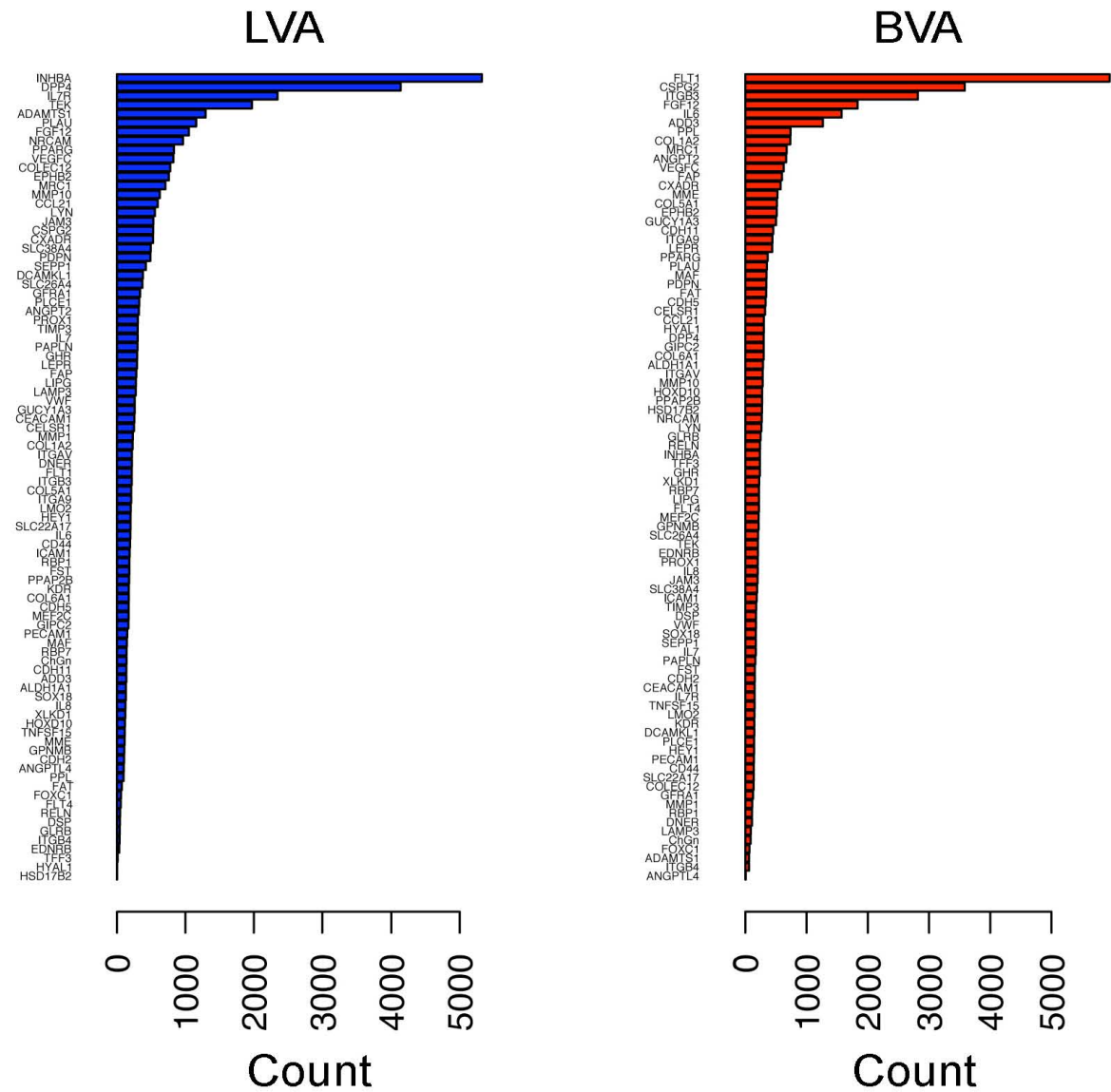
Appendix Table 2

Top 400 differentially modulated genes by VEGF-A in LEC using Multivariate Bayesian ranking analysis

MB Ranking	LEC stimulated with VEGF-A Name	Probe ID	Log2 Ratio 1 hr	4 hr.	8 hr.	24 hr.
1	early growth response 3	124744	7.306	0.238	0.308	0.463
2	early growth response 2 (Krox-20 homolog, Drosophila)	101929	6.522	-0.414	-0.206	-0.285
3	early growth response 1	147353	4.671	0.879	1.207	0.623
4	coagulation factor III (thromboplastin, tissue factor)	204787	5.860	3.093	1.424	1.559
5	N/A	209213	2.357	-1.128	-1.041	-1.699
6	activating transcription factor 3	185687	4.483	0.985	0.728	0.931
7	nuclear receptor subfamily 4, group A, member 2	123450	5.775	-0.154	0.051	0.558
8	nuclear receptor subfamily 4, group A, member 1	216600	6.072	1.846	0.123	0.653
9	v-fos FBJ murine osteosarcoma viral oncogene homolog	205128	4.676	1.846	1.819	1.243
10	N/A	183303	2.878	1.011	0.477	0.115
11	Kruppel-like factor 10	104402	2.859	0.929	0.491	-0.001
12	Kruppel-like factor 10	125028	2.834	0.845	0.630	0.193
13	coagulation factor III (thromboplastin, tissue factor)	146916	5.360	2.604	1.229	1.460
14	N/A	122171	2.095	0.146	-0.173	-0.744
15	jumonji domain containing 3	124424	2.168	-0.445	-0.869	-0.484
16	cytochrome P450, family 1, subfamily A, polypeptide 1	135086	-0.049	-1.869	-2.830	-2.051
17	prostaglandin-endoperoxide synthase 2 (prostaglandin G/H synthase and cyclooxygenase)	208388	4.575	-0.148	0.357	-0.137
18	family with sequence similarity 13, member C1	205995	0.319	-1.749	-1.979	-0.823
19	dual specificity phosphatase 5	121612	3.317	2.588	1.487	0.938
20	N/A	178581	2.694	1.288	0.516	0.599
21	zinc finger protein 36, C3H type, homolog (mouse)	179827	3.494	1.279	1.444	1.151
22	guanylate cyclase 1, soluble, alpha 3	170165	0.680	0.940	-1.154	-1.715
23	SHC (Src homology 2 domain containing) family, member 4	183641	0.344	2.615	1.045	0.400
24	chromosome 11 open reading frame 17|NUAK family, SNF1-like kinase, 2	157942	2.637	0.647	0.354	0.482
25	hairy and enhancer of split 1, (Drosophila)	176983	1.842	-0.335	-0.006	-0.228
26	kinesin family member 20A	118830	-1.084	-1.623	-1.397	0.728
27	solute carrier family 2 (facilitated glucose transporter), member 12	175805	-0.120	-1.846	-2.481	-1.424
28	Down syndrome critical region gene 1	124953	4.418	1.431	0.768	0.589
29	hairy/enhancer-of-split related with YRPW motif 1	121998	1.373	-1.139	-0.539	-1.108
30	kinesin family member 4A	115354	-0.777	-1.145	-0.719	1.225
31	ribosomal protein S6 kinase, 90kDa, polypeptide 5	152363	0.643	-0.738	-2.405	-0.106
32	carbonic anhydrase IV	196942	0.055	-0.351	-1.447	-3.247
33	topoisomerase (DNA) II alpha 170kDa	135302	-0.165	-0.395	-0.739	1.851
34	cell division cycle associated 1	147806	-0.539	-0.869	-0.625	1.457
35	SMAD, mothers against DPP homolog 7 (Drosophila)	206947	0.715	-1.260	-1.112	-0.860
36	centromere protein A, 17kDa	128411	-0.901	-0.730	-0.705	1.393
37	discs, large homolog 7 (Drosophila)	194498	-0.342	-0.630	-0.911	1.458
38	stanniocalcin 1	119453	4.020	2.647	-0.120	0.651
39	dual specificity phosphatase 1	182417	2.918	2.217	1.441	1.207
40	N/A	138125	1.170	1.633	0.265	-0.877

MB Ranking	LEC stimulated with VEGF-A		Log2 Ratio			
	Name	Probe ID	1 hr	4 hr.	8 hr.	24 hr.
41	centromere protein F, 350/400ka (mitosin)	183726	0.073	-0.272	-0.571	1.796
42	DEP domain containing 1B	206865	-0.544	-0.975	-1.279	1.065
43	aurora kinase B	203163	-0.610	-0.709	-0.636	1.537
44	protein regulator of cytokinesis 1	180626	-0.726	-0.751	-0.563	1.512
45	centrosomal protein 55kDa	198728	-0.492	-0.734	-0.553	1.480
46	solute carrier family 4, sodium bicarbonate cotransporter, member 7	163733	1.259	2.638	1.880	1.292
47	nuclear factor, interleukin 3 regulated	203863	1.709	0.030	0.108	-0.221
48	N/A	190308	-0.252	-0.685	-0.222	1.737
49	TTK protein kinase	107112	-0.521	-0.850	-0.278	1.577
50	NIMA (never in mitosis gene a)-related kinase 2	115004	-0.918	-1.137	-1.067	0.987
51	kinesin family member 2C	212531	-0.376	-0.587	-0.535	1.644
52	N/A	111700	-0.199	-0.568	0.036	1.829
53	apolipoprotein B mRNA editing enzyme, catalytic polypeptide-like 3B	138620	-0.916	-1.347	-0.883	1.068
54	baculoviral IAP repeat-containing 3	154663	2.395	-0.108	-0.044	0.036
55	SNF1-like kinase	171526	2.704	0.921	0.369	0.334
56	nucleolar and spindle associated protein 1	128435	-0.424	-0.631	-0.721	1.657
57	FBJ murine osteosarcoma viral oncogene homolog B	105390	5.350	0.229	0.031	-0.222
58	transforming, acidic coiled-coil containing protein 3	165983	-0.825	-1.252	-0.506	0.944
59	chemokine orphan receptor 1	139192	1.941	1.132	0.255	-0.142
60	mitogen-activated protein kinase kinase kinase 8	106192	2.404	0.220	-0.228	0.575
61	trophinin associated protein (tastin)	137875	-1.182	-1.208	-0.882	0.800
62	PDZ binding kinase	169723	-1.125	-1.005	-0.883	1.315
63	cyclin-dependent kinase inhibitor 2C (p18, inhibits CDK4)	112997	-0.573	-1.672	-1.590	0.539
64	N/A	125681	0.980	1.524	0.197	-0.832
65	pyruvate dehydrogenase kinase, isozyme 4	101060	-0.369	-1.822	-2.025	-1.423
66	asp (abnormal spindle)-like, microcephaly associated (Drosophila)	181685	0.162	-0.066	-0.278	2.022
67	N/A	133024	-0.642	-2.246	-2.748	-3.315
68	cyclin A2	110863	-0.567	-0.681	-0.593	1.370
69	sprouty homolog 2 (Drosophila)	207231	1.994	0.659	0.868	0.388
70	baculoviral IAP repeat-containing 5 (survivin)	104062	-0.680	-0.912	-0.807	1.171
71	chemokine (C-X-C motif) receptor 4	191821	-0.397	0.934	1.974	2.182
72	fms-related tyrosine kinase 1	219494	0.396	2.332	1.457	1.320
73	proline rich 11	123490	-0.514	-0.909	-0.813	1.123
74	polo-like kinase 1 (Drosophila)	197341	-0.897	-0.863	-0.985	0.921
75	N/A	198371	-0.997	-1.140	-1.770	0.442
76	spindle pole body component 25 homolog (S. cerevisiae)	130624	-0.592	-1.014	-0.793	1.178
77	SHC SH2-domain binding protein 1	106848	-0.572	-0.523	0.134	1.726
78	chromosome 18 open reading frame 24	205780	-0.714	-0.946	-0.345	1.225
79	prickle-like 2 (Drosophila)	134212	0.046	-1.868	-1.507	-0.900
80	anillin, actin binding protein (scraps homolog, Drosophila)	169499	-0.562	-0.488	-0.450	1.631
81	v-maf musculoaponeurotic fibrosarcoma oncogene homolog B (avian)	226336	1.215	-0.989	-0.899	-0.973
82	N/A	200967	2.667	0.366	-0.471	-0.649
83	MAX dimerization protein 3	131913	-0.523	-1.359	-1.663	0.399
84	high mobility group AT-hook 2	105728	-0.182	2.062	1.305	0.270
85	N/A	715431	0.288	1.100	1.165	-0.858
86	family with sequence similarity 64, member A	201158	-0.802	-0.532	-1.105	0.913
87	heparin-binding EGF-like growth factor	139874	2.354	1.481	0.874	1.046

MB Ranking	LEC stimulated with VEGF-A Name	Probe ID	Log2 Ratio 1 hr	4 hr.	8 hr.	24 hr.
88	barren homolog 1 (Drosophila)	177741	-0.581	-0.687	-0.161	1.426
89	phosphoinositide-3-kinase, regulatory subunit 1 (p85 alpha)	180157	1.687	0.505	0.063	-0.259
90	N/A	170545	0.957	1.485	0.132	-0.930
91	kinetochore associated 2	107406	-0.810	-1.111	-0.986	1.101
92	v-myb myeloblastosis viral oncogene homolog (avian)-like 1	207803	-0.522	-1.318	0.036	0.737
93	BUB1 budding uninhibited by benzimidazoles 1 homolog (yeast)	157194	-1.122	-0.989	-0.638	0.826
94	kinesin family member 23	160577	-0.457	-0.538	-0.242	1.513
95	phosphoglycerate dehydrogenase	210225	-0.403	-0.621	-0.224	1.452
96	hyaluronan-mediated motility receptor (RHAMM)	216917	-0.450	-0.559	-0.537	1.550
97	N/A	215658	1.332	2.110	1.582	1.585
98	thymidine kinase 1, soluble	105119	-0.759	-0.809	-0.475	1.377
99	kinesin family member 18A	177455	-0.158	-0.801	-0.649	1.446
100	prickle-like 1 (Drosophila)	143140	1.064	-0.369	-0.876	-0.308
101	chromosome 15 open reading frame 42	196613	-0.844	-0.068	0.454	1.578
102	Opa interacting protein 5	211010	-0.539	-0.800	-0.980	1.090
103	B-cell CLL/lymphoma 6 (zinc finger protein 51)	151724	2.292	0.323	0.285	0.708
104	cyclin B2	169571	-0.727	-1.086	-1.148	0.980
105	N/A	179136	1.633	-0.311	-0.205	0.199
106	adrenergic, beta-2-, receptor, surface	127856	1.102	0.315	-0.929	-0.437
107	glyoxalase domain containing 1	137815	-0.591	1.175	0.669	-0.469
108	N/A	159898	-0.868	-0.645	-0.773	1.058
109	endothelial cell-specific molecule 1	174810	0.542	2.492	2.233	3.508
110	kinesin family member 11	199107	-0.325	-0.596	-0.446	1.497
111	phosphoserine aminotransferase 1	151268	-0.433	0.255	1.460	1.317
112	kinesin family member C1	141343	-0.547	-0.719	-0.524	1.179
113	leukemia inhibitory factor (cholinergic differentiation factor)	117096	2.348	0.370	0.269	0.026
114	ubiquitin-conjugating enzyme E2C	143651	-0.417	-0.478	-0.491	1.299
115	baculoviral IAP repeat-containing 5 (survivin)	227666	-0.696	-0.628	-0.772	1.018
116	N/A	134295	0.213	-1.245	-1.175	-0.003
117	basic helix-loop-helix domain containing, class B, 2	197538	3.844	1.508	1.612	1.404
118	MLF1 interacting protein	147135	-0.525	-0.699	0.094	1.405
119	solute carrier family 38, member 4	217080	0.455	-0.846	-1.692	-0.761
120	proline/serine-rich coiled-coil 1	181161	-0.794	-1.379	-1.233	0.532
121	Rac GTPase activating protein 1	135746	-0.553	-0.694	-0.499	1.086
122	inositol 1,4,5-trisphosphate 3-kinase A	216718	0.277	1.824	1.149	-0.143
123	cyclin-dependent kinase inhibitor 3 (CDK2-associated dual specificity phosphatase)	191305	-0.512	-0.579	-0.702	1.212
124	MAP6 domain containing 1	180319	-0.055	1.554	0.545	0.316
125	transmembrane protein 100	216519	-0.288	-1.704	-1.210	-1.785
126	asp (abnormal spindle)-like, microcephaly associated (Drosophila)	205649	0.013	-0.681	-0.595	1.570
127	tumor necrosis factor, alpha-induced protein 8	128843	1.698	-0.128	-0.095	0.149
128	N/A	217029	2.200	0.977	0.786	0.738
129	N/A	128495	-0.589	-0.539	-0.329	1.395
130	amphiregulin (schwannoma-derived growth factor)	123143	1.383	1.936	0.394	0.351
131	serine/threonine kinase 6 pseudogene	683679	-0.650	-0.693	-0.475	1.028
132	cadherin 10, type 2 (T2-cadherin)	198370	0.309	-1.144	-1.206	-0.838
133	cell division cycle 2, G1 to S and G2 to M	123400	-0.457	-0.656	-0.421	1.440
134	antigen identified by monoclonal antibody Ki-67	137656	-0.521	-0.679	-0.476	1.495

167

MB Ranking	LEC stimulated with VEGF-A Name	Probe ID	Log2 Ratio 1 hr	4 hr.	8 hr.	24 hr.
135	high-mobility group box 2	216889	-0.690	-1.169	-1.097	0.652
136	protein tyrosine phosphatase, receptor type, E	541414	2.225	0.800	1.020	0.127
137	ribonucleotide reductase M2 polypeptide	134286	-0.576	-0.569	-0.363	1.698
138	6-phosphofructo-2-kinase/fructose-2,6-biphosphatase 3	198714	1.992	1.866	1.293	0.737
139	ephrin-B2	162498	0.755	-0.516	-1.167	-0.835
140	myeloid cell leukemia sequence 1 (BCL2-related)	147139	1.818	0.453	0.337	0.105
141	v-rel reticuloendotheliosis viral oncogene homolog (avian)	109539	0.959	-0.687	-0.419	0.064
142	mal, T-cell differentiation protein-like	201519	-0.313	1.677	0.776	-0.142
143	N/A	163671	-0.172	1.423	1.141	0.763
144	Rho GTPase activating protein 11A	117485	-0.073	0.011	0.318	1.696
145	pituitary tumor-transforming 3	147452	-0.575	-0.708	-0.912	0.854
146	polymerase (DNA directed), theta	112081	0.167	-0.429	0.290	1.452
147	midnolin	159555	2.462	0.864	0.542	0.391
148	potassium channel, subfamily K, member 6	206064	-0.536	1.242	0.908	0.487
149	chromosome 18 open reading frame 1	113714	0.132	-1.139	-1.452	-0.862
150	interleukin 1, beta	130322	2.151	0.852	0.563	0.950
151	cancer susceptibility candidate 5	105014	-0.450	-0.238	-0.317	1.485
152	phosphoserine aminotransferase 1	221068	-0.516	0.066	1.354	1.094
153	tumor necrosis factor, alpha-induced protein 3	168741	2.476	0.210	-0.071	0.099
154	ATPase family, AAA domain containing 3B	224173	-0.119	1.243	1.364	0.606
155	centromere protein A, 17kDa	106198	-0.873	-1.110	-0.739	1.096
156	sperm associated antigen 5	185888	-0.713	-0.663	-0.760	0.878
157	nucleoside phosphorylase	147282	1.265	1.971	1.564	1.491
158	pituitary tumor-transforming 1	204044	-0.603	-0.636	-0.787	0.935
159	gamma-aminobutyric acid (GABA) A receptor, epsilon	130287	1.430	0.864	0.351	-0.280
160	ADAM metallopeptidase with thrombospondin type 1 motif, 9	160876	2.459	0.884	0.422	-0.495
161	cyclin B1	216120	-0.852	-0.688	-0.560	0.812
162	nuclear receptor subfamily 1, group D, member 2	227856	0.585	-0.375	-1.385	-0.080
163	N/A	138397	-0.489	-0.303	0.355	1.295
164	MAD2 mitotic arrest deficient-like 1 (yeast)	138685	-0.392	-0.272	0.399	1.355
165	N/A	192975	-0.959	-1.012	-0.260	1.218
166	TPX2, microtubule-associated, homolog (Xenopus laevis)	189094	-0.848	-0.906	-0.409	1.022
167	DEP domain containing 1	205423	-0.278	-0.660	-0.356	1.362
168	v-maf musculoaponeurotic fibrosarcoma oncogene homolog (avian)	186589	0.095	-1.340	-1.613	-1.197
169	CDC45 cell division cycle 45-like (S. cerevisiae)	208272	-0.238	-0.308	0.532	1.740
170	CDC20 cell division cycle 20 homolog (S. cerevisiae)	161150	-0.771	-0.855	-0.725	0.734
171	sphingosine kinase 1	199219	-0.146	1.291	0.300	-0.128
172	regulator of G-protein signalling 16	173025	1.972	0.545	0.667	0.140
173	serine/threonine kinase 6	157917	-0.561	-0.644	-0.506	1.008
174	spermatogenesis associated 12	229375	-0.442	-1.474	-1.603	-1.650
175	serine/threonine kinase 6 pseudogene	540912	-1.043	-1.241	-1.045	0.184
176	growth arrest-specific 1	142146	-0.963	-1.757	-0.821	-0.315
177	Rho family GTPase 3	129829	1.101	-0.424	-0.641	-0.702
178	CDC20 cell division cycle 20 homolog (S. cerevisiae)	106187	-0.838	-0.769	-0.602	0.830
179	homocysteine-inducible, endoplasmic reticulum stress-inducible, ubiquitin-like domain member 1	183516	1.591	0.216	0.259	-0.006
180	lymphotoxin beta (TNF superfamily, member 3)	180671	-0.783	-1.163	-1.890	-1.534
181	N/A	164460	0.167	1.337	1.564	0.056

MB Ranking	LEC stimulated with VEGF-A	Probe ID	Log2 Ratio			
	Name		1 hr	4 hr.	8 hr.	24 hr.
182	serum deprivation response (phosphatidylserine binding protein)	156433	0.391	-0.872	-1.088	-1.016
183	bone morphogenetic protein 2	193689	2.015	1.237	1.382	0.480
184	cell division cycle associated 8	130297	-0.859	-0.746	-0.550	0.756
185	cingulin-like 1	106427	-0.077	-1.020	-1.827	-1.774
186	shugoshin-like 1 (S. pombe)	227151	-0.686	-1.152	-0.710	1.185
187	cell division cycle associated 5	135130	-0.348	-0.454	0.215	1.462
188	peptidylglycine alpha-amidating monooxygenase COOH-terminal interactor	149253	-0.985	-1.389	-0.689	0.157
189	B-cell CLL/lymphoma 6, member B (zinc finger protein)	178868	1.178	-0.071	0.047	-0.324
190	N/A	106827	-0.202	1.736	0.586	0.540
191	F-box and leucine-rich repeat protein 20	147632	0.447	-0.928	-1.064	-0.145
192	inositol 1,3,4,5,6-pentakisphosphate 2-kinase	168375	1.596	0.550	0.897	0.092
193	chromosome 10 open reading frame 114	541266	-0.028	-1.229	-1.752	-0.667
194	Ras-related associated with diabetes	149158	2.635	0.929	0.074	-0.025
195	transforming growth factor, beta 3	142790	1.346	1.832	0.339	0.043
196	chromosome 8 open reading frame 4	108623	0.139	-2.079	-2.106	-0.871
197	CCAAT/enhancer binding protein (C/EBP), delta	151000	1.621	0.476	-0.319	0.198
198	sorting nexin 22	145714	1.255	1.908	1.373	1.203
199	tumor necrosis factor, alpha-induced protein 8-like 3	151078	1.727	0.555	-0.920	-1.080
200	interferon induced with helicase C domain 1	133193	-0.034	-1.480	-0.953	-0.546
201	centromere protein E, 312kDa	165425	0.168	0.057	0.179	1.811
202	N/A	123427	1.267	-0.031	-0.279	0.190
203	solute carrier family 25 (mitochondrial carrier; phosphate carrier), member 25	183778	1.793	0.711	0.677	0.406
204	transforming growth factor, alpha	180395	0.022	-0.885	-1.195	-1.646
205	N/A	200017	0.710	1.617	1.957	0.841
206	diaphanous homolog 3 (Drosophila)	102085	-0.398	-0.434	-0.284	1.252
207	Fanconi anemia, complementation group D2	151336	-1.439	-1.088	-1.339	0.423
208	potassium intermediate/small conductance calcium-activated channel, subfamily N, member 2	102973	0.653	2.303	1.067	1.972
209	N/A	119241	0.207	-0.234	-0.205	1.343
210	ZW10 interactor	167013	-0.229	-0.277	0.156	1.494
211	p300/CBP-associated factor	183086	-0.084	-0.999	-1.729	-0.234
212	maternal embryonic leucine zipper kinase	156792	-0.332	-0.448	0.158	1.266
213	FXYD domain containing ion transport regulator 3	201258	0.934	-0.065	1.172	1.164
214	H2.0-like homeobox 1 (Drosophila)	197242	2.067	0.912	0.554	1.123
215	fibronectin leucine rich transmembrane protein 2	171313	0.241	-0.902	-0.938	-1.258
216	interferon-induced protein with tetratricopeptide repeats 2	130677	0.567	-1.331	-1.305	-0.478
217	thyroid hormone receptor interactor 13	194658	-0.799	-0.294	0.297	0.950
218	FSH primary response (LRPR1 homolog, rat) 1	187170	-0.385	-0.928	0.516	1.020
219	cAMP responsive element modulator	141393	1.269	0.673	-0.609	-0.221
220	cell division cycle associated 2	166387	-1.104	-0.481	-0.714	0.768
221	calcium/calmodulin-dependent protein kinase kinase 1, alpha	150074	-0.186	1.307	0.544	-0.041
222	kinesin family member 14	121673	0.183	-0.287	-0.060	1.792
223	neuronal PAS domain protein 2	185464	0.376	1.384	1.648	0.615
224	chemokine (C-C motif) ligand 20	133100	1.672	1.012	-0.689	-0.299
225	chromosome 1 open reading frame 21	185996	-0.010	1.436	0.772	0.651
226	histone 1, H4d	112668	-0.466	-0.594	-0.345	1.040
227	N/A	144657	0.117	-0.306	-1.379	-1.229

MB Ranking	LEC stimulated with VEGF-A		Log2 Ratio			
	Name	Probe ID	1 hr	4 hr.	8 hr.	24 hr.
228	cache domain containing 1	214499	0.397	-0.911	-1.186	-0.686
229	breast cancer 2, early onset	119580	0.272	-0.510	0.585	1.431
230	chromosome 10 open reading frame 10	178105	-0.657	0.739	0.395	0.625
231	pituitary tumor-transforming 2	130575	-0.557	-0.649	-0.895	0.680
232	high-mobility group box 2	177404	-0.732	-1.221	-0.830	0.448
233	insulin-like growth factor 1 (somatomedin C)	123381	0.489	-1.035	-1.462	-1.389
234	family with sequence similarity 54, member A	143413	-0.681	-0.255	0.285	0.950
235	N/A	144215	-0.077	1.193	0.589	-0.406
236	programmed cell death 4 (neoplastic transformation inhibitor)	144148	0.322	-0.611	-1.699	-0.838
237	KIAA0101	123361	-0.240	-0.524	-0.621	1.154
238	kelch-like 24 (Drosophila)	188332	0.321	-0.450	-1.241	0.240
239	FOS-like antigen 2	117028	0.859	-0.071	0.035	-0.831
240	cytochrome P450, family 4, subfamily X, polypeptide 1	123084	-0.247	-0.658	-1.494	-1.370
241	leucine-rich repeats and immunoglobulin-like domains 3	137001	1.365	-0.845	-0.465	-0.294
242	M-phase phosphoprotein 1	205220	0.042	-0.159	0.440	1.495
243	galanin	167511	-0.441	1.466	1.819	0.900
244	diaphanous homolog 3 (Drosophila)	108052	-0.330	-0.592	-0.402	1.411
245	interferon stimulated exonuclease gene 20kDa	118954	0.547	1.520	1.411	0.385
246	KIAA0513	104925	1.124	0.721	-0.654	-0.511
247	N/A	187106	0.293	0.193	-0.380	-1.496
248	kelch-like 4 (Drosophila)	114429	0.400	0.670	-0.590	-0.707
249	Kruppel-like factor 2 (lung)	174556	1.730	0.392	-0.742	-0.198
250	KIAA1913	229140	0.793	2.200	0.495	0.402
251	polo-like kinase 4 (Drosophila)	191973	0.125	-0.471	0.113	1.298
252	AXIN1 up-regulated 1	151956	3.185	1.228	0.922	0.440
253	nuclear receptor subfamily 4, group A, member 3	102081	3.668	0.750	0.310	0.424
254	syndecan 2 (heparan sulfate proteoglycan 1, cell surface-associated, fibroglycan)	209676	-0.117	-0.449	-1.174	-1.422
255	N/A	182019	-0.342	-0.695	-1.629	-1.191
256	solute carrier family 45, member 4	222162	1.177	0.694	-0.731	0.094
257	fatty acid binding protein 3, muscle and heart (mammary-derived growth inhibitor)	146250	0.486	1.003	1.446	2.424
258	v-myb myeloblastosis viral oncogene homolog (avian)-like 2	154410	-0.550	-0.827	-0.161	1.115
259	polymerase (RNA) I polypeptide B, 128kDa	219437	-0.624	0.729	0.525	-0.381
260	hyaluronoglucosaminidase 4	189554	0.633	0.386	0.019	1.525
261	myeloid/lymphoid or mixed-lineage leukemia (trithorax homolog, Drosophila); translocated to, 3	129350	0.066	-1.029	-1.394	-0.869
262	glycine dehydrogenase (decarboxylating; glycine decarboxylase, glycine cleavage system protein P)	114924	-1.207	-1.407	-0.895	-0.292
263	matrix metallopeptidase 19	708133	-0.141	-0.806	0.001	-1.341
264	leucine zipper protein 5	212326	-0.573	-0.698	-0.613	0.903
265	chromosome 12 open reading frame 24	214857	-0.302	0.861	1.317	-0.096
266	Bloom syndrome	199557	-0.047	-0.126	0.749	1.403
267	KIAA1370	186024	0.608	-0.625	-0.090	0.764
268	N/A	182347	-0.423	0.158	-1.147	-1.147
269	IQ motif containing GTPase activating protein 3	186522	-0.738	-0.923	-0.386	0.756
270	kinesin family member 15	188149	-0.367	-0.384	-0.180	1.259
271	pseudouridylate synthase 1	202211	-0.154	0.951	1.112	-0.023
272	chromosome 20 open reading frame 42	172479	-0.570	0.872	1.091	2.451
273	zinc finger protein 664	187860	-1.346	-1.122	-1.702	-1.286

MB Ranking	LEC stimulated with VEGF-A Name	Probe ID	Log2 Ratio 1 hr	4 hr.	8 hr.	24 hr.
274	CHK1 checkpoint homolog (S. pombe)	211140	-0.763	-0.908	0.354	0.492
275	N/A	179063	-0.454	-0.790	-0.599	0.933
276	dedicator of cytokinesis 10	107398	-0.444	1.129	0.624	-0.108
277	ADAM metallopeptidase with thrombospondin type 1 motif, 18	220286	1.239	0.343	0.032	-0.425
278	decay accelerating factor for complement (CD55, Cromer blood group system)	167208	0.620	1.662	1.701	1.651
279	l(3)mbt-like (Drosophila)	115601	0.806	-0.827	-0.439	-0.289
280	TAF4b RNA polymerase II, TATA box binding protein (TBP)-associated factor, 105kDa	127808	0.084	1.530	0.599	0.323
281	G protein-coupled receptor 125	236580	-0.923	0.276	-0.750	-0.988
282	ankyrin repeat domain 20B	161943	0.751	1.645	1.807	0.955
283	potassium channel tetramerisation domain containing 12	105004	0.096	-0.968	-2.305	-2.036
284	tissue factor pathway inhibitor 2	144600	0.207	0.965	1.285	1.261
285	phospholipase C, beta 4	100736	0.735	-0.332	-0.858	-0.479
286	acyl-CoA thioesterase 11	164864	0.031	1.338	1.805	1.203
287	WD repeats and SOF1 domain containing	196524	1.784	1.456	1.510	0.861
288	RAD51 homolog (RecA homolog, E. coli) (S. cerevisiae)	158651	-0.464	-0.242	0.527	1.183
289	dual specificity phosphatase 26 (putative)	185108	-0.468	-1.121	-0.786	0.635
290	chromosome 9 open reading frame 76	177183	-0.393	-0.767	0.250	0.730
291	N/A	236648	1.844	0.942	0.857	0.526
292	decay accelerating factor for complement (CD55, Cromer blood group system)	109858	0.598	1.262	1.023	1.600
293	carbohydrate (keratan sulfate Gal-6) sulfotransferase 1	151863	-0.218	-0.775	0.324	1.025
294	chromosome 7 open reading frame 31	172392	-0.280	-1.519	-1.114	-0.515
295	plasminogen activator, urokinase receptor	208060	0.848	2.362	2.244	1.423
296	CDC28 protein kinase regulatory subunit 1B	112634	-0.509	-0.461	-0.451	0.852
297	ubiquitin-conjugating enzyme E2T (putative)	208303	-0.276	-0.282	0.260	1.265
298	superoxide dismutase 2, mitochondrial	149133	0.937	1.328	1.353	1.534
299	shugoshin-like 2 (S. pombe)	215796	0.126	-0.463	0.012	1.131
300	Ras association (RalGDS/AF-6) domain family 8	164634	0.465	0.344	-0.184	-1.082
301	ADP-ribosylation factor-like 5B	182434	1.422	0.386	0.469	0.567
302	BCL6 co-repressor	223980	1.843	0.749	0.575	0.383
303	tumor necrosis factor (ligand) superfamily, member 10	153282	0.060	-1.419	-1.306	-0.475
304	ASF1 anti-silencing function 1 homolog B (S. cerevisiae)	161404	-0.433	-0.748	-0.009	1.021
305	breast cancer 1, early onset	124112	-0.262	-0.711	0.286	1.378
306	N/A	190904	-0.216	-0.566	-0.936	1.136
307	diacylglycerol kinase, delta 130kDa	194946	0.743	1.213	0.623	1.635
308	dihydrofolate reductase	114480	-0.459	-0.480	-0.371	0.896
309	purinergic receptor P2Y, G-protein coupled, 5	189269	0.682	-0.565	-0.704	0.262
310	nucleolar protein 5A (56kDa with KKE/D repeat)	189611	-0.089	1.276	0.936	0.191
311	chromosome 6 open reading frame 173	228202	-0.782	-0.807	-0.590	0.581
312	plasminogen activator, tissue	152725	0.385	2.268	1.835	-0.094
313	chromosome 1 open reading frame 51	190300	0.768	-0.622	-1.350	-0.758
314	N/A	716249	-0.336	-1.387	-0.329	-0.692
315	cytoplasmic polyadenylation element binding protein 4	202878	1.574	0.451	0.476	0.505
316	v-maf musculoaponeurotic fibrosarcoma oncogene homolog F (avian)	179935	1.548	0.200	-0.085	-0.135
317	SERTA domain containing 1	183615	2.051	0.518	0.331	0.180
318	chromosome 9 open reading frame 68	126803	0.832	-0.554	-0.735	-0.094
319	RALBP1 associated Eps domain containing 2	125119	0.038	-0.602	-1.691	-1.072

MB Ranking	LEC stimulated with VEGF-A		Log2 Ratio			
	Name	Probe ID	1 hr	4 hr.	8 hr.	24 hr.
320	ELOVL family member 6, elongation of long chain fatty acids (FEN1/Elo2, SUR4/Elo3-like, yeast)	216339	-0.088	0.476	1.246	0.987
321	testis-specific kinase 2	193067	-0.169	-1.151	-1.413	-0.174
322	N/A	212060	0.651	0.184	-0.906	0.249
323	E2F transcription factor 8	185998	-0.650	-0.427	-0.503	0.823
324	immediate early response 2	163612	2.048	0.846	0.654	0.455
325	N/A	109626	-0.139	-0.963	0.423	0.296
326	single-stranded DNA binding protein 2	182329	-0.064	0.374	-1.034	-0.875
327	DnaJ (Hsp40) homolog, subfamily B, member 4	103618	-0.108	-1.090	-1.386	-1.303
328	N/A	100458	-0.406	-0.189	1.244	0.610
329	6-phosphofructo-2-kinase/fructose-2,6-biphosphatase 3	213278	1.618	1.337	1.085	0.573
330	N/A	212778	-0.419	-0.448	-0.496	0.889
331	ras homolog gene family, member J	168924	0.097	0.152	-1.174	-1.221
332	synaptogyrin 3	147437	0.228	1.046	0.371	-0.462
333	mannosidase, alpha, class 1C, member 1	211828	-0.033	-0.499	-0.821	-1.521
334	regulator of G-protein signalling 2, 24kDa	116793	2.021	-0.396	-0.622	-0.552
335	synapse defective 1, Rho GTPase, homolog 1 (C. elegans)	104549	-1.572	-0.754	-0.502	-0.676
336	Fanconi anemia, complementation group B	141313	-0.125	-0.622	0.423	0.812
337	tribbles homolog 1 (Drosophila)	150749	3.576	1.384	0.629	0.148
338	low density lipoprotein receptor-related protein 8, apolipoprotein e receptor	221017	-0.052	1.371	1.880	1.195
339	ral guanine nucleotide dissociation stimulator-like 1	180843	1.352	1.298	1.210	0.607
340	chromosome 2 open reading frame 23	156624	-0.222	-1.115	-1.807	-1.107
341	nuclear receptor subfamily 1, group H, member 3	155957	-0.041	-1.067	-0.972	-1.142
342	bruno-like 5, RNA binding protein (Drosophila)	193658	-0.135	-0.924	-1.283	-1.663
343	N/A	111796	0.185	-0.097	-0.479	-1.290
344	KIAA1794	190099	-0.247	-0.386	0.066	1.325
345	ATPase family, AAA domain containing 3C	148869	-1.012	0.119	0.291	-0.526
346	chromosome 9 open reading frame 95	146066	0.240	-0.807	-1.113	-0.355
347	KIAA1914	129030	-0.072	-1.765	-1.637	-1.444
348	ADAM metallopeptidase with thrombospondin type 1 motif, 4	212524	1.173	0.632	0.504	1.441
349	interferon-related developmental regulator 2	213763	-0.597	0.319	0.873	0.133
350	trans-prenyltransferase	117679	-0.647	0.960	1.397	0.447
351	nucleolar protein family 6 (RNA-associated)	224105	-0.177	1.001	1.067	0.055
352	chromosome 14 open reading frame 145	154359	-0.393	-0.960	-0.416	0.606
353	proline-rich nuclear receptor coactivator 1	102937	0.289	-0.415	-1.110	0.065
354	solute carrier family 40 (iron-regulated transporter), member 1	165911	-0.094	-1.175	-1.151	-0.539
355	AT rich interactive domain 5B (MRF1-like)	163382	1.258	-0.064	-0.016	0.231
356	growth arrest-specific 2 like 3	137837	0.421	-0.792	-0.521	0.530
357	transmembrane protein 88	200951	1.148	-0.252	-0.498	-0.688
358	chromosome 20 open reading frame 19	213234	0.176	-0.725	-1.440	-0.389
359	phosphatidic acid phosphatase type 2C	120143	0.343	0.274	-0.464	-1.080
360	N/A	194097	0.237	-0.347	-1.197	-0.652
361	N/A	228136	0.400	-0.760	-0.843	-0.594
362	CD200 antigen	105368	1.281	0.185	-0.190	0.134
363	N/A	208543	-0.149	-0.845	-0.939	-1.469
364	N/A	197968	-0.004	-0.593	-1.479	-0.532
365	ring finger protein 150	213739	0.536	-0.398	-0.617	-0.707
366	N/A	123821	-0.326	0.914	0.385	0.728

MB Ranking	LEC stimulated with VEGF-A	Probe ID	Log2 Ratio			
	Name		1 hr	4 hr.	8 hr.	24 hr.
367	angiopoietin 2	193875	0.459	1.960	2.538	2.302
368	platelet derived growth factor C	189538	0.258	-0.440	-1.631	-1.078
369	RNA, U3 small nucleolar interacting protein 2	206116	-0.252	1.164	1.071	-0.074
370	translocase of outer mitochondrial membrane 40 homolog (yeast)	197942	-0.312	0.622	1.022	0.058
371	N/A	222424	1.014	-0.447	0.040	0.008
372	PDZ and LIM domain 4	170266	-0.120	1.400	0.736	0.204
373	Kruppel-like factor 5 (intestinal)	156864	1.531	1.405	0.768	0.801
374	v-jun sarcoma virus 17 oncogene homolog (avian)	123273	0.680	0.214	-0.654	-0.869
375	protein-L-isoaspartate (D-aspartate) O-methyltransferase domain containing 1	129701	0.064	-0.932	-1.551	-0.435
376	ST8 alpha-N-acetyl-neuraminide alpha-2,8-sialyltransferase 4	203385	0.577	0.852	0.462	1.842
377	signal transducer and activator of transcription 1, 91kDa	136002	0.105	-0.299	-1.175	-1.054
378	family with sequence similarity 64, member A	159220	-0.678	-0.423	-0.607	0.857
379	thymidylate synthetase	154415	-0.535	-0.762	-0.382	0.978
380	syntaxin 11	138768	1.237	1.059	0.561	0.027
381	zinc finger protein 323	199498	-0.548	-1.528	-1.690	-0.947
382	lunatic fringe homolog (Drosophila)	185842	-0.548	-1.205	-1.561	-1.473
383	iroquois homeobox protein 2	542107	1.811	0.531	0.258	0.245
384	RAD54 homolog B (S. cerevisiae)	115487	-0.535	-0.973	0.242	0.435
385	N/A	297413	1.511	-0.139	0.398	0.461
386	N/A	195134	-0.013	-0.138	0.346	1.469
387	ubiquitin-like, containing PHD and RING finger domains, 1	165886	-0.426	0.059	1.564	0.943
388	ring finger protein 144	101012	0.028	-1.448	-0.960	-0.841
389	coiled-coil domain containing 33	235214	0.275	-0.758	-0.085	0.557
390	peter pan homolog (Drosophila)	171791	-0.064	1.068	0.934	-0.159
391	integrin, alpha 7	185859	1.094	0.402	0.460	1.326
392	N/A	151231	1.059	-0.226	-0.036	0.990
393	desmuslin	114901	0.512	1.293	1.169	1.087
394	cell division cycle associated 7	207416	-0.198	0.856	1.190	0.045
395	hydroxysteroid dehydrogenase like 1	192606	-1.483	-0.824	-1.109	-1.230
396	apolipoprotein L, 4	147557	-0.320	-1.118	-1.958	-0.841
397	copine family member IX	214846	0.244	-0.082	-0.478	-1.135
398	CDC6 cell division cycle 6 homolog (S. cerevisiae)	130465	-0.193	-0.030	1.303	1.230
399	pecanex homolog (Drosophila)	134496	0.100	-0.838	-1.119	-0.724
400	N/A	206048	-0.048	-1.307	-0.874	-0.638

Appendix Table 3

Top 400 differentially modulated genes by VEGF-C in LEC using

Multivariate Bayesian ranking analysis

MB Ranking	LEC stimulated with VEGF-C		Log2 Ratio			
	Name	Probe ID	1 hr	4 hr.	8 hr.	24 hr.
1	v-fos FBJ murine osteosarcoma viral oncogene homolog	205128	3.255	0.995	1.516	2.035
2	early growth response 1	147353	3.731	0.563	1.185	1.358
3	early growth response 3	124744	5.491	0.119	0.460	0.708
4	coagulation factor III (thromboplastin, tissue factor)	146916	2.830	1.368	0.243	1.063
5	prostaglandin-endoperoxide synthase 2 (prostaglandin G/H synthase and cyclooxygenase)	208388	2.193	0.046	0.712	0.376
6	N/A	133024	-0.499	-1.841	-1.669	-1.644
7	early growth response 2 (Krox-20 homolog, Drosophila)	101929	4.604	-0.018	0.123	0.302
8	N/A	228964	-0.628	0.259	-1.974	-0.890
9	ADAM metallopeptidase with thrombospondin type 1 motif, 9	160876	1.965	0.669	-0.061	0.461
10	coagulation factor III (thromboplastin, tissue factor)	204787	3.240	1.563	0.711	1.095
11	p300/CBP-associated factor	183086	0.296	-0.574	-1.632	-0.487
12	N/A	178581	1.895	0.790	0.512	1.008
13	SNF1-like kinase	171526	2.100	0.462	0.547	0.356
14	zinc finger protein 36, C3H type, homolog (mouse)	179827	1.839	0.757	0.763	1.148
15	DEP domain containing 1B	206865	-0.648	-1.147	-1.255	0.259
16	protein regulator of cytokinesis 1	180626	-0.627	-0.721	-0.597	0.737
17	endothelial cell-specific molecule 1	174810	0.263	1.655	1.375	1.738
18	guanylate cyclase 1, soluble, alpha 3	170165	0.792	1.103	-0.385	-0.529
19	polo-like kinase 1 (Drosophila)	197341	-0.693	-0.867	-1.531	0.208
20	aurora kinase B	203163	-0.716	-0.931	-0.565	0.567
21	phosphoinositide-3-kinase, regulatory subunit 3 (p55, gamma)	216089	0.580	-0.944	-0.694	-0.186
22	KIAA1913	229140	0.691	1.569	-0.019	0.323
23	jumonji domain containing 3	124424	0.845	-0.459	-0.561	0.111
24	nuclear receptor subfamily 4, group A, member 1	216600	3.591	0.546	0.510	0.305
25	N/A	185597	-0.294	1.217	0.603	0.261
26	interleukin 1, beta	130322	1.674	0.759	0.389	0.854
27	lymphotoxin beta (TNF superfamily, member 3)	180671	-0.754	-0.910	-1.481	-1.483
28	latrophilin 1	127718	0.237	-0.684	0.909	0.931
29	midnolin	159555	1.809	0.596	-0.101	0.359
30	NIMA (never in mitosis gene a)-related kinase 2	115004	-0.777	-1.255	-1.057	0.071
31	cyclin-dependent kinase inhibitor 2C (p18, inhibits CDK4)	112997	-0.708	-1.589	-1.175	-0.230
32	kinesin family member 4A	115354	-0.687	-0.833	-0.986	0.409
33	chromosome 15 open reading frame 42	196613	-0.508	-0.734	-0.215	0.722
34	kinesin family member 20A	118830	-1.165	-1.511	-0.966	-0.272
35	zinc finger protein 614	147595	1.413	1.157	0.526	0.656
36	6-phosphofructo-2-kinase/fructose-2,6-biphosphatase 3	198714	1.539	0.950	0.309	0.856
37	iroquois homeobox protein 2	542107	1.430	0.511	0.036	0.179
38	SERTA domain containing 1	183615	1.292	0.023	0.145	0.053
39	thymidine kinase 1, soluble	105119	-0.672	-0.747	-0.815	0.448
40	calmin (calponin-like, transmembrane)	162511	-0.787	0.477	-0.800	-0.745
41	N/A	209213	1.349	-0.719	-0.589	-0.587

MB Ranking	LEC stimulated with VEGF-C		Log2 Ratio			
	Name	Probe ID	1 hr	4 hr.	8 hr.	24 hr.
42	N/A	191516	-1.004	-1.002	-0.157	-1.056
43	N/A	230575	0.814	0.877	-0.224	-0.196
44	N/A	210759	-0.408	0.734	-0.079	-0.873
45	apolipoprotein B mRNA editing enzyme, catalytic polypeptide-like 3B	138620	-0.892	-1.347	-0.956	-0.167
46	N/A	179136	1.263	-0.252	0.752	0.550
47	Cbp/p300-interacting transactivator, with Glu/Asp-rich carboxy-terminal domain, 1	118816	-0.722	0.172	-1.567	-1.696
48	zinc finger protein 664	187860	-1.135	-0.870	-1.731	-0.995
49	cyclin B2	169571	-0.645	-1.069	-1.038	0.125
50	nucleolar and spindle associated protein 1	128435	-0.404	-0.638	-0.706	0.754
51	fatty acid binding protein 3, muscle and heart (mammary-derived growth inhibitor)	146250	0.646	0.592	1.193	1.677
52	PDZ binding kinase	169723	-0.794	-1.040	-1.197	0.031
53	topoisomerase (DNA) II alpha 170kDa	135302	-0.264	-0.461	-0.430	0.820
54	chemokine orphan receptor 1	139192	0.877	1.014	-0.560	0.166
55	nitric oxide synthase 1 (neuronal) adaptor protein	180965	-0.573	-0.621	-0.571	0.532
56	baculoviral IAP repeat-containing 5 (survivin)	104062	-0.759	-1.065	-0.816	0.132
57	antigen identified by monoclonal antibody Ki-67	137656	-0.369	-0.573	-0.658	0.653
58	centromere protein F, 350/400ka (mitosin)	183726	-0.038	-0.358	-0.309	0.984
59	BCL6 co-repressor	223980	1.396	0.492	0.708	0.826
60	pyruvate dehydrogenase kinase, isozyme 4	101060	-1.226	-1.517	-1.566	-1.107
61	N/A	228086	0.424	-0.587	-0.740	-0.757
62	N/A	620594	1.178	1.238	0.455	0.880
63	phosphoinositide-3-kinase, regulatory subunit 1 (p85 alpha)	180157	1.059	0.190	-1.010	-0.378
64	kinesin family member C1	141343	-0.540	-1.004	-0.689	0.322
65	solute carrier family 45, member 4	222162	1.057	0.404	0.035	-0.062
66	U2AF homology motif (UHM) kinase 1	218514	1.205	0.758	0.082	0.409
67	N/A	111700	-0.345	-0.573	-0.218	0.739
68	basic helix-loop-helix domain containing, class B, 2	197538	2.672	1.042	0.791	0.821
69	N/A	144262	0.722	-0.570	1.060	1.001
70	laminin, alpha 2 (merosin, congenital muscular dystrophy)	149994	0.210	-0.230	-0.681	-1.093
71	WD and tetratricopeptide repeats 1	205123	-1.184	-0.782	-0.393	-1.027
72	B-cell CLL/lymphoma 6, member B (zinc finger protein)	178868	0.939	0.263	-0.781	-0.111
73	chromosome 2 open reading frame 23	156624	-0.090	-0.711	-1.486	-1.186
74	N/A	135436	1.225	0.265	0.564	0.722
75	t-complex 11 (mouse) like 2	193950	0.490	0.157	-0.962	-0.024
76	baculoviral IAP repeat-containing 5 (survivin)	227666	-0.804	-0.889	-1.044	0.062
77	TSC22 domain family, member 2	113125	1.437	0.464	0.408	0.353
78	inhibitor of DNA binding 2, dominant negative helix-loop-helix protein	129260	0.697	-0.801	-0.509	-0.219
79	solute carrier family 4, sodium bicarbonate cotransporter, member 7	163733	1.253	1.800	0.095	0.280
80	N/A	232041	1.789	1.290	-0.154	0.492
81	chromosome 18 open reading frame 56	223997	-0.569	0.012	-1.326	-0.239
82	calcium/calmodulin-dependent protein kinase (CaM kinase) II beta	227829	-0.139	1.219	0.531	0.446
83	elastin (supravalvular aortic stenosis, Williams-Beuren syndrome)	187671	-0.097	-0.732	0.390	-0.728
84	asp (abnormal spindle)-like, microcephaly associated (Drosophila)	181685	0.190	-0.197	-0.071	1.127
85	N/A	200967	0.816	-0.693	-0.474	-0.349
86	N/A	194279	0.481	1.623	0.460	-0.181
87	ras homolog gene family, member H	198968	-0.746	0.371	-0.300	-0.708

| MB Ranking | LEC stimulated with VEGF-C | | Log2 Ratio | | | |
	Name	Probe ID	1 hr	4 hr.	8 hr.	24 hr.
88	N/A	128294	-0.305	-1.077	-0.195	-0.965
89	R-spondin family, member 4	208221	-0.473	-0.234	0.774	-0.428
90	chromosome 15 open reading frame 2	197925	-1.093	-0.004	-0.043	-0.429
91	ribonucleotide reductase M2 polypeptide	134286	-0.418	-0.275	-0.697	0.667
92	interferon-induced protein with tetratricopeptide repeats 2	130677	0.265	-0.943	-0.741	-0.443
93	inactivation escape 1	206913	0.517	-0.239	-0.221	-0.793
94	olfactory receptor, family 51, subfamily T, member 1	152842	-0.541	-0.553	-0.426	0.623
95	ubiquitin-conjugating enzyme E2C	143651	-0.563	-0.805	-0.480	0.385
96	N/A	231275	-0.401	-0.970	-1.359	-1.122
97	kinetochore associated 2	107406	-0.549	-0.789	-0.743	0.311
98	N/A	209907	-0.177	-0.845	0.098	-0.817
99	tubby like protein 1	137311	-0.427	0.530	0.682	-0.263
100	N/A	697680	1.369	1.127	0.891	1.049
101	activating transcription factor 3	185687	2.676	1.017	0.317	0.850
102	zinc finger protein 80 (pT17)	105989	-0.691	-0.536	0.471	-0.539
103	chemokine (C-X-C motif) receptor 4	191821	-0.617	-0.079	0.433	0.569
104	nei endonuclease VIII-like 3 (E. coli)	172546	-0.340	-0.608	-0.751	0.456
105	N/A	180079	-0.379	-0.337	-0.675	-1.443
106	regulator of G-protein signalling 2, 24kDa	116793	0.343	-0.536	-0.613	-0.760
107	fibroblast growth factor receptor 1 (fms-related tyrosine kinase 2, Pfeiffer syndrome)	217844	-0.239	-0.776	-1.856	-1.826
108	N/A	175055	0.764	-0.038	0.648	-0.405
109	WD repeats and SOF1 domain containing	196524	1.886	1.506	1.455	1.019
110	gon-4 homolog (C.elegans)	191928	0.892	-0.402	0.619	-0.003
111	N/A	116001	0.531	-0.059	-0.426	-0.742
112	p21 (CDKN1A)-activated kinase 3	217739	1.234	0.815	0.660	0.090
113	N/A	234260	-0.322	-0.241	0.828	-0.536
114	N/A	121962	0.371	-0.043	-1.140	-0.233
115	glutaminyl-peptide cyclotransferase (glutaminyl cyclase)	152127	1.211	0.432	-0.131	0.339
116	hairy and enhancer of split 1, (Drosophila)	176983	1.418	-0.151	-0.608	-0.185
117	hairy/enhancer-of-split related with YRPW motif 1	121998	0.607	-0.856	-0.921	-0.567
118	aquaporin 7	124473	1.447	0.468	0.748	0.475
119	N/A	445006	1.257	0.290	0.173	0.055
120	pelota homolog (Drosophila)	222926	1.219	0.372	-0.072	0.546
121	calmegin	100646	0.547	0.755	-0.396	-0.196
122	v-maf musculoaponeurotic fibrosarcoma oncogene homolog B (avian)	226336	1.235	-0.744	-0.915	-0.040
123	vesicle-associated membrane protein 1 (synaptobrevin 1)	192759	-0.833	-0.394	0.516	-0.545
124	stanniocalcin 1	119453	1.693	-0.077	-1.126	-0.404
125	N/A	198371	-1.263	-0.805	-1.031	-0.360
126	UDP-N-acetyl-alpha-D-galactosamine:polypeptide N-acetylgalactosaminyltransferase 8 (GalNAc-T8)	142557	0.408	-0.166	0.440	1.074
127	N/A	151076	-0.580	-0.895	-0.686	-1.322
128	kinesin family member 2C	212531	-0.213	-0.632	-0.580	0.653
129	protein geranylgeranyltransferase type I, beta subunit	177456	0.674	-0.568	-0.112	0.031
130	dual specificity phosphatase 5	121612	2.564	0.889	0.576	0.682
131	N/A	154042	0.506	1.577	-0.207	-0.390
132	SHC SH2-domain binding protein 1	106848	-0.463	-0.509	-0.422	0.543
133	discs, large homolog 7 (Drosophila)	194498	-0.382	-0.617	-0.817	0.483

MB Ranking	LEC stimulated with VEGF-C		Log2 Ratio			
	Name	Probe ID	1 hr	4 hr.	8 hr.	24 hr.
134	N/A	159435	-1.060	-0.657	0.145	-0.309
135	cell division cycle associated 1	147806	-0.260	-0.687	-0.717	0.402
136	N/A	159898	-0.543	-1.043	-0.672	0.120
137	N/A	701184	0.779	0.260	0.950	-0.090
138	PBX/knotted 1 homeobox 1	137640	0.554	0.178	-0.302	0.841
139	kelch repeat and BTB (POZ) domain containing 6	201279	-0.988	0.174	-0.690	-0.196
140	chromosome 10 open reading frame 114	541266	-0.269	-1.160	-1.140	-0.608
141	N/A	236648	1.482	0.335	0.203	0.420
142	cyclin A2	110863	-0.471	-0.624	-0.823	0.328
143	T-box 3 (ulnar mammary syndrome)	115993	0.985	0.332	-0.120	-0.090
144	transmembrane protein 100	216519	-0.382	-1.114	-0.737	-1.143
145	decay accelerating factor for complement (CD55, Cromer blood group system)	167208	0.258	1.133	0.727	0.836
146	myosin IB	115188	1.464	1.054	0.992	0.824
147	cAMP responsive element binding protein 5	211684	0.865	1.104	0.352	1.002
148	SUMO1/sentrin specific peptidase 1	224778	0.574	0.079	-0.680	0.281
149	interleukin 18 receptor 1	213445	-0.072	1.337	0.137	-0.600
150	N/A	215658	0.855	1.048	0.933	1.271
151	N/A	289734	0.837	-0.312	0.469	0.070
152	N/A	169184	0.563	1.020	-0.137	0.193
153	ADAM metallopeptidase with thrombospondin type 1 motif, 9	10298121	0.848	0.167	0.413	-0.520
154	cytochrome P450, family 1, subfamily A, polypeptide 1	135086	0.301	-0.419	-1.085	-0.978
155	C-type lectin domain family 2, member L	184748	-0.983	-0.011	-0.233	0.041
156	N/A	107502	-0.329	-0.416	-0.212	0.810
157	N/A	231119	0.052	1.012	-0.001	-0.321
158	centromere protein A, 17kDa	106198	-0.835	-0.915	-0.807	0.034
159	cell division cycle 2, G1 to S and G2 to M	123400	-0.541	-0.536	-0.542	0.434
160	N/A	233248	-0.756	0.240	-0.223	0.352
161	N/A	707294	1.035	0.485	-0.036	0.179
162	N/A	215902	-0.135	-0.534	0.084	0.786
163	chromosome 14 open reading frame 4	216855	0.813	-0.028	-0.422	0.044
164	transcription elongation factor A (SII), 3	107155	-0.019	0.189	-0.034	-0.912
165	heparan sulfate (glucosamine) 3-O-sulfotransferase 1	154628	0.464	-0.268	-0.550	-0.569
166	mal, T-cell differentiation protein-like	201519	0.395	0.006	-0.530	-0.720
167	spermatogenesis associated 12	229375	-0.736	-1.057	-1.372	-0.884
168	peroxisome proliferative activated receptor, gamma, coactivator 1, alpha	147539	0.878	0.104	0.707	0.986
169	cyclin-dependent kinase inhibitor 3 (CDK2-associated dual specificity phosphatase)	191305	-0.703	-0.741	-0.683	0.345
170	WAS protein family, member 2	146329	-0.512	-0.963	-1.613	-1.092
171	N/A	113704	-0.148	-0.818	-0.465	-0.953
172	cell division cycle associated 5	135130	-0.319	-0.684	-0.480	0.546
173	chromosome 21 open reading frame 108	235773	0.996	0.363	-0.064	0.409
174	N/A	170978	-0.561	0.258	-0.729	-0.820
175	hyaluronan-mediated motility receptor (RHAMM)	216917	-0.371	-0.611	-0.673	0.520
176	chromosome 20 open reading frame 128	149623	0.981	0.915	1.040	1.087
177	chromosome 10 open reading frame 10	178105	-0.749	0.177	0.298	0.264
178	growth differentiation factor 15	182404	1.203	0.365	0.312	0.598
179	anillin, actin binding protein (scraps homolog, Drosophila)	169499	-0.200	-0.441	-0.515	0.576

MB Ranking	LEC stimulated with VEGF-C Name	Probe ID	Log2 Ratio 1 hr	4 hr.	8 hr.	24 hr.
180	melanoma antigen family C, 2	160885	0.094	1.162	0.184	0.640
181	N/A	104707	-0.171	-1.333	-0.559	-1.263
182	gap junction protein, alpha 4, 37kDa (connexin 37)	202429	0.304	-0.311	-0.802	-0.753
183	serine/threonine kinase 6	157917	-0.736	-0.985	-0.583	0.124
184	vascular endothelial growth factor C	170337	0.252	1.486	0.650	1.278
185	KIAA0101	123361	-0.383	-0.689	-0.797	0.347
186	N/A	106597	-0.591	0.127	-0.067	-1.029
187	zinc finger and BTB domain containing 26	177467	0.490	-0.596	0.178	-0.355
188	serine/threonine kinase 6 pseudogene	540912	-1.090	-1.175	-0.957	-0.506
189	N/A	148170	-0.598	-0.189	0.434	0.671
190	chromosome 1 open reading frame 61	220684	-0.878	-0.690	-0.462	-1.218
191	N/A	111200	-0.244	-1.081	-0.736	-0.794
192	inositol 1,3,4,5,6-pentakisphosphate 2-kinase	168375	1.171	0.137	0.436	0.246
193	inhibitor of DNA binding 2B, dominant negative helix-loop-helix protein	233364	0.525	-0.373	-0.515	-0.590
194	Fanconi anemia, complementation group D2	151336	-0.626	-0.844	-0.934	0.268
195	N/A	191465	-0.107	0.297	-0.012	1.262
196	protein phosphatase 1K (PP2C domain containing)	191909	-0.701	-0.157	0.208	0.397
197	TPX2, microtubule-associated, homolog (Xenopus laevis)	189094	-0.904	-0.925	-0.674	0.008
198	N/A	351669	0.922	-0.144	0.508	0.635
199	chromosome 18 open reading frame 58	173685	-0.372	-0.660	-1.354	0.043
200	family with sequence similarity 64, member A	201158	-1.002	-1.037	-0.552	0.039
201	N/A	231627	0.078	0.337	-0.213	1.127
202	forkhead box D1	108203	0.321	0.091	-1.150	-0.432
203	ankyrin repeat domain 20B	161943	0.920	1.665	1.219	0.841
204	N/A	118927	0.789	0.965	1.170	1.314
205	N/A	140753	0.953	0.493	0.118	-0.566
206	zinc finger protein 467	184463	0.330	-0.788	-0.621	-0.407
207	N/A	209417	-0.104	0.409	1.345	0.525
208	centrosomal protein 55kDa	198728	-0.445	-0.542	-0.615	0.617
209	spindle pole body component 25 homolog (S. cerevisiae)	130624	-0.623	-0.779	-0.720	0.192
210	Kruppel-like factor 5 (intestinal)	156864	0.987	0.913	0.239	0.437
211	TAP binding protein (tapasin)	143717	-0.070	0.312	-1.063	-0.620
212	N/A	171510	-0.968	0.113	-0.706	-0.469
213	N/A	400486	0.171	1.638	0.086	-0.103
214	deleted in liver cancer 1	207792	1.074	0.844	0.396	0.561
215	sperm associated antigen 5	185888	-0.666	-0.936	-0.891	0.012
216	kinesin family member 23	160577	-0.372	-0.258	-0.297	0.641
217	kinesin family member 14	121673	-0.118	-0.498	-0.225	0.844
218	AT rich interactive domain 3B (BRIGHT- like)	712742	0.997	0.058	0.136	0.306
219	growth arrest-specific 7	189097	0.828	-0.700	0.295	-0.004
220	N/A	128495	-0.244	-0.654	-0.314	0.555
221	N/A	230585	1.021	1.073	0.508	1.172
222	fatty acid synthase	154286	-0.456	0.362	-0.326	0.477
223	6-phosphofructo-2-kinase/fructose-2,6-biphosphatase 3	213278	1.241	0.797	0.200	0.602
224	N/A	159940	-0.473	0.159	0.711	-0.448
225	zinc finger protein 671	149250	-1.004	-0.163	-0.427	0.281
226	N/A	704926	1.012	0.114	1.430	0.778

MB Ranking	LEC stimulated with VEGF-C Name	Probe ID	Log2 Ratio 1 hr	4 hr.	8 hr.	24 hr.
227	zinc finger protein 407	214534	-0.671	-0.935	-0.381	-1.128
228	N/A	192010	0.733	0.591	0.748	1.286
229	galanin	167511	-0.678	0.084	0.463	-0.005
230	adiponutrin	197774	0.576	1.000	0.857	1.070
231	KIAA1193	188138	-0.362	-0.761	0.140	-0.732
232	protein tyrosine phosphatase, receptor type, E	541414	1.594	0.811	0.602	0.063
233	B-cell CLL/lymphoma 6 (zinc finger protein 51)	151724	1.593	0.725	-0.094	0.560
234	fructose-1,6-bisphosphatase 1	125158	0.399	-0.742	-0.438	0.208
235	N/A	234709	1.654	0.656	0.543	0.332
236	tigger transposable element derived 1	237079	0.012	1.208	0.819	0.185
237	N/A	113701	0.124	1.091	0.707	0.442
238	N/A	217029	1.672	0.528	0.187	0.776
239	family with sequence similarity 91, member A2	103214	0.970	1.107	0.483	0.759
240	N/A	198050	-0.812	-0.733	0.160	-0.514
241	ets variant gene 1	216791	-0.055	0.991	0.721	0.178
242	N/A	205276	0.200	-0.891	-0.442	-0.576
243	ADP-ribosylation factor-like 5B	182434	0.899	-0.132	0.306	0.595
244	ERO1-like beta (S. cerevisiae)	207998	0.984	0.057	0.032	0.322
245	N/A	232731	-0.779	0.058	-0.433	-0.837
246	high-mobility group box 2	216889	-0.680	-0.935	-0.834	-0.045
247	paraneoplastic antigen MA3	176304	-0.093	-0.147	1.078	0.491
248	dual specificity phosphatase 10	187011	0.890	-0.105	0.011	-0.247
249	UTP14, U3 small nucleolar ribonucleoprotein, homolog A (yeast)	113975	-0.401	-0.360	-0.731	-1.226
250	sodium channel, voltage-gated, type III, alpha	161435	0.610	-0.392	0.144	0.634
251	G protein-coupled receptor 133	102836	-0.649	-0.857	0.197	-0.073
252	chemokine (C-X-C motif) receptor 3	103589	-0.106	-0.978	0.211	-0.459
253	N/A	245704	0.676	-0.292	0.845	0.133
254	low density lipoprotein receptor class A domain containing 1	548189	0.200	0.504	1.093	1.043
255	N/A	232983	-0.514	-1.135	-0.044	-0.824
256	peptidoglycan recognition protein 2	117570	-0.920	-0.017	-1.544	-1.575
257	scavenger receptor class F, member 2	148950	-0.473	-0.679	-1.799	-1.494
258	insulin induced gene 1	215650	1.015	0.087	0.221	0.389
259	N/A	182347	-0.447	-0.538	-1.138	-1.092
260	myeloid/lymphoid or mixed-lineage leukemia 3|B melanoma antigen family, member 5|B melanoma antigen family, member 3	199679	1.033	0.395	0.255	0.244
261	low density lipoprotein receptor (familial hypercholesterolemia)	103382	1.135	0.609	0.422	0.664
262	N/A	181035	-0.254	-0.445	-1.424	-0.268
263	N/A	182262	-0.797	-0.068	0.028	-0.734
264	lymphocyte antigen 6 complex, locus H	173179	-0.228	0.715	0.919	0.034
265	M-phase phosphoprotein 6	226998	0.123	0.379	-0.250	1.019
266	N/A	481671	-0.590	0.127	0.459	-0.606
267	fibroblast growth factor 4 (heparin secretory transforming protein 1, Kaposi sarcoma oncogene)	116891	-0.596	0.081	-1.011	-0.822
268	N/A	148766	-0.687	-0.185	0.448	-0.375
269	trophinin associated protein (tastin)	137875	-0.821	-1.123	-0.713	-0.115
270	N/A	114047	0.921	0.102	0.048	-0.237
271	ribosomal protein S6 kinase, 90kDa, polypeptide 5	152363	0.538	-0.219	-0.717	0.258
272	N/A	194013	-0.517	-0.079	0.042	-0.887

MB Ranking	LEC stimulated with VEGF-C		Log2 Ratio			
	Name	Probe ID	1 hr	4 hr.	8 hr.	24 hr.
273	phosphoenolpyruvate carboxykinase 1 (soluble)	112194	-0.287	-0.542	0.218	0.689
274	Wilms tumor 1 associated protein	227679	0.390	0.494	-0.730	-0.178
275	N/A	143181	0.230	0.807	0.214	1.002
276	N/A	222628	-0.157	-0.578	0.558	-0.347
277	CDC45 cell division cycle 45-like (S. cerevisiae)	208272	-0.491	-0.160	-0.099	0.795
278	hepatic leukemia factor	118529	-0.492	-0.232	0.243	-0.792
279	N/A	110350	0.561	-0.108	-0.407	-0.382
280	CTAGE family, member 4	235777	0.594	0.956	1.190	0.913
281	N/A	229613	-0.667	-1.091	-0.169	-0.998
282	transmembrane channel-like 8	173591	-1.210	-1.729	-1.428	-1.317
283	KIAA0513	104925	0.501	0.010	-0.617	-0.306
284	gamma-aminobutyric acid (GABA) B receptor, 1	195643	1.111	0.973	0.690	0.523
285	WAP four-disulfide core domain 12	131425	-0.931	-1.094	-0.068	-0.647
286	zinc finger protein 516	108345	-0.355	-0.737	-1.491	-0.091
287	Rac GTPase activating protein 1	135746	-0.340	-0.594	-0.691	0.333
288	hydroxysteroid dehydrogenase like 1	192606	-1.094	-1.218	-1.043	-0.398
289	N/A	226409	0.942	0.439	-0.252	-0.085
290	N/A	200017	0.834	1.627	1.071	0.851
291	potassium voltage-gated channel, KQT-like subfamily, member 1	183314	-0.787	-0.670	-0.513	-1.077
292	N/A	183303	1.862	0.556	-0.105	0.386
293	major histocompatibility complex, class II, DO beta	172619	0.465	1.162	0.564	0.211
294	nucleoside phosphorylase	147282	0.815	1.043	0.805	1.051
295	MLF1 interacting protein	147135	-0.541	-0.602	-0.226	0.464
296	N/A	335545	0.123	-0.761	0.193	-0.409
297	N/A	207583	-0.027	-0.551	0.530	-0.671
298	N/A	142167	0.212	-0.683	0.620	-0.174
299	N/A	712826	0.612	0.212	-0.304	-0.562
300	N/A	228136	0.555	0.264	-1.032	0.054
301	l(3)mbt-like 4 (Drosophila)	172568	0.126	0.175	-0.932	-0.327
302	Kruppel-like factor 10	104402	1.722	0.236	0.008	0.168
303	centromere protein A, 17kDa	128411	-0.682	-0.641	-1.098	0.263
304	phospholipase C, beta 4	100736	0.983	0.401	0.041	-0.065
305	KIAA0892	170092	-0.527	-0.478	-1.169	0.123
306	purinergic receptor P2Y, G-protein coupled, 8	133766	0.289	0.111	0.251	-0.661
307	N/A	151825	-1.052	-0.343	0.132	0.076
308	RAD9 homolog A (S. pombe)	208053	0.511	-0.643	-0.162	-0.285
309	chromosome 18 open reading frame 24	205780	-0.412	-0.441	-0.407	0.495
310	RAB5B, member RAS oncogene family	182445	-0.727	-0.591	-1.411	-0.375
311	chromosome 3 open reading frame 32	184605	0.559	0.806	0.628	1.373
312	kinesin family member 11	199107	-0.189	-0.465	-0.451	0.641
313	N/A	232185	-0.486	-0.769	0.057	-0.791
314	N/A	129073	-0.542	-1.125	-0.091	-0.203
315	N/A	147103	0.422	0.097	-0.225	-0.947
316	zinc finger protein 710	141826	-0.407	-0.100	-1.095	-0.811
317	inositol polyphosphate-5-phosphatase, 75kDa	213370	1.263	0.890	0.290	-0.126
318	coronin 6	150942	-0.013	0.024	0.775	0.831
319	adrenergic, beta-2-, receptor, surface	127856	0.634	-0.019	-0.381	-0.273

MB Ranking	LEC stimulated with VEGF-C		Log2 Ratio			
	Name	Probe ID	1 hr	4 hr.	8 hr.	24 hr.
320	chromosome 14 open reading frame 43	212518	-0.034	0.362	-0.299	-0.814
321	protein kinase, AMP-activated, gamma 2 non-catalytic subunit	542533	0.186	-0.558	0.598	-0.397
322	leucine zipper, down-regulated in cancer 1-like	114319	-0.468	0.291	-0.704	-0.729
323	palladin, cytoskeletal associated protein	130541	0.339	0.971	-0.151	-0.126
324	N/A	179552	-0.876	-0.091	-0.832	-0.190
325	basic helix-loop-helix domain containing, class B, 3	213577	0.250	-0.585	-0.173	-0.626
326	pipecolic acid oxidase	158722	0.845	1.189	1.205	1.257
327	N/A	648566	-1.036	0.130	0.022	-0.477
328	angiotensin II receptor, type 1	105197	-0.246	-0.873	0.297	-0.382
329	chromosome 20 open reading frame 58	211587	-0.717	-0.176	0.254	-0.569
330	Rho GTPase activating protein 11A	117485	-0.103	-0.284	-0.089	0.789
331	N/A	124168	-0.053	-0.376	-0.447	-0.929
332	proline/serine-rich coiled-coil 1	181161	-1.174	-1.160	-0.728	-0.242
333	protogenin homolog (Gallus gallus)	384810	-0.304	0.534	0.130	0.538
334	N/A	190308	0.063	-0.368	-0.535	0.592
335	discoidin domain receptor family, member 1	173211	0.857	0.326	0.906	0.934
336	RALBP1 associated Eps domain containing 2	125119	0.168	-0.339	-1.021	-0.212
337	N/A	185713	0.488	0.372	0.547	1.192
338	N/A	231579	-0.256	-0.173	0.496	0.632
339	serpin peptidase inhibitor, clade B (ovalbumin), member 3	163547	-0.535	-0.212	-0.491	0.549
340	trinucleotide repeat containing 9	125060	-0.220	0.771	0.256	0.832
341	N/A	138397	-0.432	-0.313	-0.207	0.573
342	N/A	206508	0.898	-0.274	1.359	1.548
343	forkhead box I1	157201	0.431	0.238	0.894	-0.184
344	N/A	261736	1.111	0.655	0.675	0.680
345	chromosome 17 open reading frame 38	180545	-1.123	-0.266	-0.823	-0.270
346	N/A	220154	0.552	1.187	0.840	0.172
347	pellino homolog 1 (Drosophila)	113197	1.132	0.235	0.054	0.197
348	myosin VIIB	187521	-0.695	-0.284	0.368	-0.087
349	N/A	120178	-0.578	-0.074	0.285	0.467
350	chromosome 1 open reading frame 127	227197	0.766	0.222	0.638	-0.126
351	solute carrier family 25 (mitochondrial carrier; phosphate carrier), member 25	183778	1.148	0.533	0.239	0.213
352	tumor necrosis factor (ligand) superfamily, member 18	179164	-0.796	0.242	-0.779	-0.388
353	ST8 alpha-N-acetyl-neuraminide alpha-2,8-sialyltransferase 4	203385	0.249	0.460	0.350	1.051
354	kelch repeat and BTB (POZ) domain containing 2	211514	1.003	0.216	0.179	0.361
355	N/A	671775	0.826	1.030	0.312	0.457
356	N/A	567077	-0.941	-0.890	-0.363	-1.280
357	ZW10 interactor	167013	-0.377	-0.410	-0.187	0.621
358	aquaporin 2 (collecting duct)	129761	0.950	-0.299	0.559	0.237
359	N/A	107957	-0.355	-1.097	-0.917	-0.436
360	paxillin	155086	1.143	-0.211	1.404	0.953
361	N/A	235001	0.737	0.060	0.004	0.745
362	SLIT-ROBO Rho GTPase activating protein 2	165965	-0.369	-0.196	-1.122	-0.024
363	zinc finger protein 354C	128406	-0.846	0.184	-0.314	-0.400
364	N/A	181889	-1.041	-0.638	-0.761	-0.130
365	N/A	171415	0.376	1.027	0.266	0.958
366	polymerase (DNA directed), epsilon 2 (p59 subunit)	217170	-0.775	-0.742	-0.378	0.065

MB Ranking	LEC stimulated with VEGF-C	Probe ID	Log2 Ratio			
	Name		1 hr	4 hr.	8 hr.	24 hr.
367	peptidylprolyl isomerase (cyclophilin)-like 6	115831	0.335	-0.177	-0.261	-0.716
368	N/A	713730	0.209	0.325	1.251	0.102
369	calmodulin binding transcription activator 1	103913	0.638	1.175	0.624	0.665
370	CDC14 cell division cycle 14 homolog A (S. cerevisiae)	219032	0.088	1.116	0.606	0.292
371	potassium intermediate/small conductance calcium-activated channel, subfamily N, member 2	102973	0.581	1.308	0.285	0.889
372	N/A	232921	0.228	-0.125	1.124	0.185
373	ADAM metallopeptidase with thrombospondin type 1 motif, 2	224359	-0.837	0.250	-0.077	-0.565
374	dual specificity phosphatase 4	148153	0.855	0.896	0.272	0.226
375	bicaudal D homolog 2 (Drosophila)	207433	0.290	0.327	-0.767	-0.087
376	potassium channel tetramerisation domain containing 2	232722	-0.476	0.026	-1.333	-0.581
377	integrin beta 1 binding protein (melusin) 2	116020	0.512	1.173	0.809	1.080
378	WNK lysine deficient protein kinase 4	170756	-0.158	0.423	0.916	0.074
379	sprouty homolog 4 (Drosophila)	148545	0.684	0.685	0.024	0.725
380	N/A	232482	-0.932	-0.072	-0.257	-0.838
381	double homeobox, 4	177482	0.420	-0.624	0.232	0.300
382	N/A	233420	0.191	0.733	0.744	-0.162
383	polycomb group ring finger 4	167637	-0.042	-0.231	-1.134	0.248
384	chromosome 9 open reading frame 41	205667	-0.960	-0.118	-0.518	-0.730
385	solute carrier family 2 (facilitated glucose transporter), member 3	180998	0.695	-0.131	-0.287	0.063
386	ependymin related protein 1 (zebrafish)	210940	0.623	0.838	-0.021	0.656
387	N/A	248285	0.418	0.082	0.645	-0.350
388	N/A	10409147	1.054	0.386	0.107	0.359
389	N/A	102342	0.747	-0.193	-0.070	-0.014
390	MKL/myocardin-like 2	112995	-0.969	-0.315	-0.302	-0.197
391	vestigial like 2 (Drosophila)	171918	-0.820	0.240	0.001	-0.493
392	LIM domain only 6	136580	-0.456	-0.322	-0.020	-0.945
393	CDC14 cell division cycle 14 homolog A (S. cerevisiae)	176146	0.240	1.107	0.171	0.319
394	serine/threonine kinase 6 pseudogene	683679	-0.567	-0.680	-0.520	0.231
395	N/A	192975	-0.420	-0.710	-0.910	0.124
396	FBJ murine osteosarcoma viral oncogene homolog B	105390	1.288	0.002	0.424	0.040
397	TTK protein kinase	107112	-0.346	-0.587	-0.534	0.422
398	N/A	228432	-1.001	-0.278	-0.023	-0.083
399	cystathionase (cystathionine gamma-lyase)	105377	-0.953	-0.334	-0.044	-0.153
400	solute carrier family 6, member 16	191984	0.961	0.518	0.521	0.109

Appendix Table 4

Pathway classification analysis of VEGF-C induced genes in LEC

Molecular function	1h	4h	8h	24h
Transcription factor	+++	-	-	-
cytokine receptor	++	++	+	+++
Zinc finger transcription factor	++	-	-	-
Nucleic acid binding	++	-	-	-
Kinase modulator	++	-	-	-
Phosphatase	++	-	-	-
Nuclear hormone receptor	++	-	-	-
Carbohydrate phosphatase	++	-	-	-
Cytokine receptor	+	+++	-	++
Protein phosphatase	+	+	-	-
Carbohydrate transporter	+	-	-	-
Kinase inhibitor	+	-	-	-
Defense/immunity protein	-	+++	-	-
Phosphorylase	-	++	-	+++
Complement component	-	++	-	-
Growth factor	-	+	-	+
Lipase	-	+	-	+
Immunoglobulin receptor family member	-	+	-	-
Interleukin receptor	-	+	-	-
Guanylate cyclase	-	+	-	-
Storage protein	-	-	+	-
Ligand-gated ion channel	-	-	-	+
Glycosyltransferase	-	-	-	+

Biological process	1h	4h	8h	24h
MAPKKK cascade	+++	++	-	-
Nucleoside, nucleotide and nucleic acid metabolism	+++	+	-	-
Cell cycle control	+++	-	-	-
mRNA transcription	+++	-	-	-
mRNA transcription regulation	+++	-	-	-
Intracellular signaling cascade	++	++	-	-
Cell cycle	++	+	-	-
Developmental processes	++	+	-	-
Monosaccharide metabolism	++	-	-	-
Cell communication	+	+	-	-
Ligand-mediated signaling	+	+	-	-
Signal transduction	+	+	-	-
Protein phosphorylation	+	+	-	-
Oncogene	+	-	+	-
Cell proliferation and differentiation	+	-	-	-
JNK cascade	+	-	-	-
Regulation of phosphate metabolism	+	-	-	-
Complement-mediated immunity	-	++	-	-
Angiogenesis	-	+	-	+
Purine metabolism	-	+	-	+
Ion transport	-	+	-	-
Protein modification	-	+	-	-
Fatty acid metabolism	-	+	-	-
Cholesterol metabolism	-	-	+	-
Blood clotting	-	-	-	+
Synaptic transmission	-	-	-	+

+++ p-value < 0.0005; ++ p-value < 0.005; + p-value < 0.05; - not significant

8   CURRICULUM VITAE

Jay Woo Shin

PERSONAL INFORMATION

Date of Birth	April 4, 1981
Place of Birth	Seoul, South Korea
Nationality	United States of America
Sex	Male
Marital status	Single
Address	Regensdorferstrasse 9
	8049 Zurich, Switzerland
	Phone: ++41 44 633 7368
	Mobile: ++41 76 429 1037
	jay.shin@pharma.ethz.ch

EDUCATION

Ph.D. in Natural Sciences   Apr 2008
Swiss Federal Institute of Technology (ETH) Zurich, Switzerland
- Thesis: Identification of the vascular lineage-specific transcriptome and development of a novel low-density microvascular differentiation array.
- Advisor: Prof. Dr. Michael Detmar

Bachelor of Science in Computer Informatics   May 2003
Boston College, Boston, MA, USA
- Pre-medical program

RESEARCH EXPERIENCES

Research Student, Department of Biological Information   Aug 2007 - Oct 2007
Tokyo Institute of Technology, Yokohama, Japan
- Research topic: Cell-specific delivery of tumor suppressor gene using polyethylimine-complexed protein A.
- Advisor: Prof. Eiry Kobatake

Research Assistant, Cutaneous Biology Research Center   Sep 2002 - Oct 2004
Massachusetts General Hospital/Harvard Medical School, Boston, MA, USA
- Research topics: Investigation of FGF signaling in lymphangiogenesis and lymphatic re-programming of blood vascular endothelium by Prox1 regulation.
- Advisor: Prof. Dr. Michael Detmar

AWARDS & SCHOLARSHIPS

- ETH Scholarship to Tokyo Institute of Technology, Japan (2007)
- Young Investigator Scholarship, *Gordon Conference* (2006)
- European Molecular Biology Organization (EMBO) Scholarship (2006)
- Young Investigator Award, *Gene Signature Symposium.* Zurich, Switzerland (2005)

ACTIVITIES AND SKILLS

- President of Pharmaceutical Scientists' Association, PSA (2006, 2007)
- Information Technology (IT) Officer of Pharmacogenomics (2004 - present)
- Programming in C, Java, R, Perl, Python and Bioconductor implementation.
- Fluent in English and Korean. Basic in Japanese and German.

ORAL PRESENTATIONS

1. Shin J. Vascular endothelial growth factor-A mediates endocan to promote lymphangiogenesis. *3rd Cancer Network of Zurich Symposium.* Fiesch, Switzerland (January 2008).

2. Shin J (Keynote speaker). Investigation of the blood and lymph vessels growth in cancer and inflammation. *1st Young Scientists Symposium.* Munich, Germany (July 2007)**.**

3. Shin J. Identification of the vascular lineage-specific transcriptome and development of a novel low-density microvascular differentiation array. *3rd International qPCR Symposium*. Freising-Weihenstephan, Germany (March 2007).

4. Shin J. Comprehensive identification of vascular lineage-specific gene signatures and establishment of a low-density microvascular differentiation assay. *RNA Symposium*, Basel, Switzerland (November 2006).

5. Shin J. Expression profiling of endothelial lineage-specificity using vascular gene signatures. *EMBO – Advanced Analysis and Informatics on Microarray Data*, Cambridge, UK (June 2006).

6. Shin J. Comparison of two microarray-based mRNA profiling technologies for identification of novel endothelial lineage-specific genes. *2nd European Expression Array Systems meeting*, Barcelona, Spain (April 2006).

7. Shin J (Young Investigator Award). Lymphatic re-programming of blood vascular endothelium by Kaposi's sarcoma-associated herpesvirus. *Gene Signature Symposium*, Zurich, Switzerland (March 2005).

POSTER PRESENTATIONS

1. Shin J. Comprehensive identification of endothelial lineage-specific gene signatures and establishment of a low-density microvascular differentiation assay. *Gordon Research Conference – Molecular Mechanisms in Lymphatic Function and Disease*. Les Diablerets, Switzerland (September 2006).

2. Shin J. Comparison of two microarray-based mRNA profiling technologies for identification of novel endothelial lineage-specific genes. *Conference for Tumor-Host Interaction and Angiogenesis.* Ascona, Switzerland (October 2005).

3. Shin J. Prox1 promotes lineage-specific expression of FGF receptor-3 in lymphatic endothelium: A role for FGF signaling in lymphangiogenesis. *5th International Symposium on the Biology of Endothelial Cell.* Dresden, Germany (September 2005).

4. Shin J. Prox1 promotes lineage-specific expression of FGF receptor-3 in lymphatic endothelium: A role for FGF signaling in lymphangiogenesis. *5th ESH Euroconference on Angiogenesis.* Sitges, Spain (May 2005).

PUBLICATIONS

1. **Shin J**, Huggenberger R, Detmar M. Transcriptional profiling of VEGF-A and VEGF-C target genes in lymphatic endothelium reveals endocan as a novel mediator of lymphangiogenesis. Manuscript in preparation.

2. **Shin J**, Detmar M. Lymphatic-specific expression of dipeptidyl peptidase IV and its dual role in lymphatic endothelial function. Manuscript in preparation.

3. **Shin J**, Fuchs T, Gan W, Kunstfeld R, Mrowietz U, Detmar M. Quantification of vascular lineage-specific differentiation and molecular characterization of in vivo (lymph)angiogenesis by a novel low-density microvascular differentiation array. Manuscript in preparation.

4. Dadras SS, Skrzypek A, Nguyen L, **Shin J**, Schultz M, Arbiser J, Mihm MC, Detmar M. Prox-1 promotes invasion of kaposiform hemangioendotheliomas. Submitted to *Journal of Investigative Dermatology*.

5. Detmar M, **Shin J**. Angiogenesis and lymphangiogenesis in cutaneous cancer. *Exp. Dermatology* 2007 Oct;16(10): 865-866

6. **Shin J**, Min M, Larrieu-Lahargue F, Canron X, Nguyen L, Kunstfeld R, Henderson JE, Bikfalvi A, Detmar M, Hong YK. Prox1 promotes lineage-specific expression of FGF receptor-3 in lymphatic endothelium: A role for FGF signaling in lymphangiogenesis. *Mol Biol Cell.* 2006 Feb;17(2):576-84.

7. Hong YK, **Shin J**, Detmar M. The development of the lymphatic vascular system- a mystery unravels *Dev Dyn.* 2004 Nov;231(3):462-73.

8. Hong YK, Foreman K, **Shin J**, Hirakawa J, Curry CL, Sage DR, Libermann T, Dezube BJ, Fingeroth JD, Detmar M. Lymphatic re-programming of blood vascular endothelium by Kaposi's sarcoma-associated herpesvirus *Nature Genetics.* 2004 Jul;36(7):683-5.

9 ACKNOWLEDGEMENTS